

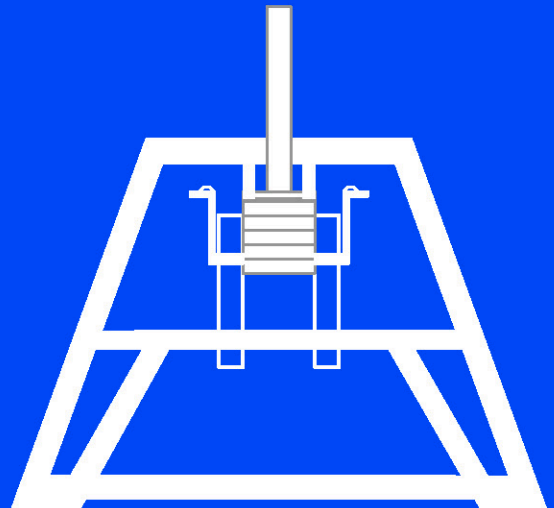
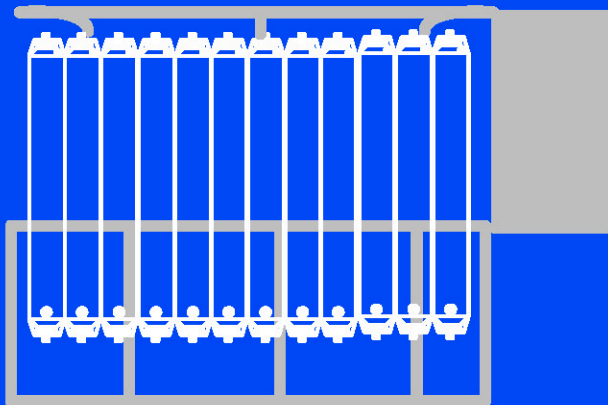
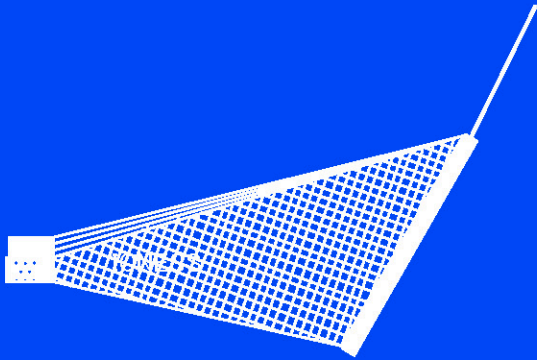
MR12-02

Preliminary Cruise Report

4 June - 12 July 2012

Issue: Aug 2012

JAMSTEC

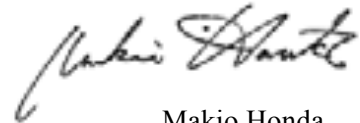


Note

This cruise report is a preliminary documentation published in approximately a month after the end of this cruise. It may not be corrected even if changes on contents are found after publication. It may also be changed without notice. Data on the cruise report may be raw or not processed. Please ask the principal investigator and persons in charge of respective observations for the latest information and permission before using. Users of data are requested to submit their results to JAMSTEC Data Integration and Analysis Group (DIAG).

September 2012

Principal Investigator of MR12-02

A handwritten signature in black ink, appearing to read 'Makio Honda', written in a cursive style.

Makio Honda
JAMSTEC

Contents of MR12-02 Preliminary Cruise Report

A. Cruise summary

- 1. Cruise information** A1
 - (1) Cruise designation
 - (2) Cruise title
 - (3) Principal investigator
 - (4) Science proposal of cruise
 - (5) Cruise period (port call)
 - (6) Cruise region (geographical boundary)
 - (7) Cruise track and stations

- 2. Outline of MR12-02** A4

- 2.1 Objective of this cruise
- 2.2 Cruise summary (highlights)

B. Text

1. Outline of MR12-02

- 1.1 Cruise summary 1
 - (1) Introduction of principal science proposal
 - (2) Objective of this cruise
 - (3) Cruise summary
 - (4) Scientific gears
- 1.2 Track and log (GODI) 8
- 1.3 Cruise participant 15

2. General observation

- 2.1 Meteorological observations
 - 2.1.1 Surface meteorological observation 18
 - 2.1.2 Ceilometer observation 26
 - 2.1.3 Lidar observations of clouds and aerosols 28
 - 2.1.4 Optical characteristics of aerosol observed by sky-radiometer 30
 - 2.1.5 Tropospheric aerosol and gas profile 31
 - 2.1.6 Continuous measurement of the water stable isotopes over the Ocean 33
- 2.2 Physical oceanographic observation
 - 2.2.1 CTD cast and water sampling 37
 - 2.2.2 Salinity measurement 44
 - 2.2.3 Shipboard ADCP 49
- 2.3 Sea surface water monitoring 52
- 2.4 Dissolved oxygen 56
- 2.5 Nutrients 60
- 2.6 pH 77
- 2.7 Dissolved inorganic carbon –DIC- 80
- 2.8 Total alkalinity 83
- 2.9 Underway pCO₂ 86

3. Special observation

3.1 BGC mooring	
3.1.1 Recovery and deployment	88
3.1.2 Instruments	100
3.1.3 Sampling schedule	103
3.1.4 Preliminary results	104
3.2 Underwater profiling buoy system (Primary productivity profiler)	
3.2.1 POPPS	106
3.2.2 RAS	112
3.3 Sediment trap experiment at station F1	118
3.4 Phytoplankton	
3.4.1 Chlorophyll a measurements by fluorometric determination	128
3.4.2 HPLC measurements of marine phytoplankton pigments	133
3.4.3 Phytoplankton abundance	138
3.4.4 Primary production and new production	140
3.4.5 P vs E curve	146
3.4.6 Oxygen evolution (gross primary production)	149
3.4.7 Absorption coefficients of phytoplankton and CDOM	151
3.5 Optical measurement	155
3.6 Drifting sediment trap	
3.6.1 Drifting mooring system	157
3.6.2 drifting sediment trap of JAMSTEC	161
3.7 Po-210 and export flux	162
3.8 Settling velocity of particles in the twilight zone	163
3.9 Zooplankton	
3.9.1 Community structure and ecological roles	164
3.9.2 Grazing pressure of microzooplankton	167
3.10 Biological study for phytoplankton and zooplankton	
3.10.1 Planktic foraminifera	169
3.10.2 Shell-bearing phytoplankton studies in the western North Pacific	171
3.11 Community structures and metabolic activities of microbes (Studies on the microbial-geochemical processes that regulate the operation of the biological pump in the subarctic and subtropical regions of the western North Pacific – IV)	173
3.12 Dissolved organic carbon	175
3.13 Chlorofluorocarbons	176
3.14 Argo float	178
3.15 Observational research on air-sea interaction in the Kuroshio-Oyashio Extension region JKEO buoy and NKEO buoy	185
3.16 Temporal changes in water properties of abyssal water in the western North Pacific	193
3.17 Development of a high-quality dissolved oxygen measurement by an optode-based oxygen sensor	197
3.18 Radiosonde observation for the validation of GOSAT and ship-borne sky radiometer Products	200
3.19 Sampling for artificial radionuclide from Fukushima	204

4. The concentrations of radionuclides in the western North Pacific 205

5. A study of the cycles of global warming related materials using their isotopomers in the western North Pacific	207
6. Validation of GOSAT products over sea using a ship-borne compact system for measuring atmospheric trace gas column densities	214
7. Multiple core	216
8. Geophysical observation	
8.1 Swath bathymetry	221
8.2 Sea surface gravity	223
8.3 Sea surface magnetic field	224
8.4 Tectonic history of the mid-Cretaceous Pacific Plate	226
9. Satellite image acquisition (MCSST from NOAA/HPRT)	228

Cover sheet: the first prize of “MR12-02 CRUISE REPORT COVER SHEET CONTEST”. The winner is Mr. Tetsuya Nakamura from Nichiyu Giken Kogyo Inc..

A. Cruise summary

1. Cruise information

(1) Cruise designation (research vessel)

MR12-02 (R/V MIRAI)

(2) Cruise title (principal science proposal) and introduction

Change in material cycles and ecosystem by the climate change and its feedback

Some disturbing effects are progressively coming to the fore in the ocean by climate change, such as rising water temperature, intensification of upper ocean stratification and ocean acidification. It is supposed that these effects result in serious damage to the ocean ecosystems. Disturbed ocean ecosystems will change a material cycle through the change of biological pump efficiency, and it will be fed back into the climate. We are aimed at clarifying the mechanisms of changes in the ocean structure in ocean ecosystems derived from the climate change,

We arranged the time-series observation stations in the subarctic gyre (K2: 47°N 160°E) and the subtropical gyre (S1: 30°N, 145°E) in the western North Pacific. In general, biological pump is more efficient in the subarctic gyre than the subtropical gyre because large size phytoplankton (diatom) is abundant in the subarctic gyre by its eutrophic oceanic condition. It is suspected that the responses against climate change are different for respective gyres. To elucidate the oceanic structures in ocean ecosystems and material cycles at both gyres is important to understand the relationship between ecosystem, material cycle and climate change in the global ocean.

There are significant seasonal variations in the ocean environments in both gyres. The seasonal variability of oceanic structures will be estimated by the mooring systems and by the seasonally repetitive ship observations scheduled for next several years.

(3) Principal Investigator (PI)

Makio Honda

Research Institute for Global Change (RIGC)

Japan Agency for Marine-Earth Science and Technology (JAMSTEC)

(4) Science proposals of cruise

Affiliation	PI	Proposal titles
University of Tokyo	Koji HAMASAKI	Studies on the microbial-geochemical processes that regulate the operation of the biological pump in the subarctic and subtropical regions of the western North Pacific – IV
Tokyo Institute of Technology	Naohiro YOSHIDA	A study of the cycles of global warming related materials using their isotopomers in the western North Pacific.
JAMSTEC	Hiroshi UCHIDA	Temporal changes in water properties of abyssal water in the western North Pacific

JAMSTEC	Toshio SUGA	Study of ocean circulation and heat and freshwater transport and their variability, and experimental comprehensive study of physical, chemical, and biochemical processes in the western North Pacific by the deployment of Argo floats and using Argo data
JAMSTEC	Hiroshi UCHIDA	Development of a high-quality dissolved oxygen measurement by an optode-based oxygen sensor
National Institute of Radiological Sciences	Tstuso AONO	The concentrations of radionuclides in the western North Pacific
JAXA	Shuji KAWAKAMI	Validation of GOSAT products over sea using a ship-borne compact system for measuring atmospheric trace gas column densities.
JAMSTEC	Yoshimi KAWAI	Observational research on air-sea interaction in the Kuroshio-Oyashio Extension region
not onboard study		
Hokkaido Univ.	Yasushi FUJIYOSHI	Continuous measurement of the water stable isotopes over the Ocean
Chiba Univ.	Masao NAKANISHI	Tectonics of the mid-Cretaceous Pacific Plate
NIES	Nobuo SUGIMOTO	Study of distribution and optical characteristics of ice/water clouds and marine aerosols
Ryukyu Univ.	Takeshi MATSUMOTO	Standardization of marine geophysical data and its application to the ocean floor geodynamics studies
Toyama Univ.	Kazuma AOKI	Maritime aerosol optical properties from measurements of Ship-borne sky radiometer

(5) Cruise period (port call)

Leg.1: 4 June 2012 (Sekinehama) – 24 June 2012 (Onahama*)

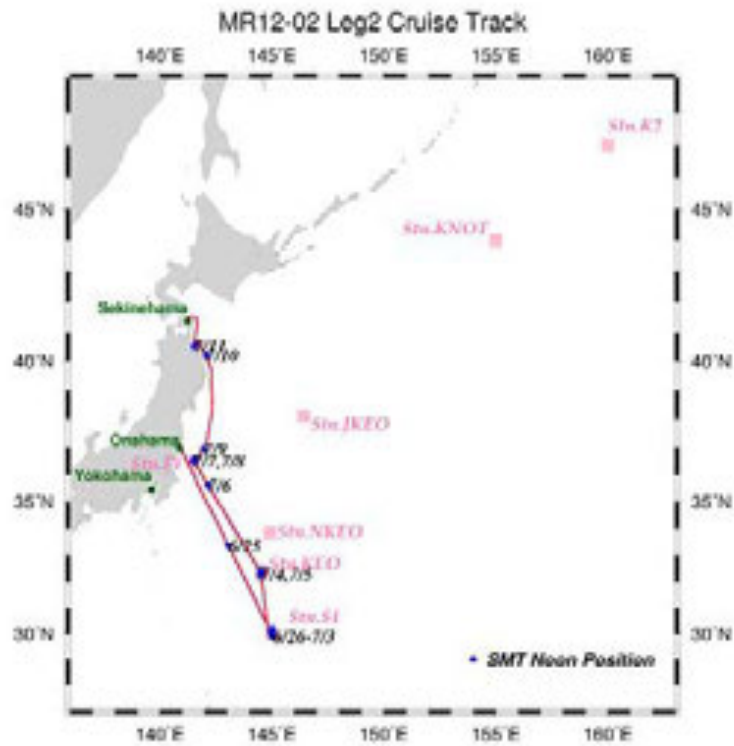
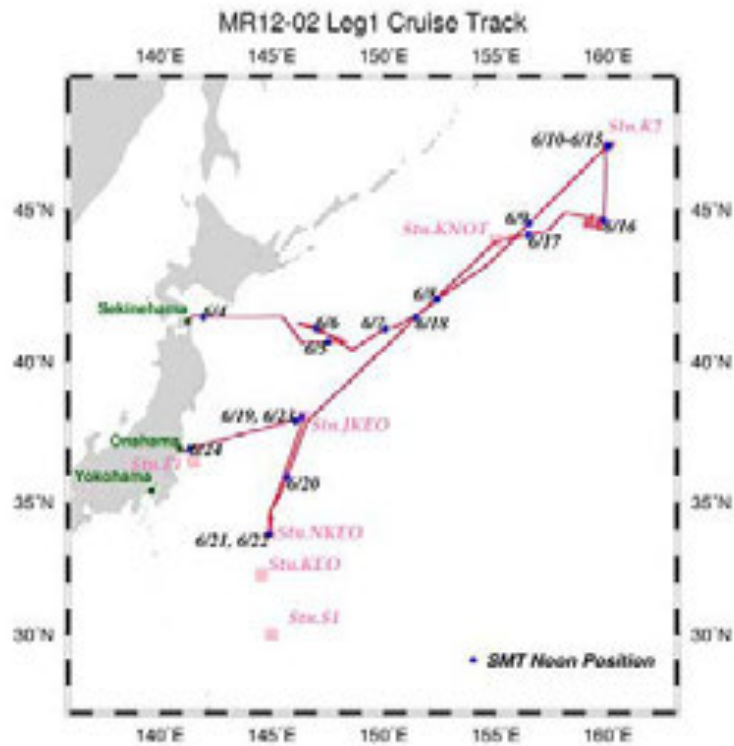
Leg.2: 24 June 2012 (Onahama*) – 12 July 2012 (Sekinehama)

* Exchange of part of participants without dock

(6) Cruise region (geographical boundary)

The western North Pacific (50°N – 30°N, 140°E – 160°W)

(7) Cruise track and stations



2. Outline of MR12-02

2.1 Objective of this cruise

Principal objective of this cruise is to observe late spring or early summer ecosystem and biogeochemical cycle at time-series stations in the sub-arctic and sub-tropical gyres. In addition, we conducted biogeochemical observation off Fukushima in order to investigate dispersion of radionuclides from the Fukushima Daiichi nuclear power plant.

Beside this, we conducted the observation of physical and biogeochemical property of meso-scale warm eddy. Moreover, JKEO / NKEO and KEO surface buoys were recovered and / or deployed.

2.2 Cruise summary (highlights)

2.2.1 Time-series observation at stations K2 and S1

(1) Nutrients

Concentrations of nutrients were measured several times at each station. Concentration of NO_3 near surface at K2 was about $17 \mu\text{mol kg}^{-1}$. Compared to winter value ($\sim 30 \mu\text{mol kg}^{-1}$), NO_3 decreased, however did not become the annual minimum value. Concentration of Si(OH)_4 was about $30 \mu\text{mol kg}^{-1}$ and this concentration was comparable to medium value of annual variability. Concentration of NO_3 upper 50m at S1 was less than $0.1 \mu\text{mol kg}^{-1}$ and comparable to the annual minimum. However, it is notable that concentration of NO_3 at surface was higher (between 0.1 and $0.7 \mu\text{mol kg}^{-1}$). It is still on argument whether this is natural increase (eolian input?) or contamination by bucket used for sampling. Unlike NO_3 , concentration of Si(OH)_4 near surface at S1 was about $2 \mu\text{mol kg}^{-1}$ and comparable to winter value or the annual maximum. It might be supported by the fact that diatom which requires Si(OH)_4 was little at S1.

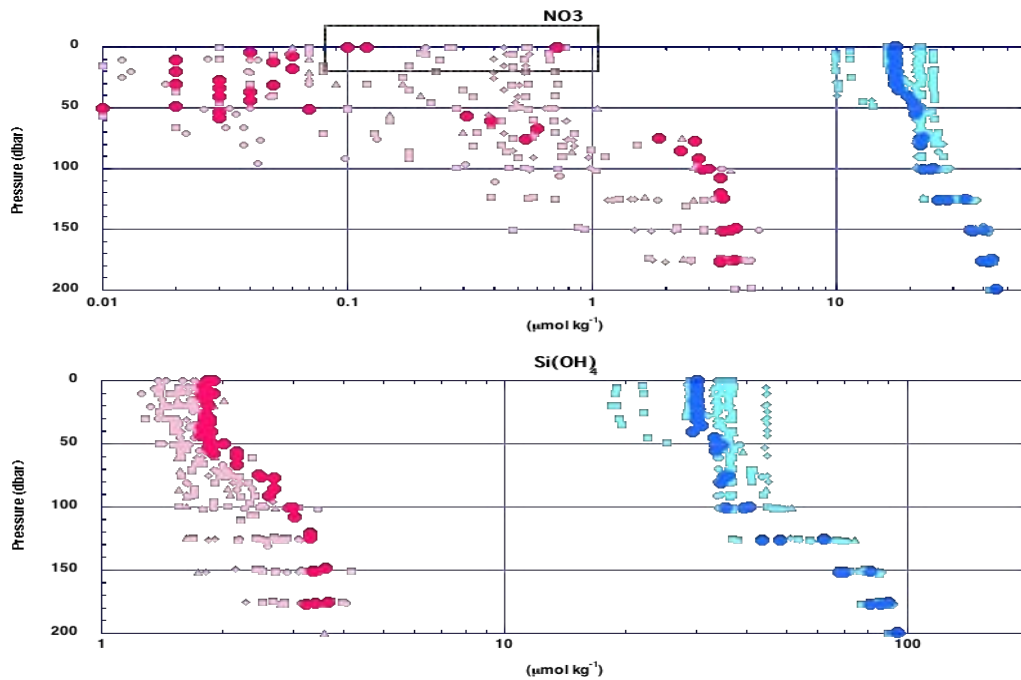


Fig. 1 Seasonal variability in nutrients: NO_3 (upper) and Si(OH)_4 (lower). Blue and red shows concentrations at K2 and S1, respectively and concentrations of dense color are data during this cruise.

(2) Pigments

Maximum chlorophyll-a (chl-a) at station K2 was about $1.2 \mu\text{g L}^{-1}$ observed at around 30 m water depth (Fig. 2a). Based on high-performance liquid chromatography (HPLC) analysis, diatom and *haptophyto* such as *coccolithophorids* were dominant species. At station S1, subsurface maximum of chl-a ($\sim 0.5 \mu\text{g L}^{-1}$) was observed at around 65 m. Dominant species of phytoplankton were *haptophyto* and *prochlorococcus* and diatom was not found. This result might support that dissolved Si(OH)_4 was not consumed largely at station S1.

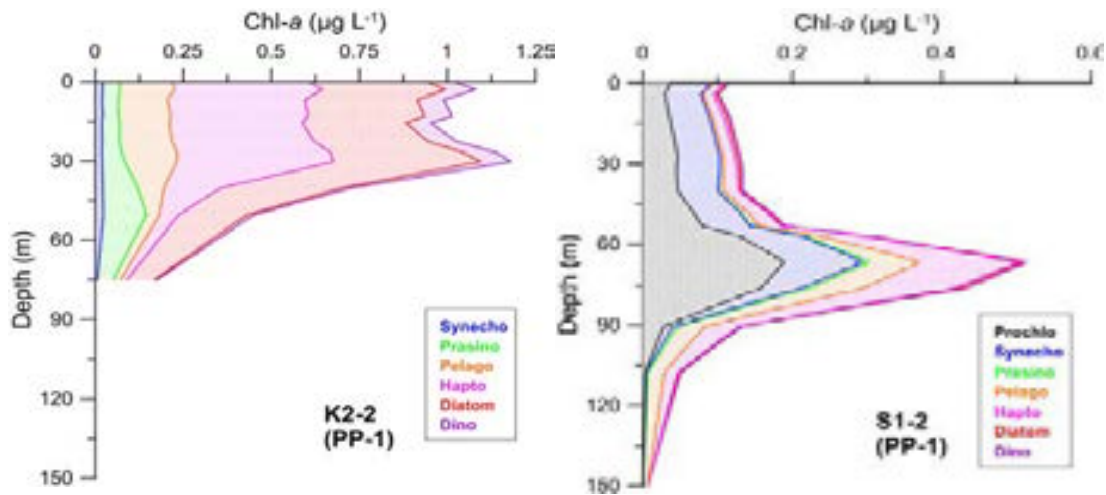


Fig. 2 Vertical profile of chlorophyll-a (chl-a) and contribution of chl-a of major major phytoplankton to total chl-a based on HPLC analysis.

(3) Primary productivity

Integrated primary productivity (PP) at station K2 ranged from approximately 400 to $600 \text{ mg-C m}^{-2} \text{ day}^{-1}$ (Fig. 3a). Based on seasonal variability in PP observed previously, PP during this cruise was close to the annual maximum. On the other hand, PP at station S1 was approximately $200 \text{ mg-C m}^{-2} \text{ day}^{-1}$. This PP coincided well with seasonal variability.

PP observed during this cruise and previously correlated well with photosynthetic available radiation (PAR) at station K2 (Fig. 3b). Thus it can be said that the major limiting factor of PP at station K2 is light condition.

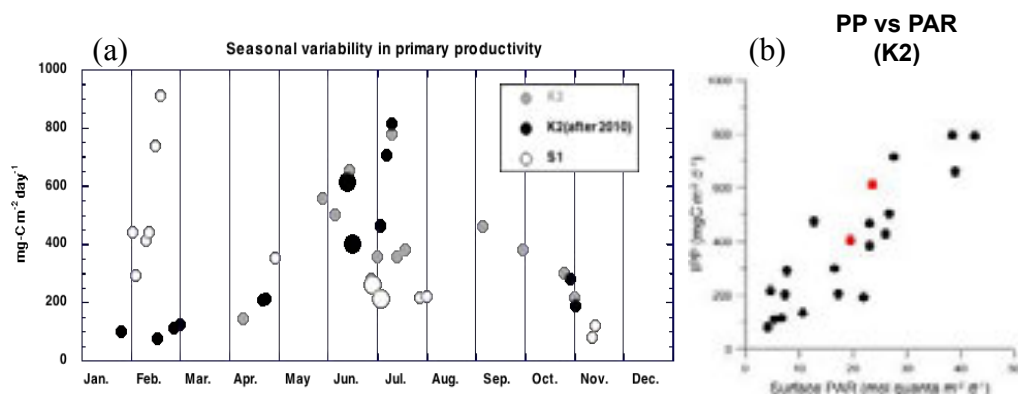


Fig. 3 (a) Seasonal variability in primary productivity (PP) at stations K2 (closed circles) and S1 (open circles). Larger circles are data obtained during this cruise. (b) relation between PP and photosynthetically available radiation (PAR) at station K2. Red circles show data obtained during this cruise

(4) Sinking particle

(Station K2) (Fig. 4a)

Based on height of sinking particle collected in collecting cups, mass flux at 200 m increased in July just after deployment. However mass flux decreased thereafter. Mass flux at 500m increased relatively in July and August 2011. Mass flux decreased between autumn 2011 and early spring 2012. Mass flux increased again in late March and April 2011. Mass flux at 4810 m was large in July and August 2011 and decreased toward winter. Mass flux also increased in April 2011 same as 500 m with time lag.

(Station S1) (Fig. 4b)

At 200 m, mass flux increased in August and decreased toward winter. Mass flux increased again in February 2012. Mass flux at 200 m was higher at S1 than K2 on average. Smaller fluxes in October 2011 and in April 2012 were observed. It might be attributed to decrease of trapping efficiency by tilt based on increase of water depth. Although seasonal variability was small, mass flux at 500 m and 4810 m were relatively higher in autumn and late winter (February and March) in 2012. Mass fluxes at these depth were smaller than those at station K2 unlike mass flux at 200 m.

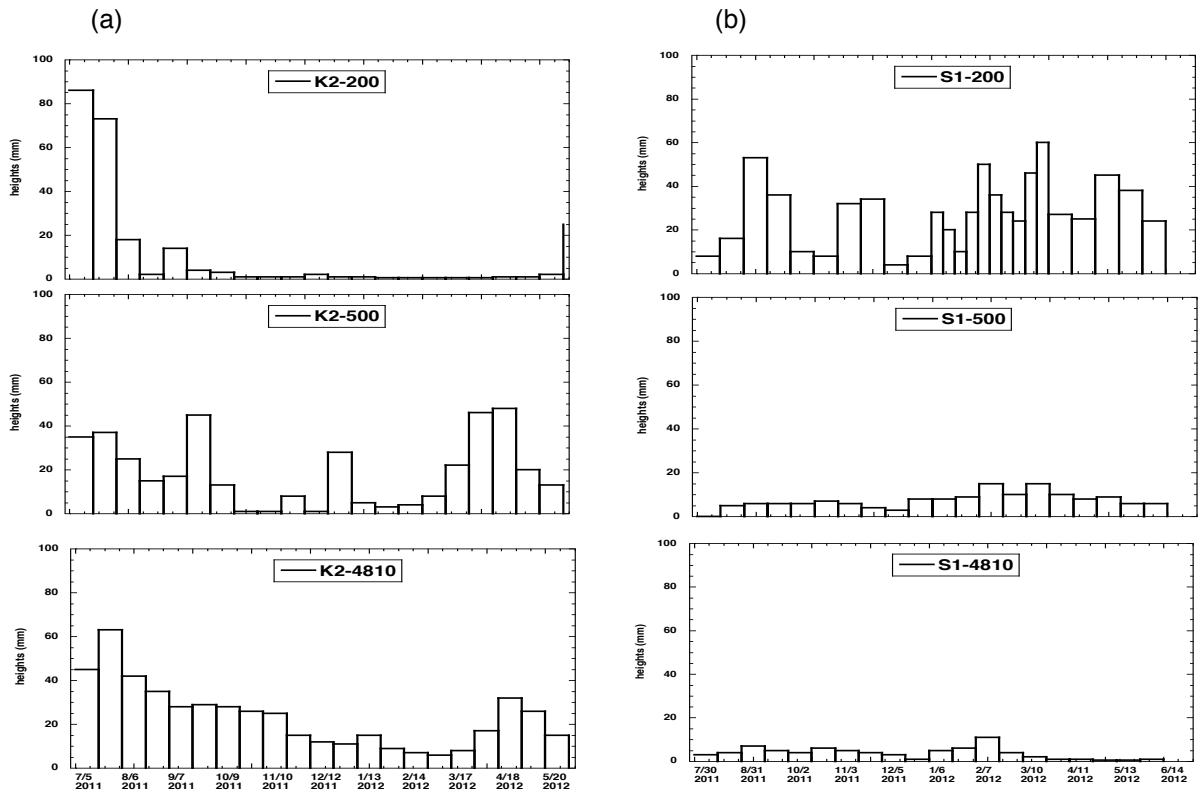


Fig. 4 Seasonal variability in sinking particle flux at (a) K2 and (b) S1. Vertical axis is height of collected materials in collecting cups.

2.2.2 Sediment trap experiment at station F1

Compared to settling particles at K2 and S1, larger materials were collected at station F1. Small increases of total mass flux at 200 m were observed in autumn 2011 and January 2012 (Fig. 5). Relatively larger flux was observed in April 2012. At 1000 m, two flux peaks were observed in September 2011 and January 2012 these increases synchronized well with shallower flux increases. Please note that several cups contained swimmer such as fish, shrimp and jellyfish. Based on vertical profile, high turbidity layer exist at around 600 m and 1000 m (Fig. 3.3.5 in the section “3.3 Sediment trap experiment at station F1”) and, therefore, horizontal supply of materials should be taken into account.

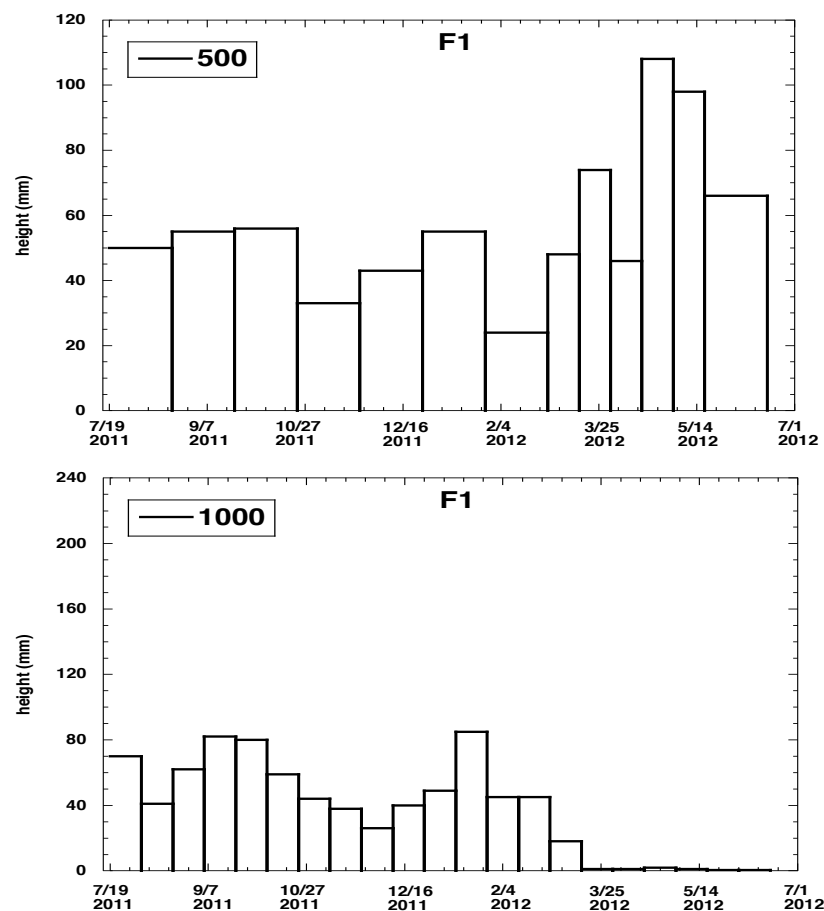


Fig. 5 Seasonal variability in total mass flux. Please note that size of collecting cup between 500 m and 1000 m are different (diameter of 500 ml cup has ca. two times higher than that of 1000 m cup).

B. Text

1. Outline of MR12-02

1.1 Cruise summary

(1) Introduction of principle science proposal

Change in material cycles and ecosystem by the climate change and its feedback

Some disturbing effects are progressively coming to the fore in the ocean by climate change, such as rising water temperature, intensification of upper ocean stratification and ocean acidification. It is supposed that these effects result in serious damage to the ocean ecosystems. Disturbed ocean ecosystems will change a material cycle through the change of biological pump efficiency, and it will be fed back into the climate. We are aimed at clarifying the mechanisms of changes in the ocean structure in ocean ecosystems derived from the climate change,

We arranged the time-series observation stations in the subarctic gyre (K2: 47°N 160°E) and the subtropical gyre (S1: 30°N, 145°E) in the western North Pacific. In general, biological pump is more efficient in the subarctic gyre than the subtropical gyre because large size phytoplankton (diatom) is abundant in the subarctic gyre by its eutrophic oceanic condition. It is suspected that the responses against climate change are different for respective gyres. To elucidate the oceanic structures in ocean ecosystems and material cycles at both gyres is important to understand the relationship between ecosystem, material cycle and climate change in the global ocean.

There are significant seasonal variations in the ocean environments in both gyres. The seasonal variability of oceanic structures will be estimated by the mooring systems and by the seasonally repetitive ship observations scheduled for next several years.

(2) Objective of this cruise

Principal objective of this cruise is to observe late spring or early summer ecosystem and biogeochemical cycle at time-series stations in the sub-arctic and sub-tropical gyres. In addition, we conducted biogeochemical observation off Fukushima in order to investigate dispersion of radionuclides from the Fukushima Daiichi nuclear power plant.

Beside this, we conducted the observation of physical and biogeochemical property of meso-scale warm eddy. Moreover, JKEO / NKEO and KEO surface buoys were recovered and / or deployed.

(3) Cruise summary (highlights)

(3-1) Time-series observation at stations K2 and S1

(1) Nutrients

Concentrations of nutrients were measured several times at each station. Concentration of NO_3 near surface at K2 was about $17 \mu\text{mol kg}^{-1}$. Compared to winter value ($\sim 30 \mu\text{mol kg}^{-1}$), NO_3 decreased, however did not become the annual minimum value. Concentration of Si(OH)_4 was about $30 \mu\text{mol kg}^{-1}$ and this concentration was comparable to medium value of annual variability. Concentration of NO_3 upper 50m at S1 was less than $0.1 \mu\text{mol kg}^{-1}$ and comparable to the annual minimum. However, it is notable that concentration of NO_3 at surface was higher (between 0.1 and $0.7 \mu\text{mol kg}^{-1}$). It is still on argument whether this is natural increase (eolian input?) or contamination by bucket used for sampling. Unlike NO_3 , concentration of Si(OH)_4 near surface at S1 was about $2 \mu\text{mol kg}^{-1}$ and comparable to winter value or the annual maximum. It might be supported by the fact that diatom which requires Si(OH)_4 was little at S1.

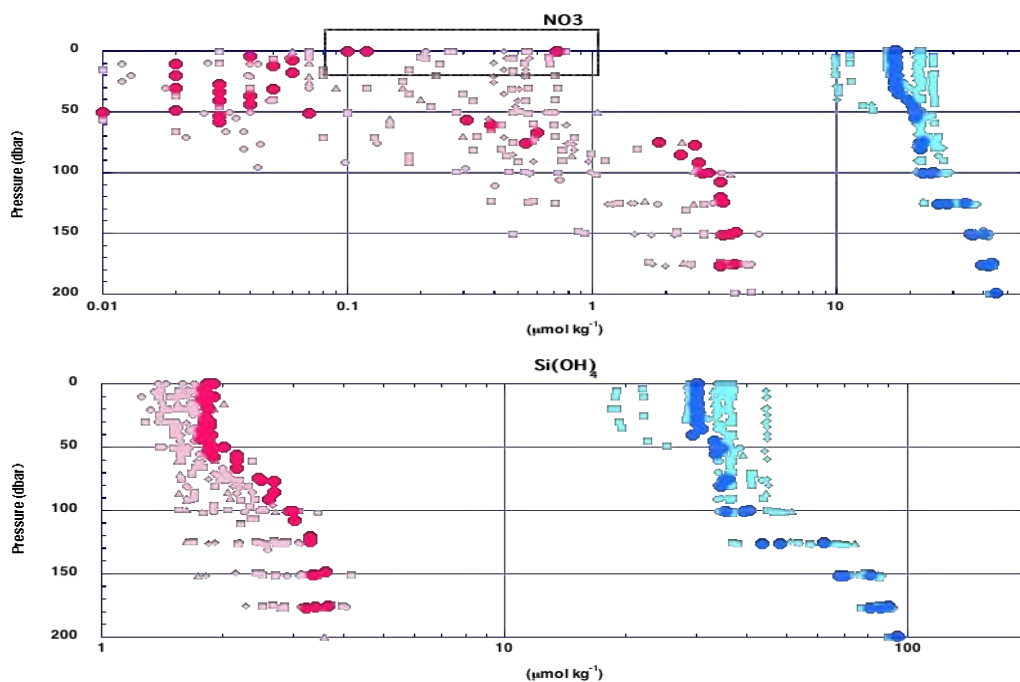


Fig. 1 Seasonal variability in nutrients: NO_3 (upper) and Si(OH)_4 (lower). Blue and red shows concentrations at K2 and S1, respectively and concentrations of dense color are data during this cruise.

(2) Pigments

Maximum chlorophyll-a (chl-a) at station K2 was about $1.2 \mu\text{g L}^{-1}$ observed at around 30 m water depth (Fig. 2a). Based on high-performance liquid chromatography (HPLC) analysis, diatom and *haptophyto* such as *coccolithophorids* were dominant species. At station S1, subsurface maximum of chl-a ($\sim 0.5 \mu\text{g L}^{-1}$) was observed at around 65 m. Dominant species of phytoplankton were *haptophyto* and *prochlorococcus* and diatom was not found. This result might support that dissolved Si(OH)_4 was not consumed largely at station S1.

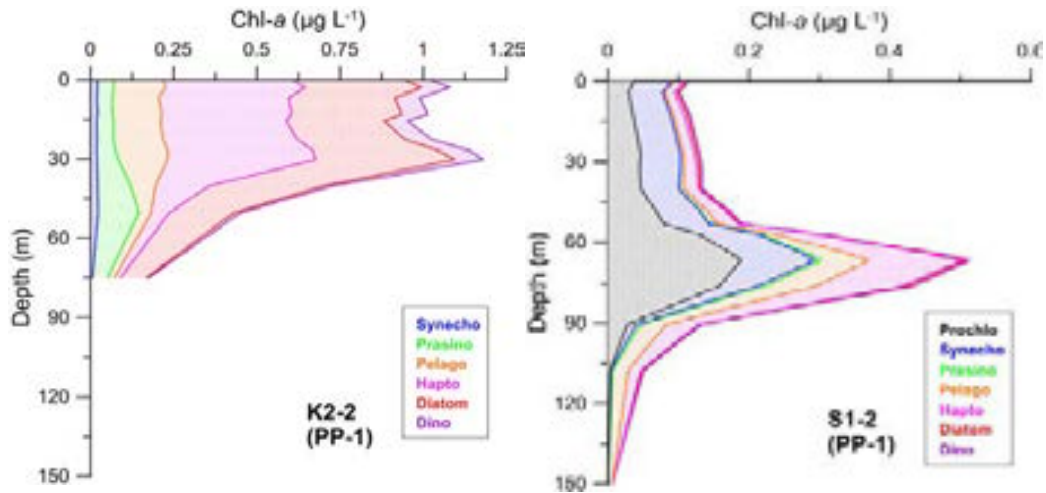


Fig. 2 Vertical profile of chlorophyll-a (chl-a) and contribution of chl-a of major major phytoplankton to total chl-a based on HPLC analysis.

(3) Primary productivity

Integrated primary productivity (PP) at station K2 ranged from approximately 400 to 600 $\text{mg-C m}^{-2} \text{day}^{-1}$ (Fig. 3a). Based on seasonal variability in PP observed previously, PP during this cruise was close to the annual maximum. On the other hand, PP at station S1 was approximately 200 $\text{mg-C m}^{-2} \text{day}^{-1}$. This PP coincided well with seasonal variability.

PP observed during this cruise and previously correlated well with photosynthetic available radiation (PAR) at station K2 (Fig. 3b). Thus it can be said that the major limiting factor of PP at station K2 is light condition.

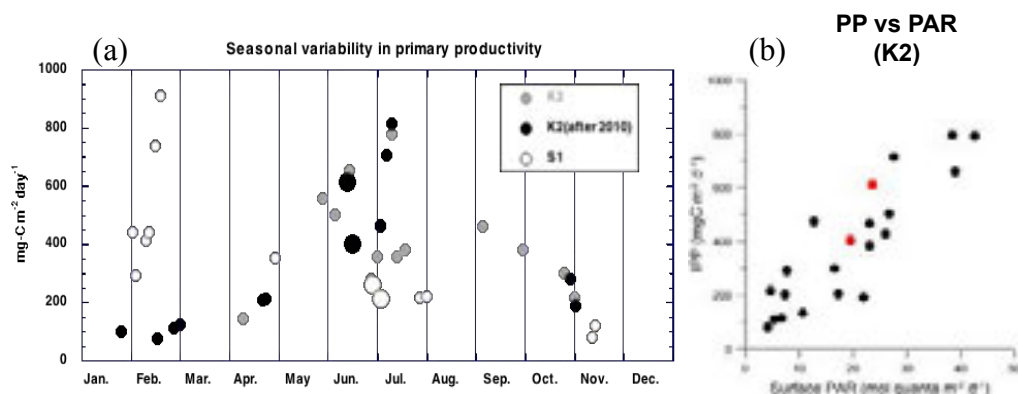


Fig. 3 (a) Seasonal variability in primary productivity (PP) at stations K2 (closed circles) and S1 (open circles). Larger circles are data obtained during this cruise. (b) relation between PP and photosynthetically available radiation (PAR) at station K2. Red circles show data obtained during this cruise

(4) Sinking particle

(Station K2) (Fig. 4a)

Based on height of sinking particle collected in collecting cups, mass flux at 200 m increased in July just after deployment. However mass flux decreased thereafter. Mass flux at 500m increased relatively in July and August 2011. Mass flux decreased between autumn 2011 and early spring 2012. Mass flux increased again in late March and April 2011. Mass flux at 4810 m was large in July and August 2011 and decreased toward winter. Mass flux also increased in April 2011 same as 500 m with time lag.

(Station S1) (Fig. 4b)

At 200 m, mass flux increased in August and decreased toward winter. Mass flux increased again in February 2012. Mass flux at 200 m was higher at S1 than K2 on average. Smaller fluxes in October 2011 and in April 2012 were observed. It might be attributed to decrease of trapping efficiency by tilt based on increase of water depth. Although seasonal variability was small, mass flux at 500 m and 4810 m were relatively higher in autumn and late winter (February and March) in 2012. Mass fluxes at these depth were smaller than those at station K2 unlike mass flux at 200 m.

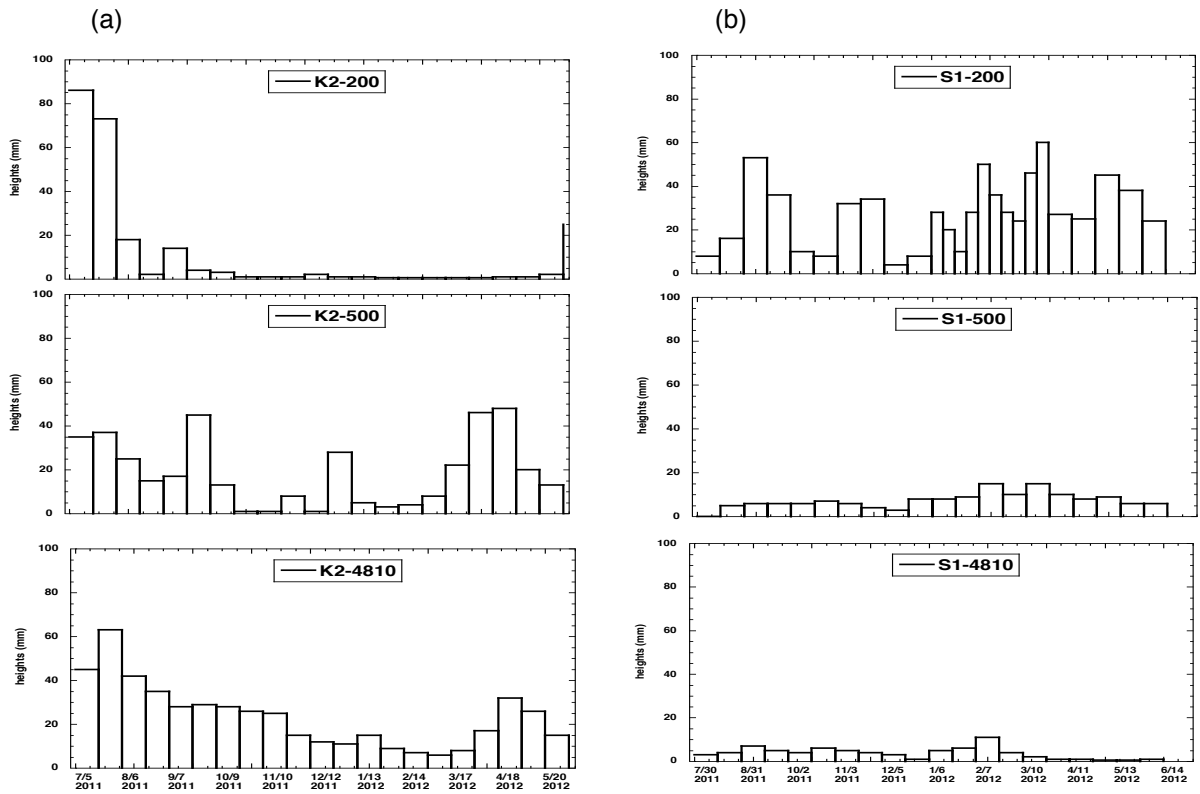


Fig. 4 Seasonal variability in sinking particle flux at (a) K2 and (b) S1. Vertical axis is height of collected materials in collecting cups.

(3-2) Sediment trap experiment at station F1

Compared to settling particles at K2 and S1, larger materials were collected at station F1. Small increases of total mass flux at 200 m were observed in autumn 2011 and January 2012 (Fig. 5). Relatively larger flux was observed in April 2012. At 1000 m, two flux peaks were observed in September 2011 and January 2012 these increases synchronized well with shallower flux increases. Please note that several cups contained swimmer such as fish, shrimp and jellyfish. Based on vertical profile, high turbidity layer exist at around 600 m and 1000 m (Fig. 3.3.5 in the section “3.3 Sediment trap experiment at station F1”) and, therefore, horizontal supply of materials should be taken into account.

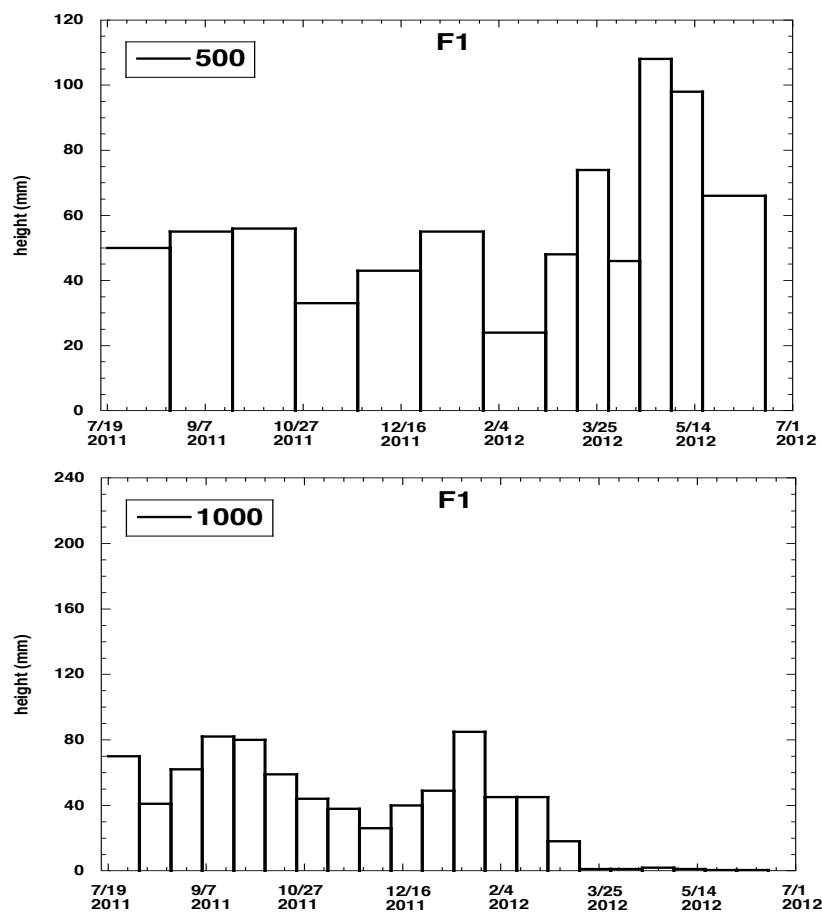


Fig. 5 Seasonal variability in total mass flux. Please note that size of collecting cup between 500 m and 1000 m are different (diameter of 500 ml cup has ca. two times higher than that of 1000 m cup).

(4) Scientific gears

All hydrocasts were conducted using 36-position 12 liter Niskin bottles carousel system with SBE CTD-DO system, fluorescence and transmission sensors. JAMSTEC scientists and MWJ (Marine Work Japan Co. Ltd.) technician group were responsible for analyzing water sample for salinity, dissolved oxygen, nutrients, CFCs, total carbon contents, alkalinity and pH. Cruise participants from JAMSTEC, Tokyo Institute of Technology, Rakuno Gakuen University, National Institute of Radiological Sciences, JAXA and University of Tokyo helped to divide seawater from Niskin bottles to sample bottles for analysis. Surface water was collected with bucket.

Optical measurement in air and underwater was conducted with PAR sensor (RAMSES-ACC) and PAR sensor on CTD, respectively.

For collecting suspended particles at station K2 and S1, Large Volume Pump (LVP) was deployed. For observing in situ particles, optical sensor called LISST (Laser In Situ Scattering and Transmissometer) and VPR (Visual Plankton recorder) were deployed by University of Tokyo and JAMSTEC, respectively.

GODI technicians group undertook responsibility for underway current direction and velocity measurements using an Acoustic Current Profiler (ADCP), geological measurements (topography, geo-magnetic field and gravity), and collecting meteorological data.

Radio zonde observation were conducted by GODI, JAMSTEC and JAXA.

For collection of zooplankton, NORPAC plankton net, and IONESS were deployed.

For conducting in situ incubation for measurement of primary productivity and collecting sinking particles at station K2, drifter was deployed at station K2 and S1. Sediment trap mooring system was also recovered and redeployed at station F1 for observation of radionuclides from the Fukushima Daiichi nuclear power plant.

For observing vertical profile of primary productivity optically, FRRF was deployed.

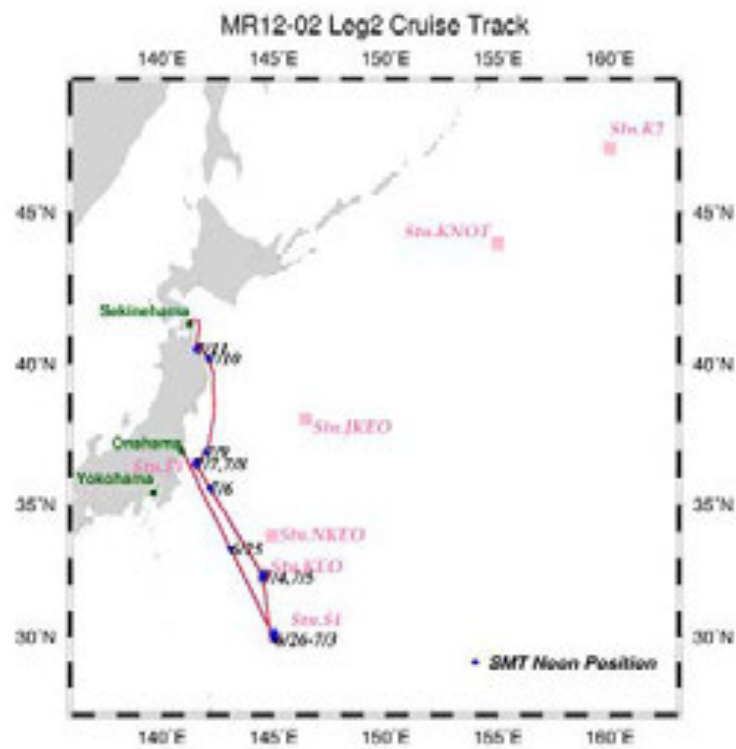
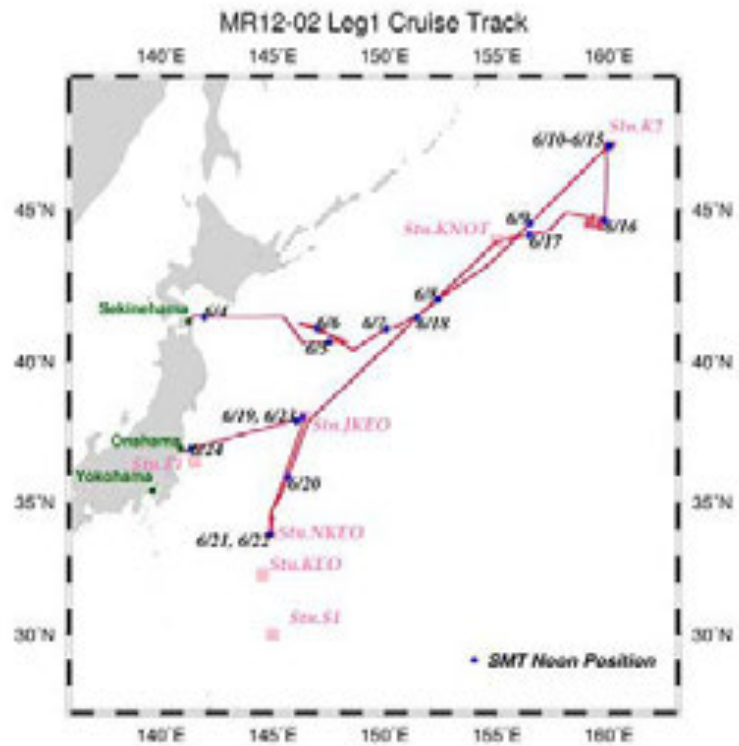
In order to conduct time-series observation in biogeochemical cycle, JAMSTEC Sediment trap mooring system and POPPS mooring system were recovered and re-deployed at station K2 and S1 (POPPS mooring only for S1).

For air-sea interaction observation, surface buoys were recovered and redeployed at stations JKEO and KEO by JAMSTEC and NOAA, respectively. Surface buoy was also deployed at station NKEO.

For observation of atmospheric chemistry (aerosol and gas), various instruments including “sky-radiometer” and ship-borne compact system for measuring atmospheric trace gas column densities were onboard and automatic measurement was conducted.

Please read text for more detail information and other instruments used for oceanographic and meteorological or atmospheric observation.

1.2 Track and log



MR12-02 Cruise log
(Leg.1)

U.T.C.		S.M.T.		Position		Event logs
Date	Time	Date	Time	Lat.	Lon.	
6.4	0:00	6.4	9:00	41-22N	141-14E	Departure from Sekinehama
	2:00		11:00	-	-	Sea surface water analysis start
	15:38	6.5	0:38	41-29.96N	145-30.03E	XCTD #01
	16:04		1:04	41-25.96N	145-34.11E	XCTD #02
	16:29		1:29	41-21.95N	145-38.14E	XCTD #03
	16:55		1:55	41-17.96N	145-42.17E	XCTD #04
	17:21		2:21	41-13.99N	145-46.13E	XCTD #05
	17:47		2:47	41-09.99N	145-50.25E	XCTD #06
	18:16		3:16	41-05.96N	145-54.36E	XCTD #07
	18:43		3:43	41-01.98N	145-58.32E	XCTD #08
	19:11		4:11	40-58.00N	146-02.29E	XCTD #09
	19:39		4:39	40-54.02N	146-06.32E	XCTD #10
	20:08		5:08	40-50.01N	146-10.40E	XCTD #11
	20:37		5:37	40-46.01N	146-14.45E	XCTD #12
	21:05		6:05	40-42.01N	146-18.38E	XCTD #13
	22:16		7:16	40-42.98N	146-27.04E	XCTD #14
	22:45		7:45	40-41.98N	146-33.69E	XCTD #15
	23:12		8:12	40-41.99N	146-40.29E	XCTD #16
	23:42		8:42	40-41.85N	146-47.20E	XCTD #17
6.5	0:12		9:12	40-40.78N	146-53.49E	XCTD #18
	0:43		9:43	40-42.21N	147-00.10E	XCTD #19
	1:13		10:13	40-42.18N	147-06.70E	XCTD #20
	1:42		10:42	40-41.94N	147-13.29E	XCTD #21
	2:11		11:11	40-41.99N	147-19.91E	XCTD #22
	2:40		11:40	40-41.99N	147-26.49E	XCTD #23
	3:09		12:09	40-41.95N	147-33.08E	XCTD #24
	3:37		12:37	40-41.92N	147-39.68E	XCTD #25
	4:06		13:06	40-41.86N	147-46.30E	XCTD #26
	4:35		13:35	40-41.80N	147-52.90E	XCTD #27
	5:02		14:02	40-41.78N	147-59.49E	XCTD #28
	5:30		14:30	40-41.75N	148-06.11E	XCTD #29
	6:01		15:01	40-41.90N	148-13.45E	XCTD #30
	6:26		15:26	40-41.97N	148-19.29E	XCTD #31
	9:40		18:40	40-56.11N	147-29.33E	CTD cast #01 (2000 m)
	11:41		20:41	40-56.45N	147-28.23E	ARGO Float #01
	11:42		20:42	40-56.48N	147-28.24E	ARGO Float #02
	18:55	6.6	3:55	41-18.00N	146-10.55E	CTD cast #02 (2000 m)
	20:50		5:50	41-18.30N	146-11.21E	ARGO Float #03
	22:31		7:31	41-14.16N	146-32.80E	CTD cast #03 (2000 m)
6.6	0:22		9:22	41-14.74N	146-33.42E	ARGO Float #04
	0:23		9:23	41-14.76N	146-33.46E	ARGO Float #05
	2:12		11:12	41-08.76N	146-58.82E	CTD cast #04 (2000 m)
	3:20		12:20	41-08.94N	146-58.76E	Radio sonde #01
	4:01		13:01	41-09.12N	146-58.75E	ARGO Float #06
	4:02		13:02	41-09.11N	146-58.78E	ARGO Float #07
	4:03		13:03	41-09.11N	146-58.79E	Surface drifting float buoy deployment #01

	4:03		13:03	41-09.11N	146-58.82E	Surface drifting float buoy deployment #02
	4:04		13:04	41-09.11N	146-58.83E	Surface drifting float buoy deployment #03
	5:11		14:11	41-05.90N	147-09.64E	CTD cast #05 (2000 m)
	7:07		16:07	41-06.32N	147-08.88E	ARGO Float #08
	7:08		16:08	41-06.30N	147-08.89E	ARGO Float #09
6.7	13:00	6.7	22:00	-	-	Time adjustment +1 hour (SMT=UTC+10h)
6.7	12:00	6.8	22:00	-	-	Time adjustment +1 hour (SMT=UTC+11h)
6.9	18:12	6.10	5:12	47-00N	160-00E	Arrival at Station K2
	21:00		8:00	47-00.34N	159-58.42E	BGC mooring recovery #1
6.10	0:50		11:50	47-00.38N	159-59.79E	Free fall optical measurements #01
	2:01		13:01	46-59.67N	159-59.88E	CTD cast #06 (5175 m)
	5:40		16:40	46-59.47N	159-59.67E	In-situ filtration #01 (200 m)
	8:00		19:00	49-59.51N	159-59.41E	Plankton net #01-1 (NORPAC: 20-0 m)
	8:08		19:08	49-59.49N	159-59.44E	Plankton net #01-2 (NORPAC: 50-20 m)
	8:18		19:18	46-59.47N	159-59.48E	Plankton net #01-2' (NORPAC: 50-20 m)
	8:28		19:28	46-59.44N	159-59.52E	Plankton net #01-3 (NORPAC: 100-50 m)
	8:41		19:41	46-59.42N	159-59.61E	Plankton net #01-4 (NORPAC: 150-100 m)
	8:55		19:55	46-59.39N	159-59.67E	Plankton net #01-5 (NORPAC: 200-150 m)
	8:10		19:10	46-59.37N	159-59.75E	Plankton net #01-6 (NORPAC: 300-200 m)
	9:34		20:34	46-59.30N	159-59.81E	Plankton net #02-1 (NORPAC: 50-0 m)
	9:45		20:45	46-59.27N	159-59.87E	Plankton net #02-2 (NORPAC: 150-0 m)
	9:58		20:58	46-59.25N	159-59.92E	Plankton net #02-3 (NORPAC: 150-0 m)
	10:04		21:04	46-59.23N	159-59.96E	Plankton net #02-4 (NORPAC: 50-0 m)
	15:30	6.11	2:30	46-59.62N	160-00.27E	CTD cast #07 (300 m)
	16:35		3:35	46-59.26N	160-00.33E	FRRF #01 (100 m)
	19:03		6:03	46-59.99N	160-10.60E	Drifting sediment trap buoy deployment #01 (200 m)
	20:55		7:55	46-59.94N	160-00.17E	FRRF #02 (100 m)
	21:53		8:53	46-59.97N	160-00.01E	CTD cast #08 (800 m)
	23:52		10:52	47-00.09N	160-00.01E	CTD cast #09 (500 m)
6.11	0:39		11:39	46-59.85N	160-00.12E	Free fall optical measurements #02 (200 m)
	1:12		12:12	46-59.47N	160-00.46E	FRRF #03 (100 m)
	1:59		12:59	46-59.79N	160-00.06E	CTD cast #10 (4000 m)
	7:54		18:54	46-59.91N	160-00.11E	FRRF #04 (100 m)
	13:00					
	16:57	6.12	3:57	47-00.05N	160-00.31E	CTD cast #11 (4903 m)
6.12	0:00		11:00	46-59.81N	159-59.79E	IONESS #01 (1000 m)
	3:09		14:09	47-03.17N	160-06.19E	CTD cast #12 (5210 m)
	7:33		18:33	47-00.75N	160-00.76E	Plankton net #03-1 (NORPAC: 500-300 m)
	8:05		19:05	47-00.91N	160-00.67E	Plankton net #03-2 (NORPAC: 700-500 m)
	8:50		19:50	47-00.99N	160-00.65E	Plankton net #03-3 (NORPAC: 1000-700 m)
	10:56		21:56	46-58.59N	159-59.32E	IONESS #02 (1000 m)
	19:03	6.13	6:03	47-00.70N	159-49.30E	Multipul corer #01
	23:24		10:24	46-56.02N	159-59.67E	Free fall optical measurements #03 (200 m)
6.13	0:09		11:09	46-56.52N	159-59.87E	IONESS #03 (1000 m)
	2:30		13:30	47-01.18N	160-00.28E	Radio sonde #02
	3:56		14:56	47-00.01N	160-00.00E	In-situ filtration #02 (4000 m)
	9:30		20:30	47-00.01N	160-00.00E	Radio sonde #03
	13:30	6.14	0:30	47-03.52N	160-12.22E	Radio sonde #04
	15:28		2:28	47-03.56N	160-17.65E	CTD cast #13 (300 m)
	16:18		3:18	47-03.76N	160-17.23E	FRRF #05 (100 m)

	18:59		5:59	47-05.95N	160-18.42E	Drifting sediment trap buoy recovery #01 (200 m)
	20:55		7:55	47-01.01N	160-03.18E	FRRF #06 (100 m)
	21:22		8:22	47-00.99N	160-03.03E	CTD cast #14 (300 m)
	22:27		9:27	47-01.02N	160-02.74E	Plankton net #04-1 (NORPAC: 20-0 m)
	22:33		9:33	47-01.03N	160-02.70E	Plankton net #04-2 (NORPAC: 50-20 m)
	22:42		9:42	47-01.07N	160-02.67E	Plankton net #04-3 (NORPAC: 100-50 m)
	22:52		9:52	47-01.07N	160-02.64E	Plankton net #04-4 (NORPAC: 150-100 m)
	23:04		10:04	47-01.10N	160-02.61E	Plankton net #04-5 (NORPAC: 200-150 m)
	23:19		10:19	47-01.13N	160-02.58E	Plankton net #04-6 (NORPAC: 300-200 m)
6.14	0:23		11:23	47-00.08N	160-00.63E	Free fall optical measurements #04 (200 m)
	0:51		11:51	46-59.86N	160-50.40E	FRRF #07 (100 m)
	1:54		12:54	47-00.01N	159-59.99E	In-situ filtration #03 (100 m)
	5:38		16:38	46-59.89N	159-59.37E	Eight-figure trace for calibration of Magnetometer #01
	7:51		18:51	47-00.26N	159-59.55E	FRRF #08 (100 m)
	10:57		21:57	46-58.86N	160-00.71E	IONESS #04 (1000 m)
	17:56	6.15	4:56	47-00.16N	160-00.95E	CTD cast #15 (2000 m)
	21:08		8:08	46-55.49N	159-59.69E	BGC mooring deployment
6.15	0:40		11:40	47-00.40N	159-58.22E	BGC mooring fixed position (5222m)
	2:51		13:51	46-58.08N	159-57.86E	In-situ filtration #04 (300 m)
	10:55		21:55	46^56.12N	159-56.75E	IONESS #05 (200 m)
	13:04	6.16	0:04	47-00N	160-00E	Departure from Station K2
	13:52		0:52	46-52.85N	159-53.58E	Cesium magnetometer towing start #01
6.16	0:30		11:30	44-46.02N	159-50.23E	XCTD #32
	0:50		11:50	44-23.70N	159-36.12E	Site survey start (Station K2- KNOT : MBES)
	2:30		13:30	44-23.55N	159-40.60E	Radio sonde #05
	11:00		22:00	-	-	Time adjustment -1 hours (SMT=UTC+10h)
	13:30		23:30	44-40.76N	159-01.61E	Radio sonde #06
	13:34		23:34	44-41.76N	159-02.15E	XCTD #33
6.17	5:00	6.17	15:00	44-03.36N	155-24.57E	Cesium magnetometer towing finish #01
	6:48		16:48	44-00N	155-00E	Arrival at Station KNOT
						Cesium magnetometer towing finish #01
	6:50		16:50	44-00.04N	154-59.96E	Site survey finish (Station K2- KNOT : MBES)
	10:36		20:36	44-00N	155-00E	CTD cast #16 (5295 m)
						Departure from Station KNOT
6.18	12:00	6.18	22:00	-	-	Time adjustment -1 hours (SMT=UTC+9h)
6.19	0:30	6.19	9:30	38-05N	146-25E	Arrival at Station JKEO
	4:00		13:00	37-55.49N	146-34.20E	K-TRITON mooring deployment
	8:41		17:41	37-54.07N	146-36.54E	K-TRITON mooring fixed position (5380m)
	9:43		18:43	37-56.32N	146-35.93E	CTD cast #17 (5366 m)
	13:33		22:33	37-56.87N	146-34.71E	Radio sonde #07
	13:36		22:36	38-05N	146-25E	Departure from Station JKEO
	15:00	6.20	0:00	37-41.20N	146-29.24E	Radio sonde #08
	16:30		1:30	37-24.71N	146-20.56E	Radio sonde #09
	18:00		3:00	37-07.92N	146-13.37E	Radio sonde #10
	19:30		4:30	36-52.01N		Radio sonde #11
6.20	14:00		23:00	34-25.74N	145-01.55E	Site survey start (Station NKEO : MBES)
	18:30	6.21	3:30	33-49.87N	144-54.07E	Site survey finish (Station NKEO : MBES)
	18:42		3:42	33-51N	144-55E	Arrival at Station NKEO
	22:57		7:57	33-50.43N	144-54.14E	CTD cast #18 (5733 m)

6.21	14:30		23:30	33-50.08N	144-53.09E	Radio sonde #12
	23:13	6.22	8:13	33-54.42N	144-55.94E	K-TRITON mooring deployment
6.22	4:04		13:04	33-50.70N	144-54.14E	K-TRITON mooring fixed position (5746m)
	4:30		13:30	33-51N	144-55E	Departure from Station NKEO
	23:24	6.23	8:24	38-05N	146-25E	Arrival at Station JKEO
	23:28		8:28	38-05.06N	146-26.87E	K-TRITON mooring recovery
6.23	3:00		12:00	38-05.18N	146-19.72E	Radio sonde #13
	5:18		14:18	38-05N	146-25E	Departure from Station JKEO
6.24	6:30	6.24	15:30	36-53.5N	140-53.8E	Arrival at off Onahama

(Leg.2)

U.T.C.		S.M.T.		Position		Event logs
Date	Time	Date	Time	Lat.	Lon.	
6.24	8:00	6.24	17:00	36-53.5N	140-53.8E	Departure from off Onahama
	14:30		23:30	35-42.85N	141-38.13E	Radio sonde #14
6.25	21:36	6.26	6:36	30-00N	145-00E	Arrival at Station S1
	22:57		7:57	30-03.93N	144-58.03E	BGC mooring recovery #2
6.26	3:00		12:00	30-03.27N	144-58.91E	Radio sonde #15
	3:58		12:58	30-00.23N	144-59.63E	CTD cast #19 (5950 m)
	8:24		17:24	30-00.22N	144-59.93E	In-situ filtration #05 (200 m)
	10:23		19:23	30-00.08N	145-00.03E	Plankton net #05-1 (NORPAC: 20-0 m)
	10:32		19:32	30-00.02N	145-00.11E	Plankton net #05-1' (NORPAC: 20-0 m)
	10:40		19:40	29-59.94N	145-00.19E	Plankton net #05-2 (NORPAC: 50-20 m)
	10:56		19:56	29-59.75N	145-00.39E	Plankton net #05-3 (NORPAC: 100-50 m)
	11:07		20:07	29-59.65N	145-00.49E	Plankton net #05-4 (NORPAC: 150-100 m)
	11:17		20:17	29-59.53N	145-00.61E	Plankton net #05-5 (NORPAC: 150-200 m)
	11:29		20:29	29-59.40N	145-00.70E	Plankton net #05-6 (NORPAC: 200-150 m)
	11:43		20:43	29-59.25N	145-00.81E	Plankton net #05-7 (NORPAC: 300-200 m)
	12:00		21:00	29-59.10N	145-00.92E	Plankton net #05-8 (NORPAC: 300-200 m)
	12:18		21:18	29-58.99N	145-00.97E	Plankton net #06-1 (NORPAC: 50-0 m)
	12:25		21:25	28-58.84N	145-01.04E	Plankton net #06-2 (NORPAC: 150-0 m)
	22:58	6.27	7:58	29-55.57N	144-59.56E	POPPS mooring recovery
6.27	2:32		11:32	29-56.17N	144-59.10E	Free fall optical measurements #05 (200 m)
	4:23		13:23	30-00.12N	145-00.12E	In-situ filtration #06 (1000 m)
	11:47		20:47	29-59.75N	145-00.62E	Plankton net #07-1 (NORPAC: 50-0 m)
	11:51		20:51	29-59.64N	145-00.72E	Plankton net #07-2 (NORPAC: 150-0 m)
	14:30		23:30	29-59.74N	145-00.33E	Radio sonde #16
	17:30	6.28	2:30	29-59.77N	144-59.80E	CTD cast #20 (300 m)
	18:33		3:33	29-59.25N	144-59.26E	FRRF #09 (200 m)
	20:50		5:50	30-07.59N	145-00.11E	Drifting sediment trap buoy deployment #02 (200 m)
	22:50		7:50	30-01.70N	144-59.35E	FRRF #10 (200 m)
	23:34		8:34	30-01.49N	144-59.30E	CTD cast #21 (300 m)
6.28	0:57		9:57	30-01.14N	144-58.95E	CTD cast #22 (800 m)
	2:28		11:28	30-00.62N	144-59.05E	Free fall optical measurements #06 (200 m)
	2:57		11:57	30-00.18N	144-59.01E	FRRF #11 (200 m)

	3:57		12:57	29-59.92N	144-59.43E	CTD cast #23 (5943 m)
	7:57		16:57	29-59.53N	144-59.58E	FRRF #12 (200 m)
	9:20		18:20	29-59.15N	144-59.78E	pCO ₂ (partial pressure of carbon dioxide sensor) #01 (300m)
	12:02		21:02	29-57.04N	145-01.18E	IONESS #06 (200 m)
	23:00	6.29	8:00	29-58.72N	145-00.09E	Plankton net #08-1 (NORPAC: 1000-700 m)
	23:49		8:49	29-58.62N	145-00.30E	Plankton net #08-2 (NORPAC: 700-500 m)
6.29	0:25		9:25	29-58.53N	145-00.54E	Plankton net #08-3 (NORPAC: 500-300 m)
	1:24		10:24	30-01.28N	145-00.86E	IONESS #07 (200 m)
	3:00		12:00	29-58.36N	144-59.68E	Radio sonde #17
	5:30		14:30	29-58.53N	144-59.69E	In-situ filtration #07 (4000 m)
	20:58	6.30	5:58	30-12.01N	145-05.94E	Multipul corer #02
6.30	0:48		9:48	30-10.60N	145-05.72E	Free fall optical measurements #07 (200 m)
	1:31		10:31	30-09.77N	145-05.46E	IONESS #08 (1000 m)
	5:30		14:30	30-04.43N	144-59.42E	In-situ filtration #08 (150 m)
	8:28		17:28	30-04.14N	144-58.85E	Plankton net #09-1 (NORPAC: 50-0 m)
	8:35		17:35	30-04.09N	144-58.84E	Plankton net #09-2 (NORPAC: 100-50 m)
	8:46		17:46	30-04.03N	144-58.84E	Plankton net #09-3 (NORPAC: 200-100 m)
	9:05		18:05	30-03.92N	144-59.88E	Plankton net #09-4 (NORPAC: 200-0 m)
	9:20		18:20	30-03.84N	144-58.89E	Plankton net #09-5 (NORPAC: 200-0 m)
	9:35		18:35	30-03.78N	144-58.91E	Plankton net #09-6 (NORPAC: 200-0 m)
	9:51		18:51	30-03.72N	144-58.92E	Plankton net #09-7 (NORPAC: 200-0 m)
	10:20		19:20	30-02.76N	144-58.77E	Eight-figure trace for calibration of Magnetometer #02
	14:30		23:30	29-57.83N	144-59.64E	Radio sonde #18
	17:31	7.1	2:31	29-49.94N	145-14.24E	CTD cast #24 (300 m)
	18:32		3:32	29-49.59N	145-14.69E	FRRF #13 (200 m)
	20:45		5:45	29-49.59N	145-13.48E	Drifting sediment trap buoy recovery #02 (200 m)
	22:50		7:50	29-55.61N	145-05.55E	FRRF #14 (200 m)
	23:32		8:32	29-55.40N	145-05.74E	CTD cast #25 (500 m)
7.1	2:29		11:29	29-53.86N	145-04.40E	Free fall optical measurements #08 (200 m)
	3:02		12:02	29-53.69N	145-04.34E	FRRF #15 (200 m)
	4:00		13:00	29-52.97N	145-02.37E	POPPS mooring deployment
	7:26		16:26	29-56.47N	144-57.99E	FRRF #16 (200 m)
	8:05		17:05	29-56.38N	144-58.47E	POPPS mooring fixed position
	8:37		17:37	29-55.34N	144-59.30E	pCO ₂ #02 (300m)
	11:58		20:58	30-04.04N	144-57.73E	IONESS #09 (1000 m)
	20:30	7.2	5:30	30-03.21N	144-58.33E	CTD cast #26 (2000 m)
	23:13		8:13	30-06.62N	145-03.43E	BGC mooring deployment
7.2	3:00		12:00	30-04.48N	144-58.35E	BGC mooring fixed position
	3:20		12:20	30-03.93N	144-58.21E	Radio sonde #19
	3:58		12:58	30-02.77N	144-59.01E	CTD cast #27 (4000 m)
	7:56		16:56	30-01.98N	144-59.55E	CTD cast #28 (2000 m)
	11:57		20:57	30-06.44N	144-56.01E	IONESS #10 (1000 m)
	15:04	7.3	0:04	30-04.41N	144-50.19E	ARGO Float #10
	15:06		0:06	30-00N	145-00E	Departure from Station S1
7.3	3:00		12:00	32-19N	144-32E	Arrival at Station KEO
	3:59		12:59	32-19.06N	144-27.75E	CTD cast #29 (5743 m)
	6:00		15:00	32-19.00N	144-27.67E	Radio sonde #20
	8:54		17:54	32-14.50N	144-29.00E	Site survey start (Station KEO: MBES)
	14:30		23:30	32-30.66N	144-43.26E	Radio sonde #21
	23:19	7.4	8:19	32-30.53N	144-37.95E	NOAA mooring deployment

7.4	4:06		13:06	32-24.08N	144-29.59E	CTD cast #30 (597 m)
	5:21		14:21	32-24.94N	144-29.85E	NOAA mooring fixed position
	7:37		16:37	32-25.32N	144-30.89E	Test of releaser for F1 mooring
	8:00		17:00	32-25.28N	144-30.86E	Radio sonde #22
	10:01		19:01	32-24.73N	144-35.96E	Radio sonde #23
	12:01		21:01	32-24.27N	144-37.50E	Radio sonde #24
	14:00		23:00	32-22.83N	144-36.91E	Radio sonde #25
	16:00	7.5	1:00	32-23.45N	144-37.14E	Radio sonde #26
	18:00		3:00	32-24.51N	144-36.56E	Radio sonde #27
	20:00		5:00	32-22.09N	144-31.31E	Radio sonde #28
	21:03		6:03	32-20.31N	144-29.01E	NOAA mooring recovery
7.5	3:00		12:00	32-18.95N	144-31.90E	Radio sonde #29
	7:42		16:42	32-19N	144-32E	Departure from Station KEO
	10:00		19:00	32-42.98N	144-15.68E	Radio sonde #30
	12:00		21:00	33-03.32N	144-00.02E	Radio sonde #31
	14:00		23:00	33-22.76N	143-46.70E	Radio sonde #32
	16:00	7.6	1:00	33-41.32N	143-33.90E	Radio sonde #33
	18:00		3:00	34-00.06N	143-18.91E	Radio sonde #34
	20:00		5:00	34-20.26N	143-05.28E	Radio sonde #35
7.6	8:12		17:12	36-29N	141-30E	Arrival at Station F1
	8:56		17:56	36-29.22N	141-30.09E	In-situ filtration #09 (100 m)
	22:48	7.7	7:48	36-27.72N	141-27.24E	WHOI mooring recovery
7.7	1:30		10:30	36-29.83N	141-30.67E	CTD cast #31 (1270 m)
	8:00		17:00	36-28.71N	141-27.95E	Radio sonde #36
	11:59		20:59	36-28.60N	141-29.81E	IONESS #11 (200 m)
	23:14	7.8	8:14	36-28.95N	141-30.12E	Multipul corer #03
7.8	3:58		12:58	36-29.16N	141-30.06E	pCO2 #03 (300m)
	7:00		16:00	36-30.03N	141-31.08E	Eight-figure trace for calibration of Magnetometer #03
	20:57	7.9	5:57	36-29.09N	141-29.94E	WHOI mooring deployment
	22:28		7:28	36-28.53N	141-28.56E	WHOI mooring fixed position
	23:12		8:12	36-29N	141-30E	Departure from Station F1
7.9	3:31		12:31	36-57.33N	142-01.97E	Radio sonde #36
	14:30	23:30	38-29.61N	142-18.84E	Radio sonde #37	
7.10	6:00	7.10	15:00	-	-	Sea surface water analysis finish
7.11	0:30	7.11	9:30	40-31.8N	141-32.58E	Arrival at Hachinohe
	8:30		17:30	40-31.8N	141-32.58E	Departure from Hachinohe
7.12	0:10	7.12	9:10	41-22N	141-14E	Arrival at Sekinehama

1.3 Cruise participants

Name	Leg.1	Leg.2	Affiliation	Appointment
Makio HONDA (Principal Investigator)	○	○	Japan Agency for Marine-Earth Science and Technology (JAMSTEC) Research Institute for Global Change (RIGC)	Team leader
Kazuhiko MATSUMOTO (Deputy PI)	○	○	JAMSTEC, RIGC	Research scientist
Minoru KITAMURA	○	○	JAMSTEC, Institute of Biogeoscience (BIOGEOS)	Research scientist
Hajime KAWAKAMI	○	○	JAMSTEC, Mutsu Institute of Oceanigraphy (MIO)	Research scientist
Masahide WAKITA	○	○	JAMSTEC, MIO	Research scientist
Tetsuichi FUJIKI	○		JAMSTEC, RIGC	Scientist
Kosei SASAOKA	○	○	JAMSTEC, RIGC	Technical support staff
Katsunori KIMOTO	○	○	JAMSTEC, RIGC	Research scientist
Miyako SATO	○		JAMSTEC, RIGC	Technical support staff
Yuriko NAKAMURA		○	JAMSTEC, RIGC	Technical support staff
Hiroshi UCHIDA	○		JAMSTEC, RIGC	Research scientist
Shigeki HOSODA	○		JAMSTEC, RIGC	Deputy Team leader
Akira NAGANO	○		JAMSTEC, RIGC	Scientist
Kyoko TANIGUCHI	○	○	JAMSTEC, RIGC	Technical support staff
Yoshihisa MINO	○	○	Nagoya University (Additional post: RIGC, JAMSTEC)	Assistant professor
Tetsuya NAKAMURA		○	Nichiyu Giken Kogyo	Engineer
Yasuhiro NAGASAWA	○		JFE Advantech	Engineer
Steven J. MANGANINI		○	Woods Hole Oceanographic Institution	Research Specialist
Keith RONNHOLM		○	University of Washington	Research Scientist
David ZIMMERMAN		○	University of Washington	Research Engineer Technician
Koji HAMASAKI	○		University of Tokyo	Associate professor
Yusuke INOUE		○	University of Tokyo	Postdoctoral researcher

Jun SUGASAWA	○	○	WDB inc.	Engineer
Ryo KANEKO	○	○	University of Tokyo	Postdoctoral researcher
Makoto ONODA	○		National Institute of Radiological Sciences	Scientist
Mario UCHIMIYA	○	○	National Institute of Polar Research	Postdoctoral researcher
Hiroshi OHYAMA	○		Japan Aerospace Exploration Agency (JAXA)	Scientist
Yoshiyuki NAKANO		○	JAMSTEC, Marine Technology Center (MARITEC)	Research scientist
Yuki OKAZAKI	○	○	Rakuno Gakuen University	Graduate student
Sebastian O. DANIELACHE	○	○	Tokyo Institute of Technology	Postdoctoral researcher
Fuyuki SHIBATA (Principal Marine Tech.)	○	○	Marine Works Japan Inc.	Marine Technician
Hirokatsu UNO	○		Same as above	Same as above
Masaki TAGUCHI		○	Same as above	Same as above
Toru IDAI	○	○	Same as above	Same as above
Kenichi KATAYAMA	○	○	Same as above	Same as above
Naoko MIYAMOTO	○	○	Same as above	Same as above
Tomoyuki TAKAMORI	○	○	Same as above	Same as above
Tatsuya TANAKA	○	○	Same as above	Same as above
Shinsuke TOYODA	○	○	Same as above	Same as above
Masanori ENOKI	○	○	Same as above	Same as above
Shin TAKADA	○	○	Same as above	Same as above
Tomonori WATAI	○	○	Same as above	Same as above
Elena HAYASHI	○	○	Same as above	Same as above
Emi DEGUCHI	○	○	Same as above	Same as above
Hideki YAMAMOTO	○	○	Same as above	Same as above
Miyo IKEDA	○	○	Same as above	Same as above

Hiroyasu SATO	○	○	Same as above	Same as above
Masahiro ORUI	○	○	Same as above	Same as above
Kanako YOSHIDA	○	○	Same as above	Same as above
Keitaro MATSUMOTO	○	○	Same as above	Same as above
Sayaka KAWAMURA	○		Same as above	Same as above
Yasushi HASHIMOTO		○	Same as above	Same as above
Katsuhisa MAENO (Principal Marine Tech.)		○	Global Ocean Development Inc. (GODI)	Marine Technician
Harumi OHTA	○		Same as above	Same as above
Toshimitsu GOTO	○	○	Same as above	Same as above

2. General observation

2.1. Meteorological observations

2.1.1. Surface Meteorological Observation

Makio HONDA	(JAMSTEC): Principal Investigator	
Katsuhisa MAENO	(Global Ocean Development Inc., GODI)	- leg2 -
Harumi OTA	(GODI)	- leg1-
Toshimitsu GOTO	(GODI)	- leg1, 2-
Ryo KIMURA	(Mirai Crew)	- leg1, 2-

(1) Objectives

Surface meteorological parameters are observed as a basic dataset of the meteorology. These parameters bring us the information about the temporal variation of the meteorological condition surrounding the ship.

(2) Methods

Surface meteorological parameters were observed throughout the MR12-02 cruise. During this cruise, we used three systems for the observation.

- i. MIRAI Surface Meteorological observation (SMet) system
- ii. Shipboard Oceanographic and Atmospheric Radiation (SOAR) system

i. MIRAI Surface Meteorological observation (SMet) system

Instruments of SMet system are listed in Table.2.1.1-1 and measured parameters are listed in Table.2.1.1-2. Data were collected and processed by KOAC-7800 weather data processor made by Koshin-Denki, Japan. The data set consists of 6-second averaged data.

ii. Shipboard Oceanographic and Atmospheric Radiation (SOAR) measurement system

SOAR system designed by BNL (Brookhaven National Laboratory, USA) consists of major three parts.

- a) Portable Radiation Package (PRP) designed by BNL – short and long wave downward radiation.
- b) Zeno Meteorological (Zeno/Met) system designed by BNL – wind, air temperature, relative humidity, pressure, and rainfall measurement.
- c) Scientific Computer System (SCS) developed by NOAA (National Oceanic and Atmospheric Administration, USA) – centralized data acquisition and logging of all data sets.

SCS recorded PRP data every 6 seconds, while Zeno/Met data every 10 seconds. Instruments and their locations are listed in Table.2.1.1-3 and measured parameters are listed in Table.2.1.1-4.

For the quality control as post processing, we checked the following sensors, before and after the cruise.

- i. Young Rain gauge (SMet and SOAR)

Inspect of the linearity of output value from the rain gauge sensor to change Input value by adding fixed quantity of test water.

ii. Barometer (SMet and SOAR)

Comparison with the portable barometer value, PTB220CASE, VAISALA.

iii. Thermometer (air temperature and relative humidity) (SMet and SOAR)

Comparison with the portable thermometer value, HMP41/45, VAISALA.

(3) Preliminary results

Figure 2.1.1-1 shows the time series of the following parameters;

Wind (SMet)

Air temperature (SMet)

Relative humidity (SMet)

Precipitation (SOAR, rain gauge)

Short/long wave radiation (SOAR)

Pressure (SMet)

Sea surface temperature (SMet)

Significant wave height (SMet)

(4) Data archives

These meteorological data will be submitted to the Data Management Group (DMG) of JAMSTEC just after the cruise.

(5) Remarks

i. SST (Sea Surface Temperature) data were available in the following periods.

02:04UTC 04 Jun. - 14:55UTC 10 Jul.

ii. SMet Young rain gauge includes invalid data at the following time due to MF/HF transmit.

04:32UTC 11 Jun.

Table.2.1.1-1 Instruments and installations of MIRAI Surface Meteorological observation system

Sensors	Type	Manufacturer	Location (altitude from surface)
Anemometer	KE-500	Koshin Denki, Japan	foremast (24 m)
Tair/RH with 43408 Gill aspirated radiation shield	HMP45A	Vaisala, Finland R.M. Young, USA	compass deck (21 m) starboard side and port side
Thermometer: SST	RFN1-0	Koshin Denki, Japan	4th deck (-1m, inlet -5m)
Barometer	Model-370	Setra System, USA	captain deck (13 m) weather observation room
Rain gauge	50202	R. M. Young, USA	compass deck (19 m)
Optical rain gauge	ORG-815DR	Osi, USA	compass deck (19 m)
Radiometer (short wave)	MS-801	Eiko Seiki, Japan	radar mast (28 m)
Radiometer (long wave)	MS-200	Eiko Seiki, Japan	radar mast (28 m)
Wave height meter	MW-2	Tsurumi-seiki, Japan	bow (10 m)

Table.2.1.1-2 Parameters of MIRAI Surface Meteorological observation system

Parameter	Units	Remarks
1 Latitude	degree	
2 Longitude	degree	
3 Ship's speed	knot	Mirai log, DS-30 Furuno
4 Ship's heading	degree	Mirai gyro, TG-6000, Tokimec
5 Relative wind speed	m/s	6sec./10min. averaged
6 Relative wind direction	degree	6sec./10min. averaged
7 True wind speed	m/s	6sec./10min. averaged
8 True wind direction	degree	6sec./10min. averaged
9 Barometric pressure	hPa	adjusted to sea surface level 6sec. averaged
10 Air temperature (starboard side)	degC	6sec. averaged
11 Air temperature (port side)	degC	6sec. averaged
12 Dewpoint temperature (starboard side)	degC	6sec. averaged
13 Dewpoint temperature (port side)	degC	6sec. averaged
14 Relative humidity (starboard side)	%	6sec. averaged
15 Relative humidity (port side)	%	6sec. averaged
16 Sea surface temperature	degC	6sec. averaged
17 Rain rate (optical rain gauge)	mm/hr	hourly accumulation
18 Rain rate (capacitive rain gauge)	mm/hr	hourly accumulation
19 Down welling shortwave radiation	W/m ²	6sec. averaged
20 Down welling infra-red radiation	W/m ²	6sec. averaged
21 Significant wave height (bow)	m	hourly
22 Significant wave height (aft)	m	hourly
23 Significant wave period (bow)	second	hourly
24 Significant wave period (aft)	second	hourly

Table.2.1.1-3 Instruments and installation locations of SOAR system

Sensors (Zeno/Met)	Type	Manufacturer	Location (altitude from surface)
Anemometer	05106	R.M. Young, USA	foremast (25 m)
Tair/RH	HMP45A	Vaisala, Finland	
with 43408 Gill aspirated radiation shield		R.M. Young, USA	foremast (23 m)
Barometer	61202V	R.M. Young, USA	
with 61002 Gill pressure port		R.M. Young, USA	foremast (23 m)
Rain gauge	50202	R.M. Young, USA	foremast (24 m)
Optical rain gauge	ORG-815DA	Osi, USA	foremast (24 m)
Sensors (PRP)	Type	Manufacturer	Location (altitude from surface)
Radiometer (short wave)	PSP	Epply Labs, USA	foremast (25 m)
Radiometer (long wave)	PIR	Epply Labs, USA	foremast (25 m)
Fast rotating shadowband radiometer		Yankee, USA	foremast (25 m)

Table.2.1.1-4 Parameters of SOAR system

Parameter	Units	Remarks
1 Latitude	degree	
2 Longitude	degree	
3 SOG	knot	
4 COG	degree	
5 Relative wind speed	m/s	
6 Relative wind direction	degree	
7 Barometric pressure	hPa	
8 Air temperature	degC	
9 Relative humidity	%	
10 Rain rate (optical rain gauge)	mm/hr	
11 Precipitation (capacitive rain gauge)	mm	reset at 50 mm
12 Down welling shortwave radiation	W/m ²	
13 Down welling infra-red radiation	W/m ²	
14 Defuse irradiance	W/m ²	

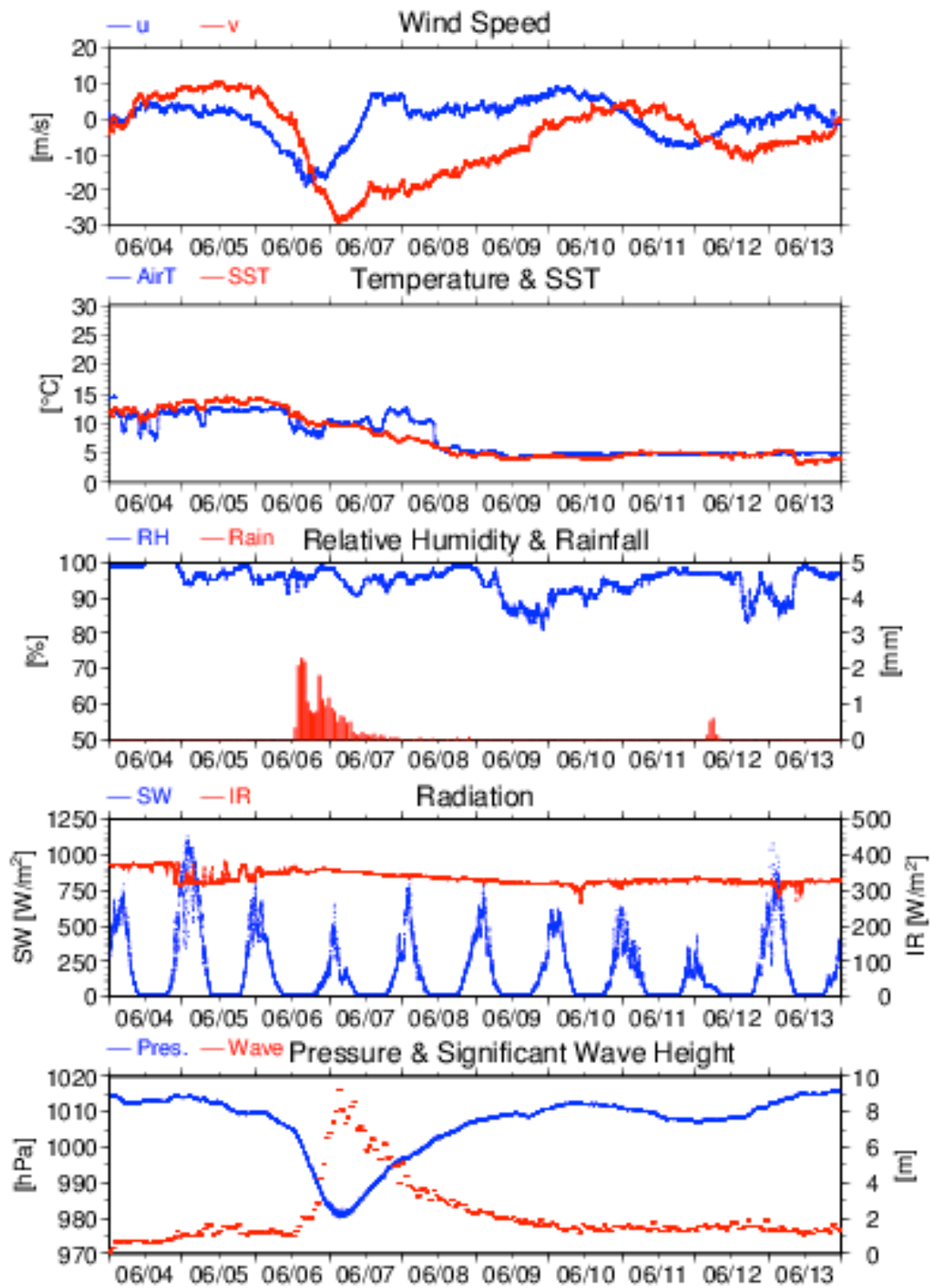


Fig.2.1.1-1 Time series of surface meteorological parameters during the MR12-02 cruise

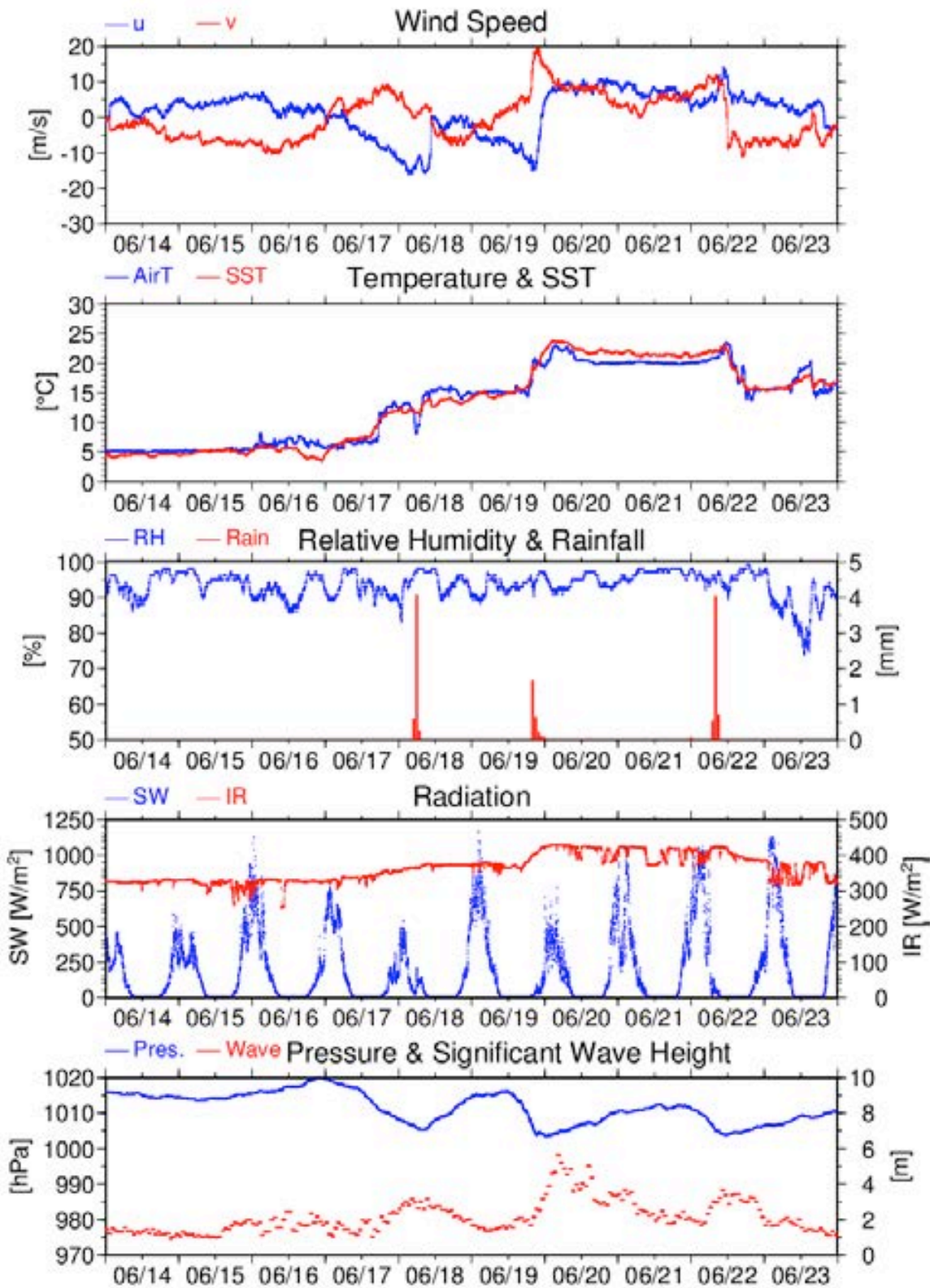


Fig.2.1.1-1 Continued

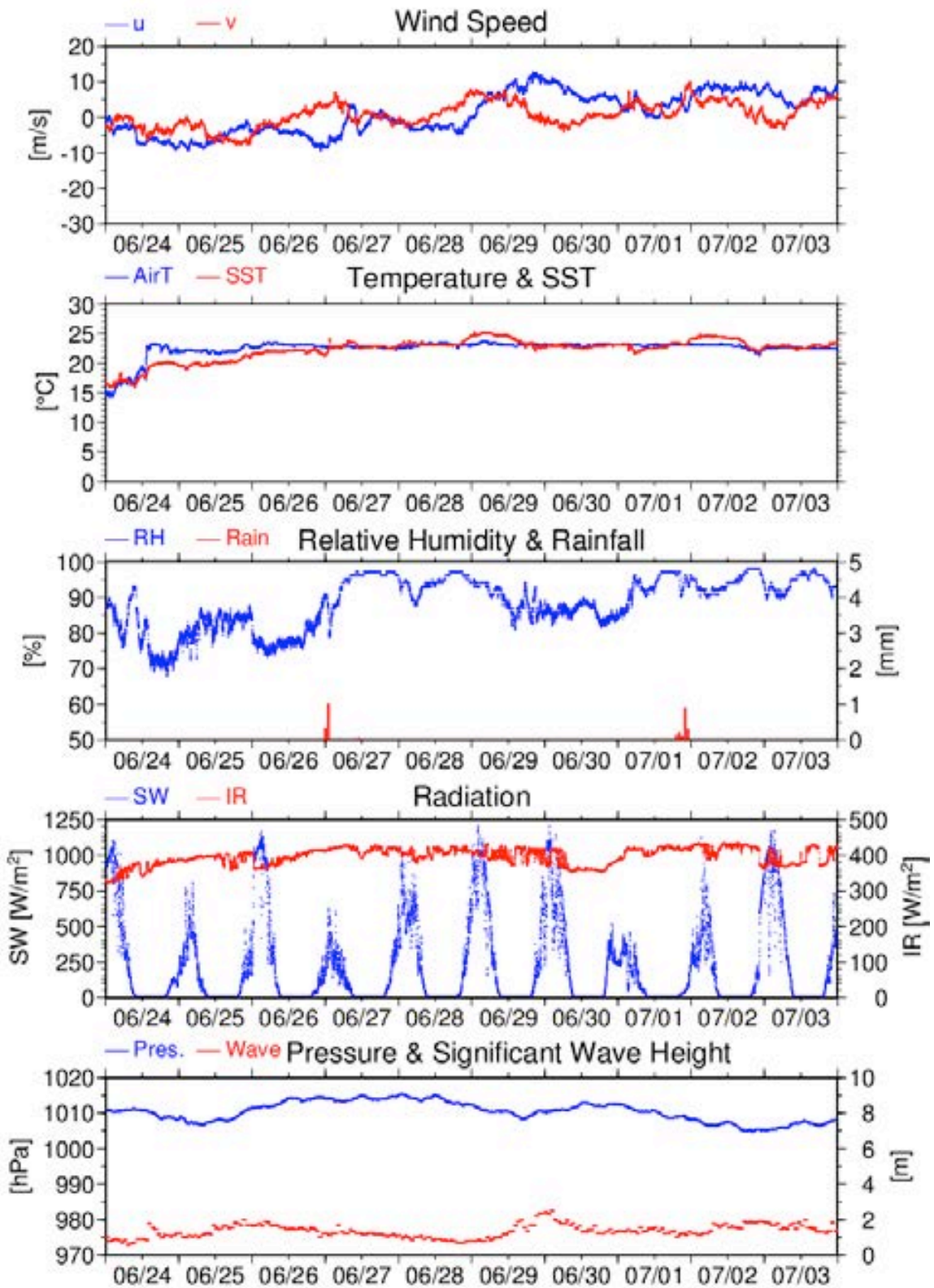


Fig.2.1.1-1 Continued

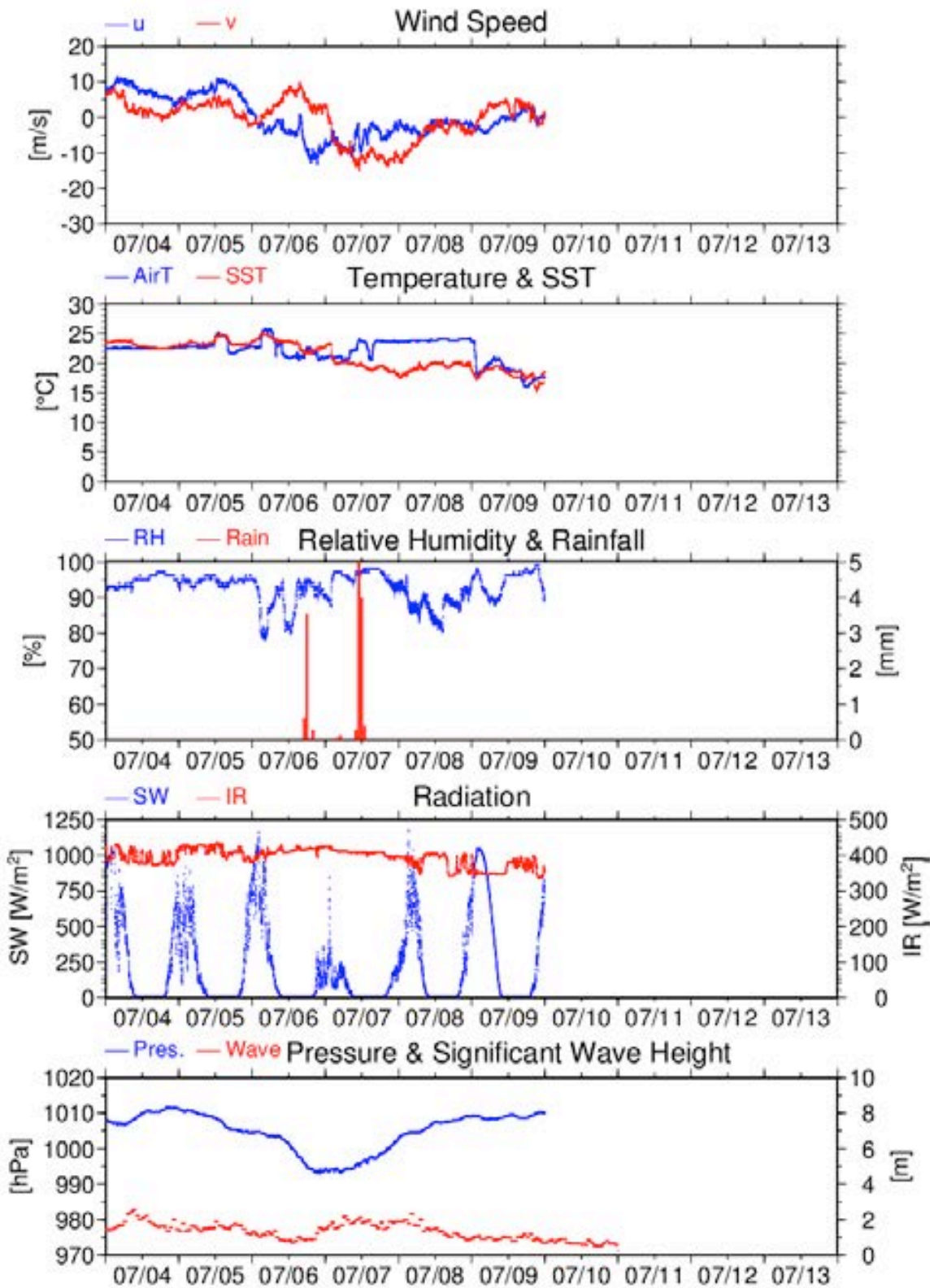


Fig.2.1.1-1 Continued

2.1.2 Ceilometer Observation

Makio HONDA	(JAMSTEC): Principal Investigator	
Katsuhisa MAENO	(Global Ocean Development Inc., GODI)	- leg2 -
Harumi OTA	(GODI)	- leg1 -
Toshimitsu GOTO	(GODI)	- leg1, 2 -
Ryo KIMURA	(Mirai Crew)	- leg1, 2 -

(1) Objectives

The information of cloud base height and the liquid water amount around cloud base is important to understand the process on formation of the cloud. As one of the methods to measure them, the ceilometer observation was carried out.

(2) Parameters

1. Cloud base height [m].
2. Backscatter profile, sensitivity and range normalized at 30 m resolution.
3. Estimated cloud amount [oktas] and height [m]; Sky Condition Algorithm.

(3) Methods

We measured cloud base height and backscatter profile using ceilometer (CT-25K, VAISALA, Finland) throughout the MR12-02 cruise from the departure of Sekinehama on 4 June 2012 to arrival of Sekinehama on 12 July 2012.

Major parameters for the measurement configuration are as follows;

Laser source:	Indium Gallium Arsenide (InGaAs) Diode
Transmitting wavelength:	905±5 nm at 25 degC
Transmitting average power:	8.9 mW
Repetition rate:	5.57 kHz
Detector:	Silicon avalanche photodiode (APD)
	Responsibility at 905 nm: 65 A/W
Measurement range:	0 ~ 7.5 km
Resolution:	50 ft in full range
Sampling rate:	60 sec
Sky Condition	0, 1, 3, 5, 7, 8 oktas (9: Vertical Visibility)
	(0: Sky Clear, 1:Few, 3:Scattered, 5-7: Broken, 8: Overcast)

On the archive dataset, cloud base height and backscatter profile are recorded with the resolution of 30 m (100 ft).

(4) Preliminary results

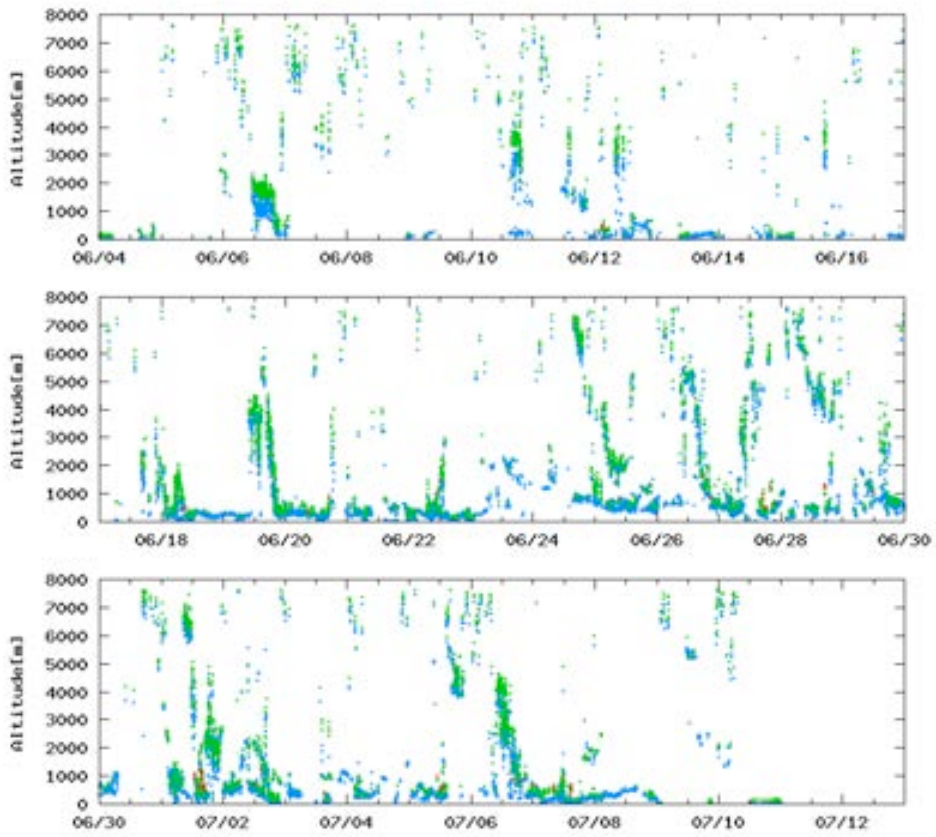
Figure 2.1.2-1 shows the time series of the lowest, second and third cloud base height.

(5) Data archives

The raw data obtained during this cruise will be submitted to the Data Management Group (DMG) in JAMSTEC.

(6) Remarks

1. Window cleaning;
22:59UTC 03 Jun., 22:51UTC 08 Jun., 04:10UTC 11 Jun., 23:22UTC 17 Jun.,
07:27UTC 25 Jun., 04:21UTC 02 Jul.



● : Lowest ● : 2nd ● : 3rd

Fig.2.1.2-1 Lowest (blue), 2nd (green) and 3rd (red) cloud base height during the cruise.

2.1.3. Lidar observations of clouds and aerosols

Nobuo SUGIMOTO (NIES)

Ichiro MATSUI (NIES)

Atsushi SHIMIZU (NIES)

Tomoaki NISHIZAWA (NIES)

Hajime OKAMOTO (Kyusyu university)

(Lidar operation was supported by Global Ocean Development Inc. (GODI).)

(1) Objectives

Objectives of the observations in this cruise is to study distribution and optical characteristics of ice/water clouds and marine aerosols using a two-wavelength polarization Mie lidar.

(2) Description of instruments deployed

Vertical profiles of aerosols and clouds are measured with a two-wavelength polarization Mie lidar. The lidar employs a Nd:YAG laser as a light source which generates the fundamental output at 1064nm and the second harmonic at 532nm. Transmitted laser energy is typically 30mJ per pulse at both of 1064 and 532nm. The pulse repetition rate is 10Hz. The receiver telescope has a diameter of 20 cm. The receiver has three detection channels to receive the lidar signals at 1064 nm and the parallel and perpendicular polarization components at 532nm. An analog-mode avalanche photo diode (APD) is used as a detector for 1064nm, and photomultiplier tubes (PMTs) are used for 532 nm. The detected signals are recorded with a transient recorder and stored on a hard disk with a computer. The lidar system was installed in a container which has a glass window on the roof, and the lidar was operated continuously regardless of weather. Every 10 minutes vertical profiles of four channels (532 parallel, 532 perpendicular, 1064, 532 near range) are recorded.

(3) Preliminary results

The two wavelength polarization Mie lidar worked well and succeeded in getting the lidar data until 5 July 2012 in the observation period. Unfortunately, the laser of the lidar stopped on 5 July due to its power failure; the lidar will work well again next cruise since the power supply was repaired after the cruise finished.

Examples of the measured data are depicted in Fig. 1. The figures indicates that the lidar can detect aerosols in the planetary boundary layer (PBL) formed below 1km, water clouds formed at the top of the PBL, ice clouds in the upper layer and rain falling from clouds. Especially, it should be noted that the lidar could detect ice clouds (cirrus) up to very high altitude of 16km since optical and microphysical properties and distributions of cirrus are key parameters for evaluating climate change. On 24 June and 3 July we could find aerosol layers above PBL (below 4km). Since the total depolarization ratios and the intensities at 1064nm for the layers seem to be low, spherical and small-size aerosols such as air pollution aerosols are probably rich in the layers.

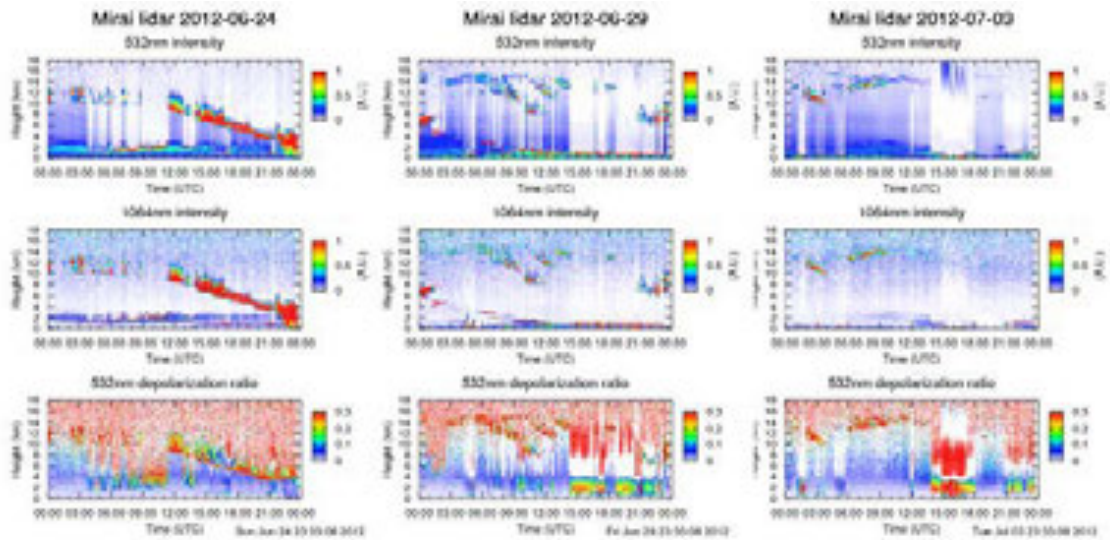


Figure 1: Time-height sections of backscatter intensities at 532nm and 1064nm and total depolarization ratios at 532nm measured on 24 June 2012, 29 June 2012, and 3 July 2012.

(4) Data archive

- Raw data

temporal resolution 10min / vertical resolution 6 m

data period (UTC): Jun. 5, 2012 – July. 5, 2012

lidar signal at 532 nm, lidar signal at 1064 nm, depolarization ratio at 532 nm

- Processed data (plan)

cloud base height, apparent cloud top height, phase of clouds (ice/water), cloud fraction

boundary layer height (aerosol layer upper boundary height),

backscatter coefficient of aerosols, particle depolarization ratio of aerosols

* Data policy and Citation

Contact NIES lidar team (nsugimot/i-matsui/shimizua/nisizawa@nies.go.jp) to utilize lidar data for productive use.

2.1.4 Optical characteristics of aerosol observed by sky radiometer

Kazuma AOKI (University of Toyama) Principal Investigator / not onboard

Tadahiro HAYASAKA (Tohoku University) Co-worker / not onboard

Sky radiometer operation was supported by Global Ocean Development Inc.

(1) Objective

Objective of the observations in this aerosol is to study distribution and optical characteristics of marine aerosols by using a ship-borne sky radiometer (POM-01 MKII: PREDE Co. Ltd., Japan). Furthermore, collections of the data for calibration and validation to the remote sensing data were performed simultaneously.

(2) Methods and Instruments

Sky radiometer is measuring the direct solar irradiance and the solar aureole radiance distribution, has seven interference filters (0.34, 0.4, 0.5, 0.675, 0.87, 0.94, and 1.02 μm). Analysis of these data is performed by SKYRAD.pack version 4.2 developed by Nakajima *et al.* 1996.

@ Measured parameters

- Aerosol optical thickness at five wavelengths (400, 500, 675, 870 and 1020 nm)
 - Ångström exponent
 - Single scattering albedo at five wavelengths
 - Size distribution of volume (0.01 μm – 20 μm)
 - Column water vapor amount from 940 nm
- # GPS provides the position with longitude and latitude and heading direction of the vessel, and azimuth and elevation angle of sun. Horizon sensor provides rolling and pitching angles.

(3) Preliminary results

This study is not onboard. Data obtained in this cruise will be analyzed at University of Toyama.

(4) Data archives

Measurements of aerosol optical data are not archived so soon and developed, examined, arranged and finally provided as available data after certain duration. All data will archived at University of Toyama (K.Aoki, SKYNET/SKY: <http://skyrad.sci.u-toyama.ac.jp/>) after the quality check and submitted to JAMSTEC.

2.1.5. Tropospheric aerosol and gas profile

Yugo KANAYA	(PI, JAMSTEC/RIGC, not on board)
Makio HONDA	(JAMSTEC/RIGC)
Fumikazu TAKETANI	(JAMSTEC/RIGC, not on board)
Xiaole PAN	(JAMSTEC/RIGC, not on board)
Yuichi KOMAZAKI	(JAMSTEC/RIGC, not on board)
Hisahiro TAKASHIMA	(JAMSTEC/RIGC, not on board)

(1) Objectives

- To quantify typical background values of atmospheric aerosol and gas over the ocean
- To clarify transport processes from source over Asia to the ocean (and also clarify the gas emission from the ocean)
- To validate satellite measurements as well as chemical transport model over the ocean
- To quantify fluorescent aerosol over the ocean

(2) Methods

(2-1) CO, O₃,

Carbon monoxide (CO) and ozone (O₃) were continually conducted during the cruise. For CO and O₃ measurements, ambient air was continually sampled on the flying bridge and drawn through ~20-m-long Teflon tubes connected to gas filter correlation CO analyzer (Model 48C, Thermo Fisher Scientific) and UV photometric based ozone analyzer (Model 49C, Thermo Fisher Scientific) in the *Research Information Center*. All measurement data was recorded by both laptop and data logger.

(2-2) Aerosol size distribution fluorescent aerosol particle

Size distribution of aerosol particle and fluorescent aerosol particle over the ocean surface were continually measured using airborne particle spectrometer (LAS-X II, PMS) and the single particle fluorescence sensor, WBS4, respectively. Ambient air was sampled from the flying bridge by a 3-m-long conductive tube, and then introduced to the each instrument. For the airborne-particle spectrometer, ambient air was passed through a diffusion dryer (Model 3062, TSI) before introducing the instrument, to achieve a low RH.

To investigate the fluorescent aerosol particle, we observed two types of fluorescence from individual particles. The instrument utilizes a continuous-wave 635 nm diode laser for the detection of particles and the determination of particle size. The scattering light signal derived from a single particle upon crossing the 635 nm-CW laser triggers two pulsed xenon UV lights (280 nm and 370 nm) for the excitation of compounds contained in the pertinent single particle. The fluorescence signals emitted from the particle are then detected by two PMTs, separately for the 310–400 nm and 420–650 nm wavelength windows.

(2-3) Ambient particle sampling

Ambient aerosol particles were collected along cruise track using High-Volume air Sampler (HV-525PM, SHIBATA). HVS was installed on the flying bridge and air was vacuumed up with speed of 500L min⁻¹. Start and stop of pumping were controlled

automatically by “Wind-direction selection system” in order to avoid collecting the particle emitted by ship’s funnel. By setting particle size selector for the HVS, two types of particles which were larger and smaller than diameter of 2.5 μm were collected on the quartz and Teflon filters, respectively. After sampling, these filters were stored in glass bottle under room temperature. We obtained 26 samples in whole cruise period.

(3) Preliminary results

These data for the whole cruise period will be analyzed.

(4) Data archives

The data will be submitted to the Data management Group (DMG) of JAMSTEC after the full analysis of the raw spectrum data is completed, which will be <2 years after the end of the cruise.

2.1.6 Continuous measurement of the water stable isotopes over the Ocean

**Yasushi FUJIYOSHI (Hokkaido Univ./JAMSTEC) Principal Investigator
(not on-board)**

**Naoyuki KURITA (JAMSTEC) (not on-board)
(Operator)**

Harumi OHTA (Global Ocean Development Inc.: GODI)

Katsuhisa MAENO (Global Ocean Development Inc.: GODI)

(1) Objective

It is well known that the variability of stable water isotopes (HDO and H₂¹⁸O) reflects the integrated history of water mass exchange that occurs during transportation from the upstream region. Thus, water isotope tracer is recognized as the powerful tool to study of the hydrological cycles in the marine atmosphere. However, oceanic region is one of sparse region of the isotope data, it is necessary to fill the data to identify the moisture sources by using the isotope tracer. In this study, to fill this sparse observation area, intense water isotopes observation was conducted along the cruise track of MR12-02.

(2) Method

Following observation was carried out throughout this cruise.

- Atmospheric moisture sampling:

Water vapor isotopes in ambient air was continuously measured using the laser instrument based on off-axis integrated cavity output spectroscopy, manufactured by Los Gatos Research, Inc. (LGR) (Water Vapor Iso- tope Analyzer, WVIA) coupled with an accessory device for the vaporization of a liquid water standard (Water Vapor Isotope Standard Source, WVISS). The WVISS is programmable from the WVIA and thus this coupled system is capable of automatically conducting a calibration routine at specific intervals.

Air intake was attached at the middle level (20m above the sea level) of the mast at the compass deck and a sampling tube (20 m length of Nylon tubing (Junron A), 8mm O.D.) was connected from air intake to a 3-way valve attached to the WVISS. A 1.0 μm filter with PTFE membrane was placed where the tube enters the air intake. Air was drawn via the pump at a flow rate of 3 l min⁻¹ to the laboratory and then a part of air was saked via the WVIA external pump at a flow rate of 0.5 l min⁻¹. Every 25 min, the 3-way valve automatically switched from ambient/outdoor inlet to WVISS standard air, whereupon standard air with a H₂O concentra- tion of 12 000 ppm was introduced to the WVIA for 5 min. After finishing the reference gas measurement, the valve switches back and ambient air sampling is resumed. Raw data from the analyzer is stored on the internal hard disk, and is transferred via ethernet cable. Calibration is undertaken as a post-processing step using the external computer system.

- Rainwater sampling

Rainwater samples gathered in rain/snow collector were collected just after

precipitation events have ended. The collected sample was then transferred into glass bottle (6ml) immediately after the measurement of precipitation amount.

- Surface seawater sampling

Seawater sample taken by the pump from 4m depth were collected in glass bottle (6ml) around the noon at the local time.

(3) Water samples for isotope analysis

Sampling of rainfall for isotope analysis is summarized in Table 2.1.6-1 (14 samples). Described rainfall amount is calculated from the collected amount of precipitation. Sampling of surface seawater taken by pump from 4m depths is summarized in Table 2.1.6-2 (37 samples).

(4) Data archive

The isotopic data of water vapor can obtain from the laser based water vapor isotope analyzer on board. The archived raw observed data (see Figure 2.1.6-1) was submitted to JAMSTEC Data Integration and Analysis Group (DIAG) after the cruise immediately. As for collected water samples, isotopes (HDO, H₂¹⁸O) analysis will be done at RIGC/JAMSTEC, and then analyzed isotopes data will be submitted to JAMSTEC DIAG.

Table 2.1.6-1 Summary of precipitation sampling for isotope analysis.

	Date	Time (UT)	Lon	Lat	Date	Time (UT)	Lon	Lat	Rain (mm)	R/S
R-1	6.4	00:00	141-14.37E	41-21.97N	6.6	14:26	148-43.22E	40-28.96N	10.2	R
R-2	6.6	14:26	148-43.22E	40-28.96N	6.7	08:01	150-17.50E	41-07.94N	157.5	R
R-3	6.7	08:01	150-17.50E	41-07.94N	6.7	23:29	152-03.04E	41-54.27N	1.2	R
R-4	6.7	23:29	152-03.04E	41-54.27N	6.10	20:36	160-00.57E	47-00.01N	2.6	R
R-5	6.10	20:36	160-00.57E	47-00.01N	6.11	21:15	160-00.34E	46-59.95N	0.1	R
R-6	6.11	21:15	160-00.34E	46-59.95N	6.12	21:32	159-49.36E	47-00.81N	0.3	R
R-7	6.12	21:32	159-49.36E	47-00.81N	6.18	11:19	149-24.15E	40-01.27N	6.6	R
R-8	6.18	11:19	149-24.15E	40-01.27N	6.20	01:51	145-43.64E	36-02.41N	5.1	R
R-9	6.20	01:51	145-43.64E	36-02.41N	6.23	00:24	146-26.44E	38-04.83 N	11.7	R
R-10	6.23	00:24	146-26.44E	38-04.83N	6.27	00:32	144-59.69E	29-55.55N	3.6	R
R-11	6.27	00:32	144-59.69E	29-55.55N	6.28	01:08	144-58.98E	30-01.18N	0.6	R
R-12	6.28	01:08	144-58.98E	30-01.18N	7.1	23:10	145-03.35E	30-05.57N	3.5	R
R-13	7.1	23:10	145-03.35E	30-05.57N	7.7	00:26	141-28.60E	36-28.97N	5.5	R
R-14	7.7	00:26	141-28.60E	36-28.97N	7.8	00:32	141-30.11E	36-30.02N	16.0	R

Table 2.1.6-2 Summary of sea surface water sampling for isotope analysis

	Sampling No.	Date	Time (UTC)	Position	
				LON	LAT
O-	1	6.4	03:00	141-56.56E	41-31.70N

O-	2	6.5	03:03	147-31.95E	40-41.93N
O-	3	6.6	02:47	146-58.83E	41-08.76N
O-	4	6.7	03:00	150-04.56E	41-07.96N
O-	5	6.8	02:00	152-23.27E	42-06.33N
O-	6	6.9	01:03	156-30.15E	44-34.56N
O-	7	6.10	01:00	159-59.73E	47-00.30N
O-	8	6.11	01:00	160-00.21E	46-59.59N
O-	9	6.12	01:03	160-02.27E	47-00.90N
O-	10	6.13	01:04	160-00.12E	46-58.29N
O-	11	6.14	01:00	160-00.40E	46-59.86N
O-	12	6.15	01:11	159-59.45E	47-00.39N
O-	13	6.16	01:00	159-49-15E	44-40.82N
O-	14	6.17	02:02	156-11.00E	44-10.19N
O-	15	6.18	02:02	151-25.58E	41-30.57N
O-	16	6.19	03:02	146-33.28E	37-55.76N
O-	17	6.20	03:00	145-40.51E	35-55.41N
O-	18	6.21	03:00	144-54.34E	33-50.54N
O-	19	6.22	03:00	144-54.20E	33-50.61N
O-	20	6.23	03:09	146-19.58E	38-04.98N
O-	21	6.24	03:00	141-19.85E	36-56.25N
O-	22	6.25	03:00	143-04.03E	33-22.07N
O-	23	6.26	03:00	144-58.91E	30-03.28N
O-	24	6.27	03:00	144-59.61E	29-56.19N
O-	25	6.28	03:00	144-58.99E	30-00.26N
O-	26	6.29	03:06	144-59.62E	29-58.16N
O-	27	6.30	03:09	145-02.31E	30-10.76N
O-	28	7.1	03:00	145-04.23E	29-53.88N
O-	29	7.2	03:00	144-58.36E	30-04.44N
O-	30	7.3	03:04	144-28.82E	32-17.10N
O-	31	7.4	03:00	144-31.58E	32-26.01N
O-	32	7.5	03:00	144-32.00E	32-18.90N
O-	33	7.6	03:04	142-08.14E	35-37.22N
O-	34	7.7	03:00	141-30.41E	36-29.88N
O-	35	7.8	03:00	141-34.50E	36-34.74N
O-	36	7.9	03:00	141-58.82E	36-56.09N
O-	37	7.10	03:00	142-04.42E	40-13.16N

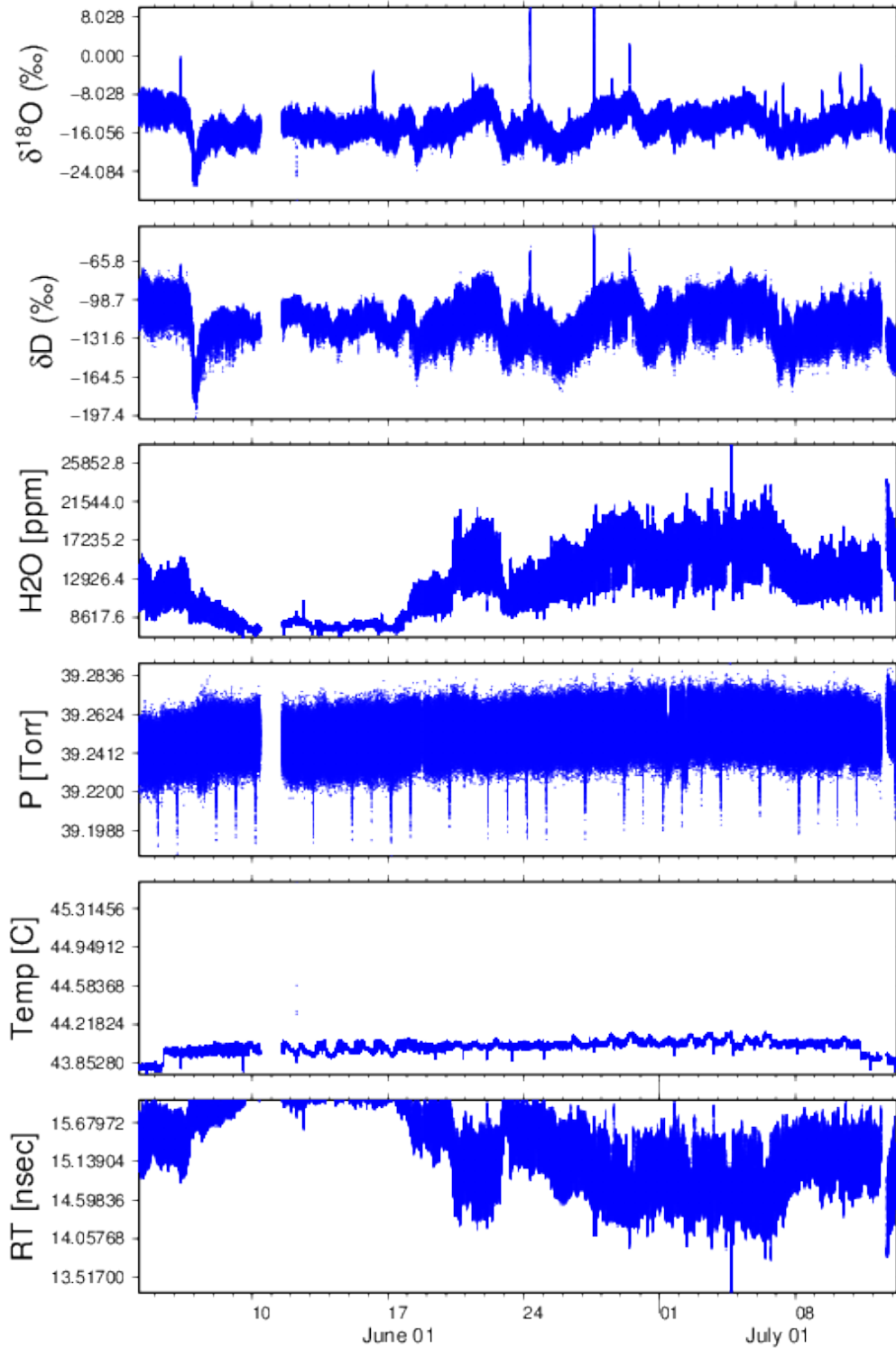


Figure 2.1.6-1
 Continuous time-series of d^{18}O , dD , H_2O concentration, cavity pressure, cavity temperature, and residence time measured by the WVIA (raw data) during the MR12-02 cruise.

2.2. Physical oceanographic observation

2.2.1. CTD cast and water sampling

Masahide WAKITA (JAMSTEC MIO): Principal investigator

Hiroshi UCHIDA * (JAMSTEC RIGC)

Shinsuke TOYODA (MWJ): Operation leader

Naoko MIYAMOTO (MWJ)

Toru IDAI (MWJ)

Hirokatsu UNO * (MWJ)

Kenichi KATAYAMA (MWJ)

Tomoyuki TAKAMORI (MWJ)

(1) Objective

Investigation of oceanic structure and water sampling.

(2) Parameters

Temperature (Primary and Secondary)

Conductivity (Primary and Secondary)

Pressure

Dissolved Oxygen

Dissolved Oxygen voltage

Transmission % and voltage

Fluorescence

Photosynthetically Active Radiation

Altimeter

(3) Instruments and Methods

CTD/Carousel Water Sampling System, which is a 36-position Carousel water sampler (CWS) with Sea-Bird Electronics, Inc. CTD (SBE9plus), was used during this cruise. 12-liter Niskin Bottles, which were washed by alkaline detergent and HCl, were used for sampling seawater. The sensors attached on the CTD were temperature (Primary and Secondary), conductivity (Primary and Secondary), pressure, dissolved oxygen, RINKO-III (dissolved oxygen sensor), transmission, fluorescence, PAR, altimeter and deep ocean standards thermometer. In the Stn.K02 cast 6, we changed PAR sensor with RINKO-III and Optode (the parameters were voltage). The Practical Salinity was calculated by measured values of pressure, conductivity and temperature. The CTD/CWS was deployed from starboard on working deck.

The CTD raw data were acquired on real time using the Seasave-Win32 (ver.7.21h) provided by Sea-Bird Electronics, Inc. and stored on the hard disk of the personal computer. Seawater was sampled during the up cast by sending fire commands from the personal computer. We stop at each layer for 30 seconds to stabilize then fire until the Stn.K02 cast 10. After the cast, we stop at each layer for 1 mini to stabilize then fire. In the Stn.K02 cast 6 and cast 9, we stop at layers for various times to test the water samples. In the Stn.S01 cast7 cast10, Stn.KEO cast2, and Stn.F01 cast1, we stop at some layers for 4 minutes to calibrate the sensor.

Spike was observed in the transmission voltage in the some casts. In the Stn.KEO cast 1, sift was observed in the transmission voltage.

In the Stn.JKO, fluorescence data was range over near surface. In addition, noise was observed in the primary conductivity and the dissolved oxygen voltage (SBE43) data of #31 bottle data.

31 casts of CTD measurements were conducted (Table 2.2.1-1).

Data processing procedures and used utilities of SBE Data Processing-Win32 (ver.7.18d) and

SEASOFT were as follows:

(The process in order)

DATCNV: Convert the binary raw data to engineering unit data. DATCNV also extracts bottle information where scans were marked with the bottle confirm bit during acquisition. The duration was set to 4.4 seconds, and the offset was set to 0.0 seconds.

In a part of the Stn.K02 cast 6 and cast 9 data, the duration was set to 1.0 seconds, and the offset was set to 0.0 seconds.

RINKOCOR (original module): Corrected of the hysteresis of RINK-III voltage.

RINKOCORROS (original module): Corrected of the hysteresis of RINKO-III voltage bottle data.

BOTTLESUM: Create a summary of the bottle data. The data were averaged over 4.4 seconds.

ALIGNCTD: Convert the time-sequence of sensor outputs into the pressure sequence to ensure that all calculations were made using measurements from the same parcel of water. Dissolved oxygen data are systematically delayed with respect to depth mainly because of the long time constant of the dissolved oxygen sensor and of an additional delay from the transit time of water in the pumped plumbing line. This delay was compensated by 6 seconds advancing dissolved oxygen sensor (SBE43) output (dissolved oxygen voltage) relative to the temperature data. RINKO-III voltage, transmission data and voltage are also delayed by slightly slow response time to the sensor. The delay was compensated by 1 second or 2 seconds advancing.

WILDEDIT: Mark extreme outliers in the data files. The first pass of WILDEDIT obtained an accurate estimate of the true standard deviation of the data. The data were read in blocks of 1000 scans. Data greater than 10 standard deviations were flagged. The second pass computed a standard deviation over the same 1000 scans excluding the flagged values. Values greater than 20 standard deviations were marked bad. This process was applied to pressure, depth, temperature, conductivity and dissolved oxygen voltage (SBE43).

CELLTM: Remove conductivity cell thermal mass effects from the measured conductivity. Typical values used were thermal anomaly amplitude $\alpha = 0.03$ and the time constant $1/\beta = 7.0$.

FILTER: Perform a low pass filter on pressure with a time constant of 0.15 second. In order to produce zero phase lag (no time shift) the filter runs forward first then backward

WFILTER: Perform a median filter to remove spikes in the fluorescence data, transmission data and voltage data. A median value was determined by 49 scans of the window. The transmission voltage data of Stn.E02 were reprocessed by the 13 scans of window, at the end of all data processing, because noise was observed in the data.

SECTIONU (original module of SECTION): Select a time span of data based on scan number in order to reduce a file size. The minimum number was set to be the starting time when the CTD package was beneath the sea-surface after activation of the pump. The maximum number of was set to be the end time when the package came up from the surface.

LOOPEDIT: Mark scans where the CTD was moving less than the minimum velocity of 0.0 m/s (traveling backwards due to ship roll).

DESPIKE (original module): Remove spikes of the data. A median and mean absolute deviation was calculated in 1-dbar pressure bins for both down and up cast, excluding the flagged values. Values greater than 4 mean absolute deviations from the median were marked bad for each bin. This process was performed 2 times for temperature, conductivity, dissolved oxygen voltage (SBE43), RINKO-III voltage. In the Stn.K02 cast 6, the optode voltage also.

DERIVE: Compute dissolved oxygen (SBE43).

BINAVG: Average the data into 1-dbar pressure bins.

DERIVE: Compute the Practical Salinity, sigma-theta and potential temperature.

SPLIT: Separate the data from an input .cnv file into down cast and up cast files.

Configuration file: MR1202A.con
MR1202B.con (Stn.K02M06)

Specifications of the sensors are listed below.

CTD: SBE911plus CTD system

Under water unit:
SBE9plus (S/N 09P54451-1027, Sea-Bird Electronics, Inc.)

Pressure sensor: DigiQuartz pressure sensor (S/N 117457)
Calibrated Date: 28 May 2012

Temperature sensors:

Primary: SBE03Plus (S/N 034811, Sea-Bird Electronics, Inc.)
Calibrated Date: 01 Mar. 2012
Secondary: SBE03-04/F (S/N 031525, Sea-Bird Electronics, Inc.)
Calibrated Date: 24 Apr. 2012

Conductivity sensors:

Primary: SBE04-04/0 (S/N 042854, Sea-Bird Electronics, Inc.)
Calibrated Date: 28 Feb. 2012
Secondary: SBE04-04/0 (S/N 042435, Sea-Bird Electronics, Inc.)
Calibrated Date: 28 Feb. 2012

Dissolved Oxygen sensor:

SBE43 (S/N 432211, Sea-Bird Electronics, Inc.)
Calibrated Date: 26 Oct. 2011
RINK-III (S/N 0024 (144002A), Alec Electronics Co. Ltd.)
Calibrated Date: 23 May 2012
RINK-III (S/N 0079 (160002A), Alec Electronics Co. Ltd.)
Calibrated Date: 23 May 2012
RINK-III (S/N 0037 (1204-2'), Alec Electronics Co. Ltd.)
Optode (S/N 1, Aanderaa Instruments AS)

Transmissometer:

C-Star (S/N CST-1363DR, WET Labs, Inc.)
Calibrated Date: 19 Apr. 2012

Fluorescence:

Chlorophyll Fluorometer (S/N 3054, Seapoint Sensors, Inc.)

Photosynthetically Active Radiation:

PAR sensor (S/N 0049, Satlantic Inc.)
Calibrated Date: 22 Jan. 2009

Altimeter:

Benthos PSA-916T (S/N 1100, Teledyne Benthos, Inc.)

Deep Ocean Standards Thermometer:

SBE35 (S/N 0045, Sea-Bird Electronics, Inc.)
Calibrated Date: 15 Apr. 2012

Carousel water sampler:

SBE32 (S/N 3221746-0278, Sea-Bird Electronics, Inc.)

Deck unit: SBE11plus (S/N 11P7030-0272, Sea-Bird Electronics, Inc.)

(4) Preliminary Results

During this cruise, 31 casts of CTD observation were carried out. Date, time and locations of the CTD casts are listed in Table 2.2.1-1.

(5) Data archive

All raw and processed data files will be submitted to the Data Management Office (DMO), JAMSTEC, and will be opened to public via “R/V MIRAI Data Web Page” in the JAMSTEC home page.

Table 2.2.2-1 CTD cast table

Table 2.1.7-1 MR12-02 CTD Castable

Stnbr	Castno	Date(UTC) (mmddyy)	Time(UTC)		BottomPosition		Depth	Wire Out	HT Above	Max Depth	Max Pressure	CTD Filename	Remark
			Start	End	Latitude	Longitude							
E01	1	060512	09:46	11:33	40-56.11N	147-29.33E	5295.0	1987.1	-	1978.0	2003.0	E01M01	Leg1 start ARGO
E05	1	060512	19:00	20:43	41-18.00N	146-10.54E	5521.0	1977.5	-	1976.0	2001.0	E05M01	ARGO
E04	1	060512	22:36	00:15	41-14.16N	146-32.87E	5429.0	1980.7	-	1977.0	2002.0	E04M01	ARGO
E03	1	060612	02:17	03:53	41-08.76N	146-58.82E	5283.0	1979.9	-	1976.0	2001.0	E03M01	ARGO
E02	1	060612	05:16	06:59	41-06.06N	147-09.63E	5155.0	1984.0	-	1978.0	2003.0	E02M01	ARGO
K02	1	061012	02:07	05:30	46-59.66N	159-59.87E	5198.0	5186.8	8.2	5176.3	5284.0	K02M01	Routine
K02	2	061012	15:36	16:15	46-59.62N	160-00.27E	5216.0	298.4	-	301.3	304.0	K02M02	P.P. / HPLC
K02	3	061012	21:57	22:43	46-59.97N	160-00.01E	5182.0	801.1	-	800.7	809.0	K02M03	Cs / Paleo
K02	4	061012	23:57	00:30	47-00.09N	160-00.01E	5184.0	500.1	-	502.2	507.0	K02M04	POM
K02	5	061112	02:04	04:27	46-59.78N	160-00.05E	5188.0	4010.2	-	4000.8	4073.0	K02M05	R.I.
K02	6	061112	17:04	23:40	47-00.01N	160-00.31E	5189.0	4909.4	-	4903.1	5002.0	K02M06	RINKO / TRAP / water sampling test
K02	7	061212	03:14	06:06	47-03.17N	160-06.18E	5217.0	5221.7	8.8	5211.1	5320.0	K02M07	Bacteria
K02	8	061312	15:33	16:09	47-03.56N	160-17.65E	5251.0	297.5	-	300.3	303.0	K02M08	P.P. / HPLC
K02	9	061312	21:28	21:55	47-00.99N	160-03.03E	5219.0	297.5	-	301.3	304.0	K02M09	P.E. / water sampling test
K02	10	061412	18:04	19:28	47-00.16N	160-00.95E	5206.0	2009.0	-	2002.5	2029.0	K02M10	Bacteria
KNT	1	061712	06:55	10:31	44-00.04N	154-59.96E	5307.0	5300.6	8.5	5295.9	5406.0	KNTM01	Routine
JKO	1	061912	09:48	13:30	37-56.32N	146-35.93E	5403.0	5386.8	10.3	5368.5	5478.0	JKOM01	Routine
NKO	1	062012	23:03	02:53	33-50.43N	144-54.14E	5759.0	5752.1	7.4	5734.3	5854.0	NKOM01	Routine
S01	1	062612	04:03	08:06	30-00.42N	144-59.63E	5953.0	5962.8	8.4	5950.7	6076.0	S01M01	Leg2 start Routine
S01	2	062712	17:35	18:23	29-59.76N	144-59.80E	5955.0	300.6	-	302.7	305.0	S01M02	P.P. / HPLC
S01	3	062712	23:39	00:08	30-01.49N	144-59.30E	5879.0	298.6	-	300.7	303.0	S01M03	POM
S01	4	062812	01:02	01:57	30-01.14N	144-58.95E	5943.0	801.7	-	801.9	809.0	S01M04	Cs / Paleo
S01	5	062812	04:02	07:21	29-59.91N	144-59.43E	5957.0	5946.1	10.3	5944.9	6070.0	S01M05	Bacteria
S01	6	063012	17:36	18:22	29-49.94N	145-14.23E	5854.0	296.5	-	300.7	303.0	S01M06	P.P. / HPLC
S01	7	063012	23:37	00:59	29-55.40N	145-05.74E	5891.0	501.6	-	503.9	508.0	S01M07	P.E. / pCO2
S01	8	070112	20:35	22:03	30-03.21N	144-58.33E	5915.0	2015.4	-	2002.5	2026.0	S01M08	Bacteria
S01	9	070212	04:02	06:30	30-02.76N	144-59.00E	5902.0	4006.9	-	4001.0	4067.0	S01M09	R.I.
S01	10	070212	08:01	09:55	30-01.98N	144-59.55E	5875.0	1990.4	-	1980.9	2004.0	S01M10	ARGO / TRAP
KEO	1	070312	04:04	08:02	32-19.06N	144-27.74E	5754.0	5756.7	8.8	5744.7	5864.0	KEOM01	Routine
KEO	2	070412	04:10	05:04	32-24.07N	144-29.58E	5760.0	593.7	-	596.9	602.0	KEOM02	Routine / Cs
FO1	1	070712	01:35	03:58	36-29.83N	141-30.66E	1281.0	1316.9	9.7	1269.7	1283.0	FO1M01	Routine / Cs

ARGO: ARGO float release point
Routine: Routine sampling cast
P.P. / HPLC: Primary Production / High Performance Liquid Chromatography cast
Cs: cesium cast
Paleo: archaeobacteria cast
RI: radioisotope cast
RINKO: RINKO test cast
TRAP: water for the TRAP
Bacteria: Bacteria sampling cast
P.E.: P vs. E curve cast

2.2.2. Salinity measurement

Masahide WAKITA (JAMSTEC MIO)

Tatsuya TANAKA (MWJ)

Kenichi KATAYAMA (MWJ)

(1) Objective

To measure bottle salinity obtained by CTD casts, bucket sampling, and The Continuous Sea Surface Water Monitoring System (TSG).

(2) Methods

a. Salinity Sample Collection

Seawater samples were collected with 12 liter Niskin-X bottles, bucket, and TSG. The salinity sample bottles of the 250ml brown glass bottles with screw caps were used for collecting the sample water. Each bottle was rinsed three times with the sample water, and filled with sample water to the bottle shoulder. The salinity sample bottles for TSG were sealed with both plastic inner caps and screw caps because we took into consideration the possibility of long term storage (for about one month). These caps were rinsed three times with the sample water before use. The bottles were stored for more than 12 hours in the laboratory before the salinity measurement.

The number of samples is shown as follows;

Table 2.2.2-1 The number of samples

Sampling type	Number of samples
CTD and Bucket	595
TSG	29
Total	624

b. Instruments and Method

The salinity measurement on R/V MIRAI was carried out during the cruise of MR12-02 using the salinometer (Model 8400B “AUTOSAL”; Guildline Instruments Ltd.: S/N 62827) with an additional peristaltic-type intake pump (Ocean Scientific International, Ltd.). A pair of precision digital thermometers (Model 9540; Guildline Instruments Ltd.: S/N 62521 and 66723) were used. The thermometer monitored the ambient temperature and the bath temperature of the salinometer.

The specifications of AUTOSAL salinometer and thermometer are shown as follows;

Salinometer (Model 8400B “AUTOSAL”; Guildline Instruments Ltd.)

Measurement Range : 0.005 to 42 (PSU)

Accuracy : Better than ± 0.002 (PSU) over 24 hours

without re-standardization

Maximum Resolution : Better than ± 0.0002 (PSU) at 35 (PSU)

Thermometer (Model 9540: Guildline Instruments Ltd.)

Measurement Range : -40 to +180 deg C

Resolution : 0.001

Limits of error \pm deg C : 0.01 (24 hours @ 23 deg C ± 1 deg C)

Repeatability : ± 2 least significant digits

The measurement system was almost the same as Aoyama *et al.* (2002). The salinometer was operated in the air-conditioned ship's laboratory at a bath temperature of 24 deg C. The ambient temperature varied from approximately 20 deg C to 25 deg C, while the bath temperature was very stable and varied within ± 0.001 deg C on rare occasion.

The measurement for each sample was carried out with the double conductivity ratio and defined as the median of 31 readings of the salinometer. Data collection was started 5 seconds after filling the cell with the sample and it took about 10 seconds to collect 31 readings by the personal computer. Data were taken for the sixth and seventh filling of the cell after rinsing five times. In the case of the difference between the double conductivity ratio of these two fillings being smaller than 0.00002, the average value of the double conductivity ratio was used to calculate the bottle salinity with the algorithm for practical salinity scale, 1978 (UNESCO, 1981). If the difference was greater than or equal to 0.00003, an eighth filling of the cell was done. In the case of the difference between the double conductivity ratio of these two fillings being smaller than 0.00002, the average value of the double conductivity ratio was used to calculate the bottle salinity. In the case of the double conductivity ratio of eighth filling did not satisfy the criteria above, we measured a ninth filling of the cell and calculated the bottle salinity. The measurement was conducted in about 6 - 10 hours per day and the cell was cleaned with soap after the measurement of the day.

(3) Preliminary Result

a. Standard Seawater

Standardization control of the salinometer was set to 498 and all measurements were carried out at this setting. The value of STANDBY was $24+5422 \pm 0003$ and that of ZERO was $0.0-0000 \pm 0001$. The conductivity ratio of IAPSO Standard Seawater batch P154 was 0.99990 (the double conductivity ratio was 1.99962) and was used as the standard for salinity. We measured 39 bottles of P154.

The specifications of SSW used in this cruise are shown as follows ;

Batch : P154
conductivity ratio : 0.99990

salinity : 34.996
Use by : 20th Oct 2014

Fig.2.2.2-1 shows the history of the double conductivity ratio for the Standard Seawater batch P154 before correction. The average of the double conductivity ratio was 1.99976 and the standard deviation was 0.00004, which is equivalent to 0.0007 in salinity.

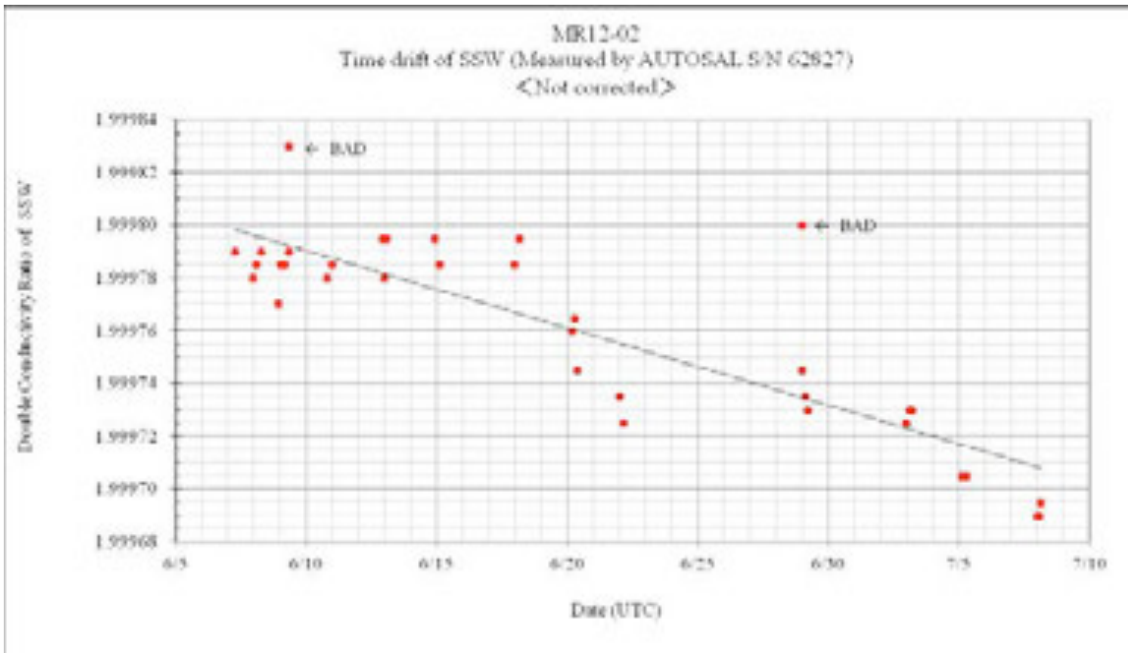


Fig. 2.2.2-1 The history of the double conductivity ratio for the Standard Seawater batch P154 (Before correction)

Fig.2.2.2-2 shows the history of the double conductivity ratio for the Standard Seawater batch P154 after correction. The average of the double conductivity ratio after correction was 1.99980 and the standard deviation was 0.00001, which is equivalent to 0.0003 in salinity.

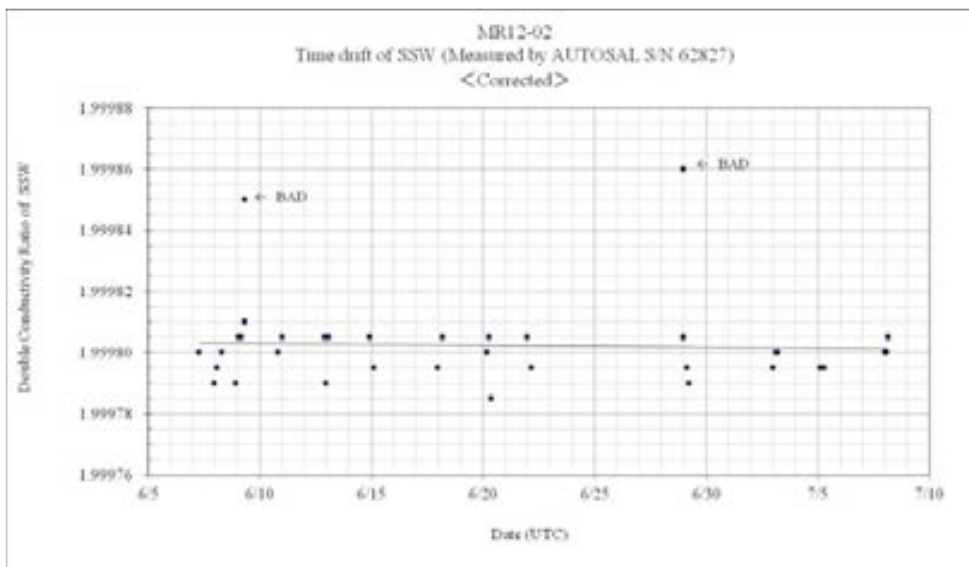


Fig. 2.2.2-2 The history of the double conductivity ratio for the Standard Seawater batch P154 (After correction)

b. Sub-Standard Seawater

Sub-standard seawater was made from deep-sea water filtered by a pore size of 0.45 micrometer and stored in a 20-liter container made of polyethylene and stirred for at least 24 hours before start measuring. It was measured about every 6 samples in order to check for the possible sudden drifts of the salinometer.

c. Replicate Samples

We estimated the precision of this method using 48 pairs of replicate samples taken from the same Niskin bottle. Fig.2.2.2-3 shows the histogram of the absolute difference between each pair of the replicate samples. The average and the standard deviation of absolute difference among 48 pairs of replicate samples were 0.0002 and 0.0001 in salinity, respectively.

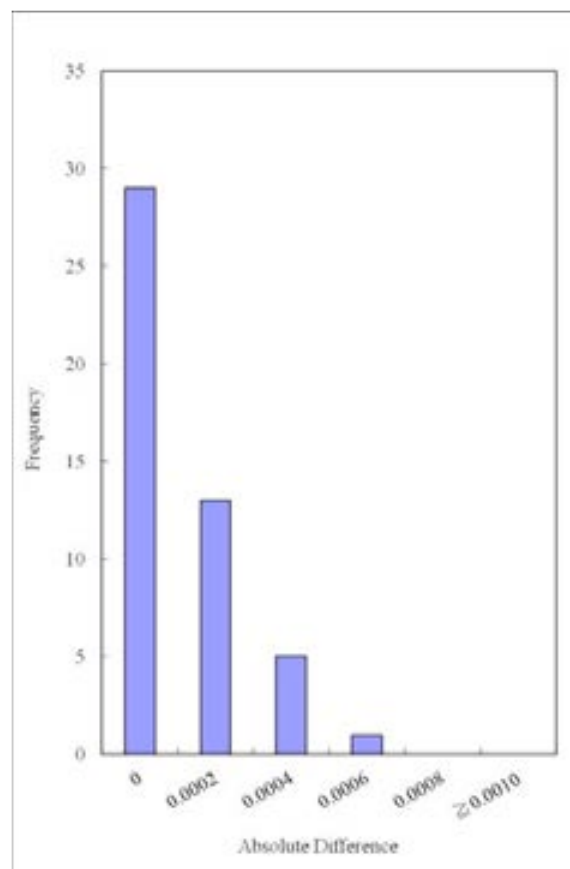


Fig. 2.2.2-3 The histogram of the double conductivity ratio for the absolute difference of replicate samples

(4) Data archive

These raw datasets will be submitted to JAMSTEC Data Management Office (DMO).

(5) Reference

- Aoyama, M. , T. Joyce, T. Kawano and Y. Takatsuki: Standard seawater comparison up to P129. Deep-Sea Research, I, Vol. 49, 1103~1114, 2002
- UNESCO : Tenth report of the Joint Panel on Oceanographic Tables and Standards. UNESCO Tech. Papers in Mar. Sci., 36, 25 pp., 1981

2.2.3 Shipboard ADCP

Makio HONDA	(JAMSTEC RIGC)	
Katsuhisa MAENO	(Global Ocean Development Inc., GODI)	- leg2 -
Harumi OTA	(GODI)	- leg1 -
Toshimitsu GOTO	(GODI)	- leg1, 2 -
Ryo KIMURA	(MIRAI Crew)	- leg1, 2 -

(1) Objective

To obtain continuous measurement of the current profile along the ship's track.

(2) Methods

Upper ocean current measurements were made in MR12-02 cruise, using the hull-mounted Acoustic Doppler Current Profiler (ADCP) system. For most of its operation the instrument was configured for water-tracking mode. Bottom-tracking mode, interleaved bottom-ping with water-ping, was made to get the calibration data for evaluating transducer misalignment angle in the shallow water. The system consists of following components;

1. R/V MIRAI has installed the Ocean Surveyor for vessel-mount ADCP (frequency 75 kHz; Teledyne RD Instruments, USA). It has a phased-array transducer with single ceramic assembly and creates 4 acoustic beams electronically. We mounted the transducer head rotated to a ship-relative angle of 45 degrees azimuth from the keel
2. For heading source, we use ship's gyro compass (Tokimec, Japan), continuously providing heading to the ADCP system directory. Additionally, we have Inertial Navigation System which provide high-precision heading, attitude information, pitch and roll, are stored in ".N2R" data files with a time stamp.
3. DGPS system (Trimble SPS751 & Fugro Multifix ver.5) providing precise ship's position.
4. We used VmDas software version 1.46.5 (TRDI) for data acquisition.
5. To synchronize time stamp of ping with GPS time, the clock of the logging computer is adjusted to GPS time every 1 minute.
6. Fresh water is charged in the sea chest to prevent biofouling at transducer face.
7. The sound speed at the transducer does affect the vertical bin mapping and vertical velocity measurement, is calculated from temperature, salinity (constant value; 35.0 psu) and depth (6.5 m; transducer depth) by equation in Medwin (1975).

Data was configured for 8-m intervals starting 23-m below sea surface. Data was recorded every ping as raw ensemble data (.ENR). Also, 60 seconds and 300 seconds averaged data were recorded as short-term average (.STA) and long-term average (.LTA) data, respectively. Major parameters for the measurement, Direct Command, are shown in

WM = 1	Profiling Mode (1-8)
WN = 100	Number of depth cells (1-128)
WP = 00001	Pings per Ensemble (0-16384)
WS = 800	Depth Cell Size (cm)
WT = 000	Transmit Length (cm) [0 = Bin Length]
WV = 0390	Mode 1 Ambiguity Velocity (cm/s radial)

2.3 Sea surface water monitoring

Masahide WAKITA (JAMSTEC): Principal Investigator
Fuyuki SHIBATA (Marine Works Japan Co. Ltd): Operation Leader
Keitaro MATSUMOTO (Marine Works Japan Co. Ltd)

(1) Objective

Our purpose is to obtain temperature, salinity, dissolved oxygen, and fluorescence data continuously in near-sea surface water.

(2) Parameters

Temperature (surface water)
Salinity (surface water)
Dissolved oxygen (surface water)
Fluorescence (surface water)

(3) Instruments and Methods

The Continuous Sea Surface Water Monitoring System (Marine Works Japan Co. Ltd.) has five sensors and automatically measures temperature, conductivity, dissolved oxygen and fluorescence in near-sea surface water every one minute. This system is located in the “*sea surface monitoring laboratory*” and connected to shipboard LAN-system. Measured data, time, and location of the ship were stored in a data management PC. The near-surface water was continuously pumped up to the laboratory from about 4.5 m water depth and flowed into the system through a vinyl-chloride pipe. The flow rate of the surface seawater was adjusted to be 7-8 dm³ min⁻¹.

a. Instruments

Software

Seamoni-kun Ver.1.30

Sensors

Specifications of the each sensor in this system are listed below.

1) Temperature and Conductivity sensor

Model:	SBE-45, SEA-BIRD ELECTRONICS, INC.
Serial number:	4552788-0264
Measurement range:	Temperature -5 to +35 °C Conductivity 0 to 7 S m ⁻¹
Initial accuracy:	Temperature 0.002 °C Conductivity 0.0003 S m ⁻¹
Typical stability (per month):	Temperature 0.0002 °C Conductivity 0.0003 S m ⁻¹
Resolution:	Temperatures 0.0001 °C Conductivity 0.00001 S m ⁻¹

2) Bottom of ship thermometer

Model: SBE 38, SEA-BIRD ELECTRONICS, INC.
 Serial number: 3852788-0457
 Measurement range: -5 to +35 °C
 Initial accuracy: ±0.001 °C
 Typical stability (per 6 month): 0.001 °C
 Resolution: 0.00025 °C

3) Dissolved oxygen sensor

Model: OPTODE 3835, AANDERAA Instruments.
 Serial number: 985
 Measuring range: 0 - 500 $\mu\text{mol dm}^{-3}$
 Resolution: <1 $\mu\text{mol dm}^{-3}$
 Accuracy: <8 $\mu\text{mol dm}^{-3}$ or 5% whichever is greater
 Settling time: <25 s

4) Dissolved oxygen sensor

Model: RINKO II, ARO-CAR/CAD
 Serial number: 13
 Measuring range: 0 - 540 $\mu\text{mol kg}^{-1}$
 Resolution: 0.1 $\mu\text{mol kg}^{-1}$ or 0.1 % whichever is greater
 Accuracy: 1 $\mu\text{mol kg}^{-1}$ or 0.1 % whichever is greater

5) Fluorometer

Model: C3, TURNER DESIGNS
 Serial number: 2300123

b. Measurements

Periods of measurement during MR12-02 are listed in Table 2.3-1.

Table 2.3-1 Events list of the Sea surface water monitoring during MR12-02

System Date [UTC]	System Time [UTC]	Events	Remarks
2012/06/04	02:56	All the measurements were started and data was available.	Cruise start
2012/06/10	17:38	All the measurements were stopped.	Filter cleaning
2012/06/10	17:58	All the measurements were started and data was available.	Restart
2012/06/16	03:01	All the measurements were stopped.	Filter cleaning
2012/06/16	03:24	All the measurements were started and data was available.	Restart
2012/06/19	04:43	All the measurements were stopped.	Filter cleaning
2012/06/19	05:03	All the measurements were started and data was available.	Restart

2012/06/29	00:42	All the measurements were stopped.	Filter cleaning
2012/06/29	01:10	All the measurements were started and data was available.	Restart
2012/07/10	05:29	All the measurements were stopped.	Cruise End

(5) Preliminary Result

Preliminary data of temperature, salinity, dissolved oxygen and fluorescence at sea surface is shown in Fig. 2.3-1.

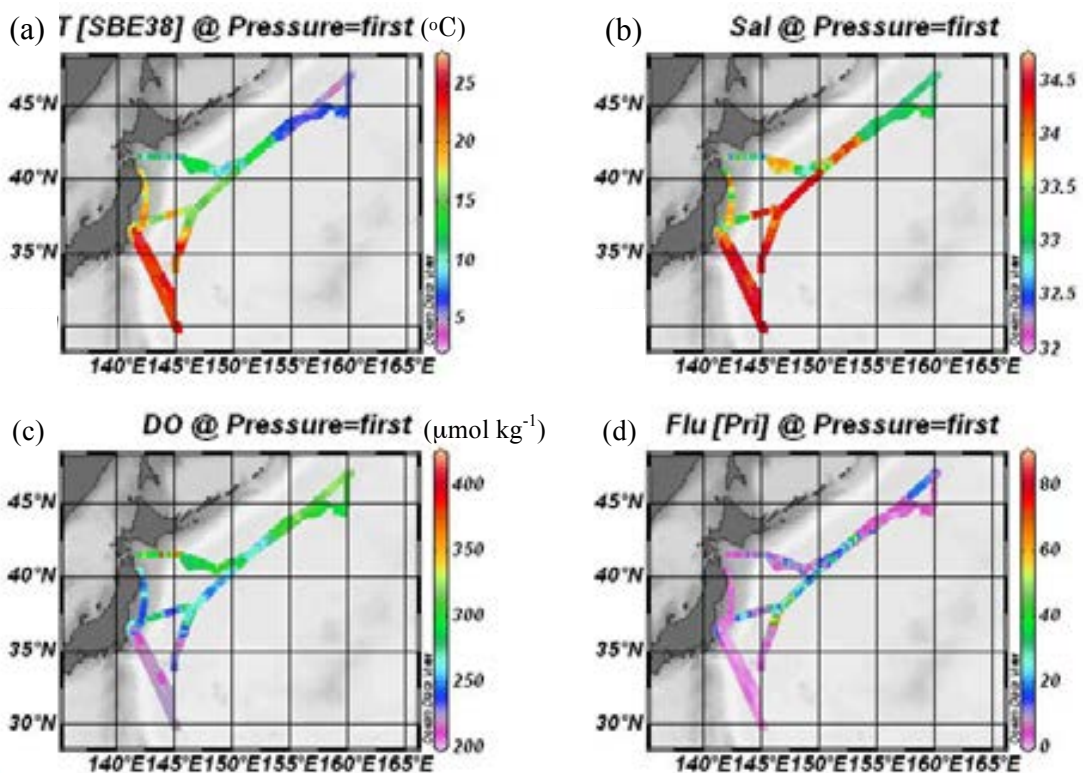


Fig. 2.3-1. Spatial and temporal distribution of (a) temperature[SBE38], (b) salinity, (c) dissolved oxygen[OPTODE] (left bottom) and (d) fluorescence[Primary] (right bottom) in MR12-02 cruise.

We took the surface water samples to compare sensor data with bottle data of salinity, dissolved oxygen and fluorescence. The results are shown in Figs. 2.3-2 - 4. All the salinity samples were analyzed by the Guideline 8400B “AUTOSAL” (see 2.2.2), and dissolve oxygen samples were analyzed by Winkler method (see 2.3), and fluorescence were analyzed by Welschmeyer method (see 3.4.1).

(6) Data archive

All data will be submitted to Chief Scientist.

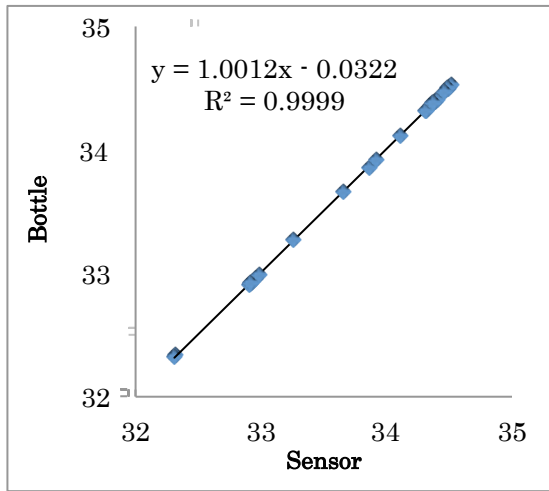


Fig. 2.3-2. Correlation of salinity between sensor and bottle data

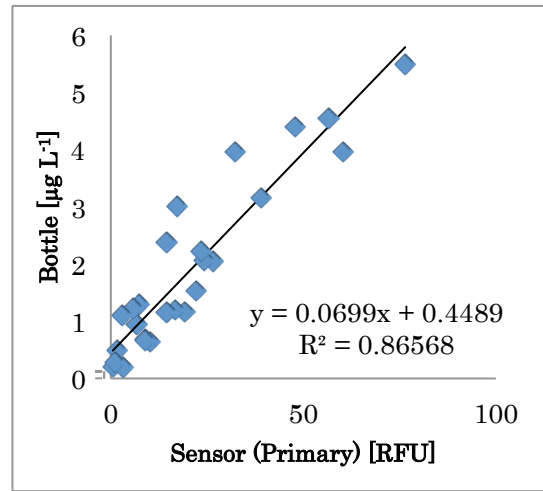


Fig. 2.3-3. Correlation of fluorescence between sensor and bottle chlorophyll data

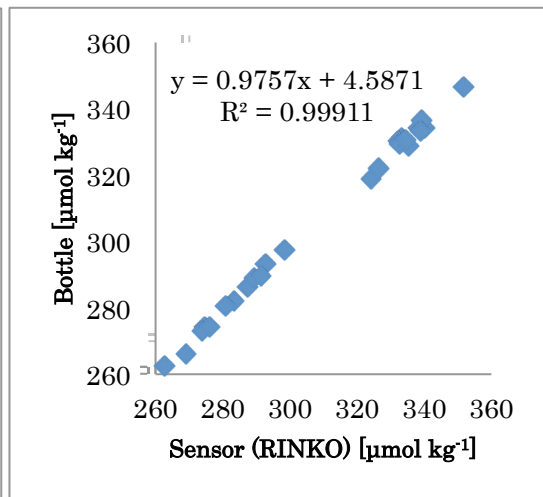
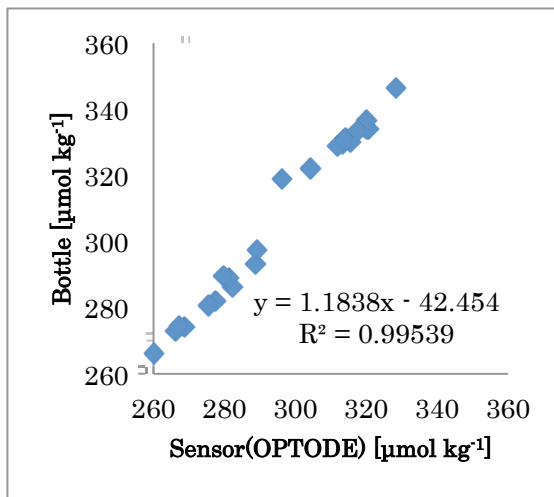


Fig. 2.3-4. Correlation of dissolved oxygen between sensor and bottle data

2.4. Dissolved oxygen

Masahide WAKITA (JAMSTEC): Principal Investigator

Fuyuki SHIBATA (Marine Works Japan Co. Ltd): Operation Leader

Keitaro MATSUMOTO (Marine Works Japan Co. Ltd)

(1) Objectives

Determination of dissolved oxygen in seawater by Winkler titration.

(2) Parameter

Dissolved Oxygen

(3) Instruments and Methods

Following procedure is based on an analytical method, entitled by “Determination of dissolved oxygen in sea water by Winkler titration”, in the WHP Operations and Methods (Dickson, 1996).

a. Instruments

Burette for sodium thiosulfate and potassium iodate;

APB-510 manufactured by Kyoto Electronic Co. Ltd. / 10 cm³ of titration vessel

APB-620 manufactured by Kyoto Electronic Co. Ltd. / 10 cm³ of titration vessel

Detector;

Automatic photometric titrator (DOT-01X) manufactured by Kimoto Electronic Co. Ltd.

Software;

DOT_Terminal Ver.1.2.0

b. Reagents

Pickling Reagent I: Manganese chloride solution (3 mol dm⁻³)

Pickling Reagent II: Sodium hydroxide (8 mol dm⁻³) / sodium iodide solution (4 mol dm⁻³)

Sulfuric acid solution (5 mol dm⁻³)

Sodium thiosulfate (0.025 mol dm⁻³)

Potassium iodide (0.001667 mol dm⁻³)

CSK standard of potassium iodide:

Lot EPJ3885, Wako Pure Chemical Industries Ltd., 0.0100N

c. Sampling

Seawater samples were collected with Niskin bottle attached to the CTD-system and surface bucket sampler. Seawater for oxygen measurement was transferred from sampler to a volume calibrated flask (ca. 100 cm³). Three times volume of the flask of seawater was overflowed. Temperature was measured by digital thermometer during the overflowing. Then two reagent solutions (Reagent I and II) of 0.5 cm³ each were added immediately into the sample flask and the stopper was inserted carefully into the flask. The sample flask was then shaken vigorously to mix the contents and to disperse the precipitate finely throughout. After the precipitate has settled at least halfway down the flask, the flask was shaken again vigorously to disperse the precipitate. The sample flasks containing pickled samples were stored in a laboratory until they were titrated.

d. Sample measurement

At least two hours after the re-shaking, the pickled samples were measured on board. 1 cm³ sulfuric acid solution and a magnetic stirrer bar were added into the sample flask and stirring began. Samples were titrated by sodium thiosulfate solution whose morality was determined by potassium iodate solution. Temperature of sodium thiosulfate during titration was recorded by a digital thermometer. During this cruise, we measured dissolved oxygen concentration using 2 sets of the titration apparatus. Dissolved oxygen concentration ($\mu\text{mol kg}^{-1}$) was calculated by sample temperature during seawater sampling, salinity, flask volume, and titrated volume of sodium thiosulfate solution without the blank. When we measured low concentration samples, titration procedure was adjusted manually.

e. Standardization and determination of the blank

Concentration of sodium thiosulfate titrant was determined by potassium iodate solution. Pure potassium iodate was dried in an oven at 130 °C. 1.7835 g potassium iodate weighed out accurately was dissolved in deionized water and diluted to final volume of 5 dm³ in a calibrated volumetric flask (0.001667 mol dm⁻³). 10 cm³ of the standard potassium iodate solution was added to a flask using a volume-calibrated dispenser. Then 90 cm³ of deionized water, 1 cm³ of sulfuric acid solution, and 0.5 cm³ of pickling reagent solution II and I were added into the flask in order. Amount of titrated volume of sodium thiosulfate (usually 5 times measurements average) gave the morality of sodium thiosulfate titrant.

The oxygen in the pickling reagents I (0.5 cm³) and II (0.5 cm³) was assumed to be 3.8×10^{-8} mol (Murray *et al.*, 1968). The blank due to other than oxygen was determined as follows. 1 and 2 cm³ of the standard potassium iodate solution were added to two flasks respectively using a calibrated dispenser. Then 100 cm³ of deionized water, 1 cm³ of sulfuric acid solution, and 0.5 cm³ of pickling reagent solution II and I each were added into the flask in order. The blank was determined by difference between the first (1 cm³ of KIO₃) titrated volume of the sodium thiosulfate and the second (2 cm³ of KIO₃) one. The results of 3 times blank determinations were averaged.

Table 2.4-1 shows results of the standardization and the blank determination during this cruise.

Date	KIO ₃ ID	Na ₂ S ₂ O ₃	DOT-01(No.1)		DOT-01(No.2)		Stations
			E.P.	Blank	E.P.	Blank	
2012/6/05	20120417-01-01	20110602-09	3.965	0.002	3.964	0.000	E01, E05, E04, E03, E02
2012/6/05	CSK EPJ3885	20110602-09	3.962	0.002	-	-	-
2012/6/10	20120417-01-02	20110602-09	3.966	0.002	3.964	0.001	K02
2012/6/17	20120417-01-03	20110602-09	3.964	0.002	3.962	0.001	KNT, JKO, NKO
2012/6/26	20120417-01-04	20110602-09	3.968	0.002	3.966	0.001	S01cast1,2,6
2012/7/2	20120417-01-05	20110602-09	3.967	0.002	3.965	0.000	S01cast10,KEO,F01

f. Repeatability of sample measurement

Replicate samples were taken at every CTD casts. Total amount of the replicate sample pairs of good measurement was 51. The standard deviation of the replicate measurement was 0.14 $\mu\text{mol kg}^{-1}$ that was calculated by a procedure in Guide to best practices for ocean CO₂

measurements Chapter4 SOP23 Ver.3.0 (2007). Results of replicate samples were shown in Table 2.4-2 and this diagram shown in Fig. 2.4-1and-2.

Table 2.4-2 Results of the standardization and the blank determinations during this cruise.

Layer	Number of replicate sample pairs	Oxygen concentration ($\mu\text{mol kg}^{-1}$) Standard Deviation.
1000m \geq	37	0.11
>1000m	13	0.11
All	50	0.11

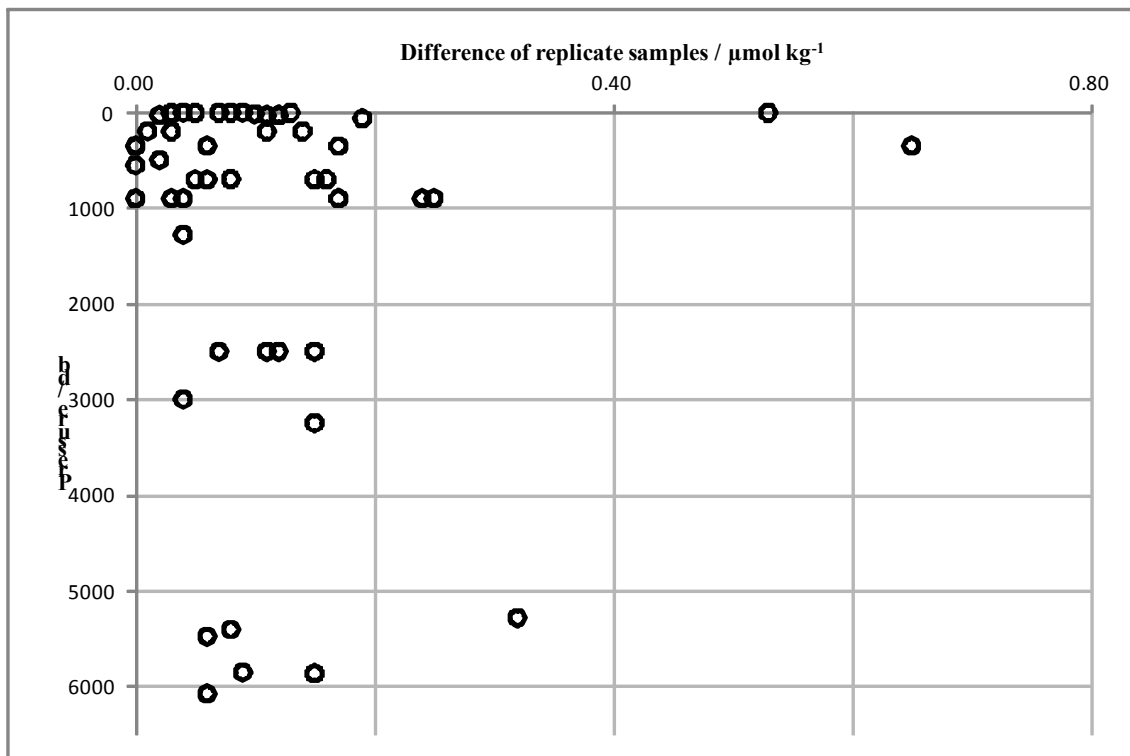


Fig. 2.4-1 Difference of replicate samples against pressure

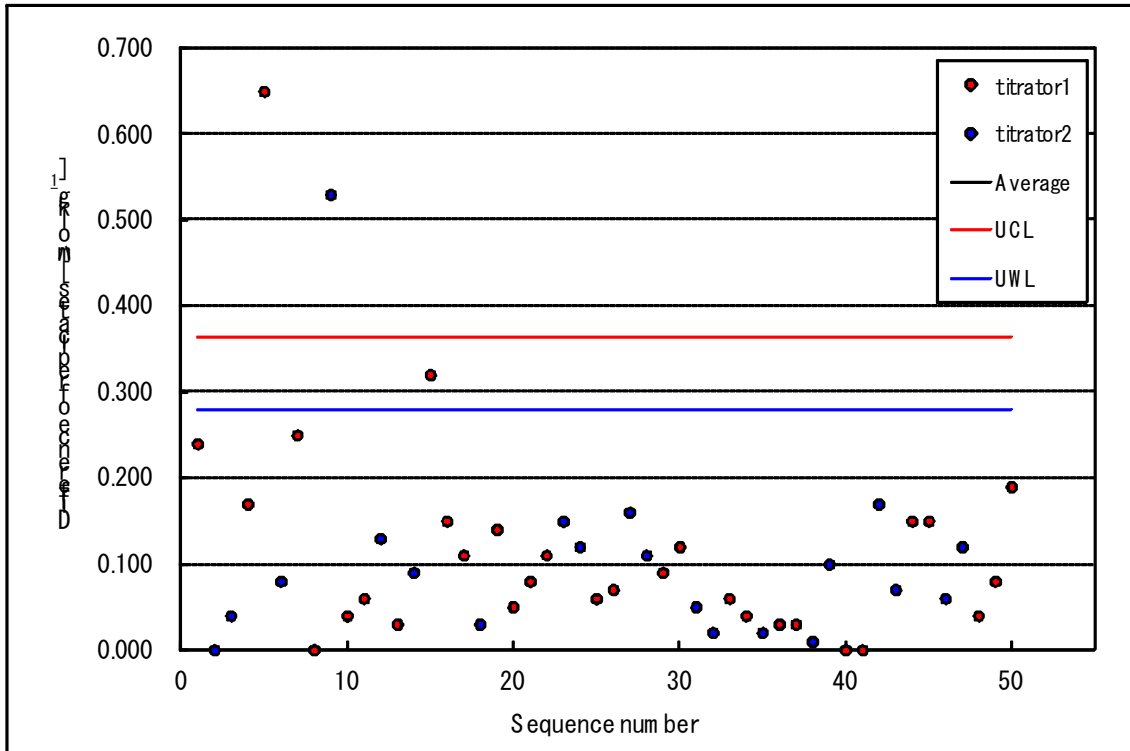


Fig. 2.4-2 Difference of replicate samples against sequence number

(4) Data archive

All data will be submitted to Chief Scientist.

(5) References

- Dickson, A.G., Determination of dissolved oxygen in sea water by Winkler titration. (1996)
- Dickson, A.G., Sabine, C.L. and Christian, J.R. (Eds.), Guide to best practices for ocean CO₂ measurements. (2007)
- Culberson, C.H., WHP Operations and Methods July-1991 "Dissolved Oxygen", (1991)
- Japan Meteorological Agency, Oceanographic research guidelines (Part 1). (1999)
- KIMOTO electric CO. LTD., Automatic photometric titrator DOT-01X Instruction manual

2.5. Nutrients

Michio AOYAMA (Meteorological Research Institute) Principal investigator

Masahide WAKITA (JAMSTEC MIO)

Masanori ENOKI (Department of Marine Science, Marine Works Japan Ltd.)

Elena Hayashi (Department of Marine Science, Marine Works Japan Ltd.)

(1) Objectives

The objectives of nutrients analyses during the R/V Mirai MR12-02 cruise in the Western North Pacific Ocean are as follows:

- Describe the present status of nutrients concentration with excellent comparability.
- Provide excellent nutrients data to biologist onboard MR12-02 to help their study.

(2) Parameters

The determinants are nitrate, nitrite, phosphate, silicate and ammonia in the western North Pacific Ocean.

(3) Summary of nutrients analysis

We made 16 runs for the samples at 12 stations (18 casts) in MR12-02. The total amount of layers of the seawater sample reached up to 558 for MR12-02. We made duplicate measurement at all layers for stations exstations E01, E02, E03, E04, and E05. The station locations for nutrients measurement is shown in Figure 2.5.1

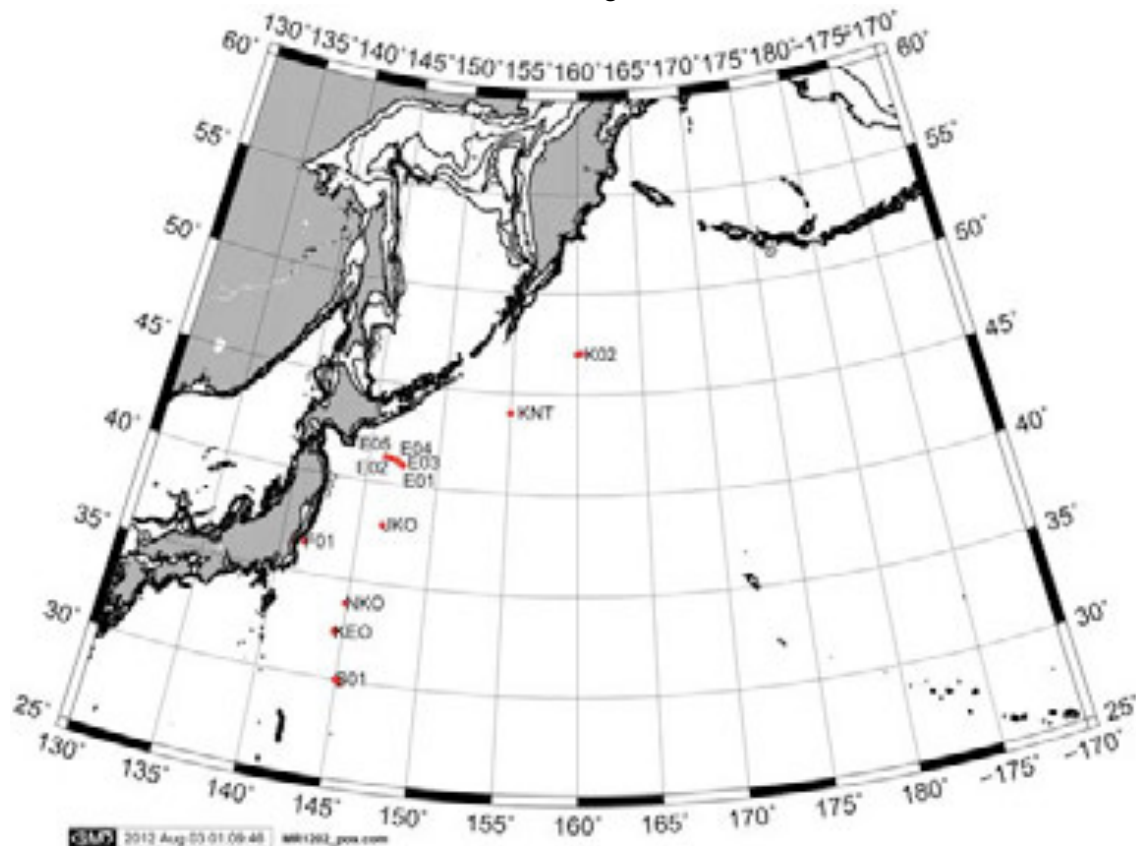


Figure 2.5.1 Sampling positions of nutrients sample.

(4) Instrument and methods

a). Analytical detail using QuAAtro system

The phosphate analysis was a modification of the procedure of Murphy and Riley (1962). Molybdic acid was added to the seawater sample to form phosphomolybdic acid which was in turn reduced to phosphomolybdous acid using L-ascorbic acid as the reductant.

Nitrate + nitrite and nitrite were analyzed according to the modification method of Grasshoff (1970). The sample nitrate was reduced to nitrite in a cadmium tube inside of which was coated with metallic copper. The sample stream with its equivalent nitrite was treated with an acidic, sulfanilamide reagent and the nitrite forms nitrous acid which reacted with the sulfanilamide to produce a diazonium ion. N-1-Naphthylethylene-diamine added to the sample stream then coupled with the diazonium ion to produce a red, azo dye. With reduction of the nitrate to nitrite, both nitrate and nitrite reacted and were measured; without reduction, only nitrite reacted. Thus, for the nitrite analysis, no reduction was performed and the alkaline buffer was not necessary. Nitrate was computed by difference.

The silicate method was analogous to that described for phosphate. The method used was essentially that of Grasshoff et al. (1983), wherein silicomolybdic acid was first formed from the silicate in the sample and added molybdic acid; then the silicomolybdic acid was reduced to silicomolybdous acid, or "molybdenum blue" using ascorbic acid as the reductant. The analytical methods of the nutrients, nitrate, nitrite, silicate and phosphate, during this cruise were same as the methods used in (Kawano et al. 2009). The details of modification of analytical methods used in this cruise are also compatible with the methods described in nutrients section in GO-SHIP repeat hydrography manual (Hydes et al., 2010)

The ammonia in seawater was mixed with an alkaline containing EDTA, ammonia as gas state was formed from seawater. The ammonia (gas) was absorbed in sulfuric acid by way of 0.5 μm pore size membrane filter (ADVANTEC PTFE) at the dialyzer attached to analytical system. The ammonia absorbed in sulfuric acid was determined by coupling with phenol and hypochlorite to form indophenols blue. Wavelength using ammonia analysis was 630 nm, which was absorbance of indophenols blue.

The flow diagrams and reagents for each parameter are shown in Figures 2.5.2 to 2.5.6.

From this cruise, we use LED lamps instead of Krypton lamp for all five channels, therefore we expect better precision of the measurements.

b). Nitrate + Nitrite Reagents

Imidazole (buffer), 0.06 M (0.4 % w/v)

Dissolved 4 g imidazole, $C_3H_4N_2$, in ca. 1000 ml DIW; added 2 ml concentrated HCl. After mixing, 1 ml Triton®X-100 (50 % solution in ethanol) was added.

Sulfanilamide, 0.06 M (1 % w/v) in 1.2M HCl

Dissolved 10 g sulfanilamide, $4-NH_2C_6H_4SO_3H$, in 900 ml of DIW, added 100 ml concentrated HCl. After mixing, 2 ml Triton®X-100 (50 % solution in ethanol) was added.

N-1-Naphthylethylene-diamine dihydrochloride, 0.004 M (0.1 % w/v)

Dissolved 1 g NED, $C_{10}H_7NHCH_2CH_2NH_2 \cdot 2HCl$, in 1000 ml of DIW and added 10 ml concentrated HCl. After mixing, 1 ml Triton®X-100 (50 % solution in ethanol) was added. This reagent was stored in a dark bottle.

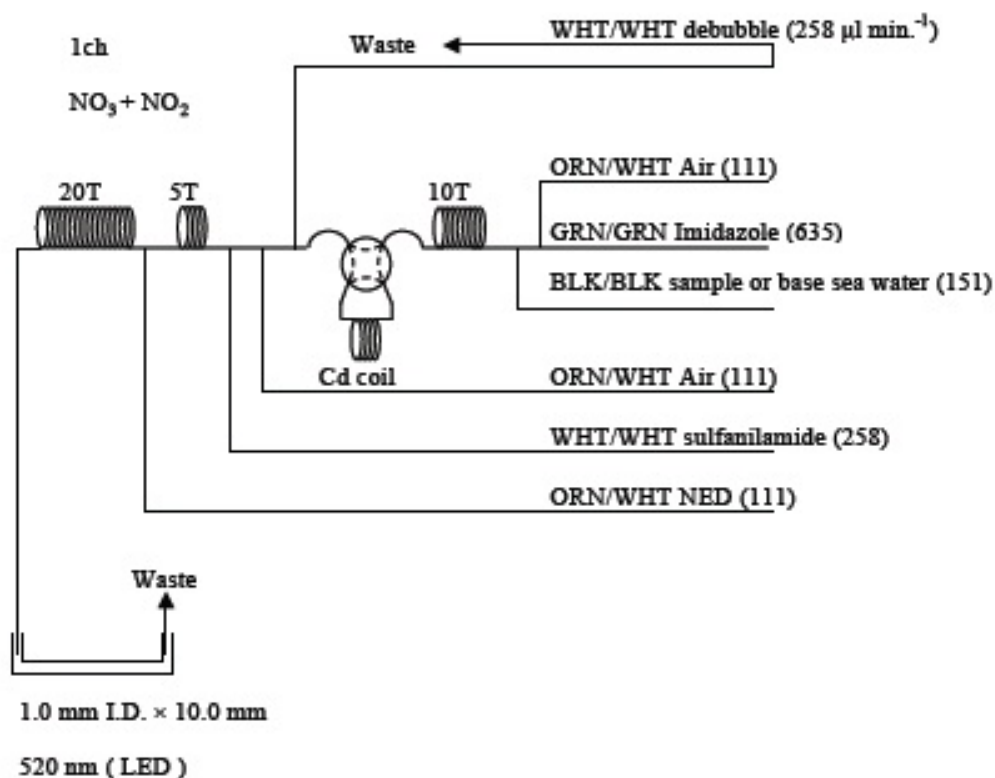


Figure 2.5.2 NO_3+NO_2 (1ch.) Flow diagram.

c). Nitrite Reagents

Sulfanilamide, 0.06 M (1 % w/v) in 1.2 M HCl

Dissolved 10g sulfanilamide, 4-NH₂C₆H₄SO₃H, in 900 ml of DIW, added 100 ml concentrated HCl. After mixing, 2 ml Triton®X-100 (50 % solution in ethanol) was added.

N-1-Naphthylethylene-diamine dihydrochloride, 0.004 M (0.1 % w/v)

Dissolved 1 g NED, C₁₀H₇NHCH₂CH₂NH₂•2HCl, in 1000 ml of DIW and added 10 ml concentrated HCl. After mixing, 1 ml Triton®X-100 (50 % solution in ethanol) was added. This reagent was stored in a dark bottle.

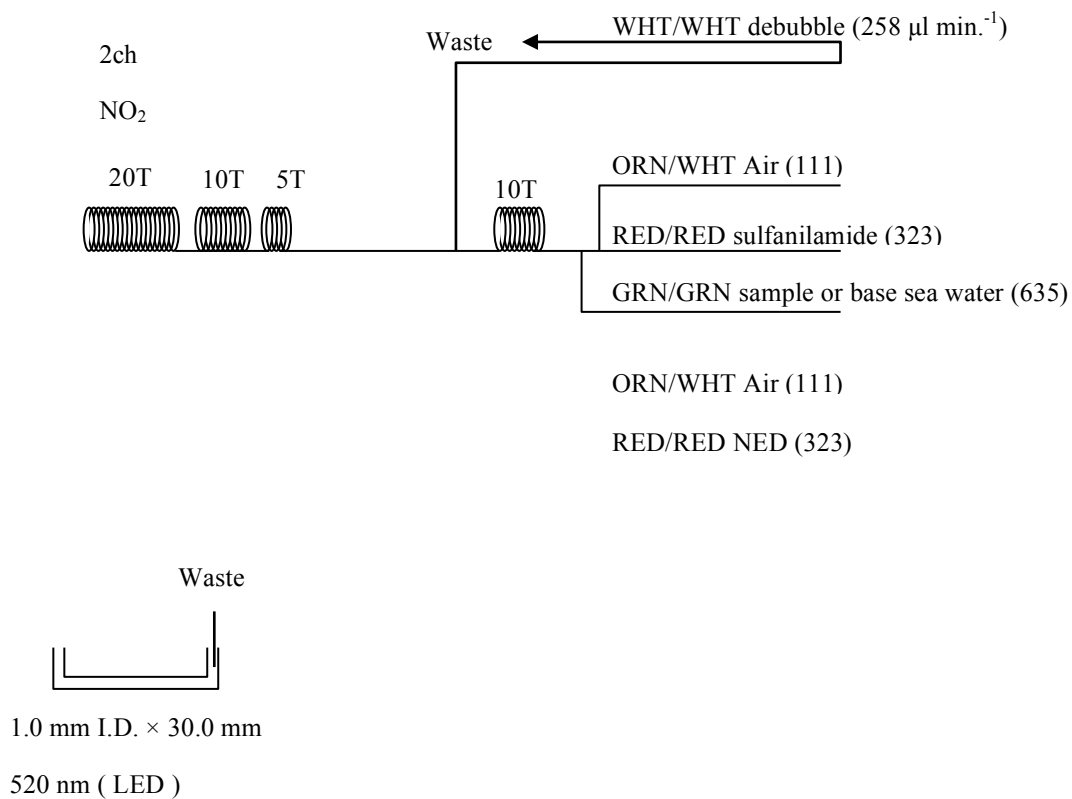


Figure 2.5.3 NO₂ (2ch.) Flow diagram.

d). Silicate Reagents

Molybdc acid, 0.06 M (2 % w/v)

Dissolved 15 g disodium molybdate (VI) dihydrate, $\text{Na}_2\text{M}_0\text{O}_4 \cdot 2\text{H}_2\text{O}$, in 980 ml DIW, added 8 ml concentrated H_2SO_4 . After mixing, 20 ml sodium dodecyl sulphate (15 % solution in water) was added.

Oxalic acid, 0.6 M (5 % w/v)

Dissolved 50 g oxalic acid anhydrous, HOOC:COOH , in 950 ml of DIW.

Ascorbic acid, 0.01M (3 % w/v)

Dissolved 2.5g L (+)-ascorbic acid, $\text{C}_6\text{H}_8\text{O}_6$, in 100 ml of DIW. This reagent was freshly prepared before every measurement.

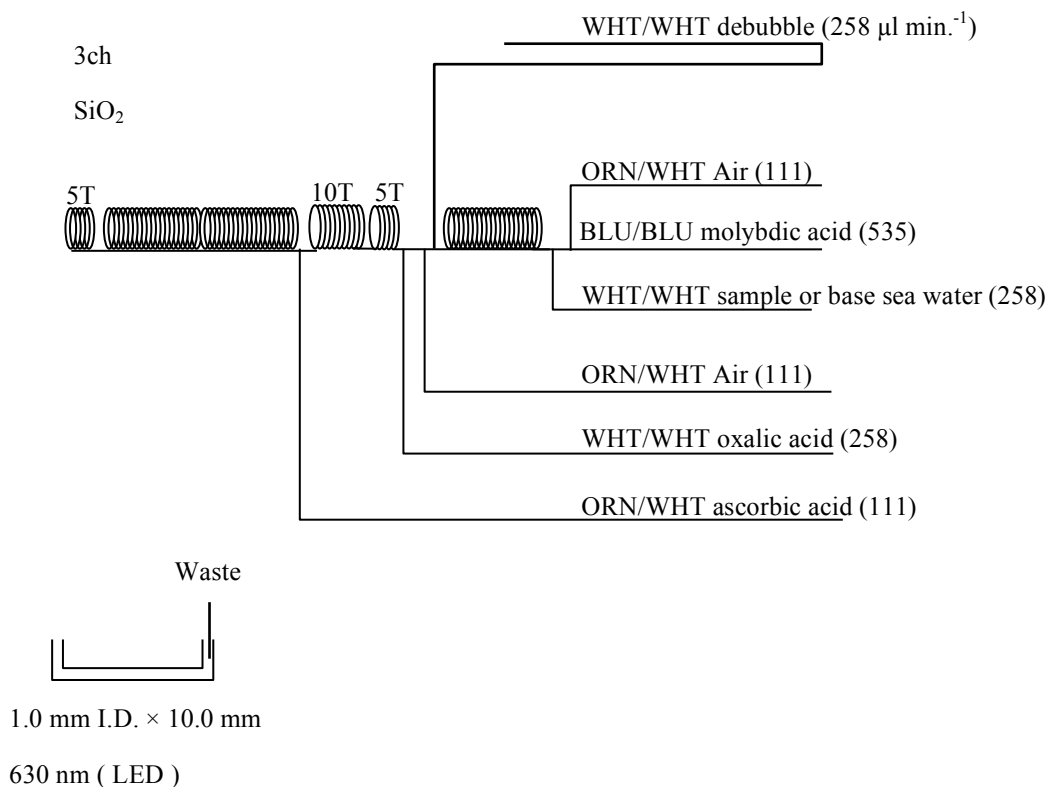


Figure 2.5.4 SiO_2 (3ch.) Flow diagram.

e). Phosphate Reagents

Stock molybdate solution, 0.03M (0.8 % w/v)

Dissolved 8 g disodium molybdate (VI) dihydrate, $\text{Na}_2\text{MoO}_4 \cdot 2\text{H}_2\text{O}$, and 0.17 g antimony potassium tartrate, $\text{C}_8\text{H}_4\text{K}_2\text{O}_{12}\text{Sb}_2 \cdot 3\text{H}_2\text{O}$, in 950 ml of DIW and added 50 ml concentrated H_2SO_4 .

Mixed Reagent

Dissolved 1.2 g L (+)-ascorbic acid, $\text{C}_6\text{H}_8\text{O}_6$, in 150 ml of stock molybdate solution. After mixing, 3 ml sodium dodecyl sulphate (15 % solution in water) was added. This reagent was freshly prepared before every measurement.

Reagent for sample dilution

Dissolved sodium chloride, NaCl , 10 g in ca. 950 ml of DIW, added 50 ml acetone and 4 ml concentrated H_2SO_4 . After mixing, 5 ml sodium dodecyl sulphate (15 % solution in water) was added.

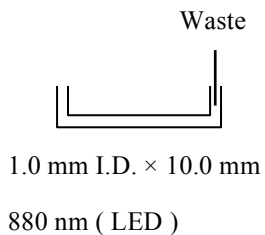
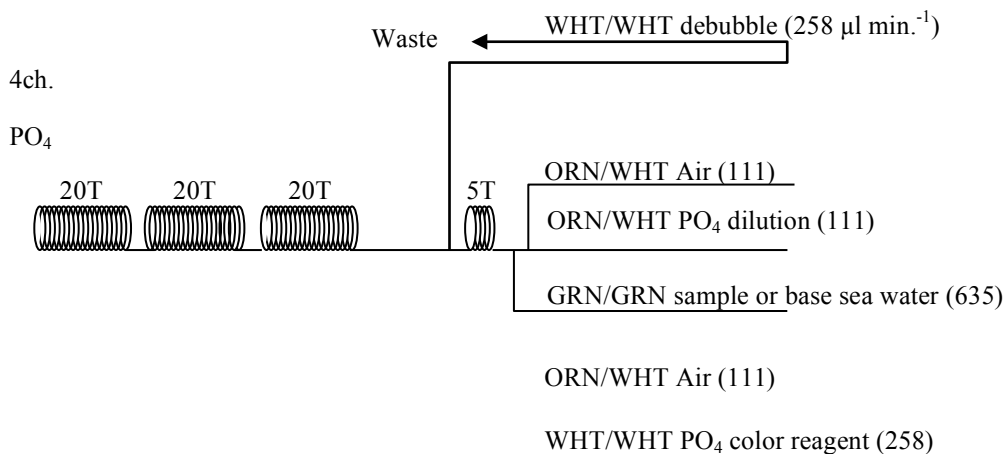


Figure 2.5.5 PO₄ (4ch.) Flow diagram.

f). Ammonia Reagents

EDTA

Dissolved 41 g EDTA (ethylenediaminetetraacetic acid tetrasodium salt), $C_{10}H_{12}N_2O_8Na_4 \cdot 4H_2O$, and 2 g boric acid, H_3BO_3 , in 200 ml of DIW. After mixing, 1 ml Triton®X-100 (30 % solution in DIW) was added. This reagent was prepared at a week about.

NaOH

Dissolved 5 g sodium hydroxide, NaOH, and 16 g EDTA in 100 ml of DIW. This reagent was prepared at a week about.

Stock Nitroprusside

Dissolved 0.25 g sodium pentacyanonitrosylferrate (II), $Na_2[Fe(CN)_5NO]$, in 100 ml of DIW and added 0.2 ml 1N H_2SO_4 . Stored in a dark bottle and prepared at a month about.

Nitroprusside solution

Mixed 4 ml stock nitroprusside and 5 ml 1N H_2SO_4 in 500 ml of DIW. After mixing, 1 ml Triton®X-100 (30 % solution in DIW) was added. This reagent was stored in a dark bottle and prepared at every 2 or 3 days.

Alkaline phenol

Dissolved 10 g phenol, C_6H_5OH , 5 g sodium hydroxide and citric acid, $C_6H_8O_7$, in 200 ml DIW. Stored in a dark bottle and prepared at a week about.

NaClO solution

Mixed 3 ml sodium hypochlorite solution, NaClO, in 47 ml DIW. Stored in a dark bottle and freshly prepared before every measurement. This reagent was prepared 0.3% available chlorine.

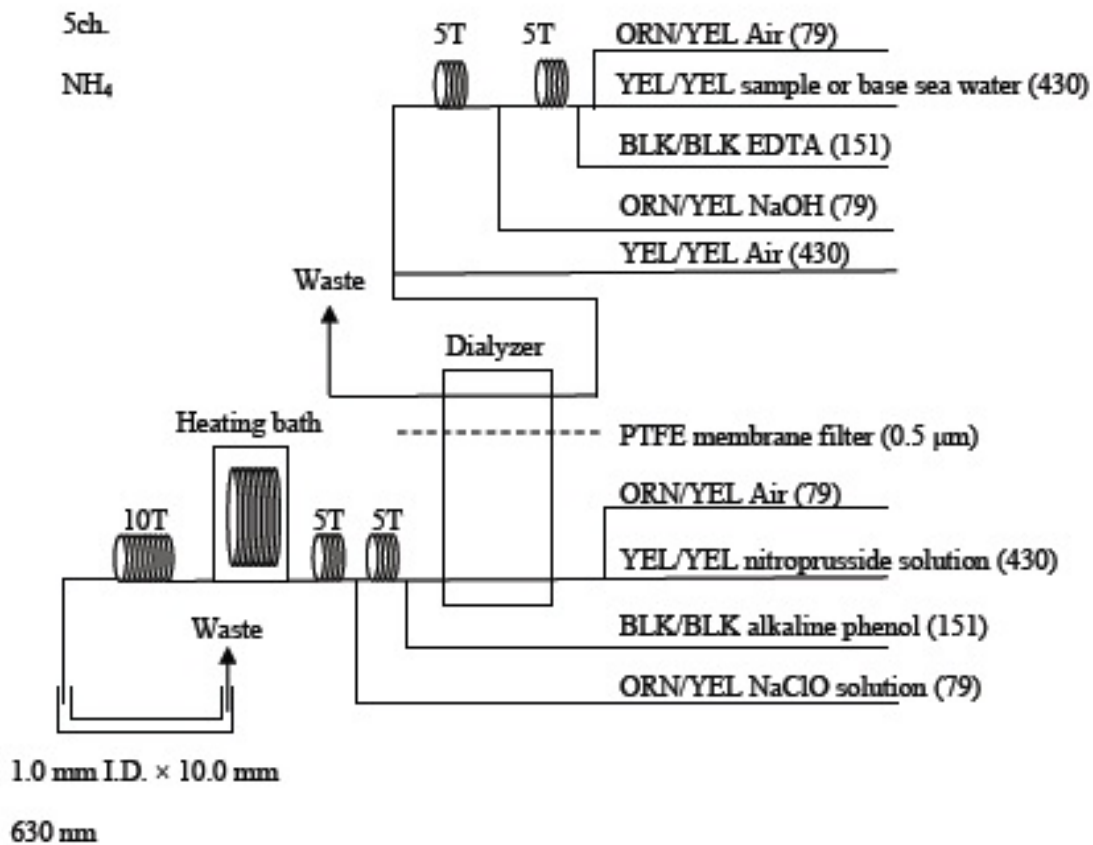


Figure 2.5.6 NH₄ (5ch.) Flow diagram.

g). Sampling procedures

Sampling of nutrients followed that oxygen, salinity and trace gases. Samples were drawn into two of virgin 10 ml polyacrylates vials without sample drawing tubes. These were rinsed three times before filling and vials were capped immediately after the drawing. The vials were put into water bath adjusted to ambient temperature, 22 ± 2 deg. C, in about 30 minutes before use to stabilize the temperature of samples in MR12-02.

No transfer was made and the vials were set an auto sampler tray directly. Samples were analyzed after collection basically within 24 hours in MR12-02.

h). Data processing

Raw data from QuAAtro was treated as follows:

- Checked baseline shift.
- Checked the shape of each peak and positions of peak values taken, and then changed the positions of peak values taken if necessary.
- Carry-over correction and baseline drift correction were applied to peak heights of each samples followed by sensitivity correction.
- Baseline correction and sensitivity correction were done basically using liner regression.
- Loaded pressure and bottle salinity from Seafile data to calculate density of seawater.
- Calibration curves to get nutrients concentration were assumed second order equations.

(5) Nutrients standards

a). Volumetric laboratory ware of in-house standards

All volumetric glass ware and polymethylpentene (PMP) ware used were gravimetrically calibrated. Plastic volumetric flasks were gravimetrically calibrated at the temperature of use within 0 to 4 K.

Volumetric flasks

Volumetric flasks of Class quality (Class A) were used because their nominal tolerances are 0.05 % or less over the size ranges likely to be used in this work. Class A flasks were made of borosilicate glass, and the standard solutions were transferred to plastic bottles as quickly as possible after they were made up to volume and well mixed in order to prevent excessive dissolution of silicate from the glass. PMP volumetric flasks were gravimetrically calibrated and used only within 0 to 4 K of the calibration temperature.

The computation of volume contained by glass flasks at various temperatures other than the calibration temperatures were done by using the coefficient of linear expansion of borosilicate crown glass.

Because of their larger temperature coefficients of cubical expansion and lack of tables constructed for these materials, the plastic volumetric flasks were gravimetrically calibrated over the temperature range of intended use and used at the temperature of calibration within 0 to 4 K. The weights obtained in the calibration weightings were corrected for the density of water and air buoyancy.

Pipettes and pipettors

All pipettes had nominal calibration tolerances of 0.1 % or better. These were gravimetrically calibrated in order to verify and improve upon this nominal tolerance.

b). Reagents, general considerations

Specifications

For nitrate standard, “potassium nitrate 99.995 suprapur®” provided by Merck, CAS No.: 7757-91-1, was used.

For phosphate standard, “potassium dihydrogen phosphate anhydrous 99.995 suprapur®” provided by Merck, CAS No.: 7778-77-0, was used.

For nitrite standard, “sodium nitrite” provided by Wako, CAS No.: 7632-00-0, was used. The assay of nitrite salts was determined according JIS K8019 were 98.31%. We used that value to adjust the weights taken.

For the silicate standard, we use “Silicon standard solution SiO₂ in NaOH 0.5 mol/l CertiPUR®” provided by Merck, CAS No.: 1310-73-2, of which lot number HC074650 was used. The silicate concentration was certified by NIST-SRM3150 with the uncertainty of 0.5 %. Factor of HC074650 was signed 1.000, however we reassigned the factor as 0.975 from the result of comparison among HC814662, HC074650 and RMNS in MR10-05 cruise.

For ammonia standard, “ammonia sulfate” provided by Wako, CAS No.: 7783-20-2, was used.

Ultra pure water

Ultra pure water (Milli-Q) freshly drawn was used for preparation of reagent, standard solutions and for measurement of reagent and system blanks.

Low-nutrients seawater (LNSW)

Surface water having low nutrient concentration was taken and filtered using 0.45 µm

pore size membrane filter. This water was stored in 20 liter cubitainer with paper box. The concentrations of nutrient of this water were measured carefully in Jan 2011.

Treatment of silicate standard due to high alkalinity

Since the silicon standard solution Merck CertiPUR® is in NaOH 0.5 mol/l, we need to dilute and neutralize to avoid make precipitation of MgOH₂ etc. When we make B standard, silicon standard solution is diluted by factor 12 with pure water and neutralized by HCl 1.0 mol/l to be about 7. After that B standard solution is used to prepare C standards.

c). Concentrations of nutrients for A, B and C standards

Concentrations of nutrients for A, B and C standards (working standards) were set as shown in Table 2.5.1. The working standard was prepared according recipes as shown in Table 2.5.2. All volumetric laboratory tools were calibrated prior the cruise as stated in chapter (5). Then the actual concentration of nutrients in each fresh standard was calculated based on the ambient, solution temperature and determined factors of volumetric laboratory wares.

The calibration curves for each run were obtained using 5 levels working standards, C-1, C-2, C-3, C-4 and C-5.

Table 2.5.1 Nominal concentrations of nutrients for A, B and C standards.

	A	B	C-1	C-2	C-3	C-4	C-5
NO ₃ (μM)	22000	900	0.03	9.2	18.3	36.6	55.0
NO ₂ (μM)	4000	20	0.00	0.2	0.4	0.8	1.2
SiO ₂ (μM)	36000	2800	0.80	28	56	111	167
PO ₄ (μM)	3000	60	0.04	0.6	1.2	2.4	3.6
NH ₄ (μM)	4000	200	0.00	0.0	2.0	4.0	6.0

Table 2.5.2 Working standard recipes.

C Std.	B-1 Std.	B-2 Std.	B-3 Std.	DIW
C-1	0 ml	0 ml	0 ml	75 ml
C-2	5 ml	5 ml	0 ml	65 ml
C-3	10 ml	10 ml	5 ml	40 ml
C-4	20 ml	20 ml	10 ml	25 ml
C-5	30 ml	30 ml	15 ml	0 ml

B-1 Std.: Mixture of nitrate, silicate and phosphate.

B-2 Std.: Nitrite.

B-3 Std.: Ammonia.

d). Renewal of in-house standard solutions

In-house standard solutions as stated in paragraph c) were renewed as shown in Table 2.5.3(a) to (c).

Table 2.5.3(a) Timing of renewal of in-house standards.

NO ₃ , NO ₂ , SiO ₂ , PO ₄ , NH ₄	Renewal
A-1 Std. (NO ₃)	maximum 1 month
A-2 Std. (NO ₂)	maximum 1 month
A-3 Std. (SiO ₂)	commercial prepared solution
A-4 Std. (PO ₄)	maximum 1 month
A-5 Std. (NH ₄)	maximum 1 month
B-1 Std. (mixture of NO ₃ , SiO ₂ , PO ₄)	8 days
B-2 Std. (NO ₂)	8 days
B-3 Std. (NH ₄)	8 days

Table 2.5.3(b) Timing of renewal of working calibration standards.

Working standards	Renewal
C Std. (mixture of B-1, B-2 and B-3 Std.)	24 hours

Table 2.5.3(c) Timing of renewal of in-house standards for reduction estimation.

Reduction estimation	Renewal
D-1 Std. (3600 µM NO ₃)	8 days
43 µM NO ₃	when C Std. renewed
47 µM NO ₂	when C Std. renewed

(6) Reference material of nutrients in seawater

To get the more accurate and high quality nutrients data to achieve the objectives stated above, huge numbers of the bottles of the reference material of nutrients in seawater (hereafter RMNS) are prepared (Aoyama et al., 2006, 2007, 2008, 2009). In the previous worldwide expeditions, such as CLIVAR cruises, the higher reproducibility and precision of nutrients measurements were required (Joyce and Corry, 1994). Since no standards were

available for the measurement of nutrients in seawater at that time, the requirements were described in term of reproducibility. The required reproducibility was 1 %, 1 to 2 %, 1 to 3 % for nitrate, phosphate and silicate, respectively. Although nutrient data from the WOCE one-time survey was of unprecedented quality and coverage due to much care in sampling and measurements, the differences of nutrients concentration at crossover points are still found among the expeditions (Aoyama and Joyce, 1996, Mordy et al., 2000, Gouretski and Jancke, 2001). For instance, the mean offset of nitrate concentration at deep waters was 0.5 $\mu\text{mol kg}^{-1}$ for 345 crossovers at world oceans, though the maximum was 1.7 $\mu\text{mol kg}^{-1}$ (Gouretski and Jancke, 2001). At the 31 crossover points in the Pacific WHP one-time lines, the WOCE standard of reproducibility for nitrate of 1 % was fulfilled at about half of the crossover points and the maximum difference was 7 % at deeper layers below 1.6 deg. C in potential temperature (Aoyama and Joyce, 1996).

During the period from 2003 to 2012, RMNS were used to keep comparability of nutrients measurement among the 9 cruises of CLIVAR project (Sato et al., 2010, Aoyama et al., 2012) , MR10-05 cruise for Arctic research (Aoyama et al., 2010) and MR10-06 cruise for “Change in material cycles and ecosystem by the climate change and its feedback” (Aoyama et al., 2011).

a). RMNS for this cruise

RMNS lots BA, AS, AY, BT, BD, and BF, which cover full range of nutrients concentrations in the North Pacific Ocean are prepared. These RMNS assignment were completely done based on random number. The RMNS bottles were stored at a room in the ship, REAGENT STORE, where the temperature was maintained 19 - 27 deg. C.

b). Assigned concentration for RMNSs

We assigned nutrients concentrations for RMNS lots BA, BS, BU, AY, BT, BD and BF as shown in Table 2.5.4.

Table 2.5.4 Assigned concentration of RMNSs.

	Nitrate	Phosphate	Silicate	Nitrite	Ammonia
BA	0.07	0.068	1.60	0.02	0.97
BS	0.07	0.064	1.61	0.02	-
BU	3.97	0.379	20.30	0.07	
AY	5.60	0.516	29.42	0.62	0.81
BT	18.21	1.320	41.00	0.47	-
BD	29.86	2.194	64.39	0.05	2.93
BF	41.39	2.809	150.23	0.02	3.05

(7) Quality control

a). Precision of nutrients analyses during the cruise

Precision of nutrients analyses during the cruise was evaluated based on the 5 to 7 measurements, which are measured every 9 to 13 samples, during a run at the concentration of C-5 std. Summary of precisions are shown as shown in Table 2.5.5. Analytical precisions

previously evaluated were 0.08 % for nitrate, 0.10 % for phosphate and 0.07 % for silicate in CLIVAR P21 revisited cruise of MR09-01 cruise in 2009, respectively. During this cruise, analytical precisions were 0.14 % for nitrate, 0.20 % for phosphate, 0.14 % for silicate, 0.29 % for nitrite and 0.40 % for ammonia in terms of median of precision, respectively. Then we can conclude that the analytical precisions for nitrate, phosphate and silicate were maintained throughout this cruise.

Table 2.5.5 Summary of precision based on the replicate analyses.

	Nitrate CV %	Nitrite CV %	Phosphate CV %	Silicate CV %	Ammonia CV%
Median	0.14	0.29	0.20	0.14	0.40
Mean	0.14	0.31	0.21	0.14	0.42
Maximum	0.18	0.77	0.44	0.26	0.50
Minimum	0.08	0.13	0.12	0.05	0.30
N	16	16	16	16	5

b). Carry over

We can also summarize the magnitudes of carry over throughout the cruise. These are small enough within acceptable levels as shown in Table 2.5.6.

Table 2.5.6 Summary of carry over throughout MR12-02.

	Nitrate %	Nitrite %	Phosphate %	Silicate %	Ammonia %
Median	0.18	0.35	0.35	0.19	0.67
Mean	0.18	0.36	0.35	0.19	0.63
Maximum	0.37	0.99	0.49	0.33	0.88
Minimum	0.00	0.00	0.14	0.05	0.27
N	16	16	16	16	5

c). Estimation of uncertainty of phosphate, nitrate and silicate concentrations

Empirical equations, eq. (1), (2) and (3) to estimate uncertainty of measurement of phosphate, nitrate and silicate are used based on measurements of 140 sets of RMNSs during the cruise MR09-01 in 2009. These empirical equations are as follows, respectively.

Phosphate Concentration C_p in $\mu\text{mol kg}^{-1}$:

$$\text{Uncertainty of measurement of phosphate (\%)} = 0.000 + 0.378 * (1/C_p) + 0.00430 * (1/C_p) * (1/C_p) \quad \text{--- (1)}$$

where C_p is phosphate concentration of sample.

Nitrate Concentration C_n in $\mu\text{mol kg}^{-1}$:

$$\text{Uncertainty of measurement of nitrate (\%)} = 0.142 + 0.431 * (1/C_n) + 0.114 * (1/C_n) * (1/C_n) \quad \text{--- (2)}$$

where C_n is nitrate concentration of sample.

Silicate Concentration C_s in $\mu\text{mol kg}^{-1}$:

$$\text{Uncertainty of measurement of silicate (\%)} = 0.047 + 4.99 * (1/C_s) + 1.879 * (1/C_s) * (1/C_s) \quad \text{--- (3)}$$

where Cs is silicate concentration of sample.

d). Empirical equation for uncertainty of ammonia

Since we do not have RM for ammonia, empirical equation of uncertainty of ammonia is created based on differences of duplicate measurements of samples taken from same niskin bottles during the cruise MR10-05. We use 102 pair of duplicate measurements and concentration of ammonia ranged from 0.02 to 1.1 $\mu\text{mol kg}^{-1}$ among all 122 pair.

Based on differences between two measurements, we estimated an empirical equation between uncertainty of measurement of ammonia and ammonia concentration where we adapted $k = 1$ as follows;

Ammonia Concentration Ca in $\mu\text{mol kg}^{-1}$:

$$\text{Uncertainty of measurement of ammonia (\%)} = 5.135 + 1.88 * (1/\text{Ca}) - 0.0099 * (1/\text{Ca}) * (1/\text{Ca}) \quad \text{--- (4)}$$

where Ca is ammonia concentration of sample.

For 28 pair, we see larger uncertainty than that estimated using empirical equation above.

(8) Problems/improvements occurred and solutions.

We observed relatively large noise during the measurements, we changed smoothing rate from 4 to 8 or 12 for CH2. We also reduce gains for CH2 from 113 to 98, and for CH4 from 182 to 158, respectively, to reduce apparent noise. These changes did not affect sample concentrations within the uncertainties. At the stations JKEO01, NKEO01, S0101 and S0102, we observed noisy plateaus for higher concentration samples for CH3, then we changed pump tubes for CH3 before we did a run for S010607. The noisy plateaus problem was solved.

(9) Station list

Table 2.5.7 List of stations

Cruise	Station	Cast	Year	Month	Date	Latitude	Longitude	
MR12-02	E01	01	2012	6	5	40.935	N	147.489 E
MR12-02	E05	01	2012	6	5	41.300	N	146.176 E
MR12-02	E04	01	2012	6	5	41.236	N	146.548 E
MR12-02	E03	01	2012	6	6	41.146	N	146.980 E
MR12-02	E02	01	2012	6	6	41.101	N	147.161 E
MR12-02	K02	01	2012	6	10	46.994	N	159.998 E
MR12-02	K02	02	2012	6	10	46.994	N	160.005 E
MR12-02	K02	06	2012	6	11	47.000	N	160.005 E
MR12-02	K02	08	2012	6	13	47.059	N	160.294 E
MR12-02	K02	09	2012	6	13	47.017	N	160.051 E
MR12-02	KNT	01	2012	6	17	44.001	N	154.999 E
MR12-02	JKO	01	2012	6	19	37.939	N	146.599 E
MR12-02	NKO	01	2012	6	21	33.841	N	144.902 E
MR12-02	S01	01	2012	6	26	30.007	N	144.994 E
MR12-02	S01	02	2012	6	27	29.996	N	144.997 E
MR12-02	S01	06	2012	6	30	29.832	N	145.237 E
MR12-02	S01	07	2012	6	30	29.923	N	145.096 E
MR12-02	S01	10	2012	7	2	30.033	N	144.993 E
MR12-02	KEO	01	2012	7	3	32.318	N	144.462 E

MR12-02	KEO	02	2012	7	4	32.401	N	144.493	E
MR12-02	F01	01	2012	7	7	36.497	N	141.511	E

(10) Data archive

All data will be submitted to JAMSTEC Data Management Office (DMO) and is currently under its control.

References

- Aminot, A. and Kerouel, R. 1991. Autoclaved seawater as a reference material for the determination of nitrate and phosphate in seawater. *Anal. Chim. Acta*, 248: 277-283.
- Aminot, A. and Kirkwood, D.S. 1995. Report on the results of the fifth ICES intercomparison exercise for nutrients in sea water, ICES coop. Res. Rep. Ser., 213.
- Aminot, A. and Kerouel, R. 1995. Reference material for nutrients in seawater: stability of nitrate, nitrite, ammonia and phosphate in autoclaved samples. *Mar. Chem.*, 49: 221-232.
- Aoyama M., and Joyce T.M. 1996, WHP property comparisons from crossing lines in North Pacific. In Abstracts, 1996 WOCE Pacific Workshop, Newport Beach, California.
- Aoyama, M., 2006: 2003 Intercomparison Exercise for Reference Material for Nutrients in Seawater in a Seawater Matrix, Technical Reports of the Meteorological Research Institute No.50, 91pp, Tsukuba, Japan.
- Aoyama, M., Susan B., Minhan, D., Hideshi, D., Louis, I. G., Kasai, H., Roger, K., Nurit, K., Doug, M., Murata, A., Nagai, N., Ogawa, H., Ota, H., Saito, H., Saito, K., Shimizu, T., Takano, H., Tsuda, A., Yokouchi, K., and Agnes, Y. 2007. Recent Comparability of Oceanographic Nutrients Data: Results of a 2003 Intercomparison Exercise Using Reference Materials. *Analytical Sciences*, 23: 1151-1154.
- Aoyama M., J. Barwell-Clarke, S. Becker, M. Blum, Braga E. S., S. C. Coverly, E. Czobik, I. Dahllof, M. H. Dai, G. O. Donnell, C. Engelke, G. C. Gong, Gi-Hoon Hong, D. J. Hydes, M. M. Jin, H. Kasai, R. Kerouel, Y. Kiyomono, M. Knockaert, N. Kress, K. A. Kroglund, M. Kumagai, S. Leterme, Yarong Li, S. Masuda, T. Miyao, T. Moutin, A. Murata, N. Nagai, G. Nausch, M. K. Ngirchchol, A. Nybakk, H. Ogawa, J. van Ooijen, H. Ota, J. M. Pan, C. Payne, O. Pierre-Duplessix, M. Pujo-Pay, T. Raabe, K. Saito, K. Sato, C. Schmidt, M. Schuett, T. M. Shammon, J. Sun, T. Tanhua, L. White, E.M.S. Woodward, P. Worsfold, P. Yeats, T. Yoshimura, A. Youenou, J. Z. Zhang, 2008: 2006 Intercomparison Exercise for Reference Material for Nutrients in Seawater in a Seawater Matrix, Technical Reports of the Meteorological Research Institute No. 58, 104pp.
- Aoyama, M., Nishino, S., Nishijima, K., Matsushita, J., Takano, A., Sato, K., 2010a. Nutrients, In: R/V Mirai Cruise Report MR10-05. JAMSTEC, Yokosuka, pp. 103-122.
- Aoyama, M., Matsushita, J., Takano, A., 2010b. Nutrients, In: MR10-06 preliminary cruise report. JAMSTEC, Yokosuka, pp. 69-83
- Gouretski, V.V. and Jancke, K. 2001. Systematic errors as the cause for an apparent deep water property variability: global analysis of the WOCE and historical hydrographic data • REVIEW ARTICLE, *Progress In Oceanography*, 48: Issue 4, 337-402.
- Grasshoff, K., Ehrhardt, M., Kremling K. et al. 1983. *Methods of seawater analysis*. 2nd rev. Weinheim: Verlag Chemie, Germany, West.
- Hydes, D.J., Aoyama, M., Aminot, A., Bakker, K., Becker, S., Coverly, S., Daniel, A., Dickson, A.G., Grosso, O., Kerouel, R., Ooijen, J. van, Sato, K., Tanhua, T., Woodward, E.M.S., Zhang, J.Z., 2010. Determination of Dissolved Nutrients (N, P, Si) in Seawater with High Precision and Inter-Comparability Using Gas-Segmented Continuous Flow Analysers, In: GO-SHIP Repeat Hydrography Manual: A Collection of Expert Reports and Guidelines. IOCCP Report No. 14, ICPO Publication Series No 134.
- Joyce, T. and Corry, C. 1994. Requirements for WOCE hydrographic programmed data reporting. WHPO Publication, 90-1, Revision 2, WOCE Report No. 67/91.
- Kawano, T., Uchida, H. and Doi, T. WHP P01, P14 REVISIT DATA BOOK, (Ryoin Co., Ltd., Yokohama, 2009).
- Kirkwood, D.S. 1992. Stability of solutions of nutrient salts during storage. *Mar. Chem.*, 38 :

151-164.

- Kirkwood, D.S. Aminot, A. and Perttila, M. 1991. Report on the results of the ICES fourth intercomparison exercise for nutrients in sea water. ICES coop. Res. Rep. Ser., 174.
- Mordy, C.W., Aoyama, M., Gordon, L.I., Johnson, G.C., Key, R.M., Ross, A.A., Jennings, J.C. and Wilson. J. 2000. Deep water comparison studies of the Pacific WOCE nutrient data set. Eos Trans-American Geophysical Union. 80 (supplement), OS43.
- Murphy, J., and Riley, J.P. 1962. *Analytica chim. Acta* 27, 31-36.
- Sato, K., Aoyama, M., Becker, S., 2010. RMNS as Calibration Standard Solution to Keep Comparability for Several Cruises in the World Ocean in 2000s. In: Aoyama, M., Dickson, A.G., Hydes, D.J., Murata, A., Oh, J.R., Roose, P., Woodward, E.M.S., (Eds.), *Comparability of nutrients in the world's ocean*. Tsukuba, JAPAN: MOTHER TANK, pp 43-56.
- Uchida, H. & Fukasawa, M. WHP P6, A10, I3/I4 REVISIT DATA BOOK Blue Earth Global Expedition 2003 1, 2, (Aiwa Printing Co., Ltd., Tokyo, 2005).

2.6. pH

Masahide WAKITA (JAMSTEC MIO): Principal Investigator
Tomonori WATAI (MWJ)
Emi DEGUCHI (MWJ)

(1) Objective

Since the global warming is becoming an issue world-widely, studies on the greenhouse gases such as CO₂ are drawing high attention. The ocean plays an important role in buffering the increase of atmospheric CO₂, and studies on the exchange of CO₂ between the atmosphere and the sea becomes highly important. Oceanic biosphere, especially primary production, has an important role concerned to oceanic CO₂ cycle through its photosynthesis and respiration. However, the diverseness and variability of the biological system make difficult to reveal their mechanism and quantitative understanding of CO₂ cycle. Dissolved CO₂ in water alters its appearance into several species, but the concentrations of the individual species of CO₂ system in solution cannot be measured directly. However, two of the four measurable parameters (alkalinity, total dissolved inorganic carbon, pH and pCO₂) can estimate each concentration of CO₂ system (Dickson et al., 2007). Seawater acidification associated with CO₂ uptake into the ocean possibly changes oceanic ecosystem and CO₂ garners in Ocean recently. We here report on board measurements of pH during MR12-02 cruise.

(2) Methods, Apparatus and Performance

(2)-1 Seawater sampling

Seawater samples were collected by 12 liter Niskin bottles mounted on the CTD/Carousel Water Sampling System and a bucket at 8 stations. Among these stations, deep and shallow casts were carried out for 2 stations. Seawater was sampled in a 100 ml glass bottle that was previously soaked in 5 % non-phosphoric acid detergent (pH13) solution at least 3 hours and was cleaned by fresh water for 5 times and Milli-Q ultrapure water for 3 times. A sampling silicone rubber tube with PFA tip was connected to the Niskin bottle when the sampling was carried out. The glass bottles were filled from the bottom smoothly, without rinsing, and were overflowed for 2 times bottle volume (about 10 seconds) with care not to leave any bubbles in the bottle. The water in the bottle was sealed by a glass made cap gravimetrically fitted to the bottle mouth without additional force. After collecting the samples on the deck, the bottles were carried into the lab and put in the water bath kept about 25 deg C before the measurement.

(2)-2 Seawater analyses

pH (-log[H⁺]) of the seawater was measured potentiometrically in the glass bottles. The pH / Ion meter (Radiometer PHM240) is used to measure the electromotive force (e.m.f.) between the glass electrode cell (Radiometer pHG201) and the reference electrode cell (Radiometer REF201) in the sample with its temperature controlled to 25 +/- 0.15 deg C.

To calibrate the electrodes, the TRIS buffer (Lot=120419-1: pH= 8.0905 pH units at 25 deg C, DelValls and Dickson, 1998) and AMP buffer (Lot=120420: pH=6.7837 pH units at 25 deg C, Dickson and Goyet, 1994) in the synthetic seawater (Total hydrogen ion concentration scale) were applied. pH_T of seawater sample (pH_{spl}) is calculated from the expression:

$$\text{pH}_{\text{spl}} = \text{pH}_{\text{TRIS}} + (E_{\text{TRIS}} - E_{\text{spl}}) / ER,$$

where electrode response ER is calculated as follows:

$$ER = (E_{\text{AMP}} - E_{\text{TRIS}}) / (\text{pH}_{\text{TRIS}} - \text{pH}_{\text{AMP}}).$$

ER value should be equal to the ideal Nernst value as follows:

$$ER = RT \ln(10) / F = 59.16 \text{ mV} / \text{pH units at 25 deg C},$$

where F is Faraday constant.

(3) Preliminary results

A replicate analysis of seawater sample was made at 4 layers (ex. 50, 300, 1600, and 4500 dbar depth) of deep cast or 2 layers (ex. 16 and 225 dbar depth) of shallow cast. The difference between each pair of analyses was plotted on a range control chart (see Figure 2.6-1). The average of the difference was 0.001 pH units ($n = 30$ pairs) with its standard deviation of 0.001 pH units. These values were lower than the value recommended by Guide (Dickson et al., 2007).

(4) Data Archive

All data will be submitted to JAMSTEC and is currently under its control.

(5) Reference

DelValls, T. A. and A. G. Dickson (1998). The pH of buffers based on 2-amino-2-hydroxymethyl-1,3-propanediol ('tris') in synthetic sea water, *Deep-Sea Research I* 45, 1541-1554.

Dickson A. G. and C. Goyet (Eds.) (1994), *Handbook of methods for the analysis of the various parameters of the carbon dioxide system in sea water*, version 2, ORNS/CDIAC-74.

Dickson, A. G., C. L. Sabine and J. R. Christian (Eds.) (2007), *Guide to best practices for ocean CO₂ measurements*, PICES Special Publication 3, 199pp.

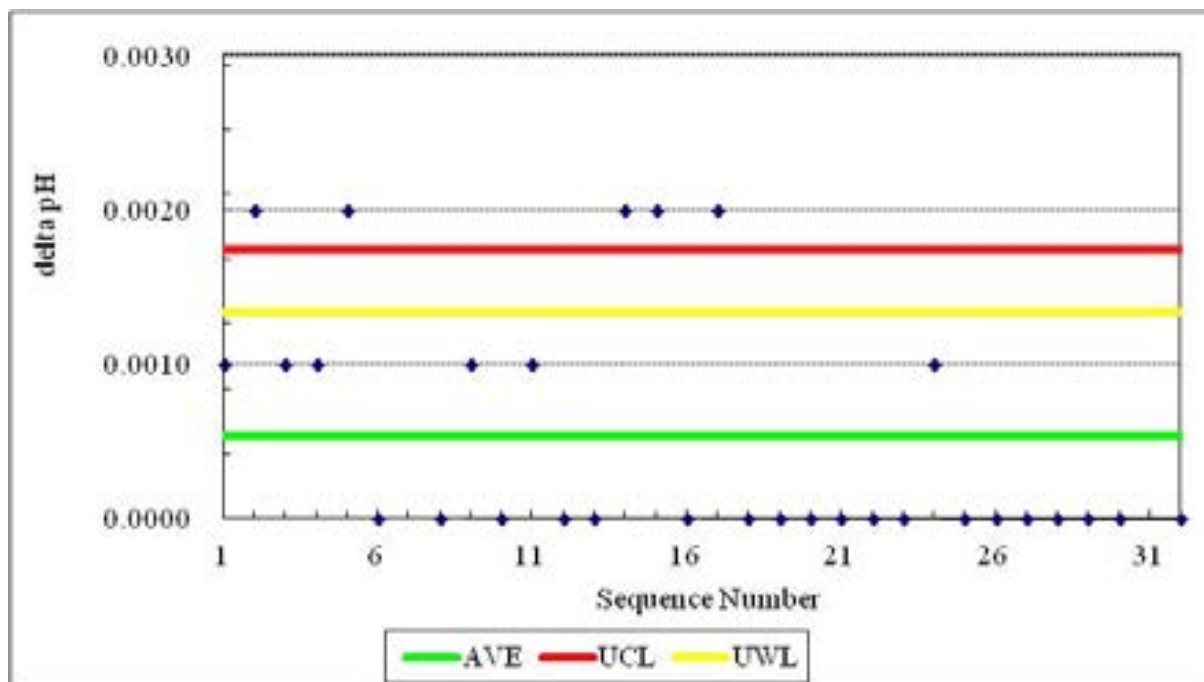


Figure 2.6-1 Range control chart of the absolute differences of replicate measurements of pH carried out during the cruise. AVE represents the average value, UCL upper control limit ($UCL = AVE * 3.267$), and UWL upper warning limit ($UWL = AVE * 2.512$) (Dickson et al., 2007).

2.7. Dissolved inorganic carbon –DIC-

Masahide WAKITA (JAMSTEC MIO): Principal Investigator

Makoto TAKADA (MWJ): Operation Leader

Tomonori WATAI (MWJ)

(1) Objective

Concentration of CO₂ in the atmosphere is now increasing at a rate of 1.5 μmol mol⁻¹ yr⁻¹ owing to human activities such as burning of fossil fuels, deforestation, and cement production. The ocean plays an important role in buffering the increase of atmospheric CO₂, therefore the urgent tasks are to clarify the mechanism of the oceanic CO₂ absorption and to estimate of CO₂ absorption capacity of the oceans. Oceanic biosphere, especially primary production, has an important role concerned to oceanic CO₂ cycle through its photosynthesis and respiration. However, the diverseness and variability of the biological system make difficult to reveal their mechanism and quantitative understanding of the CO₂ cycle. When CO₂ dissolves in water, chemical reaction takes place and CO₂ alters its appearance into several species. Concentrations of the individual species of the CO₂ system in solution cannot be measured directly, but calculated from two of four parameters: total alkalinity, total dissolved inorganic carbon, pH and pCO₂ (Dickson et al., 2007). We here report on-board measurements of DIC performed during the MR12-02 cruise.

(2) Methods, Apparatus and Performance

(2)-1 Seawater sampling

Seawater samples were collected by 12 liter Niskin bottles mounted on the CTD/Carousel Water Sampling System and a bucket at 8 stations. Among these stations, deep and shallow casts were carried out for 2 stations. Seawater was sampled in a 300 ml glass bottle (SHOTT DURAN) that was previously soaked in 5 % non-phosphoric acid detergent (pH = 13) solution at least 3 hours and was cleaned by fresh water for 5 times and Milli-Q deionized water for 3 times. A sampling silicone rubber tube with PFA tip was connected to the Niskin bottle when the sampling was carried out. The glass bottles were filled from the bottom, without rinsing, and were overflowed for 20 seconds. They were sealed using the polyethylene inner lids with its diameter of 29 mm with care not to leave any bubbles in the bottle. After collecting the samples on the deck, the glass bottles were carried to the laboratory to be measured. Within one hour after the sampling, 3 ml of the sample (1 % of the bottle volume) was removed from the bottle and poisoned with 100 μl of over saturated solution of mercury chloride. Then the samples were sealed by the polyethylene inner lids with its diameter of 31.9 mm and stored in a refrigerator at approximately 5 deg C until analyzed. Before the analysis, the samples were put in the water bath kept about 20 deg C for one hour.

(2)-2 Seawater analysis

Measurements of DIC were made with total CO₂ measuring system (Nippon ANS, Inc.). The system comprise of seawater dispensing unit, a CO₂ extraction unit, and a coulometer (Model 3000, Nippon ANS, Inc.)

The seawater dispensing unit has an auto-sampler (6 ports), which dispenses the seawater from a glass bottle to a pipette of nominal 21 ml volume. The pipette was kept at 20 ± 0.05 deg C by a water jacket, in which water circulated through a thermostatic water bath (RTE 10, Thermo).

The CO₂ dissolved in a seawater sample is extracted in a stripping chamber of the CO₂ extraction unit by adding phosphoric acid (10 % v/v). The stripping chamber is made approx. 25 cm long and has a fine frit at the bottom. First, the certain amount of acid is taken to the constant volume tube from an acid bottle and transferred to the stripping chamber from its bottom by nitrogen gas (99.9999 %). Second, a seawater sample kept in a pipette is introduced to the stripping chamber by the same method as that for an acid. The seawater and phosphoric acid are stirred by the nitrogen bubbles through a fine frit at the bottom of the stripping chamber. The stripped CO₂ is carried to the coulometer through two electric dehumidifiers (kept at 0.5 deg C) and a chemical desiccant (Mg(ClO₄)₂) by the nitrogen gas (flow rates of 140 ml min⁻¹).

Measurements of 1.5 % CO₂ standard gas in a nitrogen base, system blank (phosphoric acid blank), and seawater samples (6 samples) were programmed to repeat. The variation of our own made JAMSTEC DIC reference material or 1.5 % CO₂ standard gas signal was used to correct the signal drift results from chemical alternation of coulometer solutions.

(3) Preliminary results

During the cruise, 459 samples were analyzed for DIC. A replicate analysis was performed at the interval decided beforehand and the difference between each pair of analyses was plotted on a range control chart (Figure 2.7-1). The average of the differences was 0.48 μmol kg⁻¹ (n = 32). The standard deviation was 0.42 μmol kg⁻¹, which indicates that the analysis was accurate enough according to the Guide to best practices for ocean CO₂ measurements (Dickson et al., 2007).

(4) Data Archive

These data obtained in this cruise will be submitted to the Data Management Office (DMO) of JAMSTEC, and will open to the public via “R/V Mirai Data Web Page” in JAMSTEC home page.

(5) Reference

Dickson, A. G., C. L. Sabine, and J. R. Christian (2007), *Guide to best practices for ocean CO₂ measurements*, PICES Special Publication 3, 199pp.

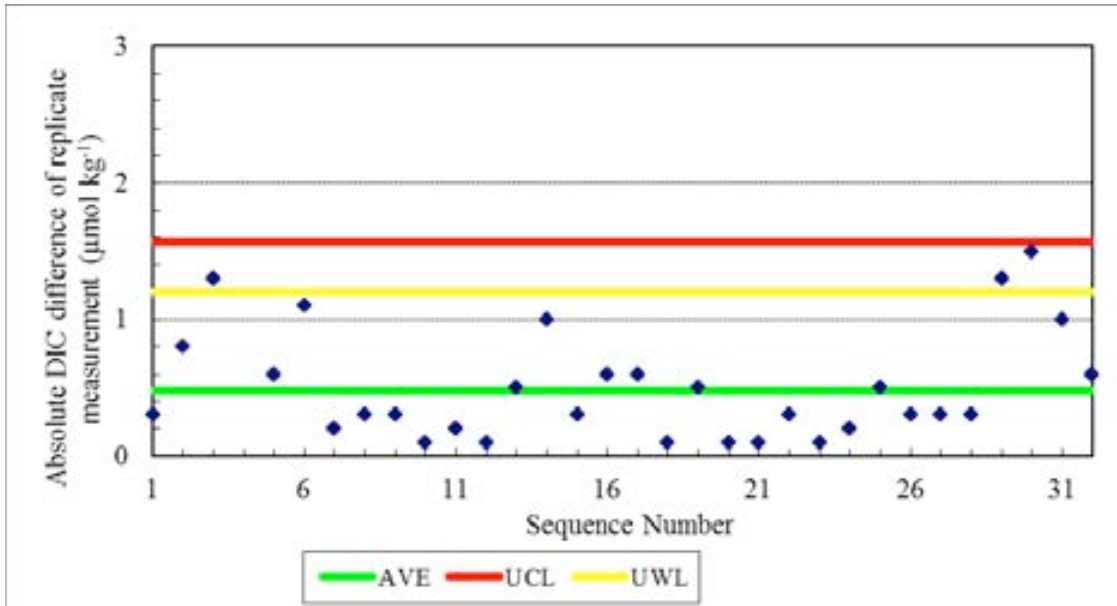


Figure 2.7-1 Range control chart of the absolute differences of replicate measurements of DIC carried out during this cruise. UCL and UWL represents the upper control limit ($UCL=AVE*3.267$) and upper warning limit ($UWL=AVE*2.512$), respectively.

2.8. Total alkalinity

Masahide WAKITA (JAMSTEC MIO): Principal Investigator

Tomonori WATAI (MWJ): Operation Leader

Makoto TAKADA (MWJ)

(1) Objective

Global warming is becoming an issue world-widely, therefore studies on green house gases, especially carbon dioxide (CO₂), are indispensable. The ocean currently absorbs one third of the 6 Gt of carbon emitted into the atmosphere each year by human activities, such as burning of fossil fuels, deforestation, and cement production. When CO₂ dissolves in sea water, chemical reaction takes place and CO₂ alters its appearance into several species and make the oceanic CO₂ cycle complicated. Oceanic biological activity, especially oceanic primary production, plays an important role concerned to the CO₂ cycle through its photosynthesis and respiration. The concentrations of the individual CO₂ species cannot be measured directly, however, two of four measurable parameters: total alkalinity, total dissolved inorganic carbon, pH, and pCO₂, can clarify the whole distribution of the CO₂ species (Dickson et al., 2007). We here report on-board measurements of total alkalinity performed during the MR12-02 cruise.

(2) Methods, Apparatus and Performance

(2)-1 Seawater sampling

Seawater samples were collected by 12 liter Niskin bottles mounted on the CTD/Carousel Water Sampling System and a bucket at 8 stations. Among these stations, deep and shallow casts were carried out for 2 stations. The seawater from the Niskin bottle was filled into the 125 ml borosilicate glass bottles (SHOTT DURAN) using a sampling silicone rubber tube with PFA. The water was filled into the bottle from the bottom smoothly, without rinsing, and overflowed for 2 times bottle volume (10 seconds) with care not to leave any bubbles in the bottle. These bottles were pre-washed in advance by soaking in 5 % non-phosphoric acid detergent (pH = 13) for more than 3 hours, and then rinsed 5 times with tap water and 3 times with Milli-Q deionized water. The samples were stored in a refrigerator at approximately 5 deg C before the analysis, and were put in the water bath with its temperature of about 25 deg C for one hour just before analysis.

(2)-2 Seawater analyses

The TA was measured using a spectrophotometric system (Nippon ANS, Inc.) using a scheme of Yao and Byrne (1998). The constant volume of sample seawater, with its value of approx. 42 ml, was transferred from a sample bottle into the titration cell kept at 25 deg C in a thermostated compartment. Then, the sample seawater was circulated through the tube connecting the titration cell and the pH cell in the spectrophotometer (Carry 50 Scan, Varian) by a peristaltic pump. The length and volume of the pH cell are 8 cm and 13 ml, respectively, and its temperature is also kept at 25 deg C in a thermostated compartment. The TA is calculated by measuring two sets of absorbance at three wavelengths (750, 616 and 444 nm); one is the absorbance of seawater sample before injecting an acid with indicator solution (bromocresol green sodium) and another is the absorbance after the injection. For mixing acid and seawater, and for degassing CO₂ from the mixed solution sufficiently, they are circulated between the titration and pH cell by a peristaltic pump for 8 and half minutes before the measurement.

The TA is calculated based on the following equation:

$$\begin{aligned} \text{pH}_T = & 4.2699 + 0.002578 * (35 - S) \\ & + \log ((R(25) - 0.00131) / (2.3148 - 0.1299 * R(25))) \\ & - \log (1 - 0.001005 * S), \end{aligned} \quad (1)$$

$$\begin{aligned} A_T = & (N_A * V_A - 10^{\text{pH}_T} * \text{DensSW}(T, S) * (V_S + V_A)) \\ & * (\text{DensSW}(T, S) * V_S)^{-1}, \end{aligned} \quad (2)$$

where R(25) represents the difference of absorbance at 616 and 444 nm between before and after the injection. The absorbance of wavelength at 750 nm is used to subtract the variation of absorbance caused by the system. DensSW (T, S) is the density of seawater at temperature (T) and salinity (S), N_A the concentration of the added acid, V_A and V_S the volume of added acid and seawater, respectively.

To keep the high analysis precision, some treatments were carried out during the cruise. The acid with indicator solution stored in 1 L DURAN bottle is kept in a bath with its temperature of 25 deg C, and about 10 ml of it is discarded at first before the batch of measurement. For mixing the seawater and the acid with indicator solution sufficiently, TYGON tube used on the peristaltic pump was periodically renewed. Absorbance measurements were done 10 times during each analysis, and the stable last five and three values are averaged and used for above listed calculation for before and after the injection, respectively.

(3) Preliminary results

A few replicate samples were taken at most of stations and the difference between each pair of analyses was plotted on a range control chart (see Figure 2.8-1). The average of the difference was $0.8 \mu\text{mol kg}^{-1}$ ($n = 24$) with its standard deviation of $0.7 \mu\text{mol kg}^{-1}$, which indicates that the analysis was accurate enough according to the Guide to best practices for ocean CO_2 measurements (Dickson et al., 2007).

(4) Data Archive

These data obtained in this cruise will be submitted to the Data Management Office (DMO) of JAMSTEC, and will be opened to the public via “R/V Mirai Data Web Page” in JAMSTEC home page.

(5) References

Dickson, A. G., C. L., Sabine, and J. R. Christian (2007), *Guide to best practices for ocean CO_2 measurements*; *PICES Special Publication 3*, 199pp.

Yao, W., and R. H. Byrne (1998), Simplified seawater alkalinity analysis: Use of linear array spectrometers. *Deep-Sea Research I*, 45, 1383-1392.

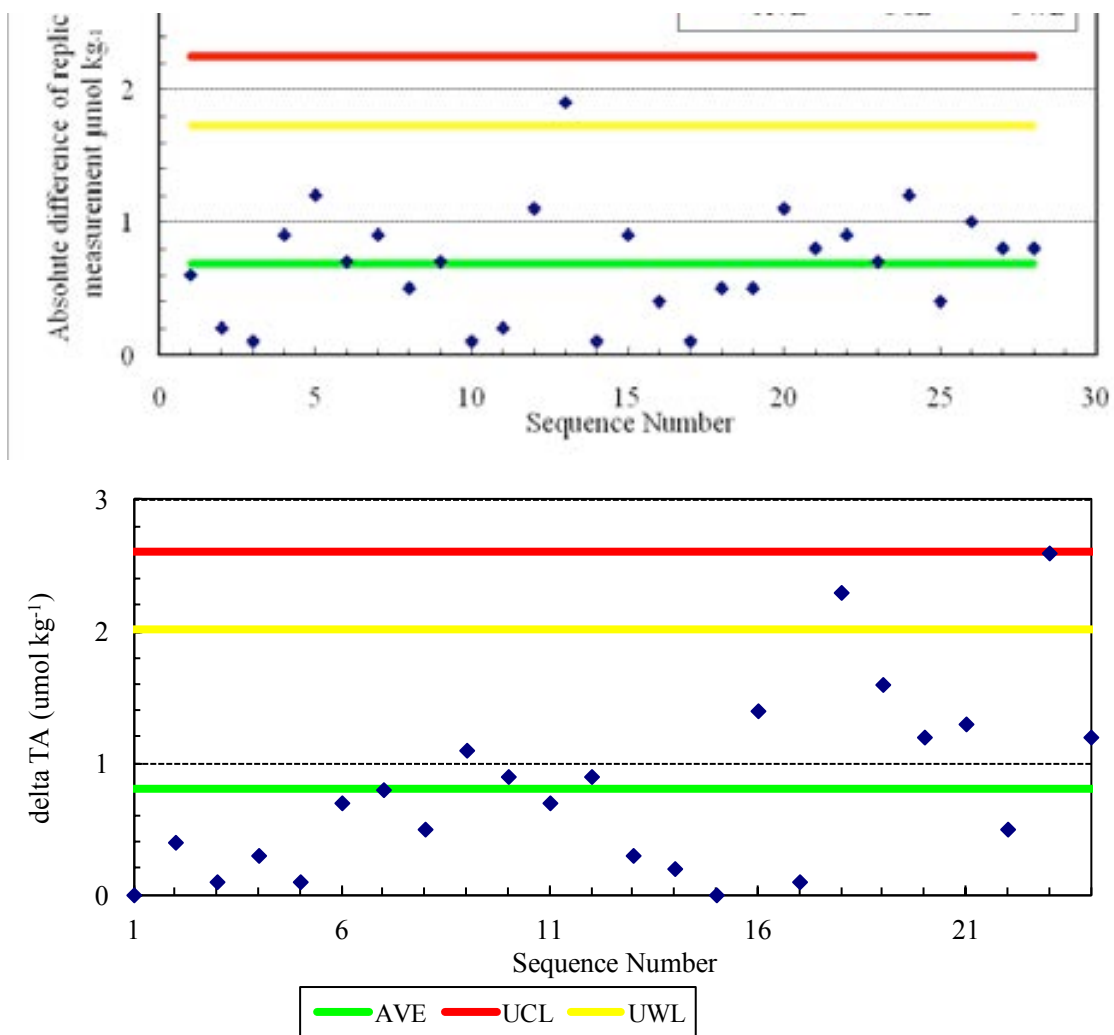


Figure 2.8-1 Range control chart of the absolute differences of replicate measurements carried out in the analysis of TA during the MR12-02 cruise. UCL and UWL represents the upper control limit ($\text{UCL}=\text{AVE}\times 3.267$) and upper warning limit ($\text{UWL}=\text{AVE}\times 2.512$), respectively.

2.9. Underway pCO₂

Masahide WAKITA (JAMSTEC MIO): Principal Investigator

Tomonori WATAI (MWJ): Operation Leader

Makoto TAKADA (MWJ)

Emi DEGUCHI (MWJ)

(1) Objectives

Concentrations of CO₂ in the atmosphere are increasing at a rate of 1.5 ppmv yr⁻¹ owing to human activities such as burning of fossil fuels, deforestation, and cement production. Oceanic CO₂ concentration is also considered to be increased with the atmospheric CO₂ increase, however, its variation is widely different by time and locations. Underway pCO₂ observation is indispensable to know the pCO₂ distribution, and it leads to elucidate the mechanism of oceanic pCO₂ variation. We here report the underway pCO₂ measurements performed during MR12-02 cruise.

(2) Methods, Apparatus and Performance

Oceanic and atmospheric CO₂ concentrations were measured during the cruise using an automated system equipped with a non-dispersive infrared gas analyzer (NDIR; LI-7000, Li-Cor). Measurements were done every about one and a half hour, and 4 standard gasses, atmospheric air, and the CO₂ equilibrated air with sea surface water were analyzed subsequently in this hour. The concentrations of the CO₂ standard gases were 300.081, 349.963, 399.976 and 450.234 ppmv. Atmospheric air taken from the bow of the ship (approx.30 m above the sea level) was introduced into the NDIR by passing through a electrical cooling unit, a mass flow controller which controls the air flow rate of 0.5 L min⁻¹, a membrane dryer (MD-110-72P, perma pure llc.) and chemical desiccant (Mg(ClO₄)₂). The CO₂ equilibrated air was the air with its CO₂ concentration was equivalent to the sea surface water. Seawater was taken from an intake placed at the approximately 4.5 m below the sea surface and introduced into the equilibrator at the flow rate of 4 - 5 L min⁻¹ by a pump. The equilibrated air was circulated in a closed loop by a pump at flow rate of 0.7 - 0.8 L min⁻¹ through two cooling units, a membrane dryer, the chemical desiccant, and the NDIR.

(3) Preliminary results

Cruise track during pCO₂ observation is shown in Figure 2.9-1. Temporal variations of both oceanic and atmospheric CO₂ concentration (xCO₂) are shown in Fig. 2.9-2.

(4) Data Archive

Data obtained in this cruise will be submitted to the Data Management Office (DMO) of JAMSTEC, and will be opened to the public via "R/V Mirai Data Web Page" in JAMSTEC home page.

(5) Reference

Dickson, A. G., Sabine, C. L. & Christian, J. R. (2007), Guide to best practices for ocean CO₂ measurements; PICES Special Publication 3, 199pp.

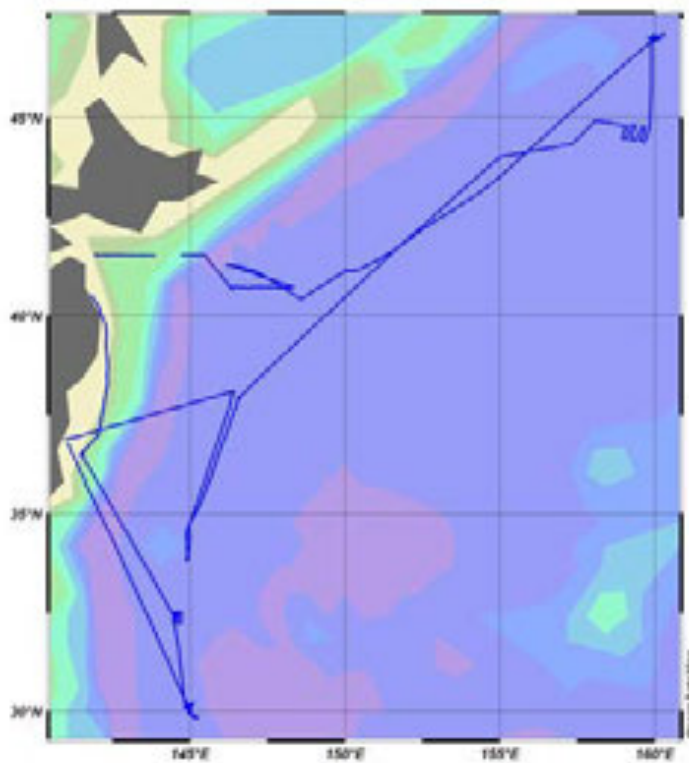


Figure 2.9-1 Observation map

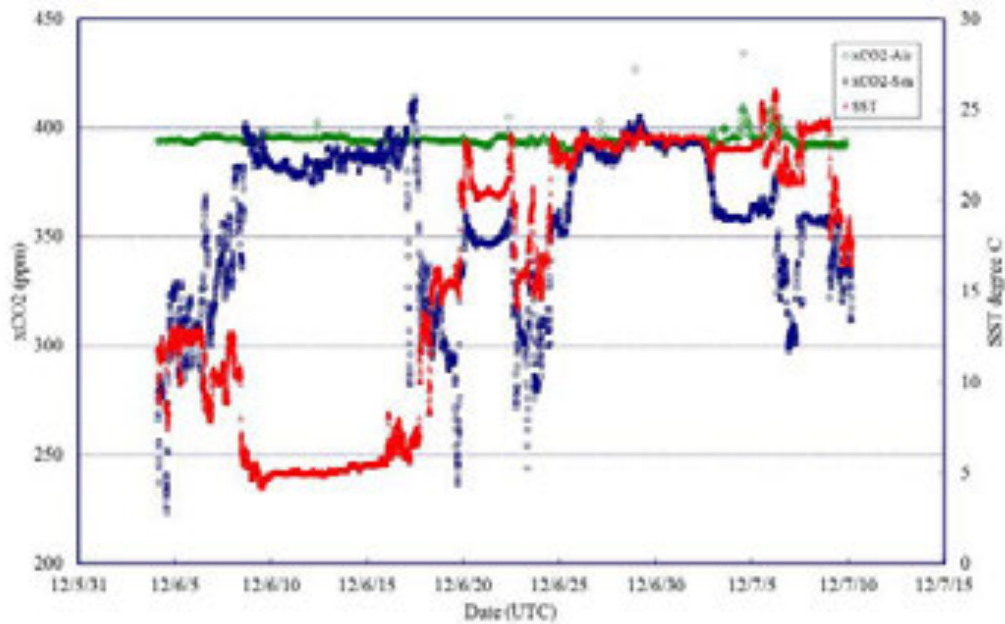


Figure 2.9-2 Temporal variations of oceanic and atmospheric CO₂ concentration (xCO₂). Blue dots represent oceanic xCO₂ variation and green atmospheric xCO₂. SST variation (red) is also shown.

3. Special observation

3.1 BGC mooring

3.1.1 Recovery and deployment

Makio HONDA (JAMSTEC MIO)

Hajime KAWAKAMI (JAMSTEC MIO)

Toru IDAI (MWJ)

Hirokatsu UNO (MWJ)*

Masaki TAGUCHI (MWJ)**

Tomoyuki TAKAMORI (MWJ)

***Leg1, **Leg2**

The one BGC mooring system was designed for biogeochemistry at Station K-2 and S-1 in the Western Subarctic Gyre. We recovered BGC mooring at Station K-2 and S-1 which were deployed at MR11-05 and deployed BGC mooring at Station K-2 and S-1. Before deployment, sea floor topography was surveyed with Sea Beam. In order to place the top of mooring systems 150m depth, precise water depths for mooring positions was measured by an altimeter (Datasonics PSA900D) mounted on CTD / CWS. Mooring works took approximately 5 hours for each mooring system. After sinker was dropped, we positioned the mooring systems by measuring the slant ranges between research vessel and the acoustic releaser. The position of the mooring is finally determined as follow:

Table 3.1.1-1 Mooring positions for respective mooring systems

	Recovery	Deployment	Recovery	Deployment
Station & type	K-2 BGC	K-2 BGC	S-1 BGC	S-1 BGC
Mooring Number	K2BGC110703	K2BGC120614	S1BGC110729	S1BGC120701
Working Date	Jun.09 th 2012	Jun. 14 st 2012	Jun. 26 th 2012	Jul. 01 th 2012
Latitude	47° 00.34 N	47° 00.40N	30° 03.93 N	30° 03.93 N
Longitude	159° 58.42 E	159° 58.22 E	144° 58.03 E	144° 58.21 E
Sea Beam Depth	5,218 m	5,210 m	5,924 m	5,922 m

The BGC mooring consists of a advance buoy with 30m pick up rope, a 64” syntactic top float with 3,000 lbs (1,360 kg) buoyancy, instruments, wire and nylon ropes, glass floats (Benthos 17” glass ball), dual releasers (Edgetech) and 4,660 lbs (2,116 kg). sinker with mace plate. Two ARGOS compact mooring locators and one submersible recovery strobe are mounted on the top float. This mooring system was planned to keep the following time-series observational instruments are mounted approximately 150 m below sea surface. It is 10 m longer than real depth because recovered depth sensor which was installed on the Sediment trap shows 10 m deeper than our expected by mooring tilt.

On the BGC mooring, 3 Sediment Traps are installed on the 200 m, 500 m and 5,000 m. Extra CTD (SBE-37) and Do Sensor (Arec) are mounted on the dual acoustic releasers. Also extra RIGO Depth Sensor and Back Scattero meter are mounted on 200m Sediment Trap.

Details for each instrument are described later (section 3.1.2). Serial numbers for instruments are as follows:

Table 3.1.1-2 Serial numbers of instruments

	Recover		Deployment	
Station and type	K-2 BGC	S-1 BGC	K-2 BGC	S-1 BGC
Mooring Number	K2BGC110703	S1BGC110729	K2BGC120614	S1BG120701
ARGOS	18842 / 52111	18841 / 52112	18842 / 52111	18841 / A02-108
ARGOS ID	18577 / 5373	18570 / 5374	18577 / 5373	18570 / 115728
Strobe	Benthos 233	234	NO2-044	Benthos 233
Sediment Trap×3				
Nichiyu (200m)	ST98025	ST98080	ST98025	ST98080
Rigo Depth Sensor	DP1158	DP1142	DP1158	DP1142
Back Scattero meter	Non	Non	906	891
Mark7-21 (500m)	989	No ID	10238-02	878
Mark7-21(5000m)	10558-01	878	10558-01	10236-01
Releaser	27809	27864	27824	27805
Releaser	28386	27815	34040	28531
SBE-37	2731	2730	2731	2730
AREC DO sensor	05	03	051	052

Table 3.1.1-3 Recovery BGC Mooring Record at K-2

Project	Time-Series	Depth	5,206.2	m
Area	North Pacific	Planned Depth	5,216.2	m
Station	K2 BGC	Length	5,068.2	m
Target Position	47°00.350	N	Depth of Buoy	150
	159°58.326		E	Peribd
ACOUSTIC RELEASERS				
Type	Edgetech	Edgetech		
Serial Number	27809	28386		
Receive F.	11.0	kHz	11.0	kHz
Transmit F.	14.0	kHz	14.0	kHz
RELEASE C.	344535	354501		
Enable C.	360320	376513		
Disable C.	360366	376530		
Battery	2 years	2 years		
Release Test	OK	OK		
RECOVERY				
Recorder	Toru Idai	Work Distance	1.4	Nm ile
Ship	R/V MIRAI	Send Enable C.	19:34	
Cruise No.	MR12-02	Slant Range	-	m sec
Date	2012/6/9	Send Release C.	19:38	
Weather	o	Discovery Buoy	19:41	
Wave Height	1.9	Pos. of Top Buoy	47°00.35	N
Seabed Depth	5,215		159°58.33	E
Ship Heading	<330>	Pos. of Start	47°00.26	N
Ship Ave. Speed	0.5		159°58.80	E
Wind	<290> 5.9	Pos. of Finish	47°01.38	N
Current	<030> 25.7		159°58.24	E

Table 3.1.1-4 Recovery BGC Mooring Record at S-1

Project	Time-Series	Depth	5,920.0	m
Area	North Pacific	Planned Depth	5,915.0	m
Station	S1 BGC	Length	5,752.3	m
Target Position	30°03.8656	N	Depth of Buoy	150
	144°58.0275	E	Period	1
ACOUSTIC RELEASERS				
Type	Edgetech	Edgetech		
Serial Number	27864	27815		
Receive F.	11.0	kHz	11.0	kHz
Transmit F.	14.0	kHz	14.0	kHz
RELEASE C.	344421	344657		
Enable C.	357724	361035		
Disable C.	357762	361073		
Battery	2 years	2 years		
Release Test	OK	OK		
RECOVERY				
Recorder	Toru Idai	Work Distance	0.7	Nm ile
Ship	R/V MIRAI	Send Enable C.	21:45	
Cruise No.	MR12-02	Slant Range	-	m
Date	2012/6/25	Send Release C.	21:50	
Weather	c	Discovery Buoy	21:51	
Wave Height	1.8	m	Pos. of Top Buoy	30°03.76
Depth	5,905	m		144°58.13
Ship Heading	<350>	Pos. of Start	30°03.24	N
Ship Ave.Speed	0.3		knot	144°58.03
Wind	<010>	Pos. of Finish	30°03.93	N
Current	<130>		15.4	cm/sec
				E

Table 3.1.1-5 Deployment BGC Mooring Record at K-2

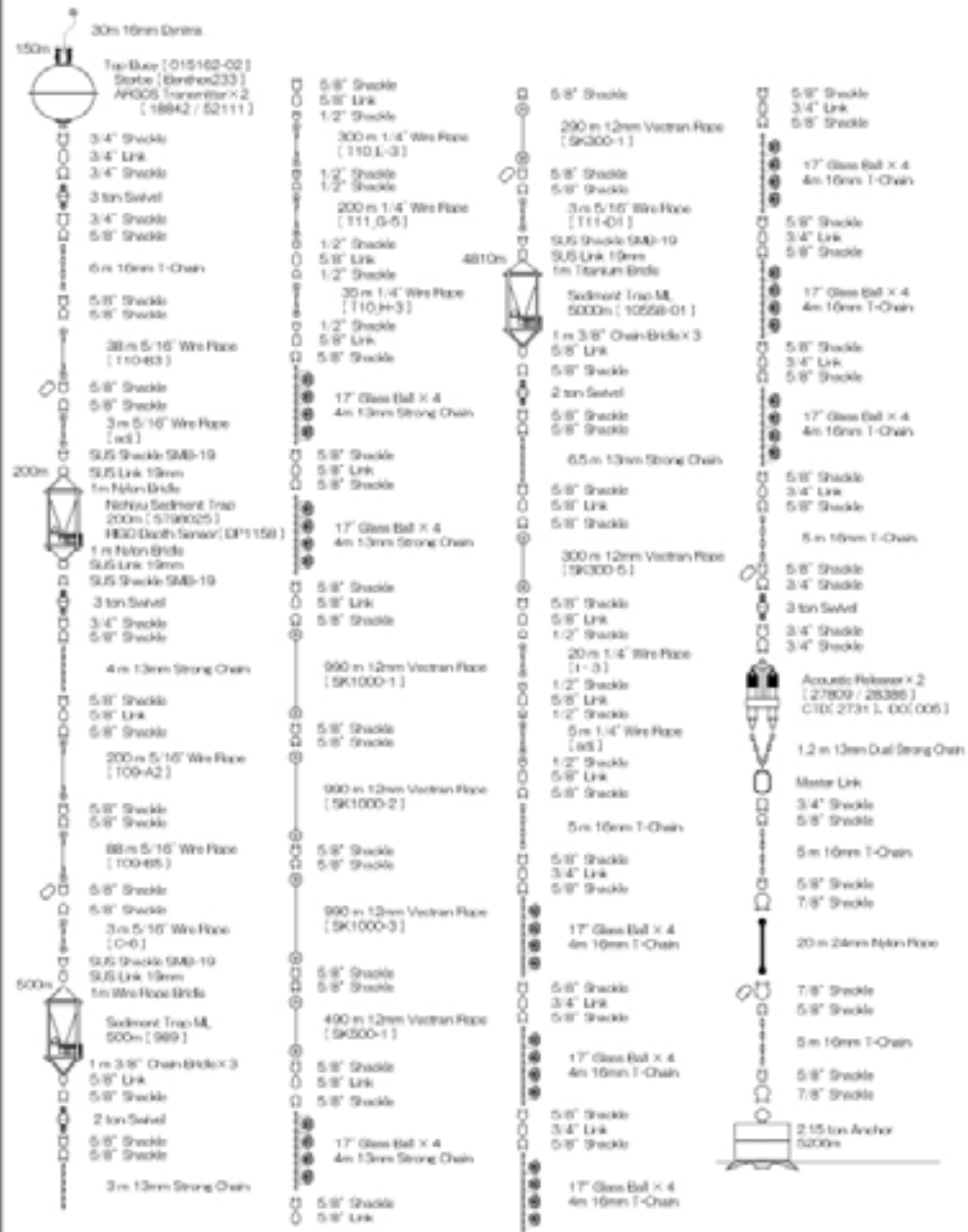
Project	Time-Series	Depth	5,206.2	m
Area	North Pacific	Planned Depth	5,216.2	m
Station	K2 BGC	Length	5,068.2	m
Target Position	47°00.350 N	Depth of Buoy	150	m
	159°58.326 E	Period	1	year
ACOUCTIC RELEASERS				
Type	Edgetech	Edgetech		
Serial Number	27824	34040		
Receive F.	11.0 kHz	11.0 kHz		
Transmit F.	14.0 kHz	14.0 kHz		
RELEASE C.	344674	233770		
Enable C.	361121	221130		
Disable C.	361167	221155		
Battery	2 years	2 years		
Release Test	OK	OK		
DEPLOYMENT				
Recorder	Toru Idai	Start	5.0	Nm ile
Ship	R/V MIRAI	Overshoot	690	m
Cruise No.	MR12-02	Let go Top Buoy	21:08	
Date	2012/6/14	Let go Anchor	23:58	
Weather	o	Sink Top Buoy	0:37	
Wave Hight	1.0 m	Pos. of Start	46°55.49	N
Seabeam Depth	5,210 m		159°59.69	E
Ship Heading	<345>	Pos. of Drop. Anc.	47°00.69	N
Ship Ave.Speed	2.0 knot		159°58.21	E
Wind	<330> 5.4 m/s	Pos. of Mooring	47°00.40	N
Current	<340> 10.3 cm/sec		159°58.22	E

Table 3.1.1-6 Deployment BGC Mooring Record at S-1

Project	Time-Series	Depth	5,920.0	m
Area	North Pacific	Planned Depth	5,915.0	m
Station	S1 BGC	Length	5,752.3	m
Target Position	30°03.8656 N	Depth of Buoy	150	m
	144°58.0275 E	Period	1	year
ACOUSTIC RELEASERS				
Type	Edgetech	Edgetech		
Serial Number	27805	28531		
Receive F.	11.0 kHz	11.0 kHz		
Transmit F.	14.0 kHz	14.0 kHz		
RELEASE C.	344611	223065		
Enable C.	360631	200405		
Disable C.	360677	200426		
Battery	2 years	2 years		
Release Test	OK	OK		
DEPLOYMENT				
Recorder	Toru Idai	Start	5.5	Nm ile
Ship	R/V MIRAI	Overshoot	356	m
Cruise No.	MR12-02	Let go Top Buoy	23:13	
Date	2012/7/1	Let go Anchor	2:31	
Weather	r	Sink Top Buoy	3:07	
Wave Hight	1.6 m	Pos. of Start	30°06.62	N
Seabed Depth	5,922 m		145°03.43	E
Ship Heading	<240>	Pos. of Drop. Anc.	30°03.79	N
Ship Ave.Speed	1.5 knot		144°57.82	E
Wind	<240> 9.3 m/s	Pos. of Mooring	30°03.93	N
Current	<187> 36.0 cm/sec		144°58.21	E

MR12-02 BGC Recovery FINAL

K2



JPAC NW PACIFIC BGC MOORING

Station K2, 5206.2m

Fig. 3.1.1-1 Recovery BGC Mooring Figure at K-2

MR12-02 BGC Recovery FINAL

S1

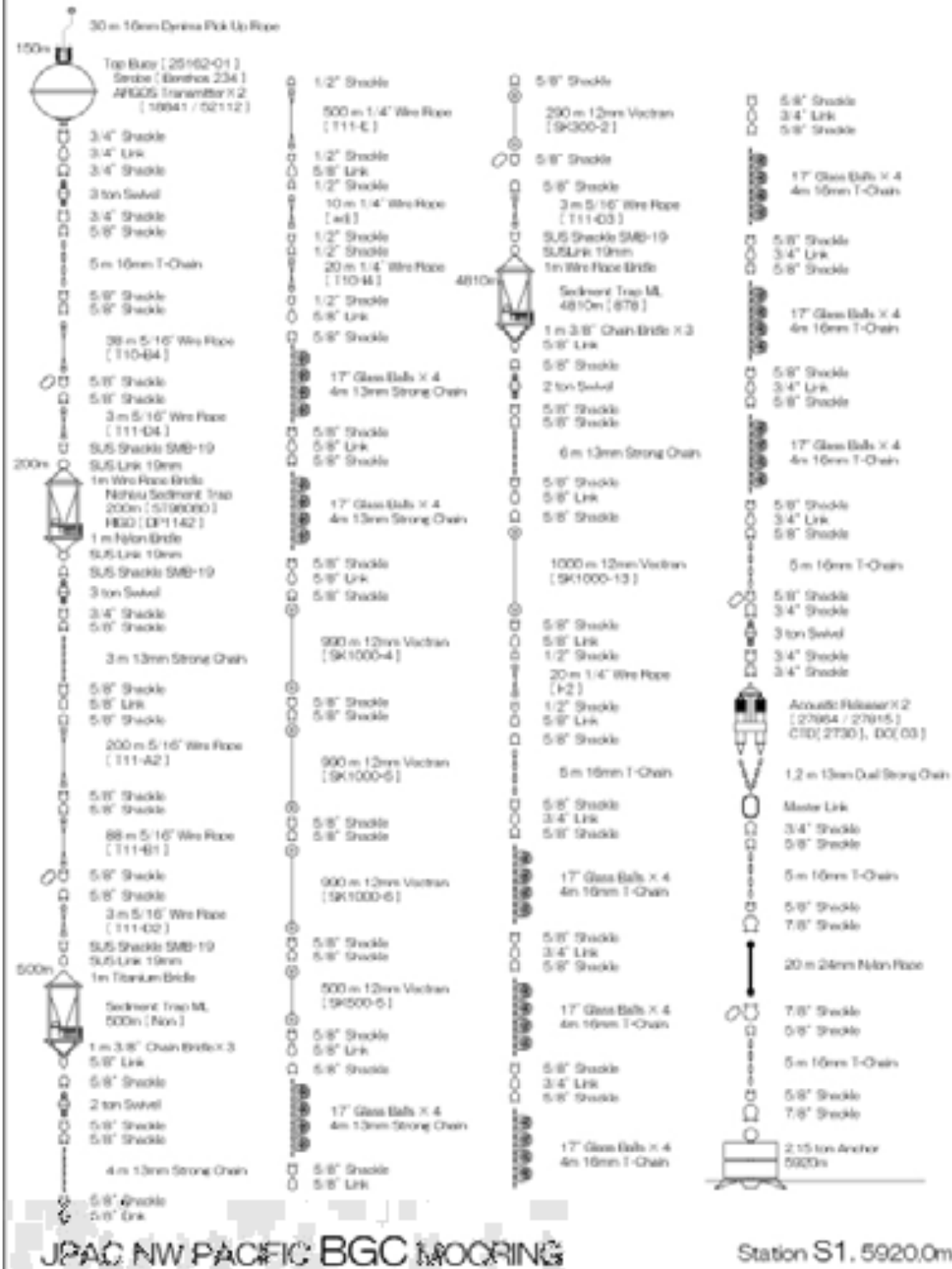
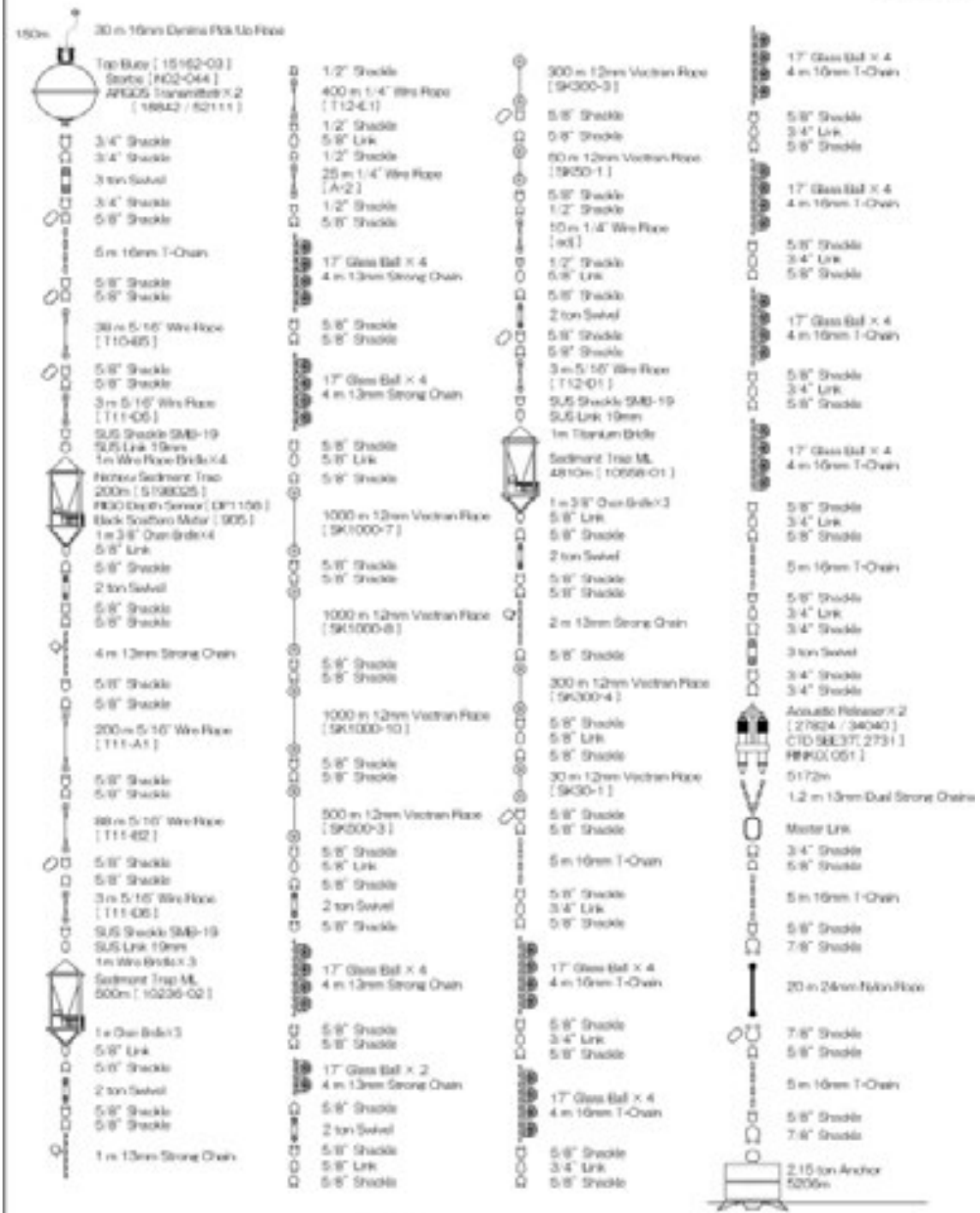


Fig. 3.1.1-2 Recovery BGC Mooring Figure at S-1

MR12-02 BGC Deployment FINAL

K2



JPAC NW PACIFIC BGC MOORING

Station K2. 5206.2m

Fig. 3.1.1-3 Deployment BGC Mooring Figure at K-2

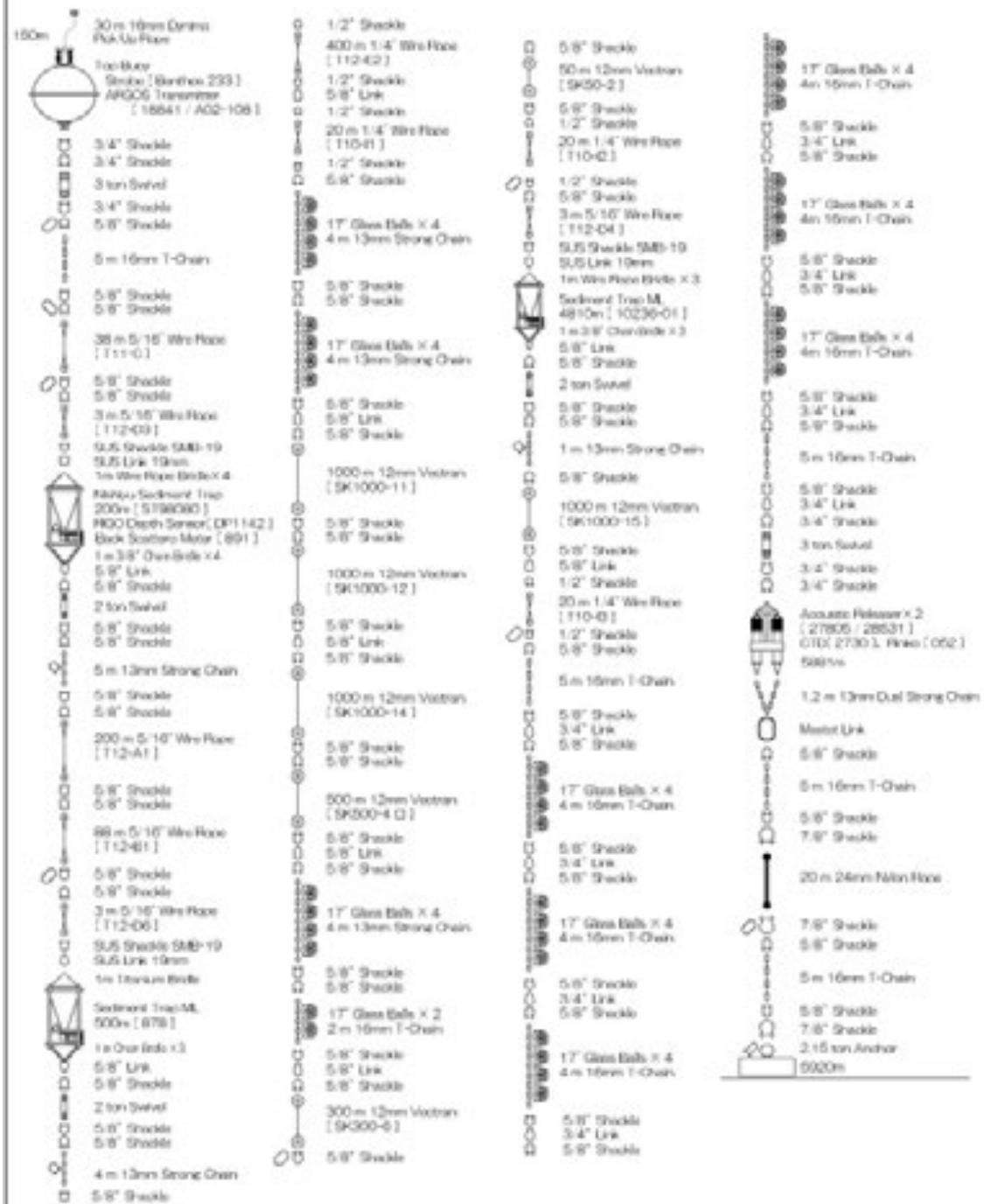


Fig. 3.1.1-4 Deployment BGC Mooring Figure at S-1

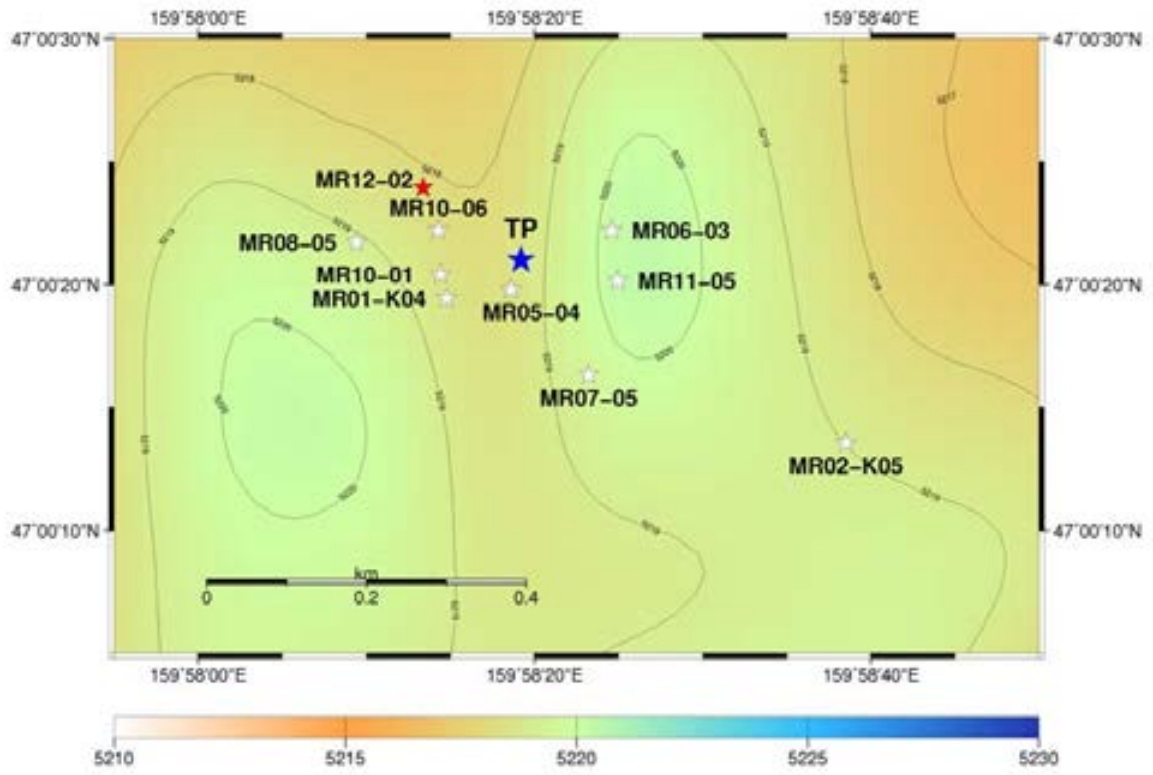


Fig. 3.1.1-5 History of deployment positions of BGC Mooring at K2

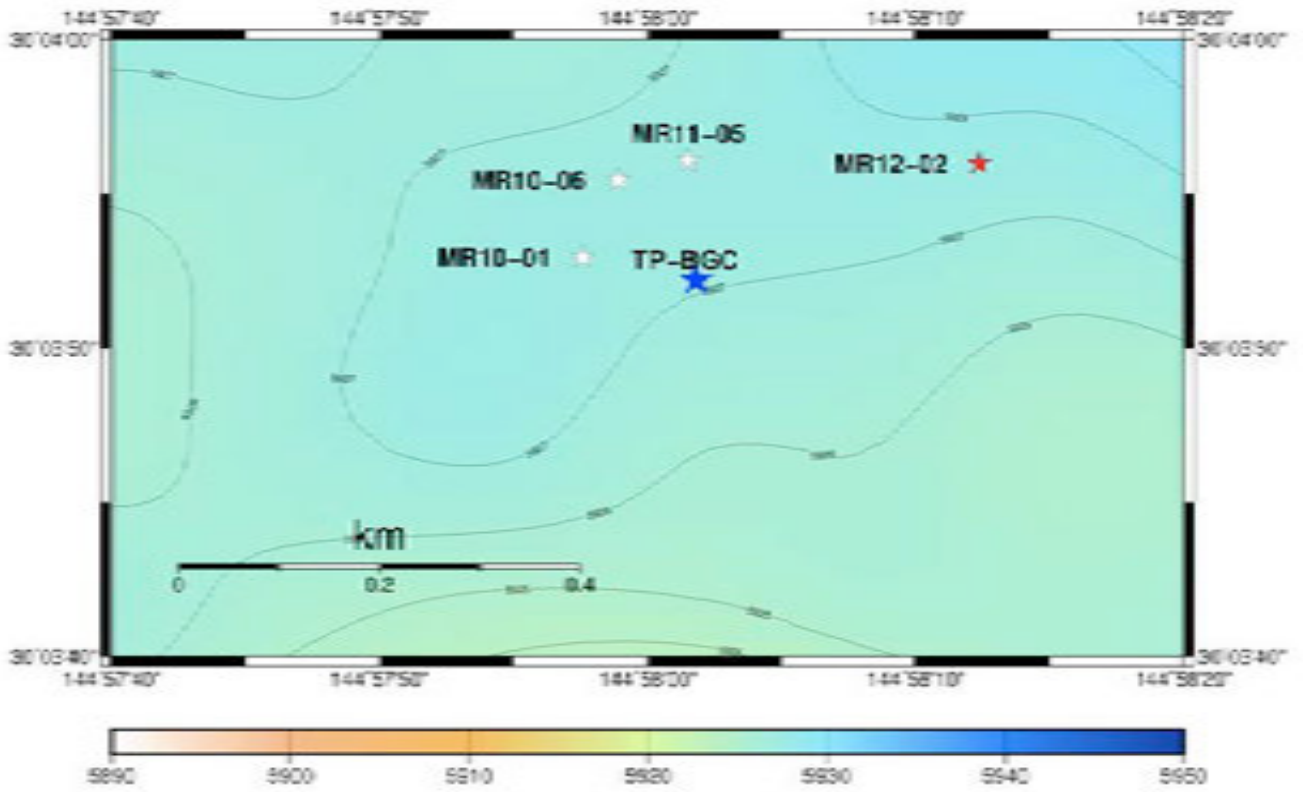


Fig. 3.1.1-5 History of deployment positions of BGC Mooring at S1

3.1.2 Instruments

On mooring systems, the following instruments are installed.

(1) ARGOS CML (Compact Mooring Locator)

The Compact Mooring Locator is a subsurface mooring locator based on SEIMAC's Smart Cat ARGOS PTT (Platform Terminal Transmitter) technology. Using CML, we can know when our mooring has come to the surface and its position. The CML employs a pressure sensor at the bottom. When the CML is turned ON, the transmission is started immediately every 90 seconds and then when the pressure sensor works ON by approximately 10 dbar, the transmission is stopped. When the top buoy with the CML comes to the surface, the pressure sensor will work OFF and the transmission will be started. Smart Cat transmissions will be initiated at this time, allowing us to locate our mooring. Depending on how long the CML has been moored, it will transmit for up to 120 days on a 90 second repetition period. Battery life, however, is affected by how long the CML has been moored prior to activation. A longer pre-activation mooring will mean less activation life.

Principle specification is as follows:

(Specification)

Transmitter:	Smart Cat PTT
Operating Temp.:	+35 [deg] to -5 [deg]
Standby Current:	80 microamps
Smart Cat Freq.:	401.650 MHz
Battery Supply:	7-Cell alkaline D-Cells
Ratings:	+10.5VDC nom., 10 Amp Hr
Hull:	6061-T6 Aluminum
Max Depth:	1,000 m
Length:	22 inches
Diameter:	3.4 inches
Upper flange:	5.60 inches
Dome:	Acrylic
Buoyancy:	-2.5 (negative) approx.
Weight	12 pounds approx.

(2) Submersible Recovery Strobe

The NOVATECH Xenon Flasher is intended to aid in the marking or recovery of oceanographic instruments, manned vehicles, remotely operated vehicles, buoys or structures. Due to the occulting (firing closely spaced bursts of light) nature of this design, it is much more visible than conventional marker strobes, particularly in poor sea conditions.

(Specification)

Repetition Rate:	Adjustable from 2 bursts per second to 1 burst every 3 seconds.
Burst Length:	Adjustable from 1 to 5 flashes per burst. 100 ms between flashes nominal.
Battery Type:	C-cell alkaline batteries.
Life:	Dependent on repetition rate and burst length. 150 hours with a one flash burst every 2 seconds.
Construction:	Awl-grip painted, Hard coat anodized 6061 T-6 aluminum housing.
Max. Depth:	7,300m
Daylight-off:	User selected, standard

Pressure Switch: On at surface, auto off when submerged below 10m.
 Weight in Air: 4 pounds
 Weight in Water: 2 pounds
 Diameter: 1.7 inches nominal
 Length: 21-1/2 inches nominal

(3) Depth Sensor

RMD Depth sensor is digital memory type and designed for mounting on the plankton net and instrument for mooring and so on. It is small and right weight for easy handling. Sampling interval is chosen between 2 and 127 seconds or 1 and 127 minutes and sampled Time and Depth data. The data is converted to personal computer using exclusive cable (printer interface).

(Specification)

Model: RMD-500
 Operating Depth: 0 ~ 500m
 Precision: 0.5% (F.S.)
 Accuracy: 1/1300
 Memory: 65,534 data (128kbyte)
 Battery: lithium battery (CR2032) DC6V
 Battery Life: 65,000 data or less than 1 year
 Sample interval: 2 ~ 127 seconds or 1 ~ 127 minutes
 Broken Pressure: 20MPa
 Diameter: 50mm
 Length: 150mm
 Main Material: vinyl chloride resin
 Cap material: polyacetal resin
 Weight: 280g

(4) CTD SBE-37

The SBE 37-SM MicroCAT is a high-accuracy conductivity and temperature (pressure optional) recorder with internal battery and memory. Designed for moorings or other long duration, fixed-site deployments, the MicroCAT includes a standard serial interface and nonvolatile FLASH memory. Constructed of titanium and other non-corroding materials to ensure long life with minimum maintenance, the MicroCAT's depth capability is 7000 meters; it is also available with an optional 250-meter plastic *ShallowCAT* housing.

(Specification)

Measurement Range

Conductivity: 0 - 7 S/m (0 - 70 mS/cm)

Temperature: -5 to 35 °C

Optional Pressure: 7000 (meters of deployment depth capability)

Initial Accuracy

Conductivity: 0.0003 S/m (0.003 mS/cm)

Temperature: 0.002 °C

Optional Pressure: 0.1% of full scale range

Typical Stability (per month)

Conductivity: 0.0003 S/m (0.003 mS/cm)

Temperature: 0.0002 °C

Optional Pressure: 0.004% of full scale range
Resolution

Conductivity: 0.00001 S/m (0.0001 mS/cm)

Temperature: 0.0001 °C

Optional Pressure: 0.002% of full scale range

Time Resolution 1 second

Clock Accuracy 13 seconds/month

Quiescent Current * 10 microamps

Optional External Input Power 0.5 Amps at 9-24 VDC

Housing, Depth Rating, and Weight (without pressure sensor)

Standard Titanium, 7000 m (23,000 ft)

Weight in air: 3.8 kg (8.3 lbs)

Weight in water: 2.3 kg (5.1 lbs)

(sampling parameter)

Sampling start time: Jun. 30th2012 00:00:00

Sampling interval: 1800 seconds

(5) JFE Advantech optical dissolved oxygen sensor, Riniko

JFE Advantech optical dissolved oxygen sensor, Riniko, is based on the oxygen luminescence quenching. The Riniko used has a datalogger with an internal battery and memory in a titanium housing designed for mooring observation. Data is sampled at 1-hour intervals.

(Manufacturer's specification)

Model: Riniko I (ARO-USB)

Sensor Type: Luminescence quenching

Operating Range: 0 ~ 200%

Resolution: 0.01 ~ 0.04%

Precision: ±2%FS (linearity)

Memory: 1GB mini SD card

Sampling interval: 0.1 ~ 600 seconds

Burst time: 1 ~ 1,440 minutes

Sample number: 1 ~ 18,000

Battery: CR-V3 lithium battery, 3.3Ah (maximum 2 batteries)

Housing material: Titanium

Size: φ54 mm × 232 mm

Weight: 0.9 kg in air, 0.6 kg in water

Depth rating: 7000 m

3.1.3 Sampling schedule

After retrieving sample / data, replacement of new battery and initialization of schedule (Table 3.1.3), sediment trap mooring system at K2 (S1) was deployed on 15 June 2012 (2 July 2012). This mooring system will be recovered during MR13-04 cruise (July 2013).

K2				S1			
	21cup		26cup		21cup		26cup
	500 m, 4810 m		200m		500 m, 4810 m		200m
Int	18		18	Int	18		18
1	2012/6/16	1	2012/6/16	1	2012/7/3	1	2012/7/3
2	2012/7/4	2	2012/7/4	2	2012/7/21	2	2012/7/21
3	2012/7/22	3	2012/7/22	3	2012/8/8	3	2012/8/8
4	2012/8/9	4	2012/8/9	4	2012/8/26	4	2012/8/26
5	2012/8/27	5	2012/8/27	5	2012/9/13	5	2012/9/13
6	2012/9/14	6	2012/9/14	6	2012/10/1	6	2012/10/1
7	2012/10/2	7	2012/10/2	7	2012/10/19	7	2012/10/19
8	2012/10/20	8	2012/10/20	8	2012/11/6	8	2012/11/6
9	2012/11/7	9	2012/11/7	9	2012/11/24	9	2012/11/24
10	2012/11/25	10	2012/11/25	10	2012/12/12	10	2012/12/12
11	2012/12/13	11	2012/12/13	11	2012/12/30	11	2012/12/30
12	2012/12/31	12	2012/12/31	12	2013/1/17	12	2013/1/17
13	2013/1/18	13	2013/1/18	13	2013/2/4	13	2013/2/4
14	2013/2/5	14	2013/2/5	14	2013/2/22	14	2013/2/22
15	2013/2/23	15	2013/2/23	15	2013/3/12	15	2013/3/12
16	2013/3/13	16	2013/3/13	16	2013/3/30	16	2013/3/30
17	2013/3/31	17	2013/3/31	17	2013/4/17	17	2013/4/17
18	2013/4/18	18	2013/4/18	18	2013/5/5	18	2013/5/5
19	2013/5/6	19	2013/5/6	19	2013/5/23	19	2013/5/23
20	2013/5/24	20	2013/5/24	20	2013/6/10	20	2013/6/10
21	2013/6/11	21	2013/6/11	21	2013/6/28	21	2013/6/28
	2013/6/29	22	2013/6/29		2013/7/16	22	2013/7/16
		23	2013/7/8			23	2013/7/25
		24	2013/7/17			24	2013/8/3
		25	2013/7/26			25	2013/8/12
		26	2013/8/4			26	2013/8/21
			2013/8/13				2013/8/30
Int. 9 days				Int. 9 days			

K2		S1	
Deployment date	2012/6/15	Deployment date	2012/7/2
MR13-04 start date	ca. 2013.7.01	MR13-04 start date	ca. 2013.7.10
Recovery date	ca. 2013.7.04	Recovery date	ca. 2013.7.13

3.1.4 Preliminary results

(1) Water depth of 200m sediment trap

Depth of 200 m sediment trap was monitored by a depth sensor (RIGO RMD) each 1.5 hour during mooring period.

Depth of K2 200m sediment trap increased largely by 225 m in September 2011. Except this period, trap depth was approximately 211 m. Trap depth decreased gradually from 214 m to 210m. This was likely attributed to the extension of Vectran rope of mooring system during mooring period.

Depth of S1 200 m sediment trap was deepened several times during mooring period. In October 2011, 200 m sediment trap was deepened to 260 m. In the early November 2011, water depth increased temporary by 300 m. In April 2012, 200 m sediment trap was also deepened to 280 m. Compared to station K2, the effect of temporal current or eddy on mooring system is likely stronger at station S1.

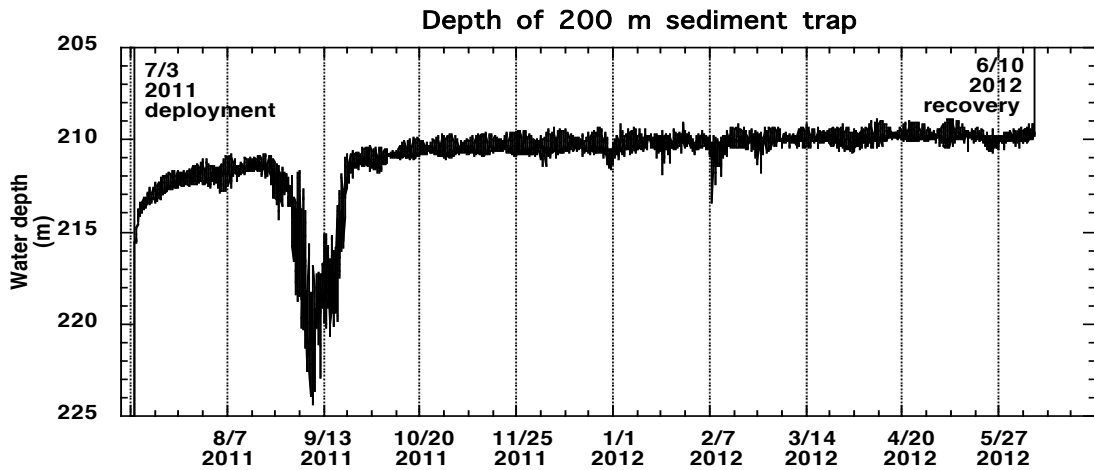


Fig. 3.1.4.1 Seasonal variability in water depths of 200 m sediment trap (K2)

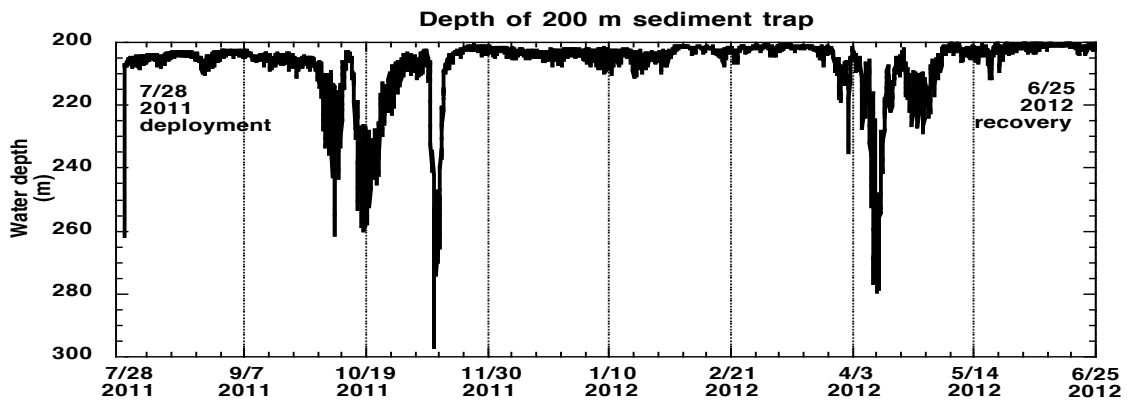


Fig. 3.1.4.2 Seasonal variability in water depths of 200 m sediment trap (S1)

(2) Sediment trap

Sediment trap mooring systems deployed in July 2010 were recovered on in June 2012. Settling particle was collected in collecting cups exchanged each 16 days (or 8 days for part of samples at station S1).

(Station K2)

Based on height of sinking particle collected in collecting cups, mass flux at 200 m increased in July just after deployment. However mass flux decreased thereafter. Mass flux at 500m increased relatively in July and August 2011. Mass flux decreased between autumn 2011 and early spring 2012. Mass flux increased again in late March and April 2011. Mass flux at 4810 m was large in July and August 2011 and decreased toward winter. Mass flux also increased in April 2011 same as 500 m with time lag.

(Station S1)

At 200 m, mass flux increased in August and decreased toward winter. Mass flux increased again in February 2012. Mass flux at 200 m was higher at S1 than K2 on average. Smaller fluxes in October 2011 and in April 2012 were observed. It might be attributed to decrease of trapping efficiency by tilt based on increase of water depth (Fig. 3.1.4.2).

Although seasonal variability was small, mass flux at 500 m and 4810 m were relatively higher in autumn and late winter (February and March) in 2012. Mass fluxes at these depths were smaller than those at station K2 unlike mass flux at 200 m.

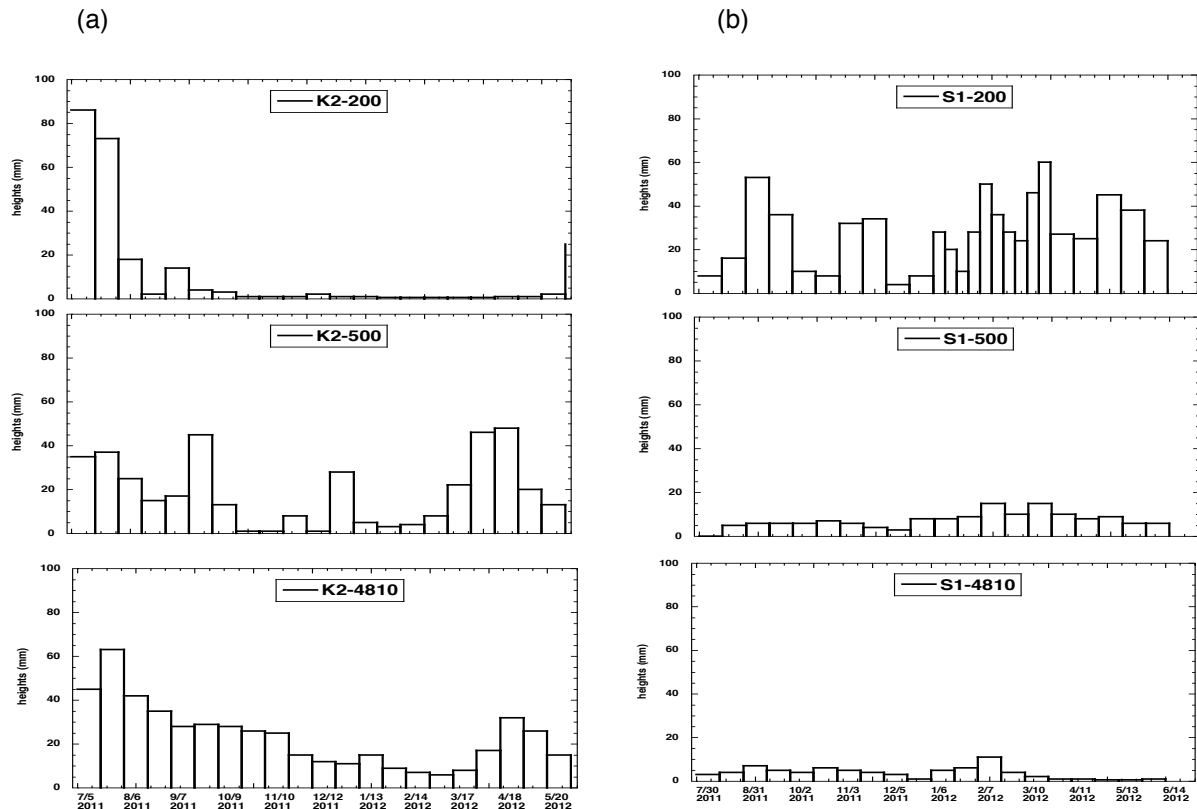


Fig. 3.1.4.3 Seasonal variability in sinking particle flux at (a) K2 and (b) S1. Vertical axis is height of collected materials in collecting cups.

3.2 Underwater profiling buoy system (Primary productivity profiler)

3.2.1 POPPS

Tetsuichi FUJIKI (JAMSTEC)

Yoshihisa MINO (JAMSTEC)

Toru IDAI (MWJ)

Tetsuya NAKAMURA (Nichiyu Giken Kogyo)

(1) Objective

An understanding of the variability in phytoplankton productivity provides a basic knowledge of how aquatic ecosystems are structured and functioning. The primary productivity of the world oceans has been measured mostly by the radiocarbon tracer method or the oxygen evolution method. As these traditional methods use the uptake of radiocarbon into particulate matter or changes in oxygen concentration in the bulk fluid, measurements require bottle incubations for periods ranging from hours to a day. This methodological limitation has hindered our understanding of the variability of oceanic primary productivity. To overcome these problems, algorithms for estimating primary productivity by using satellite ocean color imagery have been developed and improved. However, one of the major obstacles to the development and improvement of these algorithms is a lack of *in situ* primary productivity data to verify the satellite estimates.

During the past decade, the utilization of active fluorescence techniques in biological oceanography has brought marked progress in our understanding of phytoplankton photosynthesis in the oceans. Above all, fast repetition rate (FRR) fluorometry reduces the primary electron acceptor (Q_a) in photosystem (PS) II by a series of subsaturating flashlets and can measure a single turnover fluorescence induction curve in PSII. The PSII parameters derived from the fluorescence induction curve provide information on the physiological state related to photosynthesis and can be used to estimate gross primary productivity. FRR fluorometry has several advantages over the above-mentioned traditional methods. Most importantly, because measurements made by FRR fluorometry can be carried out without the need for time-consuming bottle incubations, this method enables real-time high-frequency measurements of primary productivity. In addition, the FRR fluorometer can be used in platform systems such as moorings, drifters, and floats.

The current study aimed to assess the vertical and temporal variations in PSII parameters and primary productivity in the western Pacific, by using an underwater profiling buoy system that uses the FRR fluorometer (system name: Primary productivity profiler)

(2) Methods

a) Primary productivity profiler

The primary productivity profiler (original design by Nichiyu Giken Kogyo) consisted mainly of an observation buoy equipped with a submersible FRR fluorometer (Diving Flash, Kimoto Electric), a scalar irradiance sensor (QSP-2200, Biospherical Instruments), a CTD sensor (MCTD, Falmouth Scientific) and a dissolved oxygen sensor (Compact Optode, Alec Electronics), an underwater winch, an acoustic Doppler current profiler (Workhorse Long

Ranger, Teledyne RD Instruments) and an acoustic releaser (Fig. 1). The observation buoy moved between the winch depth and the surface at a rate of 0.2 m s^{-1} and measured the vertical profiles of phytoplankton fluorescence, irradiance, temperature, salinity and dissolved oxygen. The profiling rate of the observation buoy was set to 0.2 m s^{-1} to detect small-scale variations (approx. 1 m) in the vertical profile. To minimize biofouling of instruments, the underwater winch was placed below the euphotic layer so that the observation buoy was exposed to light only during the measurement period. In addition, the vertical migration of observation buoy reduced biofouling of instruments.

b) Measurement principle of FRR fluorometer

The FRR fluorometer consists of closed dark and open light chambers that measure the fluorescence induction curves of phytoplankton samples in darkness and under actinic illumination. To allow relaxation of photochemical quenching of fluorescence, the FRR fluorometer allows samples in the dark chamber to dark adapt for about 1 s before measurements. To achieve cumulative saturation of PSII within $150 \mu\text{s}$ — i.e., a single photochemical turnover — the instrument generates a series of subsaturating blue flashes at a light intensity of $25 \text{ mmol quanta m}^{-2} \text{ s}^{-1}$ and a repetition rate of about 250 kHz. The PSII parameters are derived from the single-turnover-type fluorescence induction curve by using the numerical fitting procedure described by Kolber et al. (1998). Analysis of fluorescence induction curves measured in the dark and light chambers provides PSII parameters such as fluorescence yields, photochemical efficiency and effective absorption cross section of PSII, which are indicators of the physiological state related to photosynthesis. Using the PSII parameters, the rate of photosynthetic electron transport and the gross primary productivity can be estimated.

c) Site description and observations

The primary productivity profiler deployed at station S1 in MR11-05 was recovered on 26 June 2012 (UTC). In addition, the primary productivity profiler was newly-deployed on 1 July 2012 (UTC) (Fig. 2, target position: $29^{\circ} 56.268 \text{ N}$, $144^{\circ} 58.513 \text{ E}$, 5915 m; actual position: $29^{\circ} 56.376 \text{ N}$, $144^{\circ} 58.472 \text{ E}$, 5914 m). The measurements began on 8 July 2012 and will continue until 30 June 2013. The buoy system will be recovered in MR13-04.

Measurement schedule at station S1 (Japan time)

1. 12/07/08 02:00	2. 12/07/08 11:00	3. 12/07/11 11:00	4. 12/07/14 02:00
5. 12/07/14 11:00	6. 12/07/17 11:00	7. 12/07/20 02:00	8. 12/07/20 11:00
9. 12/07/23 11:00	10. 12/07/26 02:00	11. 12/07/26 11:00	12. 12/07/29 11:00
13. 12/08/01 02:00	14. 12/08/01 11:00	15. 12/08/04 11:00	16. 12/08/07 02:00
17. 12/08/07 11:00	18. 12/08/10 11:00	19. 12/08/13 02:00	20. 12/08/13 11:00
21. 12/08/16 11:00	22. 12/08/19 02:00	23. 12/08/19 11:00	24. 12/08/22 11:00
25. 12/08/25 02:00	26. 12/08/25 11:00	27. 12/08/28 11:00	28. 12/08/31 02:00
29. 12/08/31 11:00	30. 12/09/03 11:00	31. 12/09/06 02:00	32. 12/09/06 11:00
33. 12/09/09 11:00	34. 12/09/12 02:00	35. 12/09/12 11:00	36. 12/09/15 11:00
37. 12/09/18 02:00	38. 12/09/18 11:00	39. 12/09/21 11:00	40. 12/09/24 02:00
41. 12/09/24 11:00	42. 12/09/27 11:00	43. 12/09/30 02:00	44. 12/09/30 11:00

45. 12/10/03 11:00	46. 12/10/06 02:00	47. 12/10/06 11:00	48. 12/10/09 11:00
49. 12/10/12 02:00	50. 12/10/12 11:00	51. 12/10/15 11:00	52. 12/10/18 02:00
53. 12/10/18 11:00	54. 12/10/21 11:00	55. 12/10/24 02:00	56. 12/10/24 11:00
57. 12/10/27 11:00	58. 12/10/30 02:00	59. 12/10/30 11:00	60. 12/11/02 11:00
61. 12/11/05 02:00	62. 12/11/05 11:00	63. 12/11/08 11:00	64. 12/11/11 02:00
65. 12/11/11 11:00	66. 12/11/14 11:00	67. 12/11/17 02:00	68. 12/11/17 11:00
69. 12/11/20 11:00	70. 12/11/23 02:00	71. 12/11/23 11:00	72. 12/11/26 11:00
73. 12/11/29 02:00	74. 12/11/29 11:00	75. 12/12/02 11:00	76. 12/12/05 02:00
77. 12/12/05 11:00	78. 12/12/08 11:00	79. 12/12/11 02:00	80. 12/12/11 11:00
81. 12/12/14 11:00	82. 12/12/17 02:00	83. 12/12/17 11:00	84. 12/12/20 11:00
85. 12/12/23 02:00	86. 12/12/23 11:00	87. 12/12/26 11:00	88. 12/12/29 02:00
89. 12/12/29 11:00	90. 13/01/01 11:00	91. 13/01/04 02:00	92. 13/01/04 11:00
93. 13/01/07 11:00	94. 13/01/10 02:00	95. 13/01/10 11:00	96. 13/01/13 11:00
97. 13/01/16 02:00	98. 13/01/16 11:00	99. 13/01/19 11:00	100. 13/01/22 02:00
101. 13/01/22 11:00	102. 13/01/25 11:00	103. 13/01/28 02:00	104. 13/01/28 11:00
105. 13/01/31 11:00	106. 13/02/03 02:00	107. 13/02/03 11:00	108. 13/02/06 11:00
109. 13/02/09 02:00	110. 13/02/09 11:00	111. 13/02/12 11:00	112. 13/02/15 02:00
113. 13/02/15 11:00	114. 13/02/18 11:00	115. 13/02/21 02:00	116. 13/02/21 11:00
117. 13/02/24 11:00	118. 13/02/27 02:00	119. 13/02/27 11:00	120. 13/03/02 11:00
121. 13/03/05 02:00	122. 13/03/05 11:00	123. 13/03/08 11:00	124. 13/03/11 02:00
125. 13/03/11 11:00	126. 13/03/14 11:00	127. 13/03/17 02:00	128. 13/03/17 11:00
129. 13/03/20 11:00	130. 13/03/23 02:00	131. 13/03/23 11:00	132. 13/03/26 11:00
133. 13/03/29 02:00	134. 13/03/29 11:00	135. 13/04/01 11:00	136. 13/04/04 02:00
137. 13/04/04 11:00	138. 13/04/07 11:00	139. 13/04/10 02:00	140. 13/04/10 11:00
141. 13/04/13 11:00	142. 13/04/16 02:00	143. 13/04/16 11:00	144. 13/04/19 11:00
145. 13/04/22 02:00	146. 13/04/22 11:00	147. 13/04/25 11:00	148. 13/04/28 02:00
149. 13/04/28 11:00	150. 13/05/01 11:00	151. 13/05/04 02:00	152. 13/05/04 11:00
153. 13/05/07 11:00	154. 13/05/10 02:00	155. 13/05/10 11:00	156. 13/05/13 11:00
157. 13/05/16 02:00	158. 13/05/16 11:00	159. 13/05/19 11:00	160. 13/05/22 02:00
161. 13/05/22 11:00	162. 13/05/25 11:00	163. 13/05/28 02:00	164. 13/05/28 11:00
165. 13/05/31 11:00	166. 13/06/03 02:00	167. 13/06/03 11:00	168. 13/06/06 11:00
169. 13/06/09 02:00	170. 13/06/09 11:00	171. 13/06/12 11:00	172. 13/06/15 02:00
173. 13/06/15 11:00	174. 13/06/18 11:00	175. 13/06/21 02:00	176. 13/06/21 11:00
177. 13/06/24 11:00	178. 13/06/27 02:00	179. 13/06/27 11:00	180. 13/06/30 11:00

(3) Data archives

The data will be submitted to JAMSTEC Data Management Office.

(4) References

Kolber, Z. S., O. Prášil and P. G. Falkowski. 1998. Measurements of variable chlorophyll fluorescence using fast repetition rate techniques: defining methodology and experimental protocols. *Biochim. Biophys. Acta.* 1367: 88-106.

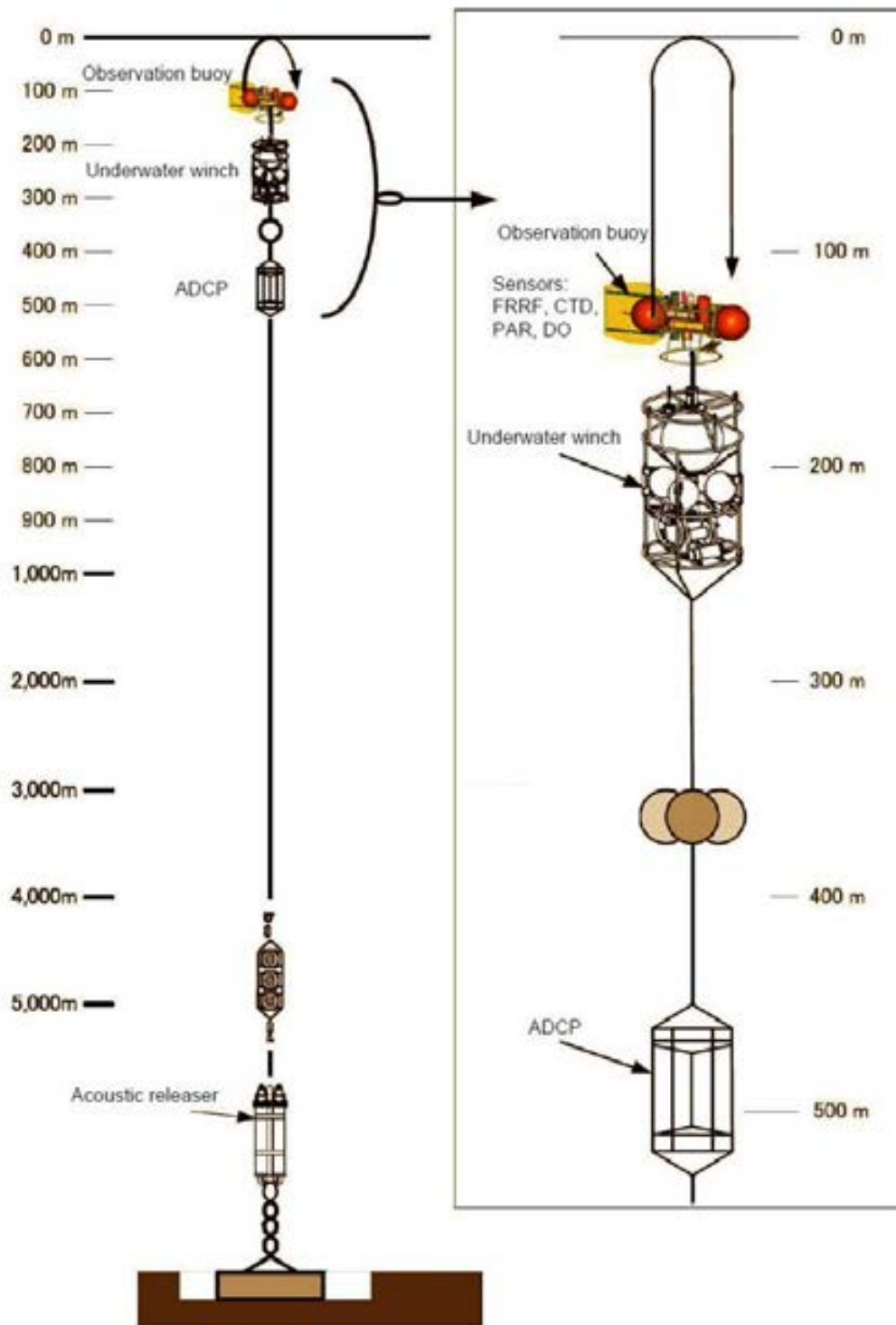


Figure 1. Schematic diagram of the primary productivity profiler.

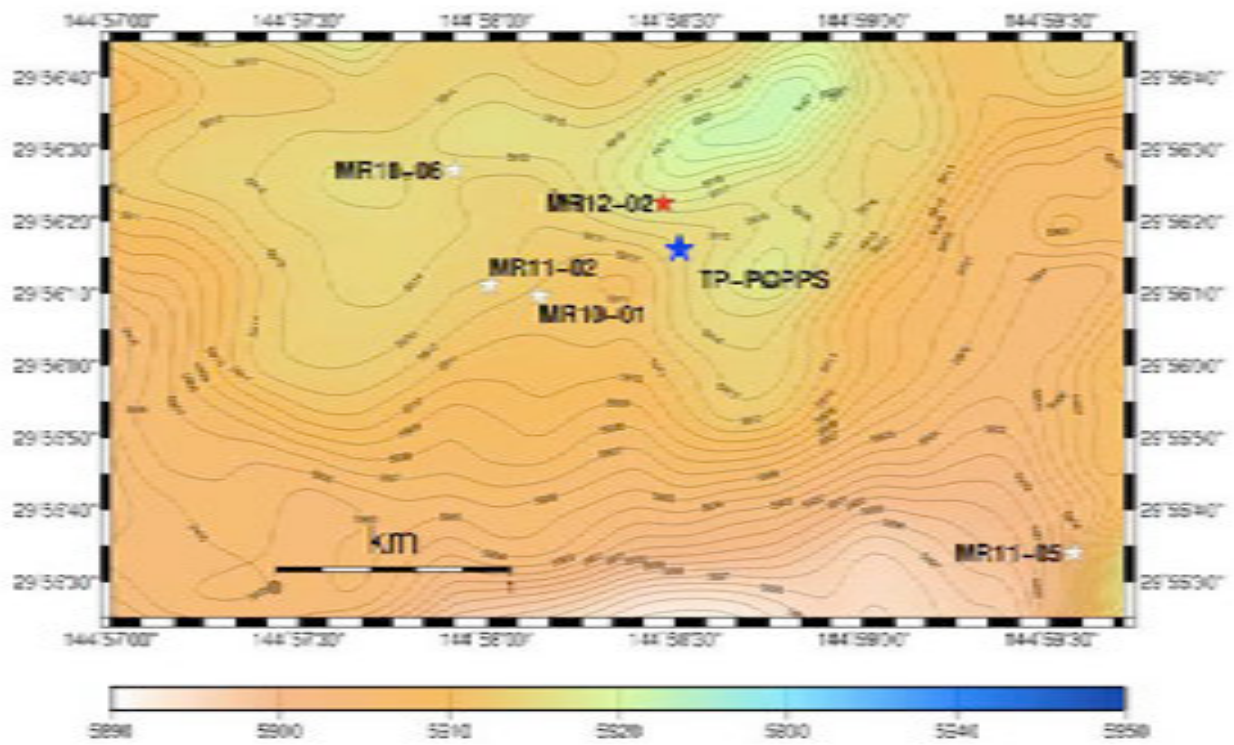


Figure 3. History of deployment positions of POPPS mooring at S1

3.2.2 RAS

Masahide WAKITA (JAMSTEC MIO)

3.2.2.1 RAS Preliminary results

(1) Pressure, temperature and salinity at RAS

Pressure, temperature and salinity by SBE-37 SM (Sea-birds) were observed every a half hour attached on RAS and POPPS WINCH frames. RAS and POPPS WINCH were located at ~380db and ~350db, respectively (Fig. 1a). Temperature and salinity at RAS and WINCH were generally constant all year around (Fig. 1b and 1c). However, both RAS and WINCH were sometimes deepened by approximately 60 db. It was noteworthy that both RAS and WINCH were deepened in autumn 2011 and spring 2012. It is suspected that strong current took place and mooring system might be largely forced to be tilted.

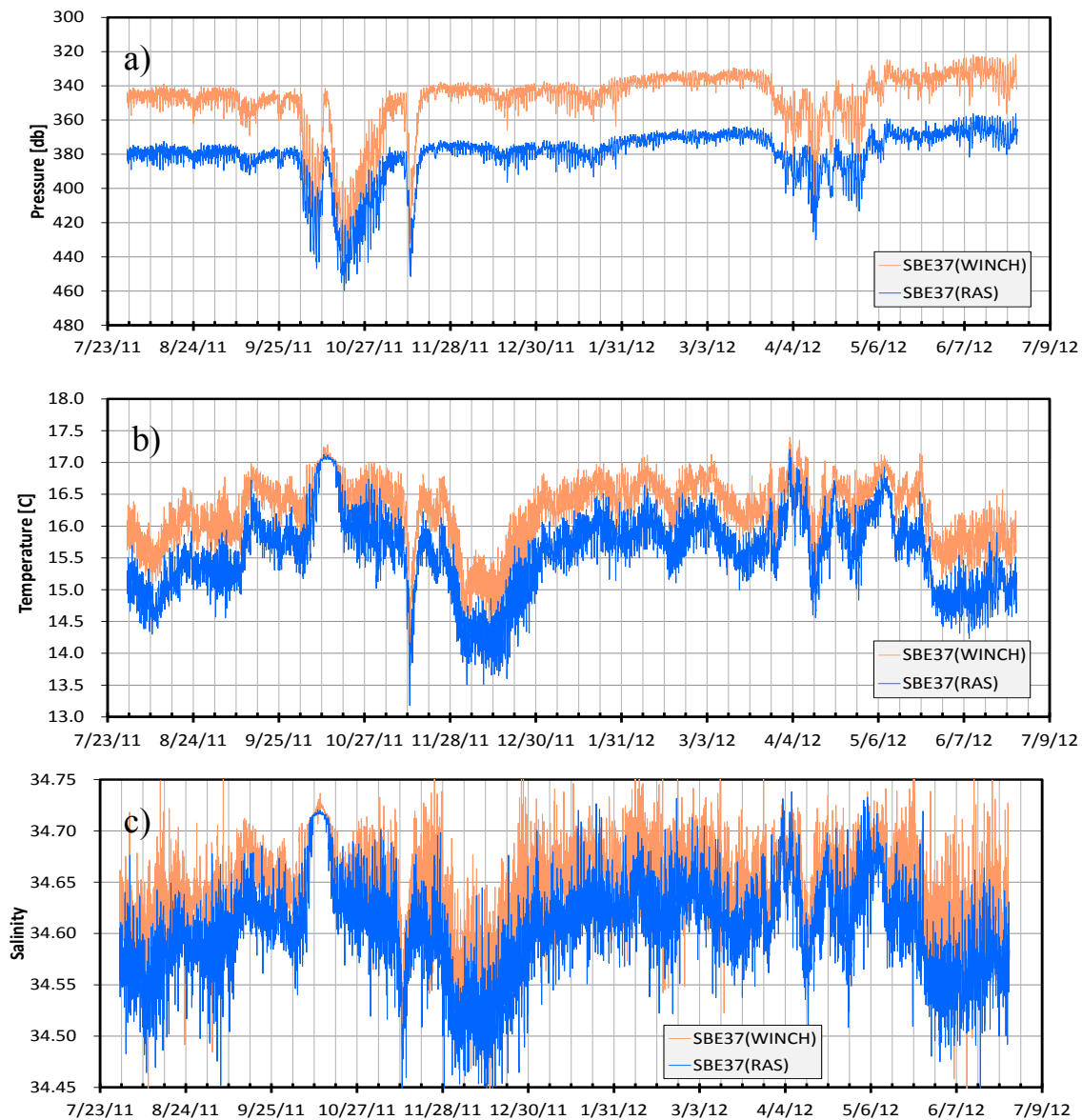


Figure 1 Pressure (a), temperature (b) and Salinity (c) at RAS and POPPS during deployment.

(4) Chemical analysis of RAS sample

RAS worked following schedule and obtained samples of dissolved inorganic carbon (DIC), total alkalinity (TA), nutrients (Phosphate, Nitrate + Nitrite, Silicate), dissolved organic carbon (DOC), $^{15}\text{NO}_3^-$ and salinity (Table 1). DOC and $^{15}\text{NO}_3^-$ will be measured by AORI and Nagoya Univ/RIGC, respectively. However, some sample volume after collecting (#2, #4, #7, #9, #18, #19, #21, #31, #39 and #48) were quite small. These samples leaked with holes and couldn't measure DIC, TA, nutrients, DOC, $^{15}\text{NO}_3^-$ and salinity

Salinity of RAS seawater samples was measured by salinometer (AutoLab YEO-KAL) (Fig 2a). Salinity of RAS samples should be lower than ambient seawater, because RAS samples were diluted with HgCl_2 solution and Milli-Q water. Salinity measured by salinometer was slightly lower than that observed by SBE-37 sensor (CTD) by $0.3 \pm 0.3\%$. RAS samples (~500ml) were diluted with 0.5 ml of HgCl_2 for preservative and 1.0 ml of Milli-Q water for pressure-resistance of sample tube (~0.3%). For RAS samples with hole on bags (#2, #4, #7, #9, #18, #19, #21, #31, #39 and #48), high salinity should be attributed to contamination of high saline seawater in the sample bag containers (not shown). For chemical properties, the dilutions of RAS samples by HgCl_2 were corrected by a ratio of salinity by SBE-37 to that by salinometer. Preliminary results of chemical analysis of RAS sample are shown in Figs. 2b to 2f.

Concentrations of nutrients (phosphate, nitrate, silicate) for the first sample (collected on 31 July 2011) were comparable to previous values observed before deployments (MR11-05) and calculation values from sigma theta by using relationship between sigma theta and nutrients. However, phosphate and nitrate decreased in late spring (#38, #41-#43, #46) (Figs. 2c-2d).

Both DIC and TA concentrations were smaller than those observed before deployments (MR11-05) and calculation values from sigma theta by $\sim 80 \pm 20$ (DIC) and 50 ± 10 (TA) $\mu\text{mol kg}^{-1}$. We did not use HCl for anti-biofouling, because HCl affected DIC analysis (Honda and Watanabe, 2007). However, DIC became lower than DIC and TA observed by hydrocasting even if seawater was collected without HCl. CO_2 degassing might take place during deployment or analysis, regardless of usage of HCl. Most of sample bags that metalized Polyethylene lined peeled after deployment, which CO_2 might degas from this peeled part of sample bag during deployment. Unfortunately RAS sample might not be available for measurements of DIC and TA of RAS samples.

Table 1 RAS sample list at S1.

RAS No.	Date		RIGC				AORI		RIGC/NU	RIGC	Memo
	Interval 8 days		Volume	DIC	TA	Nutrients	DOC		¹⁵ NO ₃ ⁻	Salinity	
	#	mm/dd/yyyy					Time(JST)	20ml			
1	07/31/2011	3:00:00	M	1	1	1	1	1	1		
2	07/31/2011	3:40:00	S	AORI : Control							Holes in sampling bag
3	07/31/2011	4:20:00	M	AORI : Glucose 1mM							
4	07/31/2011	5:00:00	S	AORI : Control							Holes in sampling bag
5	07/31/2011	5:40:00	M	AORI : Glucose 1mM							
6	08/08/2011	3:00:00	M	1	1	1	2	0	1	1	
7	08/16/2011	3:00:00	S	0	0	1	0	0	0	1	Holes in sampling bag
8	08/24/2011	3:00:00	M	1	1	1	2	0	1	1	
9	09/01/2011	3:00:00	S	0	0	0	0	0	0	0	Holes in sampling bag
10	09/09/2011	3:00:00	M	1	1	1	2	0	1	1	
11	09/17/2011	3:00:00	M	1	1	1	2	0	1	1	
12	09/25/2011	3:00:00	M	1	1	1	2	0	1	1	
13	10/03/2011	3:00:00	M	1	1	1	2	0	1	1	
14	10/11/2011	3:00:00	M	1	1	1	2	0	1	1	
15	10/19/2011	3:00:00	M	1	1	1	2	0	1	1	
16	10/27/2011	3:00:00	M	1	1	1	2	0	1	1	
17	11/04/2011	3:00:00	M	1	1	1	2	0	1	1	
18	11/12/2011	3:00:00	S	0	0	0	0	0	0	0	Holes in sampling bag
19	11/20/2011	3:00:00	S	0	0	0	0	0	0	0	Holes in sampling bag
20	11/28/2011	3:00:00	M	1	1	1	2	0	1	1	
21	12/06/2011	3:00:00	S	0	1	1	0	0	0	1	Holes in sampling bag
22	12/14/2011	3:00:00	M	1	1	1	2	0	1	1	
23	12/22/2011	3:00:00	M	1	1	1	2	0	1	1	
24	12/30/2011	3:00:00	M	1	1	1	2	0	1	1	
25	01/07/2012	3:00:00	M	1	1	1	2	0	1	1	
26	01/15/2012	3:00:00	M	1	1	1	2	0	1	1	
27	01/23/2012	3:00:00	M	1	1	1	2	0	1	1	
28	01/31/2012	3:00:00	M	1	1	1	2	0	1	1	
29	02/08/2012	3:00:00	M	1	1	1	2	0	1	1	
30	02/16/2012	3:00:00	M	1	1	1	2	0	1	1	
31	02/20/2012	3:00:00	S	0	0	1	0	0	0	1	Holes in sampling bag
32	02/24/2012	3:00:00	M	1	1	1	2	0	1	1	
33	02/28/2012	3:00:00	M	1	1	1	2	0	1	1	
34	03/03/2012	3:00:00	M	1	1	1	2	0	1	1	
35	03/07/2012	3:00:00	M	1	1	1	2	0	1	1	
36	03/11/2012	3:00:00	M	1	1	1	2	0	1	1	
37	03/19/2012	3:00:00	M	1	1	1	2	0	1	1	
38	03/27/2012	3:00:00	M	1	1	1	2	0	1	1	
39	04/04/2012	3:00:00	S	0	0	0	0	0	0	0	Holes in sampling bag
40	04/12/2012	3:00:00	M	1	1	1	2	0	1	1	
41	04/20/2012	3:00:00	M-	1	1	1	1	1	0	1	
42	04/28/2012	3:00:00	M	1	1	1	2	0	1	1	
43	05/06/2012	3:00:00	M	1	1	1	2	0	1	1	
44	05/14/2012	3:00:00	M	1	1	1	2	0	1	1	
45	05/22/2012	3:00:00	M	1	1	1	2	0	1	1	
46	05/30/2012	3:00:00	M	1	1	1	2	0	1	1	
47	06/07/2012	3:00:00	M	1	1	1	2	0	1	1	
48	06/15/2012	3:00:00	S	0	0	0	0	0	0	0	Holes in sampling bag

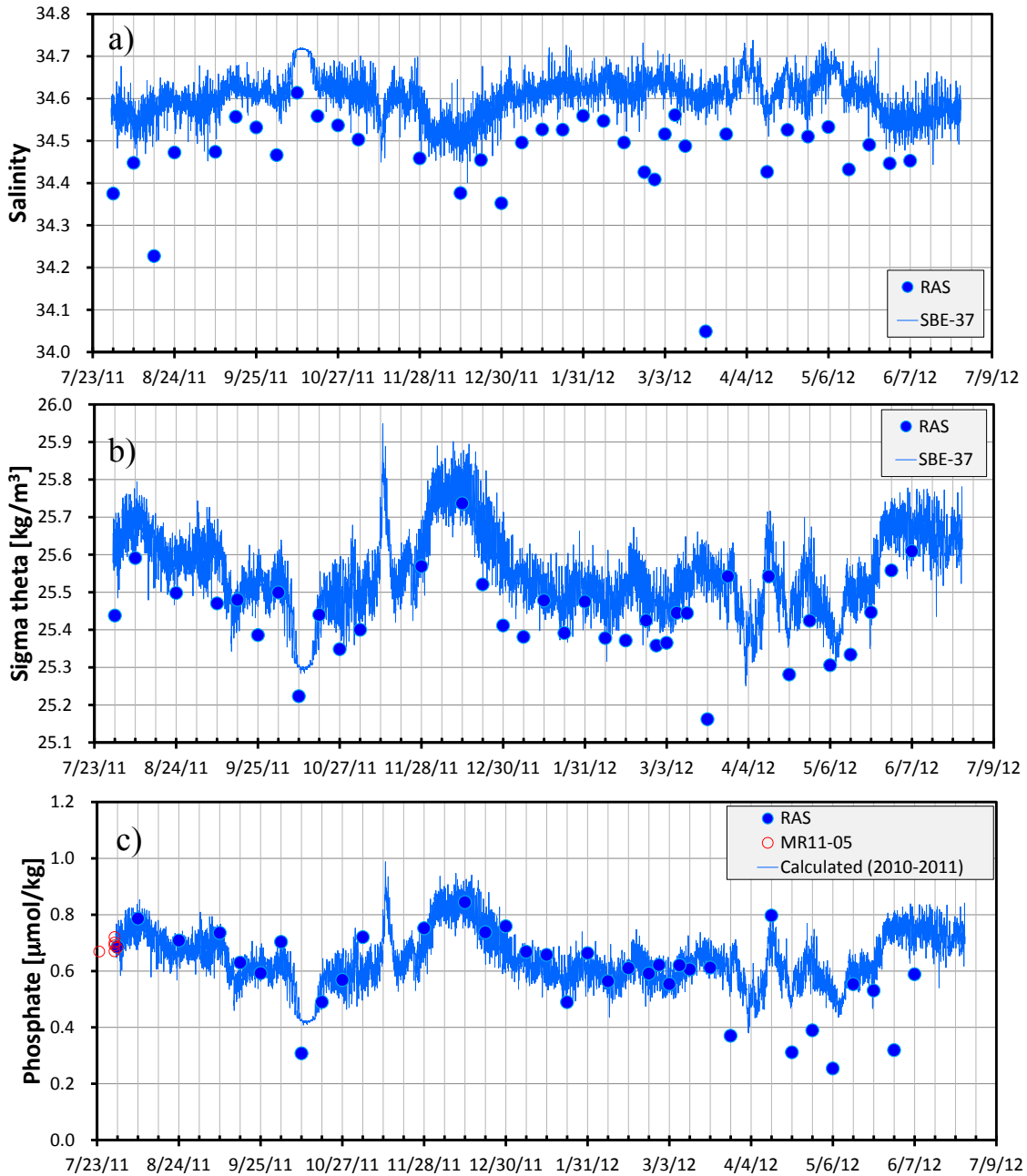


Figure 2 Measurements of salinity (a), sigma theta (b), phosphate (c), nitrate (d), silicate (e), TA and DIC (f) collected by RAS during deployment. Thin lines were the salinity value calculated from sigma theta by using TA or DIC from 2010 to 2011(c-f), because with nutrients, DIC and TA. Opened circles (○) show the measurements by hydrocasting before mooring deployment.

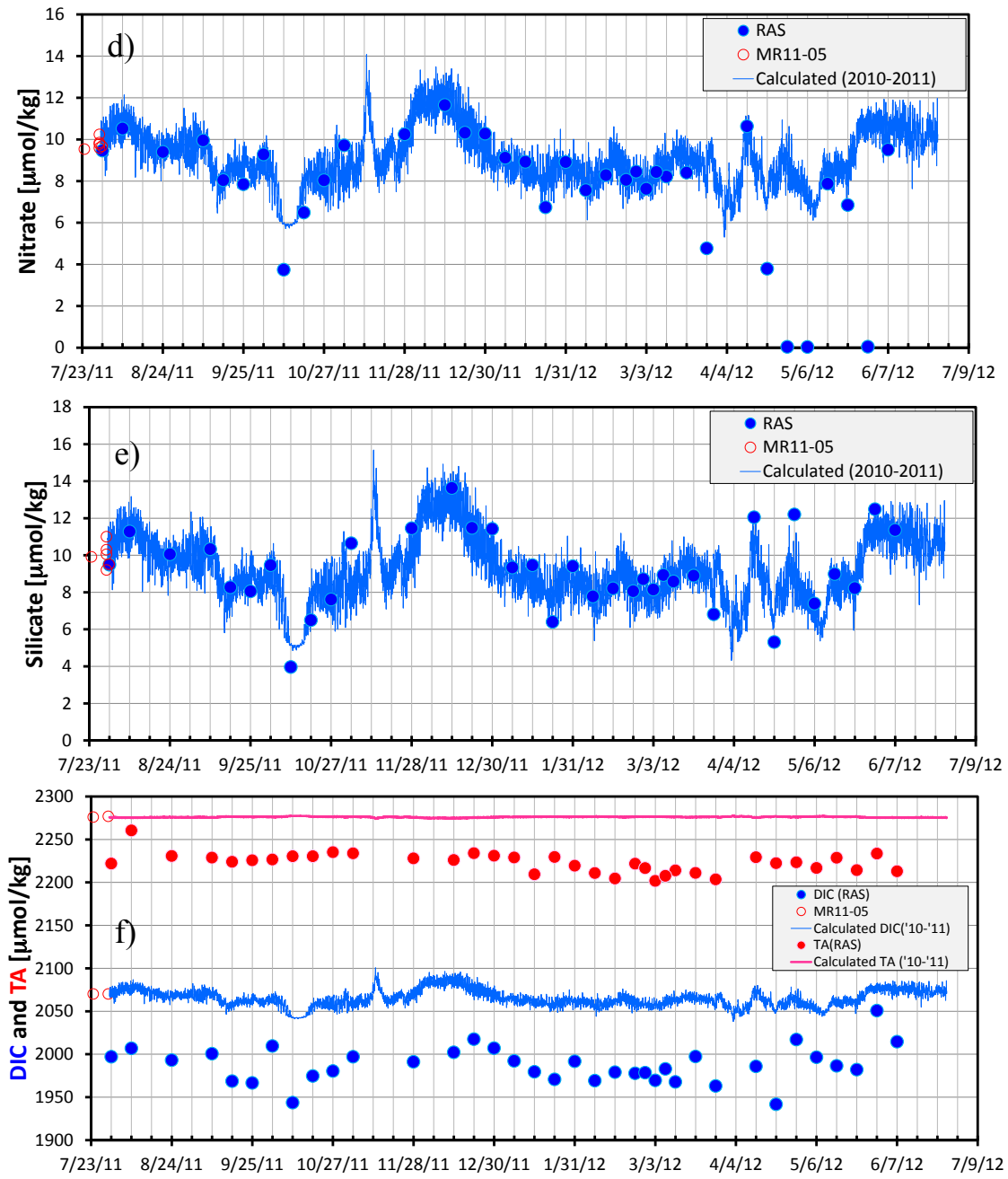


Figure 2 (continued) .

3.2.2.2 RAS Sampling schedule

Sampling schedule of time-series remote automatic water sampler (RAS) of POPPS mooring at station S1 is as follows;

S1 RAS 250m POPPS

RAS No.	Date		Memo
	Interval 8 days		
#	mm/dd/yyyy	Time(JST)	
1	07/02/2012	19:00:00	Saturated HgCl ₂ 0.5ml
2	07/02/2012	19:40:00	Saturated HgCl ₂ 0.5ml
3	07/10/2012	19:00:00	Saturated HgCl ₂ 0.5ml
4	07/18/2012	19:00:00	Saturated HgCl ₂ 0.5ml
5	07/26/2012	19:00:00	Saturated HgCl ₂ 0.5ml
6	08/03/2012	19:00:00	Saturated HgCl ₂ 0.5ml
7	08/11/2012	19:00:00	Saturated HgCl ₂ 0.5ml
8	08/19/2012	19:00:00	Saturated HgCl ₂ 0.5ml
9	08/27/2012	19:00:00	Saturated HgCl ₂ 0.5ml
10	09/04/2012	19:00:00	Saturated HgCl ₂ 0.5ml
11	09/12/2012	19:00:00	Saturated HgCl ₂ 0.5ml
12	09/20/2012	19:00:00	Saturated HgCl ₂ 0.5ml
13	09/28/2012	19:00:00	Saturated HgCl ₂ 0.5ml
14	10/06/2012	19:00:00	Saturated HgCl ₂ 0.5ml
15	10/14/2012	19:00:00	Saturated HgCl ₂ 0.5ml
16	10/22/2012	19:00:00	Saturated HgCl ₂ 0.5ml
17	10/30/2012	19:00:00	Saturated HgCl ₂ 0.5ml
18	11/07/2012	19:00:00	Saturated HgCl ₂ 0.5ml
19	11/15/2012	19:00:00	Saturated HgCl ₂ 0.5ml
20	11/23/2012	19:00:00	Saturated HgCl ₂ 0.5ml
21	12/01/2012	19:00:00	Saturated HgCl ₂ 0.5ml
22	12/09/2012	19:00:00	Saturated HgCl ₂ 0.5ml
23	12/17/2012	19:00:00	Saturated HgCl ₂ 0.5ml
24	12/25/2012	19:00:00	Saturated HgCl ₂ 0.5ml
25	01/02/2013	19:00:00	Saturated HgCl ₂ 0.5ml
26	01/10/2013	19:00:00	Saturated HgCl ₂ 0.5ml
27	01/18/2013	19:00:00	Saturated HgCl ₂ 0.5ml
28	01/26/2013	19:00:00	Saturated HgCl ₂ 0.5ml
29	02/03/2013	19:00:00	Saturated HgCl ₂ 0.5ml
30	02/11/2013	19:00:00	Saturated HgCl ₂ 0.5ml
31	02/19/2013	19:00:00	Saturated HgCl ₂ 0.5ml
32	02/27/2013	19:00:00	Saturated HgCl ₂ 0.5ml
33	03/07/2013	19:00:00	Saturated HgCl ₂ 0.5ml
34	03/15/2013	19:00:00	Saturated HgCl ₂ 0.5ml
35	03/23/2013	19:00:00	Saturated HgCl ₂ 0.5ml
36	03/31/2013	19:00:00	Saturated HgCl ₂ 0.5ml
37	04/08/2013	19:00:00	Saturated HgCl ₂ 0.5ml
38	04/16/2013	19:00:00	Saturated HgCl ₂ 0.5ml
39	04/24/2013	19:00:00	Saturated HgCl ₂ 0.5ml
40	05/02/2013	19:00:00	Saturated HgCl ₂ 0.5ml
41	05/10/2013	19:00:00	Saturated HgCl ₂ 0.5ml
42	05/18/2013	19:00:00	Saturated HgCl ₂ 0.5ml
43	05/26/2013	19:00:00	Saturated HgCl ₂ 0.5ml
44	06/03/2013	19:00:00	Saturated HgCl ₂ 0.5ml
45	06/11/2013	19:00:00	Saturated HgCl ₂ 0.5ml
46	06/19/2013	19:00:00	Saturated HgCl ₂ 0.5ml
47	06/27/2013	19:00:00	Saturated HgCl ₂ 0.5ml
48	07/05/2013	19:00:00	Saturated HgCl ₂ 0.5ml

Interval 40 minutes
for duplicate sampling

3.3 Sediment trap experiment at station F1

Makio HONDA (JAMSTEC)

Hajime KAWAKAMI (JAMSTEC)

Cris GERMAN (Woods Hole Oceanographic Institution, WHOI)

Steven J. MANGANINI (WHOI)

In order to collect time-series sinking particle and certify how and when artificial radioactive nuclides are transported vertically near the Fukushima Daiichi nuclear power plant, time-series sediment traps were deployed at approximately 500 m and 1000 m at station F1 in July 2011. Sampling interval are 16 days at 1000 m and 32 days at 500 m (16 days in March and April 2012). Before deployment, collecting cups were filled up with seawater based 10% buffered formalin. This observation is cooperative research with Woods Hole Oceanographic Institution (PI: Cris German). This mooring system was recovered and redeployed during this cruise.

3.3.1 Preliminary result

(1) Total Mass Flux

Onboard, we measured heights of sinking particle collect in collecting cups with scale in order to know general view of seasonal variability.

Small increases of total mass flux at 200 m were observed in autumn 2011 and January 2012 (Fig. 3.3.1). Relatively larger flux was observed in April 2012. At 1000 m, two flux peaks were observed in September 2011 and January 2012 these increases synchronized well with shallower flux increases. Please note that several cups contained swimmer such as fish, shrimp and jelly fish.

(2) Seasonal variability in temperature, water depth, current velocity and direction

On mooring system, ADCP was installed at ca. 475 m and 975 m and measured seasonal variability in temperature, water depth, current velocity and direction during deployment.

Water depth at 475 m ADCP varied between 474 m and 469 m (Fig. 3.3.2). At the beginning of October 2011, water depth of 475 m ADCP water decreased by about 3 m temporally while water depth of 975 m ADCP decreased by about 4 m at the beginning of December 2011 and increased gradually to 977 m. At this moment, the cause of this motion is unknown and open question. Water temperature at 475 m was about 4°C and relatively stable by February 2012 (Fig. 3.3.2). Water temperature varied largely between 3°C and 7°C thereafter. Water temperature at 975 m were relatively stable and about 3.1°C.

Current velocity at 475 m and 975 m varied from 0 cm sec⁻¹ to 30 cm sec⁻¹, and were on average 6 cm sec⁻¹ and 4 cm sec⁻¹, respectively (Fig. 3.3.3). Strong dominant current direction did not exist and, however, current tended to flow toward south (Fig. 3.3.4).

It is noted that layers with lower beam transmittance were observed at around 700 m and below 1100 m during the last cruise (MR11-05: MR11-05) while these layers were not clear

during this cruise (Fig. 3.3.5). Horizontal transport of materials should be taken into account when the results are discussed.

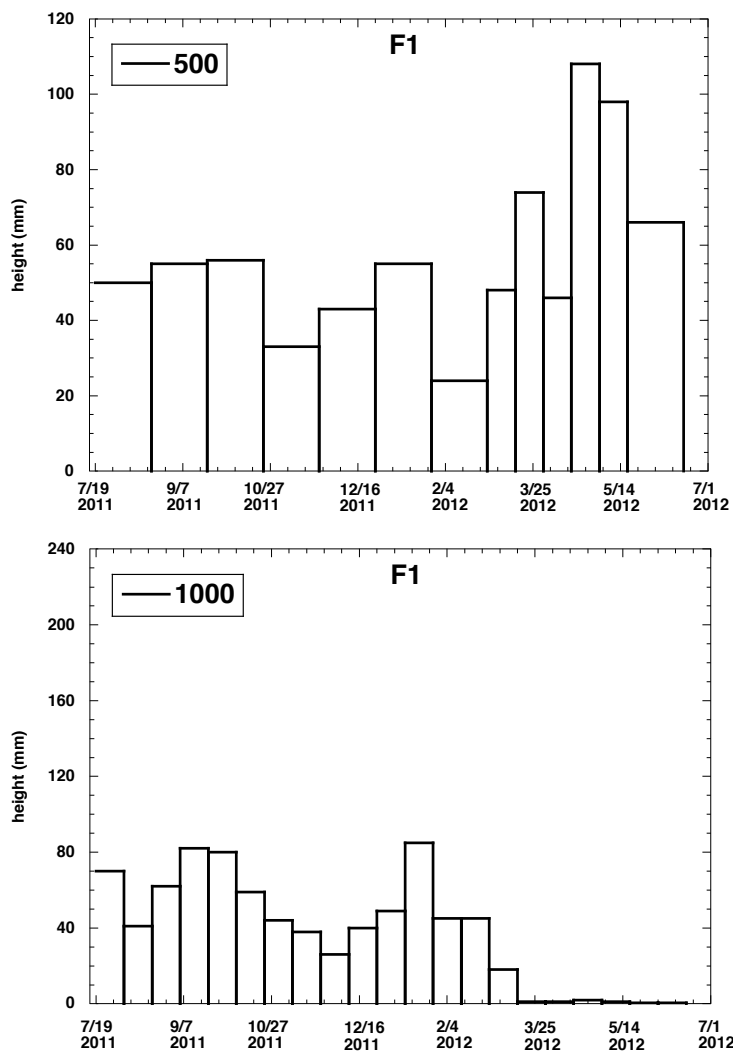


Fig. 3.3.1 Seasonal variability in total mass flux. Please note that size of collecting cup between 500 m and 1000 m are different (diameter of 500 ml cup has ca. two times higher than that of 1000 m cup).

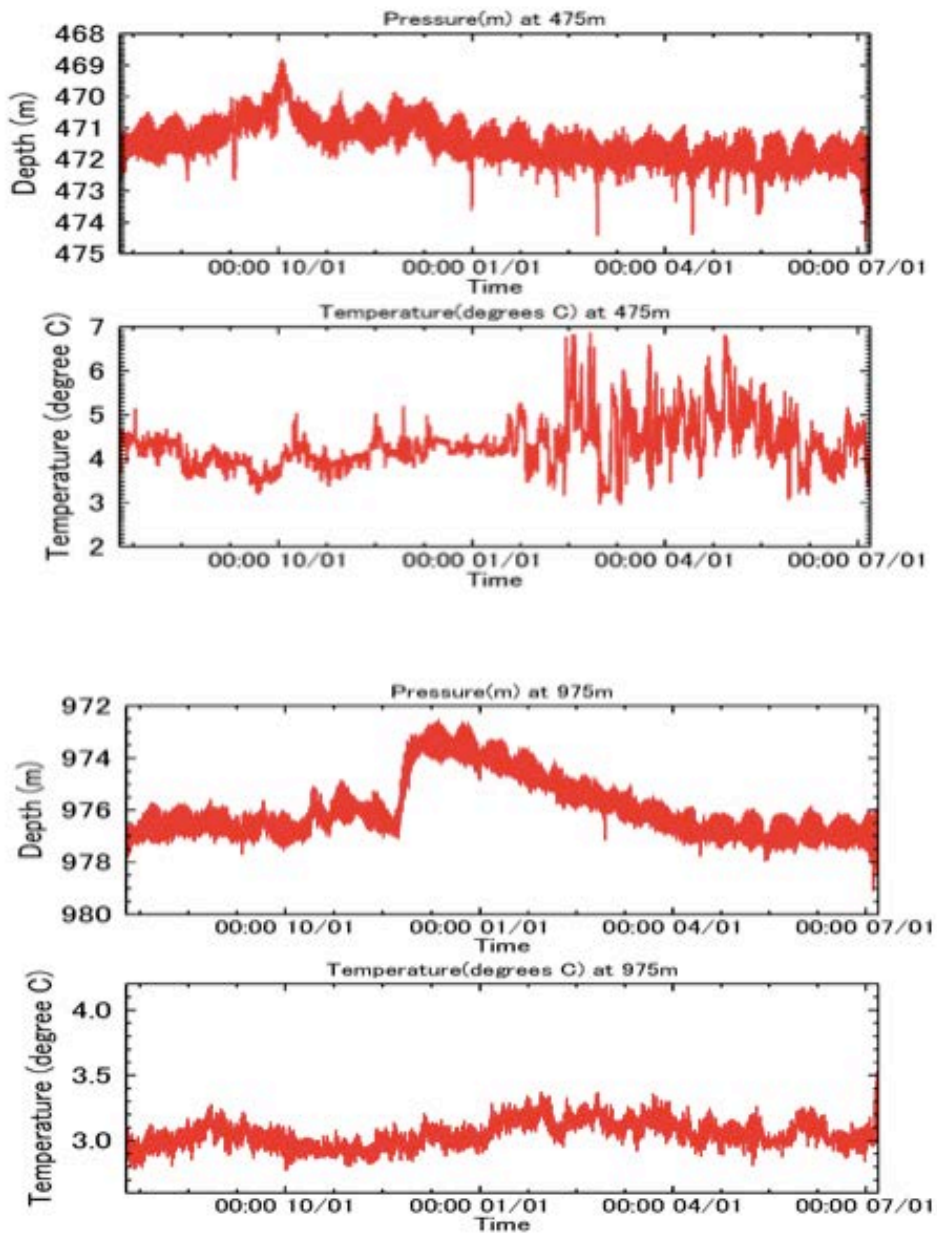


Fig. 3.3.2 Seasonal variability in pressure and temperature measured by ADCP at ca. 475 m and 975 m.

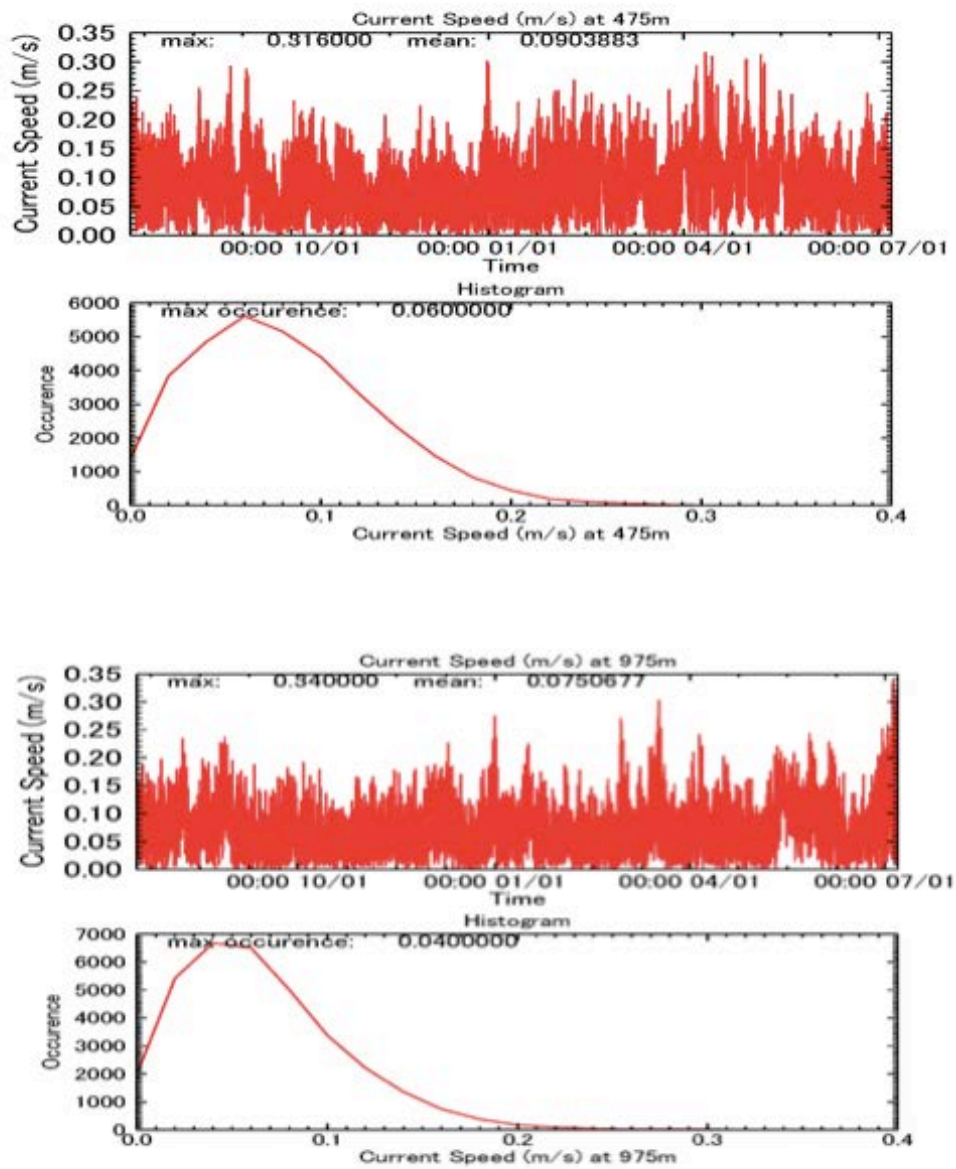


Fig. 3.3.3 Seasonal variability in current velocity measured by ADCP at ca. 475 m and 975 m.

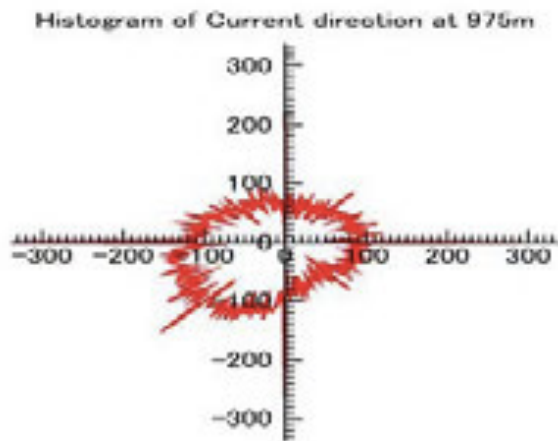
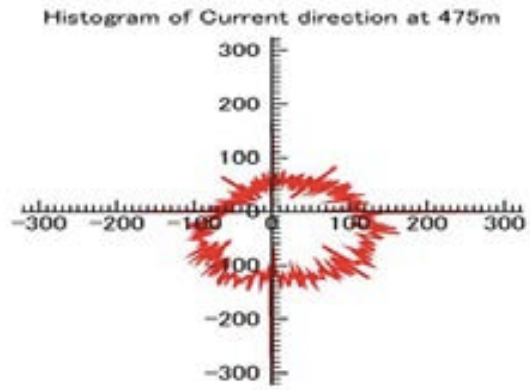


Fig. 3.3.4 Histogram of current direction measured by ADCP at ca. 475 m and 975 m.

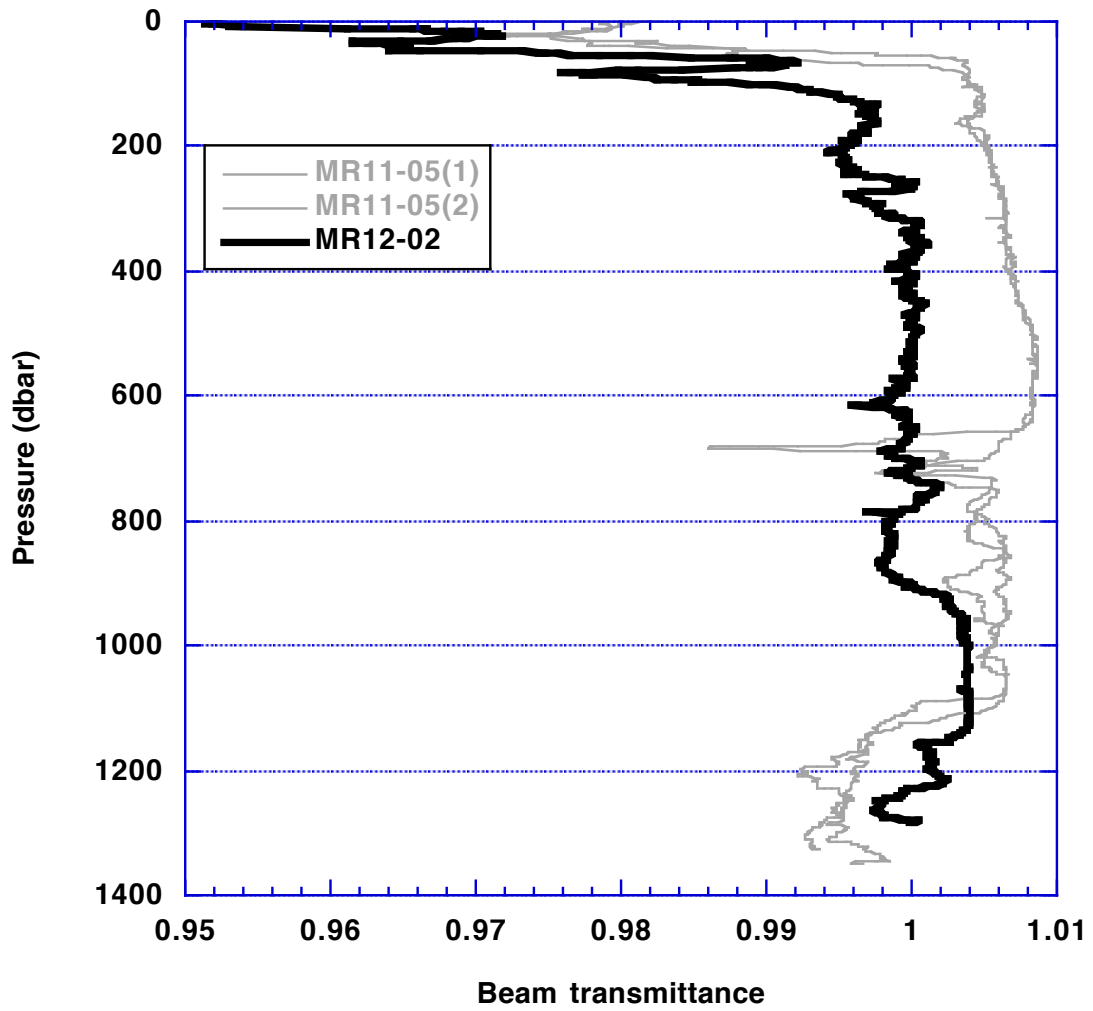


Fig. 3.3.5 Vertical profile of beam transmittance during MR12-02 cruise (black line) and MR11-05 (gray lines)

3.3.2 Redeployment

After retrieving sample / data, replacement of new battery and initialization of schedule (Table 3.3.1), sediment trap mooring system was deployed on 9 July 2012. Designs of mooring system are shown in Table 3.3.2 and Fig. 3.3.5. Anchor position and ambient topography is shown in Fig. 3.3.6. Various information about deployment (Releaser, anchor position, and working log) are shown in Table 3.3.3. This mooring system will be recovered in July 2013.

Table 3.3.1 Schedule (opening day of each cup)

	1000m		500m	
		21		13
		17		34
1	2012/7/10	1	2012/7/10	
2	2012/7/27	2	2012/8/13	
3	2012/8/13	3	2012/8/16	
4	2012/8/30	4	2012/10/20	
5	2012/9/16	5	2012/11/23	
6	2012/10/3	6	2012/12/27	
7	2012/10/20	7	2013/1/30	
8	2012/11/8	8	2013/3/5	
9	2012/11/23	9	2013/3/22	interval
10	2012/12/10	10	2013/4/8	17
11	2012/12/27	11	2013/4/25	
12	2013/1/13	12	2013/5/12	
13	2013/1/30	13	2013/5/29	
14	2013/2/16		2013/7/2	
15	2013/3/5			
16	2013/3/22			
17	2013/4/8			
18	2013/4/25			
19	2013/5/12			
20	2013/5/29			
21	2013/6/15			
	2013/7/2			

Table 3.3.2 design of ST mooring system (2012 – 2013)
(Major difference from 2011-2012 version is no current meter.)

Mooring I.D.		Fukushima WHOI Sediment Trap Mooring (F1)										
Water Depth		1300.00										
Connections	Item #	Description	Weight (lb/m.ea)	Quantity #	Item Length Item	Item Weight Item	Mooring Length (m)	Above Bottom mab	Below Surface mbs	Mooring Weight(lb) (lb)top to bottom	Mooring Weight(lb) (lb)bottom to top no anchor	Mooring Weight(lb) (lb)bottom to top with anchor
A4	1	GLASS BALLS 17"on 1m,3/8 chain	-50.00	18.00	18.00	-900.00	18.00	840.04	459.96	-900.00	-654.56	1112.14
A	2	wire rope 1/4"	0.27	1.00	20.00	5.32	38.00	822.04	477.96	-894.68	245.44	2012.14
A	3	chain, 3/8"	4.49	1.00	2.00	8.98	40.00	802.04	497.96	-885.70	240.12	2006.82
A	4	bridle (3-wire rope)	10.16	1.00	1.00	10.16	41.00	800.04	499.96	-875.54	231.14	1997.84
ST-500m	5	SEDIMENT TRAP MK7	121.00	1.00	1.52	121.00	42.52	799.04	500.96	-754.54	220.98	1987.68
	6	bridle,(3-1m 3/8 chain)	23.20	1.00	1.00	23.20	43.52	797.52	502.48	-731.34	99.98	1866.88
A	7	chain, 3/8"	4.49	1.00	2.00	8.98	45.52	796.52	503.48	-722.36	76.78	1843.48
A	8	wire rope 1/4"	0.27	1.00	461.00	122.83	506.52	794.52	505.48	-599.73	67.80	1834.50
A4	9	GLASS BALLS 17"on 1m,3/8 chain	-50.00	10.00	10.00	-500.00	516.52	333.52	966.48	-1099.73	-54.82	1711.88
A	10	wire rope 1/4"	0.15	1.00	20.00	3.00	536.52	323.52	976.48	-1096.73	445.18	2211.88
A	11	chain, 3/8"	4.49	1.00	2.00	8.98	538.52	303.52	996.48	-1087.75	442.18	2208.88
	12	bridle (3-wire rope)	10.16	1.00	1.00	10.16	539.52	301.52	998.48	-1077.59	433.20	2199.90
ST-1000m	13	SEDIMENT TRAP MK7	121.00	1.00	1.52	121.00	541.04	300.52	999.48	-956.59	423.04	2169.74
A	14	bridle,(3-1m 3/8 chain)	23.20	1.00	1.00	23.20	542.04	299.00	1001.00	-933.39	302.04	2068.74
A	15	chain, 3/8"	4.49	1.00	2.00	8.98	544.04	298.00	1002.00	-924.41	278.84	2045.54
A	16	wire rope 1/4"	0.27	1.00	176.00	46.82	720.04	296.00	1004.00	-877.60	269.86	2036.56
B	17	chain, 3/8"	4.49	1.00	2.00	8.98	722.04	120.00	1180.00	-868.62	223.04	1989.74
B	18	ACOUSTIC RELEASE (ORE Tandem)	160.00	1.00	1.00	160.00	723.04	118.00	1182.00	-708.62	214.06	1980.76
B	19	chain, 3/8"	4.49	1.00	2.00	8.98	725.04	117.00	1183.00	-699.64	54.06	1820.76
A	20	wire rope 1/4"	0.27	1.00	50.00	13.30	775.04	115.00	1185.00	-686.34	45.08	1825.08
A	21	wire rope 1/4"	0.27	1.00	50.00	13.30	825.04	65.00	1235.00	-673.04	31.78	1811.78
B	22	nylon rope,3/4"	0.05	1.00	10.00	0.52	835.04	15.00	1285.00	-672.52	18.48	1798.48
B	23	chain, 3/8"	4.49	1.00	4.00	17.96	839.04	5.00	1295.00	-654.56	17.96	1797.96
Anchor-1300m	24	ANCHOR	0.89	2000.00	1.00	1780.00	840.04	1.00	1299.00	1125.44		1780.00
A = 1/2"shackle - 5/8" pear ring - 1/2"shackle												
B = 1/2"shackle - 5/8" pear ring - 5/8"shackle												

MR12-02 WHOI Deployment FINAL

F1

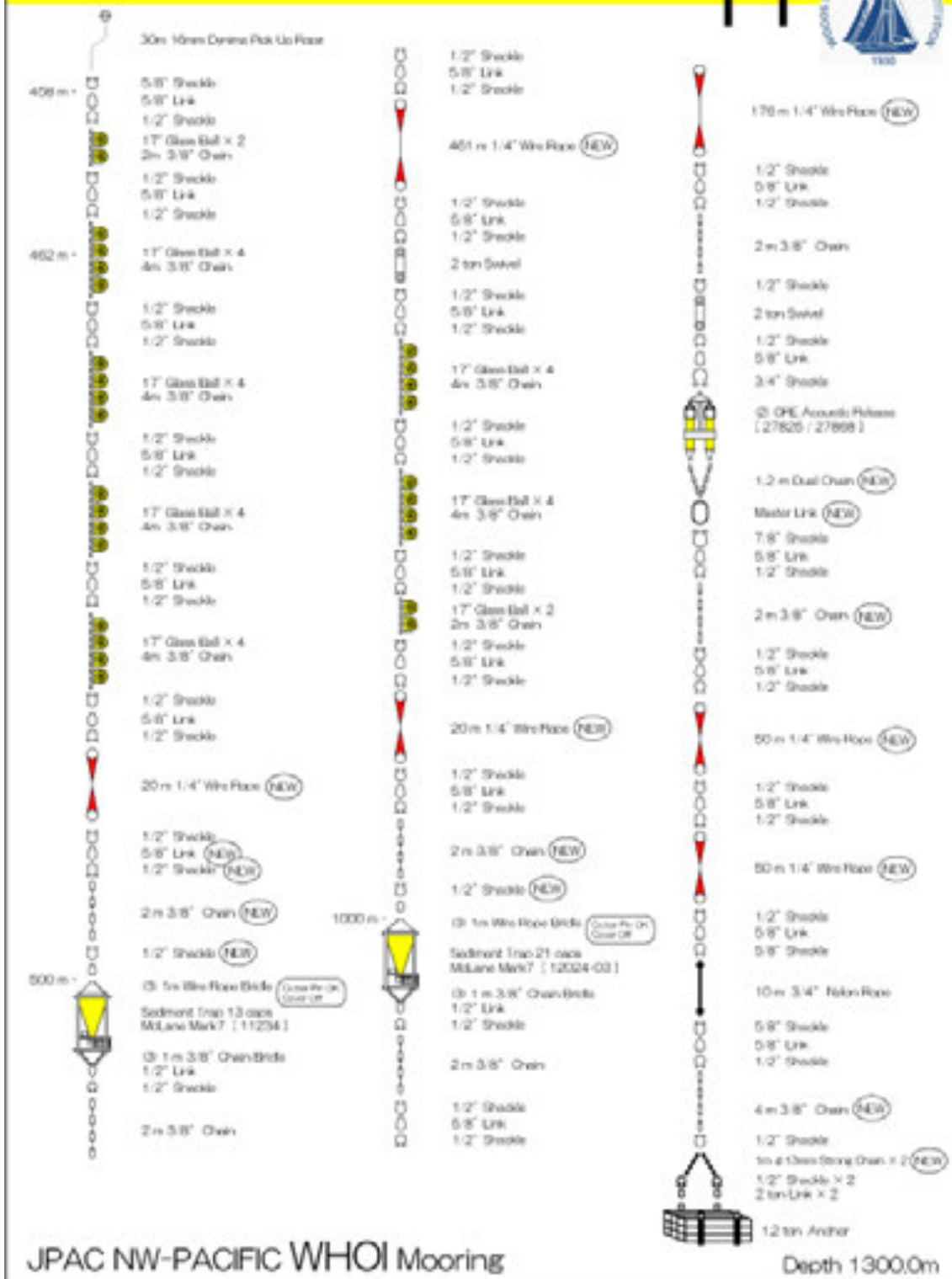


Fig. 3.3.5 Design of F1 sediment trap mooring system

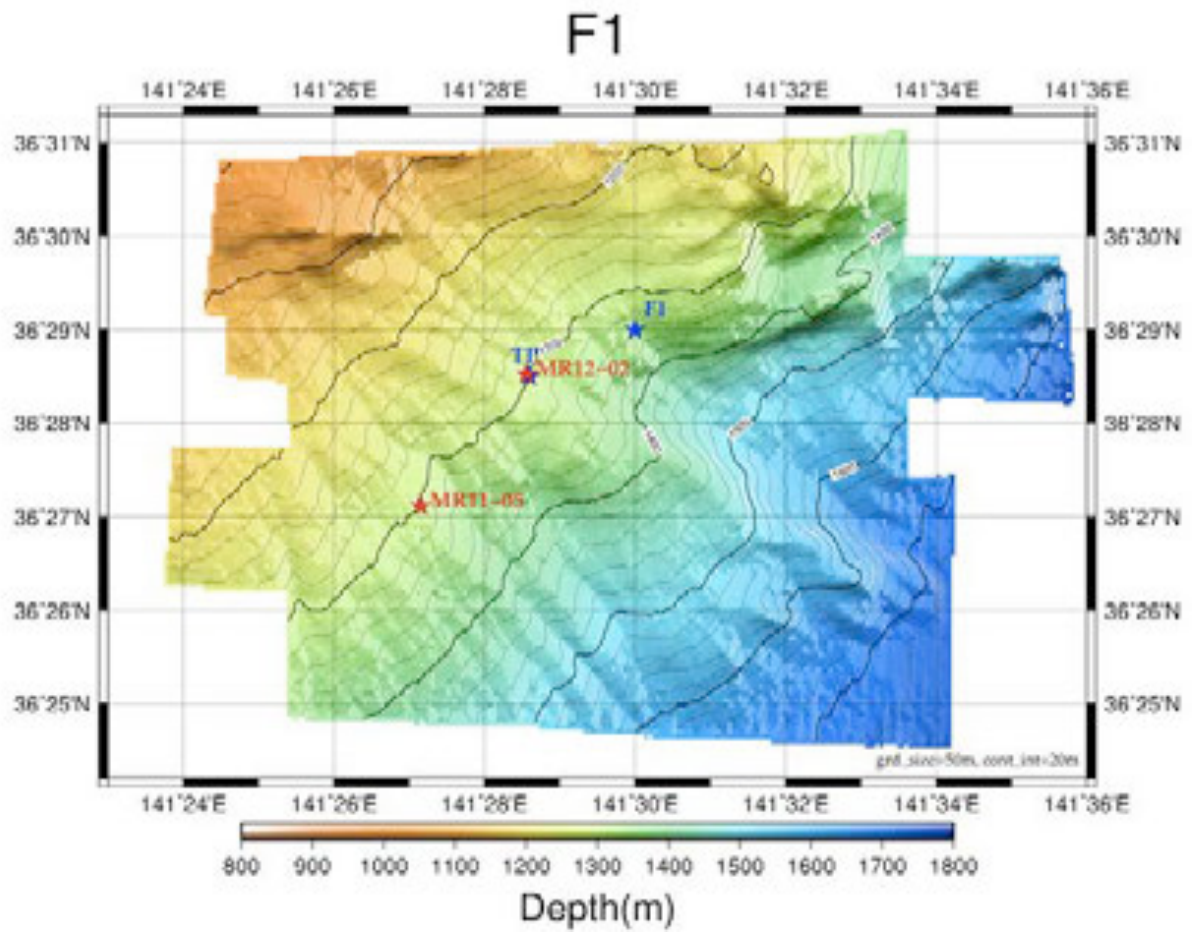


Fig. 3.3.6 Anchor position of F1 sediment trap (MR12-02).
Former anchor position (MR11-05) is also shown for comparison.

Table 3.3.3 Deployment log sheet

Mooring Number	F1WHOI120708		
Project	Time-Series	Depth	1,300.0 m
Area	North Pacific	Planned Depth	1,300.0 m
Station	F1	Length	842.0 m
Target Position	36°28.50 N	Depth of Buoy	457 m
	141°28.60 E	Period	1 year
ACOUCTIC RELEASERS			
Type	Edgetech	Edgetech	
Serial Number	27825	27868	
Receive F.	11.0 kHz	11.0 kHz	
Transmit F.	14.0 kHz	14.0 kHz	
RELEASE C.	344176	335534	
Enable C.	356736	322710	
Disable C.	356770	322756	
Battery	2 years	2 years	
Release Test	-	-	
DEPLOYMENT			
Recorder	Toru Idai	Start	0.8 Nmile
Ship	R/V MIRAI	Overshoot	- m
Cruise No.	MR12-02	Let go Top Buoy	20:57
Date	2012/7/8	Let go Anchor	22:12
Weather	bc	Sink Top Buoy	22:17
Wave Hight	0.9 m	Pos. of Start	36°29.09 N
Seabeam Depth	1,298 m		141°29.94 E
Ship Heading	<225>	Pos. of Drop. Anc.	36°28.42 N
Ship Ave.Speed	- knot		141°28.53 E
Wind	<NNE> 4.0 m/s	Pos. of Mooring	36°28.53 N
Current	<040> 36.0 cm/sec		141°28.56 E

3.4 Phytoplankton

3.4.1 Chlorophyll *a* measurements by fluorometric determination

Kazuhiko MATSUMOTO (JAMSTEC)

Hideki YAMAMOTO (MWJ)

Hironori SATO (MWJ)

Masahiro ORUI (MWJ)

Keitaro MATSUMOTO (MWJ)

1. Objective

Phytoplankton biomass can estimate as the concentration of chlorophyll *a* (chl-*a*), because all oxygenic photosynthetic plankton contain chl-*a*. Phytoplankton exist various species in the ocean, but the species are roughly characterized by their cell size. The objective of this study is to investigate the vertical distribution of phytoplankton and their size fractionations as chl-*a* by using the fluorometric determination.

2. Sampling

Samplings of total chl-*a* were conducted from 16 depths between the surface and 200 m at all observational stations. At the cast for primary production, water samples were collected at eight depths from among the surface, 1%, 3%, 5%, 7%, 13%, 33%, 60% light depths relative to the surface and at five other depths between the surface and 200 m at the station of K2 and S1.

3. Instruments and Methods

Water samples (0.15–0.5 L) for total chl-*a* were filtered (<0.02 MPa) through 25mm-diameter Whatman GF/F filter. Size-fractionated chl-*a* were obtained by sequential filtration (<0.02 MPa) of 1 L water sample through 10- μ m, 3- μ m and 1- μ m polycarbonate filters (47-mm diameter) and Whatman GF/F filter (25-mm diameter). Phytoplankton pigments retained on the filters were immediately extracted in a polypropylene tube with 7 ml of N,N-dimethylformamide (Suzuki and Ishimaru, 1990). Those tubes were stored at –20°C under the dark condition to extract chl-*a* for 24 hours or more.

Fluorescences of each sample were measured by Turner Design fluorometer (10-AU-005), which was calibrated against a pure chl-*a* (Sigma-Aldrich Co.). We applied two kind of fluorometric determination for the samples of total chl-*a*: “Non-acidification method” (Welschmeyer, 1994) and “Acidification method” (Holm-Hansen *et al.*, 1965). Size-fractionated samples were applied only “Non-acidification method”. Analytical conditions of each method were listed in table 1.

4. Preliminary Results

The results of total chl-*a* at station K2 and S1 were shown in Figure 1 and 2. The results of total chl-*a* at station KNOT, JKEO NKEO and KEO were shown in Figure 3. The results of size fractionated chl-*a* were shown in Figure 4.

5. Data archives

The processed data file of pigments will be submitted to the JAMSTEC Data

Integration and Analysis Group (DIAG) within a restricted period. Please ask PI for the latest information.

6. Reference

- Suzuki, R., and T. Ishimaru (1990), An improved method for the determination of phytoplankton chlorophyll using N, N-dimethylformamide, *J. Oceanogr. Soc. Japan*, 46, 190-194.
- Holm-Hansen, O., Lorenzen, C. J., Holmes, R.W. and J. D. H. Strickland (1965), Fluorometric determination of chlorophyll. *J. Cons. Cons. Int. Explor. Mer.* 30, 3-15.
- Welschmeyer, N. A. (1994), Fluorometric analysis of chlorophyll *a* in the presence of chlorophyll *b* and pheopigments. *Limnol. Oceanogr.* 39, 1985-1992.

Table 1. Analytical conditions of “Non-acidification method” and “Acidification method” for chlorophyll *a* with Turner Designs fluorometer (10-AU-005).

	Non-acidification method	Acidification method
Excitation filter (nm)	436	340-500
Emission filter (nm)	680	>665
Lamp	Blue Mercury Vapor	Daylight White

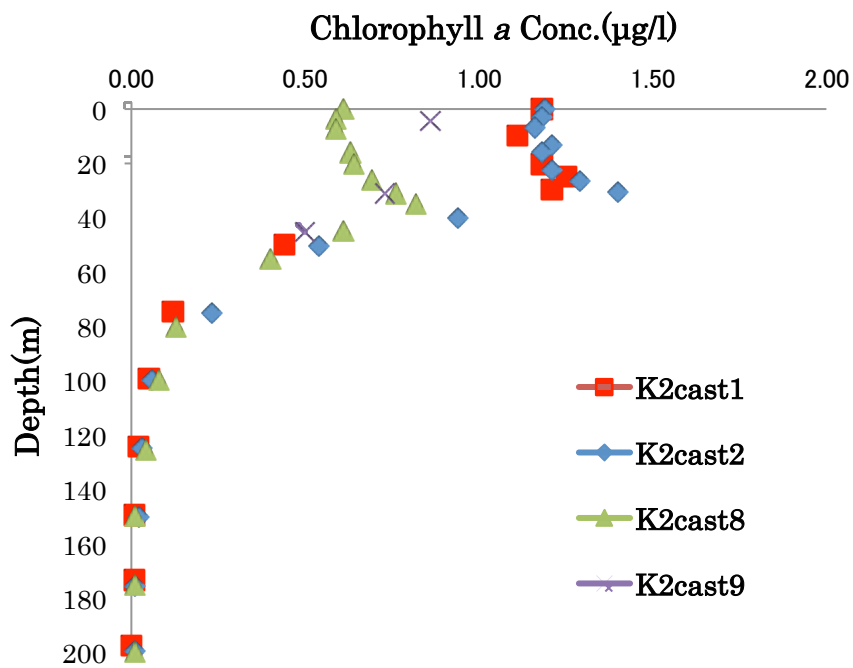


Figure 1. Vertical distribution of chlorophyll *a* at Stn. K2 cast 1, 2, 8 and 9

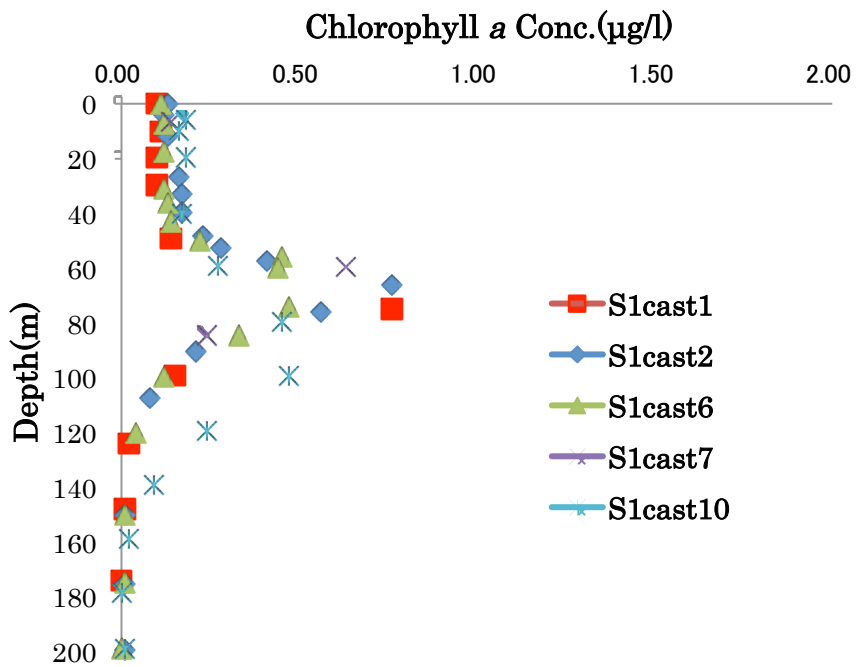


Figure 2. Vertical distribution of chlorophyll *a* at Stn. S1 cast 1, 2, 6, 7 and 10

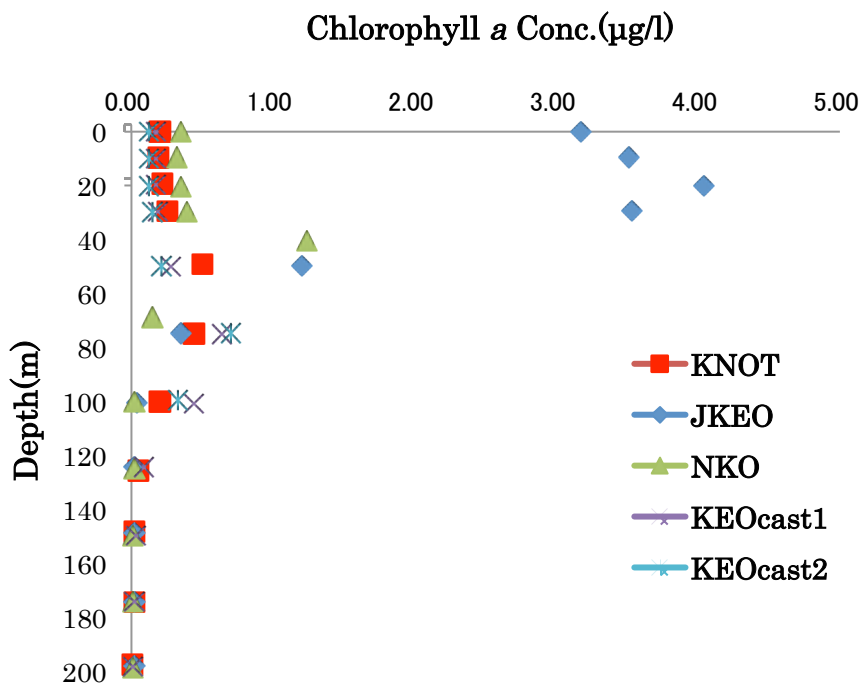


Figure 3. Vertical distribution of chlorophyll *a* at Stn. KNOT, JKEO, NKEO, KEO cast 1 and KEO cast 2.

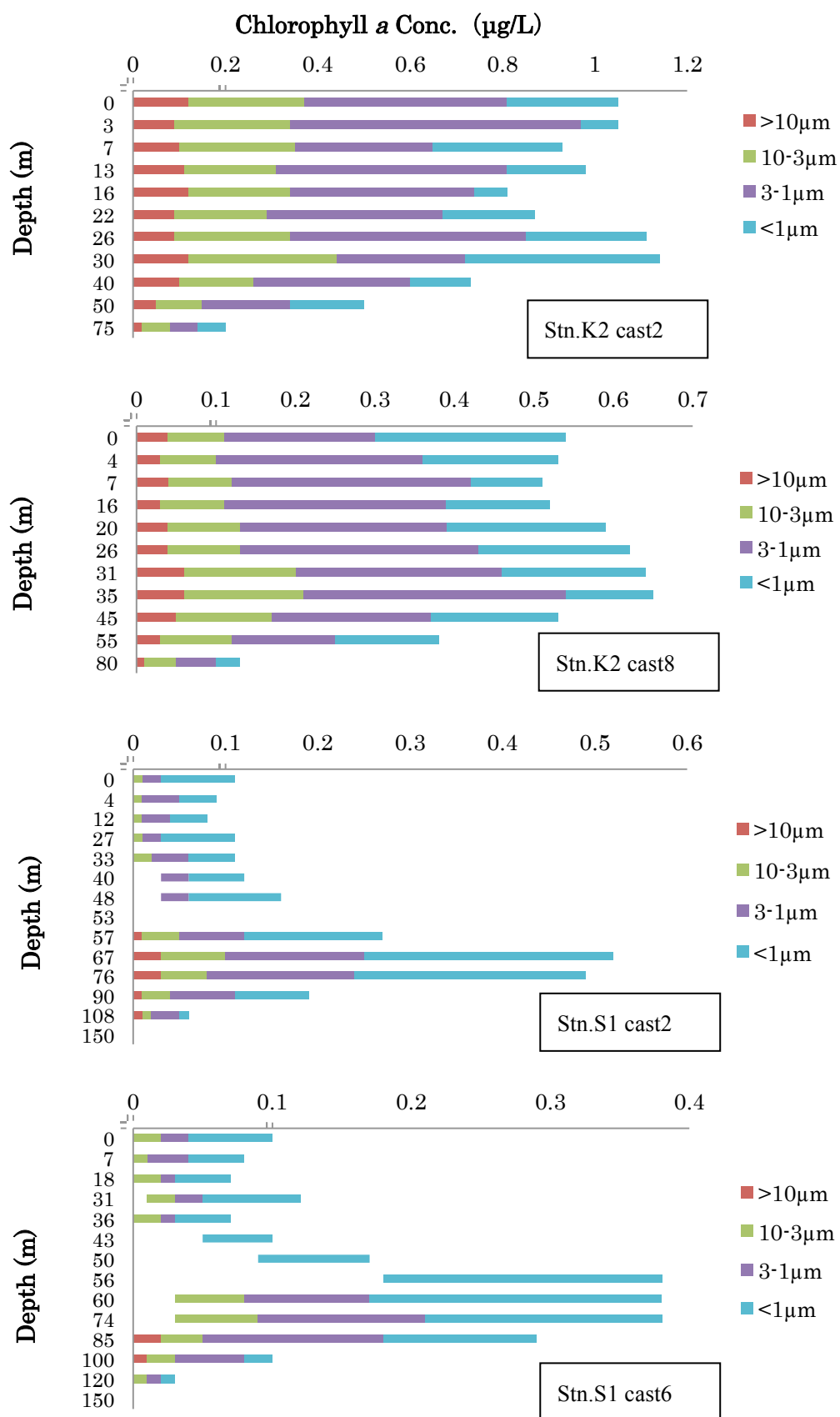


Figure 4. Vertical distribution of size-fractionated chlorophyll *a*

3.4.2 HPLC measurements of marine phytoplankton pigments

Kazuhiko MATSUMOTO (JAMSTEC RIGC)

Hironori SATO (MWJ)

(1) Objective

The chemotaxonomic assessment of phytoplankton populations present in natural seawater requires taxon-specific algal pigments as good biochemical markers. A high-performance liquid chromatography (HPLC) measurement is an optimum method for separating and quantifying phytoplankton pigments in natural seawater. In this cruise, we measured the marine phytoplankton pigments by HPLC to investigate the marine phytoplankton community structure in the western North Pacific.

(2) Methods, Apparatus and Performance

Seawater samples were collected from 11 or 14 depths between the surface and 200 m at the cast for the primary production. Sampling depths were determined by the light intensity at eight depths from among the surface, 0.5%, 1%, 2.5%, 5%, 10%, 25%, 50% light depths relative to the surface and at three other depths between the surface and 200 m. Seawater samples were collected using Niskin bottles, except for the surface water, which was taken by a bucket. Seawater samples (2 to 3L) were filtered (<0.02 MPa) through the 47-mm diameter Whatman GF/F filter. To remove retaining seawater in the sample filters, GF/F filters were vacuum-dried in a freezer (0 °C) within 6 hours. Subsequently, phytoplankton pigments retained on a filter were extracted in a glass tube with 4 ml of N,N-dimethylformamide (HPLC-grade) for at least 24 hours in a freezer (-20 °C), and analyzed by HPLC within a few days.

Residua cells and filter debris were removed through polypropylene syringe filter (pore size: 0.2 µm) before the analysis. The samples injection of 500 µl was conducted by auto-sampler with the mixture of extracted pigments (350 µl), pure water (150 µl) and internal standard (10 µl). Phytoplankton pigments were quantified based on C₈ column method containing pyridine in the mobile phase (Zapata *et al.*, 2000).

(i) HPLC System

HPLC System was composed by Agilent 1200 modular system, G1311A Quaternary pump (low-pressure mixing system), G1329A auto-sampler and G1315D photodiode array detector.

(ii) Stationary phase

Analytical separation was performed using a YMC C₈ column (150×4.6 mm). The column was thermostatted at 35 °C in the column heater box.

(iii) Mobile phases

The eluant A was a mixture of methanol: acetonitrile: aqueous pyridine solution (0.25M pyridine), (50:25:25, v:v:v). The eluant B was a mixture of methanol: acetonitrile: acetone (20:60:20, v:v:v). Organic solvents for mobile phases were used reagents of

HPLC-grade.

(iv) Calibrations

HPLC was calibrated using the standard pigments (Table 1). The solvents of pigment standards were displaced to N,N-dimethylformamide, but the concentrations were determined with spectrophotometer by using its extinction coefficient in ethanol or acetone.

(v) Internal standard

Ethyl-apo-8'-carotenoate was added into the samples prior to the injection as the internal standard. The mean chromatogram area and its coefficient of variation (CV) of internal standard were estimated as the following two samples:

Standard samples (Figure 1): 195.9 ± 2.8 (n = 38), CV=1.4%

Seawater samples: 201.4 ± 2.9 (n = 76), CV=1.5%

(vi) Pigment detection and identification

Chlorophylls and carotenoids were detected by photodiode array spectroscopy (350~800 nm). Pigment concentrations were calculated from the chromatogram area at different five channels (Table 1). First channel was allocated at 409 nm of wavelength for the absorption maximum of Pheophorbide *a* and Pheophytin *a*. Second channel was allocated at 431 nm for the absorption maximum of chlorophyll *a*. Third channel was allocated at 440 nm for the absorption maximum of [3,8-divinyl]-protochlorophyllide. Fourth channel was allocated at 450 nm for other pigments. Fifth channel was allocated at 462 nm for chlorophyll *b*.

(3) Preliminary results

Vertical profiles of major pigments (Chlorophyll *a*, Chlorophyll *b*, Divinyl chlorophyll *a*, Fucoxanthin, 19'-hexanoyloxyfucoxanthin, 19'-butanoyloxyfucoxanthin and zeaxanthin) at the station K2 and S1 were shown in Figure 2 and 3.

(4) Data archives

The processed data file of pigments will be submitted to the JAMSTEC Data Integration and Analyses Group (DIAG) within a restricted period. Please ask PI for the latest information.

(5) Reference

Zapata M, Rodriguez F, Garrido JL (2000), Separation of chlorophylls and carotenoids from marine phytoplankton: a new HPLC method using a reversed phase C₈ column and pyridine-containing mobile phases, *Mar. Ecol. Prog. Ser.*, 195, 29-45.

Table 1. Retention time and wavelength of identification for pigment standards.

No.	Pigment	Productions	Retention Time (minute)	Wavelength of identification (nm)
1	Chlorophyll <i>c3</i>	DHI Co.	8.054	462
2	Chlorophyllide <i>a</i>	DHI Co.	10.082	431
3	[3,8-Divinyl]-Protochlorophyllide	DHI Co.	11.000	440
4	Chlorophyll <i>c2</i>	DHI Co.	11.334	450
5	Peridinin	DHI Co.	14.537	450
6	Pheophorbide <i>a</i>	DHI Co.	16.650	409
7	19'-butanoyloxyfucoxanthin	DHI Co.	17.885	450
8	Fucoxanthin	DHI Co.	19.185	450
9	Neoxanthin	DHI Co.	19.539	440
10	Prasincoxanthin	DHI Co.	20.866	450
11	19'-hexanoyloxyfucoxanthin	DHI Co.	21.616	450
12	Violaxanthin	DHI Co.	21.667	440
13	Diadinoxanthin	DHI Co.	24.293	450
14	Dinoxanthin	DHI Co.	25.725	440
15	Antheraxanthin	DHI Co.	25.707	450
16	Alloxanthin	DHI Co.	26.992	450
17	Diatoxanthin	DHI Co.	27.949	450
18	Zeaxanthin	DHI Co.	28.694	450
19	Lutein	DHI Co.	28.898	450
20	Ethyl-apo-8'-carotenoate	Sigma-Aldrich Co.	30.793	462
21	Crococanthin	DHI Co.	32.867	450
22	Chlorophyll <i>b</i>	Sigma-Aldrich Co.	33.303	462
23	Divinyl chlorophyll <i>a</i>	DHI Co.	34.518	440
24	Chlorophyll <i>a</i>	Sigma-Aldrich Co.	34.798	431
25	Pheophytin <i>a</i>	DHI Co.	37.174	409
26	Alpha-carotene	DHI Co.	37.853	450
27	Beta-carotene	DHI Co.	38.064	450

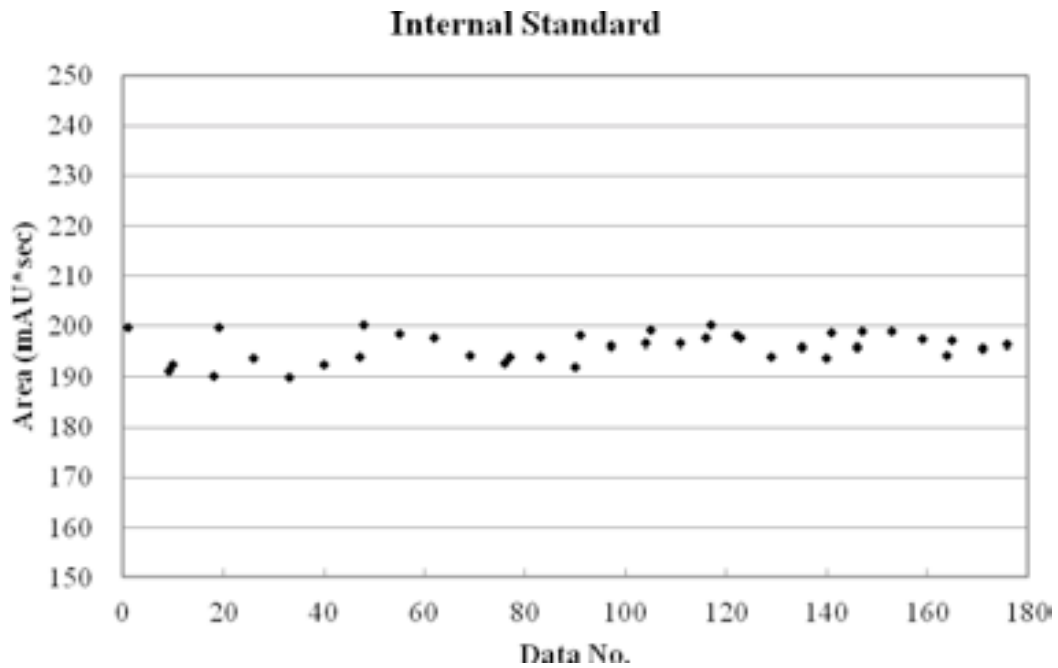


Figure 1. Variability of chromatogram areas for the internal standard.

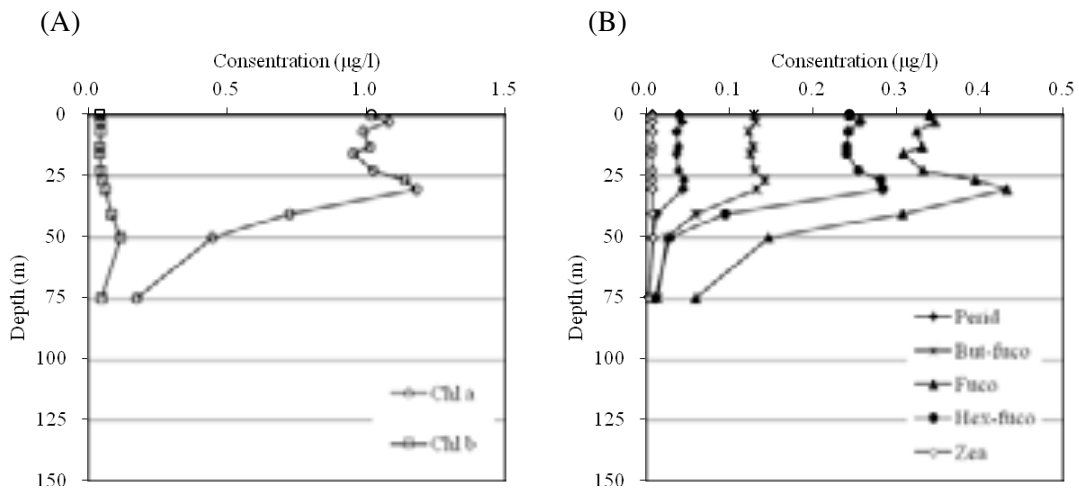


Figure 2-(A). Vertical distributions of major phytoplankton pigments (Chlorophyll *a*, Chlorophyll *b*) at Stn.K2 cast2.

Figure 2-(B). Vertical distributions of major phytoplankton pigments (Fucoxanthin, 19'-hexanoyloxyfucoxanthin, 19'-butanoyloxyfucoxanthin, Peridinin and Zeaxanthin) at Stn.K2 cast2.

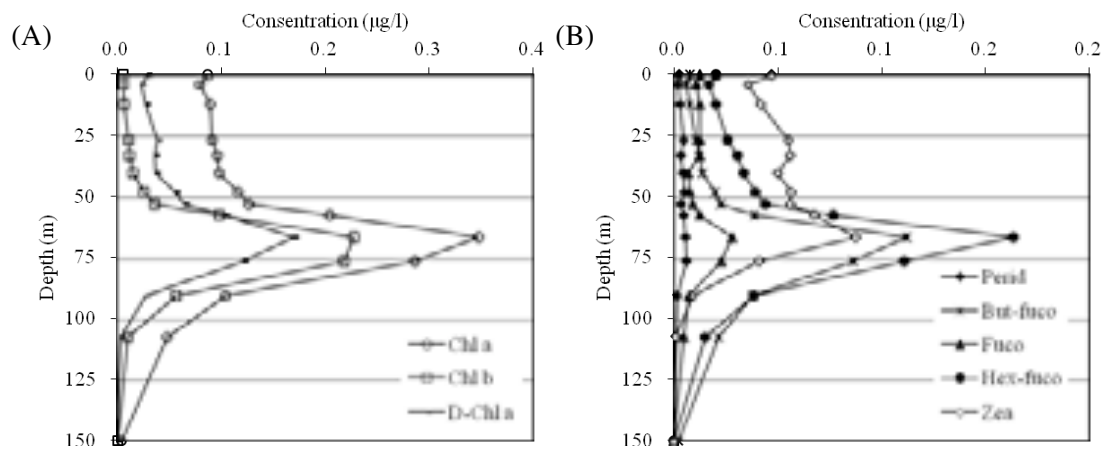


Figure 3-(A). Vertical distributions of major phytoplankton pigments (Chlorophyll *a*, Chlorophyll *b*, Divinyl chlorophyll *a*) at Stn.S1 cast2.

Figure 3-(B). Vertical distributions of major phytoplankton pigments (Fucoxanthin, 19'-hexanoyloxyfucoxanthin, 19'-butanoyloxyfucoxanthin, Peridinin and Zeaxanthin) at Stn.S1 cast2.

3.4.3 Phytoplankton abundance

Kazuhiko MATSUMOTO (JAMSTEC RIGC)

(1) Objectives

The main objective of this study is to estimate phytoplankton abundances and their taxonomy in the subarctic gyre and the subtropical gyre in the western North Pacific. Phytoplankton abundances were measured with two kinds of methods: microscopy for large size phytoplankton and flowcytometry for small size phytoplankton.

(2) Sampling

Samplings were conducted using Niskin bottles, except for the surface water, which was taken by a bucket. Samplings were carried out at the two observational stations of K2 and S1.

(3) Methods

1) Microscopy

Water samples were placed in 500 ml plastic bottle at station K2 and in 1000 ml plastic bottle at station S1. Samples were fixed with neutral-buffered formalin solution (1% final concentration). The microscopic measurements are scheduled after the cruise.

2) Flowcytometry

2)-1 Equipment

The flowcytometry system used in this research was BRYTE HS system (Bio-Rad Laboratories Inc). System specifications are follows:

Light source: 75W Xenon arc lamp

Excitation wavelength: 350-650 nm

Detector: high-performance PMT

Analyzed volume: 75 μ l

Flow rate: 10 μ l min⁻¹

Sheath fluid: Milli-Q water

Filter block: B2 as excitation filter block, OR1 as fluorescence separator block

B2 and OR1 have ability as follows:

B2: Excitation filter 390-490 nm

 Beam-splitter 510 nm

 Emission filter 515-720 nm

OR1: Emission filter 1 565-605 nm

 Beam-splitter 600 nm

 Emission filter 2 >615 nm

2)-2 Measurements

The water samples were fixed immediately with glutaraldehyde (1% final concentration) and stored in the dark at 4°C. The analysis by the flow cytometer was acquired on board within 24 hours after the sample fixation. Calibration was achieved with standard beads

of 0.356 – 9.146 μm (Polysciences, Inc.). Standard beads of 2.764 μm were added into each sample prior to the injection of flow cytometer as internal standard. Phytoplankton cell populations were estimated from the forward light scatter signal. Acquired data were stored in list mode file and analyzed with WinBryte software. Phytoplankton are classified with prokaryotic cyanobacteria (*Prochlorococcus* and *Synechococcus*) and other eukaryotes on the basis of scatter and fluorescence signals. *Synechococcus* is discriminated by phycoerythrin as the orange fluorescence, while other phytoplankton are recognized by chlorophylls as the red fluorescence without the orange fluorescence. *Prochlorococcus* and picoeukaryotes were distinguished with their cell size, but it was difficult to identify the abundance of *Prochlorococcus* accurately in the surface mixed layer due to its decreased chlorophyll fluorescence. The cell size was estimated using the empirically-determined relationship between cell diameter (d_{cell}) and bead diameter (d_{bead}) with the forward light scatter signal (FS) by Blanchot *et al.*, (2001) as follows.

$$d_{\text{cell}} = d_{\text{bead}} (\text{FS})^{1/5}$$

(4) Data Archive

All data will be submitted to Data Integration and Analysis Group (DIAG), JAMSTEC.

(5) Reference

Blanchot J, André J-M, Navarette C, Neveux J, Radenac M-H (2001), Picophytoplankton in the equatorial Pacific: vertical distributions in the warm pool and in the high nutrient low chlorophyll conditions, *Deep-Sea Research I* 48, 297-314.

3.4.4 Primary production and new production

Kazuhiko MATSUMOTO (JAMSTEC RIGC)

Miyo IKEDA (MWJ)

Kanako YOSHIDA (MWJ)

Masahiro ORUI (MWJ)

(1) Objective

Quantitative assessment of temporal and spatial variation in carbon and nitrate uptake in the surface euphotic layer should be an essential part of biogeochemical studies in the western North Pacific. Primary production (PP) was measured as incorporation of inorganic C¹³, and new production (NP), measurement of nitrate uptake rate was conducted with ¹⁵N stable isotope tracer at K2, and S1 stations.

(2) Methods

1) *Sampling, incubation bottle and filter*

Sampling was begun at predawn immediately before the incubation experiment. Seawater samples were collected using Teflon-coated and acid-cleaned Niskin bottles, except for the surface water, which was taken by a bucket. Samplings were conducted at eight depths within the euphotic depth in response to the light levels of the incubation containers adjusted with the blue acrylic plate. Two kinds of baths were prepared for PP and NP (bath-1), and for oxygen evolution (bath-2). The light levels of the incubation containers in each bath were shown in Table 3.4.4-1. The light depths relative to the surface had been estimated by SPMR sensor on the previous day of the sampling. The incubated depths were corrected by SPMR sensor on the incubation day. Seawater samples were placed into acid-cleaned clear polycarbonate bottles in duplicate for PP and NP, and in a single for the dark and the time-zero samples. The time-zero sample was filtered immediately after the addition of ¹³C and ¹⁵N solution. The PP incubation was conducted in a single for bath-2. Filtration of seawater sample was conducted with pre-combusted glass fiber filters (Whatman GF/F 25 mm) with temperature of 450 degree C for at least 4 hours.

2) *Incubation*

Each bottle was spiked with sufficient NaH¹³CO₃ just before incubation so that ¹³C enrichment was about 10% of ambient dissolved inorganic carbon as final concentration of 0.2 mmol dm⁻³ (Table 3.4.4-2). The ¹⁵N-enriched NO₃, K¹⁵NO₃ solution, was injected to the incubation bottles (except PP bottles), resulting that the final concentration of ¹⁵N enrichment was about 10% of ambient nitrate (Table 3.4.4-3). Incubation was begun at predawn and continued for 24 h. The simulated *in situ* method was conducted in the on-deck bath cooled by running surface seawater or by immersion cooler.

3) *Measurement*

After 24 hours incubation, samples were filtered though GF/F filter, and the filters were kept in a freezer (-20 degree C) on board until analysis. Before analysis, the filters were dried in the oven (45 degree C) for at least 20 hours, and inorganic carbon was removed by acid

treatment in a HCl vapor bath for 30 minutes. All samples were measured by a mass spectrometer ANCA-SL system at MIRAI during this cruise.

Instruments: preprocessing equipment ROBOPLEP-SL (Europa Scientific Ltd.; now SerCon Ltd.)
stable isotope ratio mass spectrometer EUROPA20-20 (Europa Scientific Ltd.; now SerCon Ltd.)

Methods: Dumas method, Mass spectrometry

Precision: All specifications are for n=5 samples.

It is a natural amount and five time standard deviation of the analysis as for amount 100 µg of the sample. We measured repeatability 4 times in this cruise. ^{13}C (0.04 - 0.10 ‰), ^{15}N (0.09 - 0.29 ‰)

Reference Material: The third-order reference materials L-aspartic acid (SHOKO Co., Ltd.)

4) Calculation

(a) Primary Production

Based on the balance of ^{13}C , assimilated organic carbon (ΔPOC) is expressed as follows (Hama *et al.*, 1983):

$$^{13}\text{C}_{(\text{POC})} * \text{POC} = ^{13}\text{C}_{(\text{sw})} * \Delta\text{POC} + (\text{POC} - \Delta\text{POC}) * ^{13}\text{C}_{(0)}$$

This equation is converted to the following equation;

$$\Delta\text{POC} = \text{POC} * (^{13}\text{C}_{(\text{POC})} - ^{13}\text{C}_{(0)}) / (^{13}\text{C}_{(\text{sw})} - ^{13}\text{C}_{(0)})$$

where $^{13}\text{C}_{(\text{POC})}$ is concentration of ^{13}C of particulate organic carbon after incubation, *i.e.*, measured value(%). $^{13}\text{C}_{(0)}$ is that of particulate organic carbon before incubation, *i.e.*, that for samples as a blank.

$^{13}\text{C}_{(\text{sw})}$ is concentration of ^{13}C of ambient seawater with a tracer. This value for this study was determined based on the following calculation;

$$^{13}\text{C}_{(\text{sw})} (\%) = [(\text{TDIC} * 0.011) + 0.0002] / (\text{TDIC} + 0.0002) * 100$$

where TDIC is concentration of total dissolved inorganic carbon at respective bottle depth (mol dm^{-3}) and 0.011 is concentration of ^{13}C of natural seawater (1.1%). 0.0002 is added ^{13}C (mol) as a tracer. Taking into account for the discrimination factor between ^{13}C and ^{12}C (1.025), primary production (PP) was, finally, estimated by

$$\text{PP} = 1.025 * \Delta\text{POC}$$

(b) New production

NO_3 uptake rate or new production (NP) was estimated with following equation:

$$\text{NP} (\mu\text{g dm}^{-3} \text{ day}^{-1}) = (^{15}\text{N}_{\text{excess}} * \text{PON}) / (^{15}\text{N}_{\text{enrich}}) / \text{day}$$

where $^{15}\text{N}_{\text{excess}}$, PON and $^{15}\text{N}_{\text{enrich}}$ are excess ^{15}N (measured ^{15}N minus ^{15}N natural abundance, 0.366 atom%) in the post-incubation particulate sample (%), particulate nitrogen content of the sample after incubation (mg dm^{-3}) and ^{15}N enrichment in the dissolved fraction (%), respectively.

(3) Preliminary results

Fig. 3.4.4.1 and 3.4.4.2 show the vertical profile of primary production (PP) and the diurnal change of photosynthetically available radiation (PAR) observed by PUV-510B (Biospherical Instruments Inc.).

(4) Data archives

All data will be submitted to JAMSTEC Data Integration and Analyses Group (DIAG).

Table 3.4.4-1 Light intensity of simulated *in situ* bath

Number	Bath 1	Bath 2 (with oxygen evolution)
#1	100%	100%
#2	65%	66%
#3	37.5%	40%
#4	18.1%	13.4%
#5	13.3%	9.3%
#6	6.3%	4.6%
#7	3.8%	3.1%
#8	0.7%	1.7%

Table 3.4.4-2 Sampling cast table and spike ¹³C concentration

Incubation type	CTD cast	NaH ¹³ CO ₃ (μmol dm ⁻³)
SIS	K02M02	200
SIS	K02M08	200
SIS	S01M02	200
SIS	S01M06	200

Table 3.4.4-3 Sampling cast table and spike ¹⁵N concentration

Incubation type	CTD cast	Light Intensity	K ¹⁵ NO ₃ (μmol dm ⁻³)
SIS	K02M02	All layers	2.0
SIS	K02M08	100% - 3.8%	1.8
		0.7%	2.0
SIS	S01M02	100% - 3.8%	0.01
		0.7%	0.05
SIS	S01M06	100%	0.05
		65% - 3.8%	0.01
		0.7%	0.2

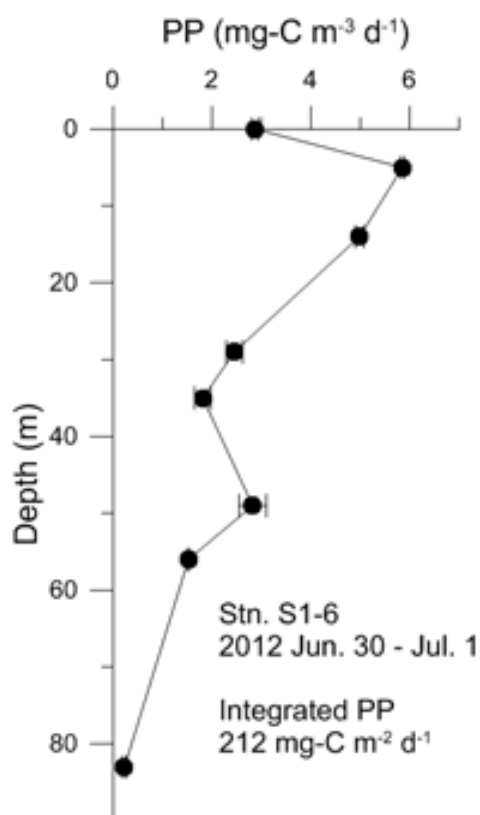
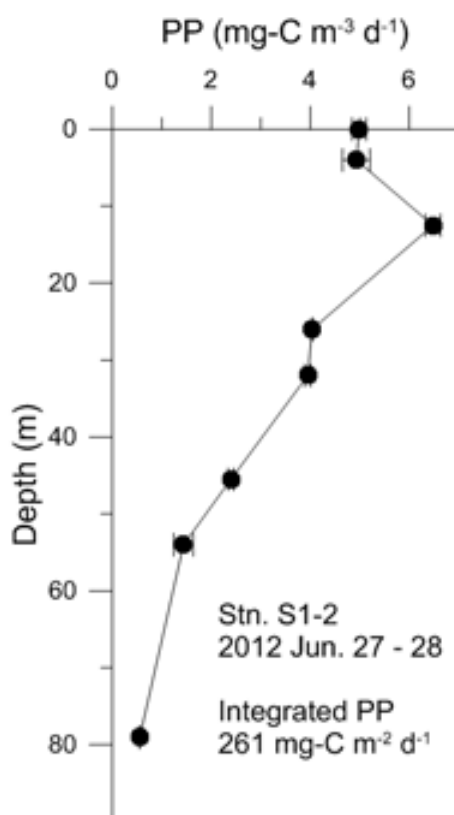
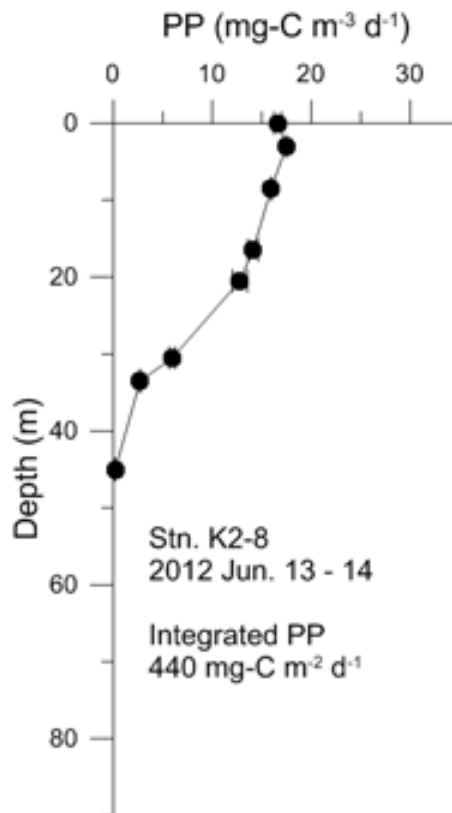
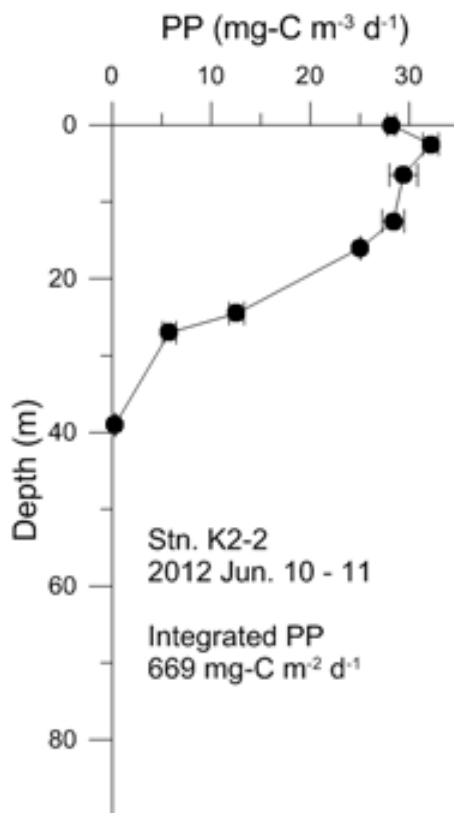


Figure 3.4.4.1 Vertical profile of primary production

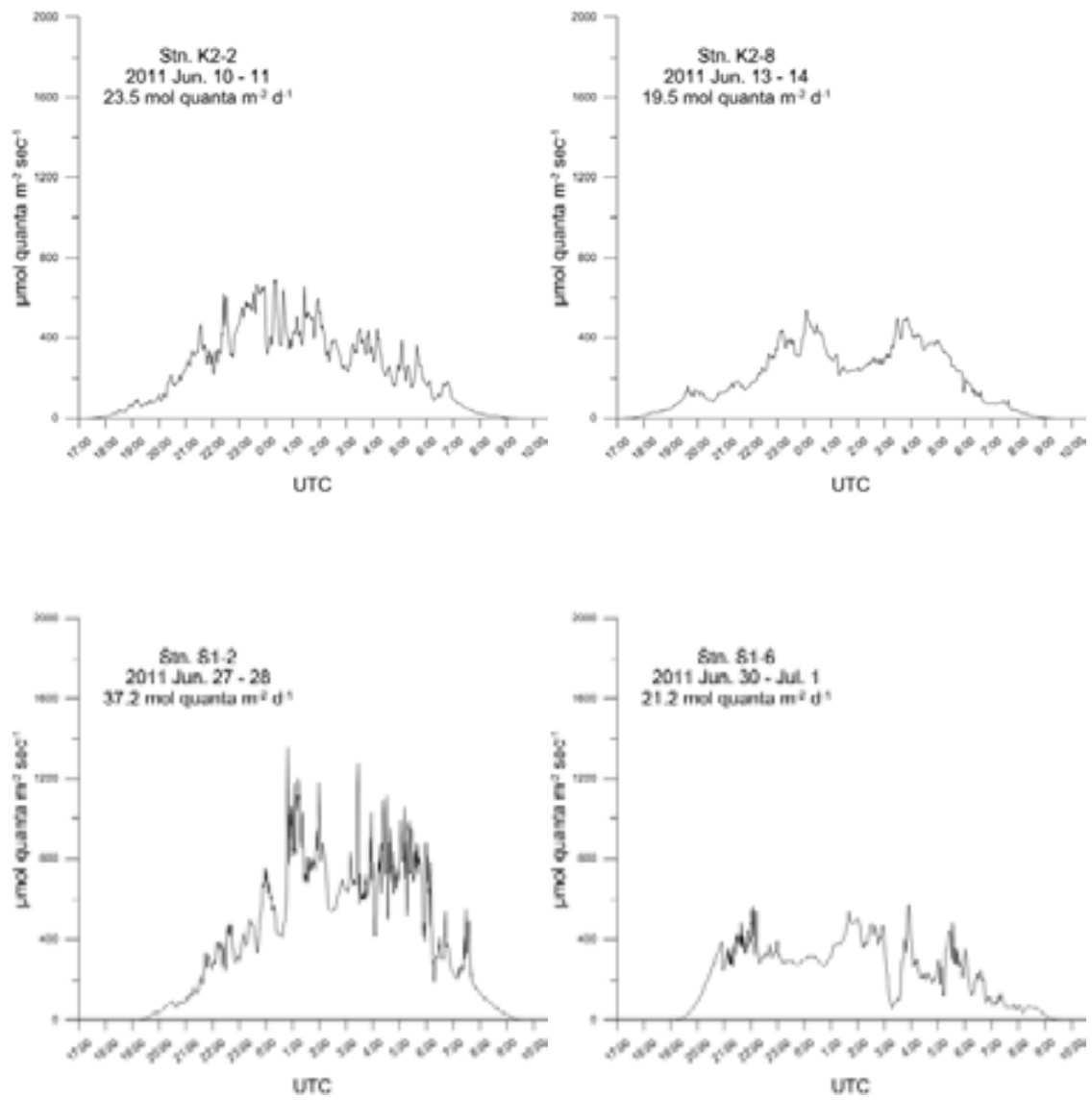


Figure 3.4.4.2 Photosynthetically available radiation (PAR) during incubation experiment

3.4.5 P vs. E curve

Kazuhiko MATSUMOTO (JAMSTEC RIGC)

Miyo IKEDA (MWJ)

Kanako YOSHIDA (MWJ)

Masahiro ORUI (MWJ)

(1) Objectives

The objective of this study is to estimate the relationship between phytoplankton photosynthetic rate (P) and scalar irradiance (E) in the western North Pacific.

(2) Methods

1) Sampling

Samplings were carried out at two observational stations of K2 and S1. Sample water was collected at three depths of different irradiance level, using Teflon-coated and acid-cleaned Niskin bottles.

2) Incubation

Three incubators filled in water were used, illuminated at one end by a 500W halogen lamp. Water temperature was controlled by circulating water cooler (Fig. 3.4.5-1). Water samples were poured into acid-cleaned clear nine flasks (approx. 1 liter) and arranged in the incubator linearly against the lamp after adding the isotope solutions. The isotope solutions of 0.2 mmol dm^{-3} (final concentration) of $\text{NaH}^{13}\text{CO}_3$ solution were spiked. All flasks were controlled light intensity by shielding with a neutral density filter on lamp side. The light intensities inside the flasks were shown in Table 3.4.5. The incubations were begun at about local noon and continued for 3 h. Filtration of seawater sample was conducted with glass fiber filters (Whatman GF/F 25 mm) which precombusted with temperature of 450 degree C for at least 4 hours.

3) Measurement

After the incubation, samples were treated as same as the primary production experiment. During the cruise, All incubator samples were measured by a mass spectrometer ANCA-SL system at MIRAI. The analytical function and parameter values used to describe the relationship between the photosynthetic rate (P) and scalar irradiance (E) are best determined using a least-squares procedure from the following equation.

$$P = P_{\max}(1 - e^{-\alpha E/P_{\max}})e^{-bE/P_{\max}} : (\text{Platt et al., 1980})$$

where, P_{\max} is the light-saturated photosynthetic rate, α is the initial slope of the P vs. E curve, b is a dimensionless photoinhibition parameter.

(3) Preliminary results

The P vs. E curve obtained at the station of K2 (4m) and S1 (7m) is shown in Fig. 3.4.5-2.

(4) Data archives

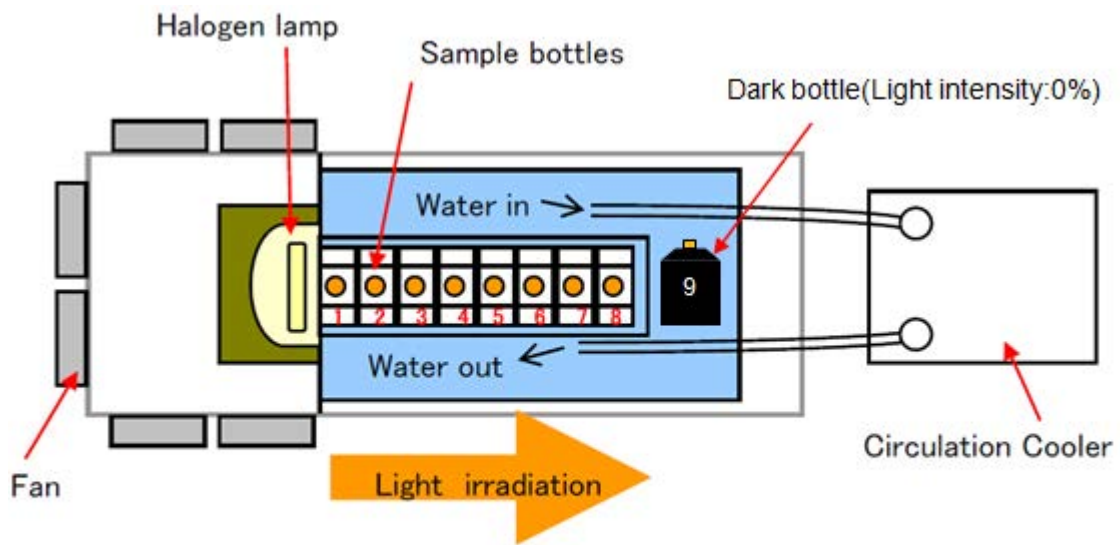
All data will be submitted to JAMSTEC Data Integration and Analyses Group (DIAG).

(5) Reference

Platt, T., Gallegos, C.L. and Harrison, W.G., 1980. Photoinhibition of photosynthesis in natural assemblages of marine phytoplankton. *Journal of Marine Research*, 38, 687-701.

Table 3.4.5 Light Intensity of P vs. E measurements

	Bath A	Bath B	Bath C
Bottle No.	Light intensity ($\mu\text{E m}^{-2} \text{sec}^{-1}$)		
1	2100	2200	2000
2	1000	1100	960
3	420	500	460
4	195	220	200
5	90	105	94
6	44	44	42
7	20	18.5	17.5
8	8	7.8	7.2
9	0.1	0.1	0.1



Fan: AC100V 50/60HZ 14/13W or 16/15W

Halogen lamp: 500W

Fig. 3.4.5-1 Look down view of Incubator for Photosynthesis and irradiation curve

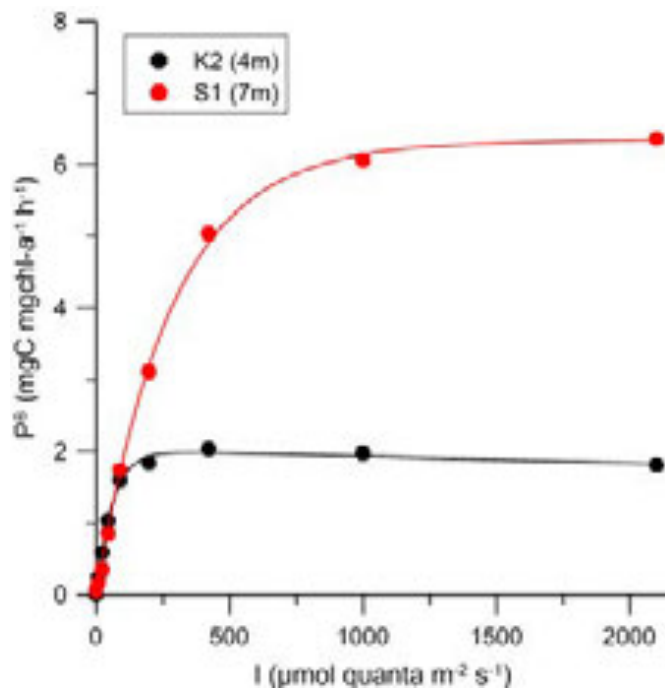


Fig. 3.4.5-2 P vs. E curve

3.4.6. Oxygen evolution

Tetsuichi FUJIKI (JAMSTEC)

Yoshihisa MINO (JAMSTEC)

Osamu ABE (Nagoya University)

3.4.6.1. Gross primary productivity

(1) Objective

An understanding of the variability in phytoplankton productivity provides a basic knowledge of how aquatic ecosystems are structured and functioning. Primary productivity in the world's oceans has been measured mostly by the carbon tracer or oxygen evolution methods. In incubations of 24 hours, the former method provides the values closest to net primary productivity (NPP), while the latter comes closest to gross primary productivity (GPP). The GPP is defined as total amount of oxygen released by phytoplankton photosynthesis. The NPP/GPP ratio provides fundamental information on the metabolic balance and carbon cycle in the ocean. In the MR12-02, the GPP were measured using the ^{18}O spike method and fast repetition rate (FRR) fluorometry.

(2) Methods

^{18}O spike method

Seawater samples were collected from eight depths corresponding to light levels of approximately 100, 60, 35, 13, 7, 5, 3 and 1 % of surface light intensity, using a bucket (surface only) and 12-L Niskin-X bottles attached to a CTD rosette system. The samples were spiked with enriched ^{18}O -labeled water (diluted 8 times of 97 % H_2^{18}O water obtained from Cambridge Isotope Laboratories) and then were incubated under light conditions that simulated those of the original sampling depth. The dark bottles were wrapped with aluminum foil. After 24 h incubation, ~100 mL of subsample were drawn into pre-evacuated gas extraction vessels and capped.

After measurements of the isotopic composition of O_2 in the laboratory on land, the GPP is calculated from the isotopic composition of dissolved oxygen in initial and incubated samples using the following equation (Bender et al. 2000).

$$\text{GPP} = \{[\delta^{18}\text{O}(\text{O}_2)_f - \delta^{18}\text{O}(\text{O}_2)_i] / [\delta^{18}\text{O}_{\text{water}} - \delta^{18}\text{O}(\text{O}_2)_i]\} \times (\text{O}_2)_i$$

where the subscripts i and f are the isotopic composition of O_2 in initial and final samples, $(\text{O}_2)_i$ is the oxygen concentration of the initial water sample, and $\delta^{18}\text{O}_{\text{water}}$ is the isotopic composition of the enriched water.

FRR fluorometry

Measurement principle of FRR fluorometer can be found in the section 3.2 (POPSS mooring). The FRR fluorometer together with a scalar irradiance sensor (QSP-2200, Biospherical Instruments) and a pressure gauge (ABH500PSC1B, Honeywell International) were deployed several times a day using a ship winch. These instrument packages lowered gently through the water column to 100m (200m for S1) depth and up again at a rate of 0.2 m s^{-1} and measured vertical

profiles of GPP.

(3) Data archives

The data will be submitted to JAMSTEC Data Management Office.

(4) References

Bender, M. L., M. L. Dickson and J. Orchardo. 2000. Net and gross production in the Ross Sea as determined by incubation experiments and dissolved O₂ studies. *Deep-Sea Res. II* 47: 3141–3158.

3.4.6.2. Vertical distribution of isotopic composition of dissolved oxygen

(1) Objective

$\Delta^{17}\text{O}$ of dissolved O₂, which is defined approximately as $\delta^{17}\text{O} - 0.5\delta^{18}\text{O}$, is a unique tracer for primary productivity and gas transfer between atmosphere and water. This can be treated as a conservative component in subsurface (hypolimnion) waters, thus we could reconstruct past changes of productivity from subsurface $\Delta^{17}\text{O}$ values when the water was in the surface. Objective of this study is to clarify inter-annual variation of primary productivity at the subduction area of north Pacific intermediate water (NPIW) using vertical distribution $\Delta^{17}\text{O}$.

(2) Sampling

In this cruise, vertical water sampling was conducted at Station K2 and S1. At Station K2, 36 samples were obtained from 10m to bottom. One hundred and fifty mL of water was collected to 300mL vacuum flasks of 300mL except for anoxic layer, which expands from 200 to 1400m at Station K2. In this layer, 1L water was collected to 2L vacuum flasks for gaining sufficient signals in IRMS. At Station S1, 36 sample were obtained as well. Between 900 and 1800m, large vacuum flaks were used for sampling, and small flasks were used for other depths.

After the bottling, less soluble gases such as oxygen, argon and nitrogen are released to vacuum headspaces within 24 hours at room temperature. These gases will be collected using a vacuum line in the laboratory. Then O₂ gas will be purified using molecular sieve packed column and measured by isotope ratio mass spectrometer (IRMS) for $\Delta^{17}\text{O}$.

(3) Expected results

Previous investigations for $\Delta^{17}\text{O}$ has been limited to surface mixed layer and used for “present” primary productivity at the surface water. This study will first investigate whether this parameter would be really conserved the surface condition. On that basis, $\Delta^{17}\text{O}$ values for NPIW water masses from each location can be regarded as those surface values when water masses were at the surface. Compare to surface $\Delta^{17}\text{O}$, subsurface $\Delta^{17}\text{O}$ values would be controlled not only by primary productivity and gas transfer between atmosphere and water, but also by the amount of isopycnal and diapycnal mixing. With regard to gas exchanges between air-water, and stratified water masses could be quantified by measuring degrees of super-saturation for nitrogen and/or noble gases.

3.4.7 Absorption coefficients of phytoplankton and colored dissolved organic matter (CDOM)

Kosei SASAOKA (JAMSTEC RIGC)

(1) Objectives

Absorption coefficients of particulate matter (phytoplankton and non-phytoplankton particles, defined as ‘detritus’) and colored dissolved organic matter (CDOM) play an important role in determining the optical properties of seawater. In particular, light absorption by phytoplankton is a fundamental process of photosynthesis, and their chlorophyll *a* (Chl-*a*) specific coefficient, a_{ph}^* , can be essential factors for bio-optical models to estimate primary productivities. Absorption coefficients of CDOM are also important parameters to validate and develop the bio-optical algorithms for ocean color sensors. The objectives of this study are to characterize the absorption spectra of phytoplankton and CDOM in the western North Pacific.

(2) Methods

Seawater samples for absorption coefficient of total particulate matter ($a_p(\lambda)$) were performed using Niskin bottles and a bucket. Samples were collected in 3000ml dark bottles and filtered (300 – 3000 ml) through 25-mm What-man GF/F glass-fiber filters under low vacuum pressure (<100 mmHg) on board. After filtration, the optical density of total particulate matter on filter ($OD_{fp}(\lambda)$) between 350 and 750 nm at a rate of 0.5 nm was immediately measured by a dual beam multi-purpose spectrophotometer (MPS-2400, Shimadzu Co.), and absorption coefficient was determined from the OD according to the quantitative filter technique (QFT) (Mitchell, 1990). A blank filter with filtered seawater was used as reference. All spectra were normalized to 0.0 at 750nm to minimize difference between sample and reference filter. To determine the optical density of non-pigment detrital particles ($OD_{fd}(\lambda)$), the filters were then soaked in methanol for a few hours and rinsed with filtered seawater to extract and remove the pigments (Kishino et al., 1985), and its absorption coefficient was measured again by MPS-2400. These measured optical densities on filters ($OD_{fp}(\lambda)$ and $OD_{fd}(\lambda)$) were converted to optical densities in suspensions ($OD_{sp}(\lambda)$ and $OD_{sd}(\lambda)$) using the pathlength amplification factor of Cleveland and Weidemann (1993) as follows:

$$OD_{sp}(\lambda) = 0.378 OD_{fp}(\lambda) + 0.523 OD_{fp}(\lambda)^2 \text{ and}$$
$$OD_{sd}(\lambda) = 0.378 OD_{fd}(\lambda) + 0.523 OD_{fd}(\lambda)^2.$$

The absorption coefficient of total particles ($a_p(\lambda)$ (m^{-1})) and non-pigment detrital particles ($a_d(\lambda)$ (m^{-1})) are computed from the corrected optical densities ($OD_s(\lambda)$):

$$a_p(\lambda) = 2.303 \times OD_{sp}(\lambda) / L \quad (L = V / S), \text{ and}$$
$$a_d(\lambda) = 2.303 \times OD_{sd}(\lambda) / L \quad (L = V / S),$$

Where S is the clearance area of the filter (m^2) and V is the volume filtered (m^3). Absorption coefficient of phytoplankton ($a_{ph}(\lambda)$) was obtained by subtracting $a_d(\lambda)$ from $a_p(\lambda)$ as follows:

$$a_{ph}(\lambda) = a_p(\lambda) - a_d(\lambda).$$

Finally, we will calculate chl-*a* normalized specific absorption spectra (a_{ph}^*) to divide a_{ph} by chl-*a* concentrations obtained from HPLC.

Seawater samples for absorption coefficient of CDOM ($a_y(\lambda)$) were collected in 250ml bottles using a bucket and the continuous sea surface water monitoring system (TSG). After letting the CDOM samples rest for a few hours to equilibrate to room temperature, samples were filtered through a 47-mm Nuclepore membrane filter (pore size = 0.2 μm). Optical densities of the CDOM ($OD_y(\lambda)$) in this filtered seawater were measured in the range from 300 to 800 nm using 10-cm pathlength glass cells with MPS-2400. Milli-Q water was used as a reference. A blank (Milli-Q water versus Milli-Q water) was subtracted from each wavelength of the spectrum. The absorption coefficient of CDOM ($a_y(\lambda)$ (m^{-1})) was calculated from measured optical densities ($OD_y(\lambda)$) as follows:

$$a_y(\lambda) = 2.303 \times OD_y(\lambda) / L \quad (\text{L is the cuvette pathlength (m)}).$$

(3) Preliminary results

Some examples of absorption spectra of phytoplankton ($a_{ph}(\lambda)$) and CDOM ($a_y(\lambda)$) were shown in Fig.3.4.7-1 and Fig.3.4.7-2, respectively.

(4) Data archive

The data from this study will be submitted to Data Integration and Analysis Group (DIAG) of JAMSTEC.

(5) References

- Mitchell, B.G., 1990, Algorithms for determining the absorption coefficient of aquatic particulates using the quantitative filter technique (QFT), *Ocean Optics X*, SPIE 1302, 137-148.
- Kishino, M., Takahashi, M., Okami, N. and Ichimura, S., 1985, Estimation of the spectral absorption coefficients of phytoplankton in the sea, *Bulletin of Marine Science*, 37, 634-642.
- Cleveland, J.S. and Weidemann, A.D., 1993, Quantifying absorption by aquatic particles: a multiple scattering correction for glass fiber filters, *Limnology and Oceanography*, 38, 1321-1327.

Table 3.4.7-1 List of sampling for absorption coefficients of phytoplankton and CDOM during MR12-02.

Station	Date (UT)	Time (UT)	Latitude	Longitude	Sampling type	Cast No.	Particle absorbance	CDOM absorbance	Remarks
E03	2012/06/06	02:15-03:53	41-08.8N	146-58.8E	CTD	1	O(6m)	O(6m)	-
TSG02	2012/06/07	1:41	41-08.2N	150-01.7E	TSG	-	-	O	-
TSG03	2012/06/08	0:35	41-59.0N	152-10.8E	TSG	-	-	O	-
TSG04	2012/06/09	0:03	44-26.0N	156-18.1E	TSG	-	-	O	-
K2	2012/06/10	15:34-16:15	47-00.0N	160-00.0E	CTD+Bucket	2	O	O(0m)	Shallow (P.P.-1)
K2	2012/06/13	15:31-16:10	47-03.6N	160-17.7E	CTD+Bucket	8	O	O(0m)	Shallow (P.P.-2)
K2	2012/06/13	21:25-21:55	47-01.0N	160-03.0E	CTD	9	O	-	Shallow (PE)
TSG10	2012/06/16	0:12	44-50.5N	159-50.4E	TSG	-	-	O	-
TSG11	2012/06/17	1:08	44-12.2N	156-25.6E	TSG	-	-	O	-
KNOT	2012/06/17	09:20-09:32	44-00.0N	155-00.0E	Bucket	1	O(0m)	O(0m)	Routine
TSG14	2012/06/18	1:17	41-37.4N	151-34.7E	TSG	-	-	O	-
TSG20	2012/06/19	2:07	37-55.9N	146-32.9E	TSG	-	-	O	-
JKEO	2012/06/19	12:20-12:28	37-56.3N	147-00.0E	Bucket	1	O(0m)	O(0m)	Routine
NKEO	2012/06/21	01:45-01:55	33-50.4N	144-54.1E	Bucket	1	O(0m)	O(0m)	Routine
TSG24	2012/06/23	1:58	38-05.3N	146-21.5E	TSG	-	-	O	-
TSG25	2012/06/24	2:07	36-58.6N	141-30.6E	TSG	-	-	O	-
TSG26	2012/06/25	2:06	33-32.4N	142-57.7E	TSG	-	-	O	-
S1	2012/06/27	17:32-18:23	30-00.0N	145-00.0E	CTD+Bucket	2	O	O(0m)	Shallow (P.P.-1)
S1	2012/06/27 - 06/28	23:37-00:08	30-01.5N	145-00.0E	CTD	3	O	-	Shallow (POM)
S1	2012/06/30	17:33-18:22	29-49.9N	145-14.2E	CTD+Bucket	6	O	O(0m)	Shallow (P.P.-2)
S1	2012/6/30 - 07/01	23:34-01:00	29-55.4N	145-05.7E	CTD	7	O	-	Shallow (PE)
KEO	2012/07/03	06:54-07:04	32-19.1N	144-27.7E	Bucket	1	O(0m)	O(0m)	Routine
F1	2012/07/07	02:32-02:39	36-29.8N	141-30.7E	Bucket	1	O(0m)	O(0m)	Routine

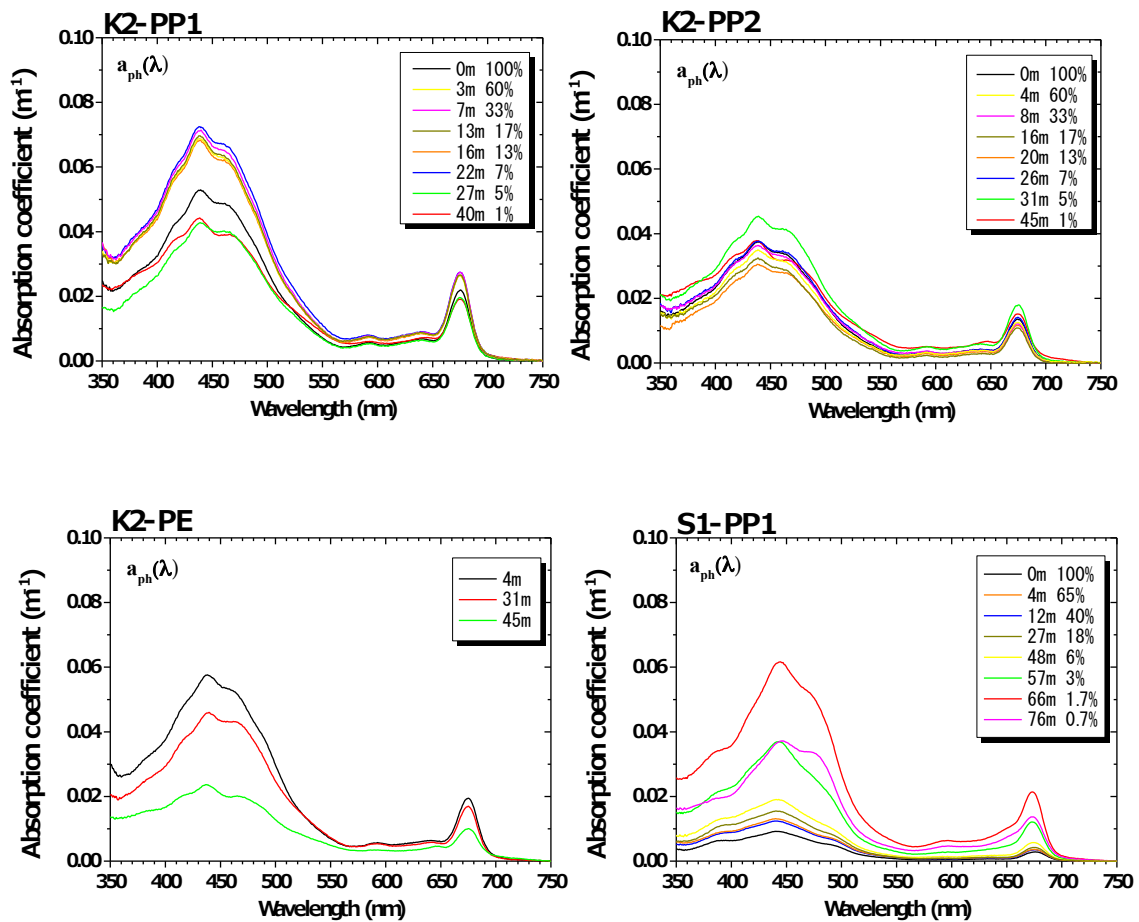


Fig.3.4.7-1 Absorption spectra of phytoplankton ($a_{ph}(\lambda)$) at Stn.K2 and S1. All spectra were normalized to 0.0 at 750nm.

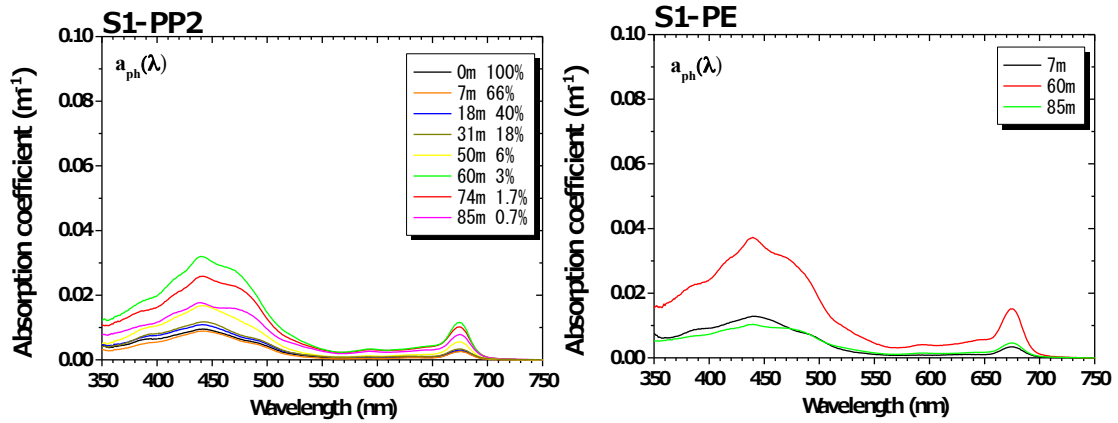


Fig.3.4.7-1 (Continued)

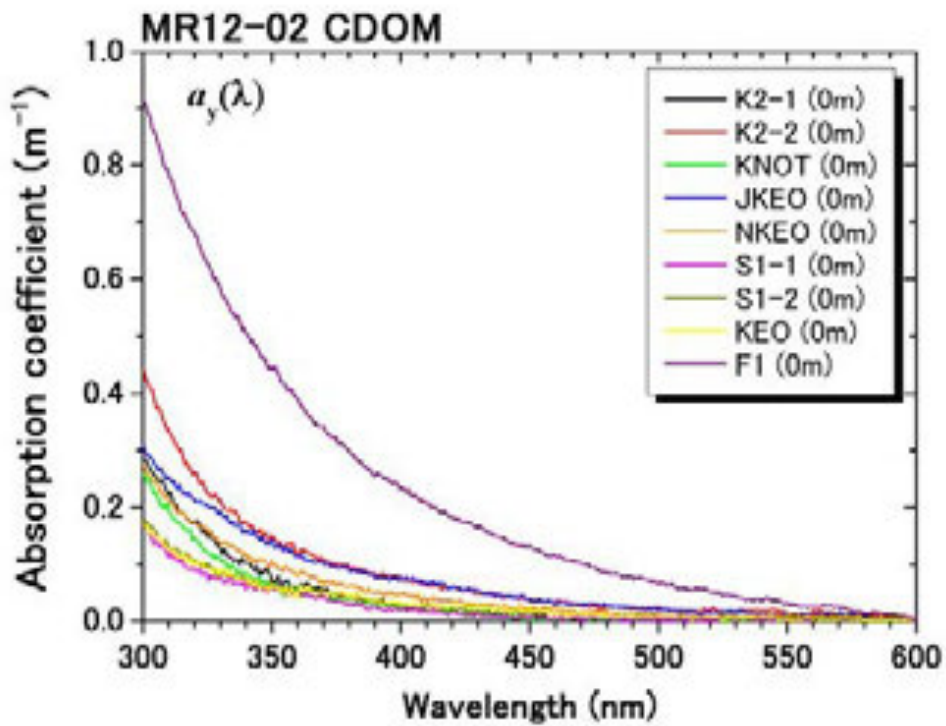


Fig.3.4.7-2 Absorption spectra of CDOM ($a_y(\lambda)$) collected by a bucket (0m depth) at each stations. All spectra were normalized to 0.0 at 600nm.

3.5 Optical measurement

Makio HONDA (JAMSTEC RIGC)

Kazuhiko MATSUMOTO (JAMSTEC RIGC)

(1) Objective

The objective of this measurement is to investigate the air and underwater light conditions at respective stations and to determine depths for *in situ* or simulated *in situ* measurement of primary production by using carbon stable isotope (C-13) during late autumn. In addition, optical data can be used for the validation of satellite data.



(2) Description of instruments deployed

The instrument consisted of the SeaWiFS Profiling Multichannel Radiometer (SPMR) and SeaWiFS Multichannel Surface Reference (SMSR). The SPMR was deployed in a free fall mode through the water column (see right picture). The SPMR profiler called “Free Fall” has a 13 channel irradiance sensors (Ed), a 13 channel radiance sensors (Lu), tilt sensor, and fluorometer. The SMSR has a 13 channel irradiance sensors (Es) and tilt meter (Table 1).

These instruments observed the vertical profiles of visible and ultra violet light and chlorophyll concentration.

Table 1. Center wavelength (nm) of the SPMR/SMSR

Es	379.5	399.6	412.2	442.8	456.1	490.9	519.0	554.3	564.5	619.5	665.6	683.0	705.9
Ed	380.0	399.7	412.4	442.9	455.2	489.4	519.8	554.9	565.1	619.3	665.5	682.8	705.2
Lu	380.3	399.8	412.4	442.8	455.8	489.6	519.3	554.5	564.6	619.2	665.6	682.6	704.5

Optical measurements by Free Fall were conducted at our time-series station K2 and S1. Measurements should be ideally conducted at median time. However observations were conducted irregularly because of limited ship-time and other observation’s convenience (Table 2). The profiler was dropped twice a each deployment to a depth of 200 m. The SMSR was mounted on the anti-rolling system’s deck and was never shadowed by any ship structure. The profiler descended at an average rate of 1.0 m/s with tilts of less than 3 degrees except near surface.

Observed data was analyzed by using software “Satlantic PPROSOFT 6” and extinction rate and photosynthetically available radiation (PAR) were computed.

Table 2 Locations of optical observation and principle characteristics
(Date and Time in LST: UTC+11hr at station K2, UTC+9hr at station S1)

Date and Time	Station	Lat./Long.	Surface PAR (quanta cm ⁻² sec ⁻¹)	Euphotic layer* (m)	Memo
2012.06.10 11:57	K2	47N/160E	6.5 x 10 ¹⁶	~ 50	1 day before PP incubation #1
2012.06.11 11:47	K2	47N/160E	4.4 x 10 ¹⁶	~ 46	during PP incubation #1
2012.06.13 10:32	K2	47N/160E	6.8 x 10 ¹⁶	~ 55	1 day before PP incubation #2
2012.06.14 11:30	K2	47N/160E	4.6 x 10 ¹⁶	~ 54	during PP incubation #2
2012.06.27 11:40	S1	30N/145E	3.2 x 10 ¹⁶	~ 82	1 day before PP incubation #1
2012.06.28 11:34	S1	30N/145E	5.8 x 10 ¹⁶	~ 82	during PP incubation #1
2012.06.30 09:55	S1	30N/145E	1.3 x 10 ¹⁷	~ 91	1 day before PP incubation #2
2012. 7. 1 11:40	S1	30N/145E	4.4 x 10 ¹⁶	~ 92	during PP incubation #2

* Euphotic layer: 0.5% of surface PAR

(3) Preliminary result

We deployed “Free Fall sensor” four times at station K2 and S1 (Table 2). Surface PAR ranged from approximately 3.2 x 10¹⁶ to 1.3 x 10¹⁷ quanta cm⁻² sec⁻¹ and surface PAR at S1 was approximately 20% higher than that at K2 on average (5.6 x 10¹⁶ and 6.6 x 10¹⁶ quanta cm⁻² sec⁻¹ at K2 and S1, respectively). The euphotic layers, that is defined as water depth with 0.5 % of surface PAR, were approximately 52 m at station K2 and 85 m at station S1. It is likely attributed to the amount of particulate materials, *i.e.* phytoplankton, in the water column: the amount of phytoplankton was likely smaller at S1 than those at K2 although surface PAR was higher at S1. This was supported by the fact that higher chlorophyll-a and primary productivity at station K2.

(4) Data archive

Optical data were filed on two types of file.

(BIN file) digital data of upwelling radiance and downwelling irradiance each 1 m from near surface to approximately 150 m for respective wave-lengths with surface PAR data during “Free Fall” deployment

(PAR file) in situ PAR each 1 m from near surface to approximately 100 m with extinction coefficient with surface PAR data during “Free Fall” deployment

These data files will be submitted to JAMSTEC Data Integration and Analyses Group (DIAG).

3.6 Drifting sediment trap

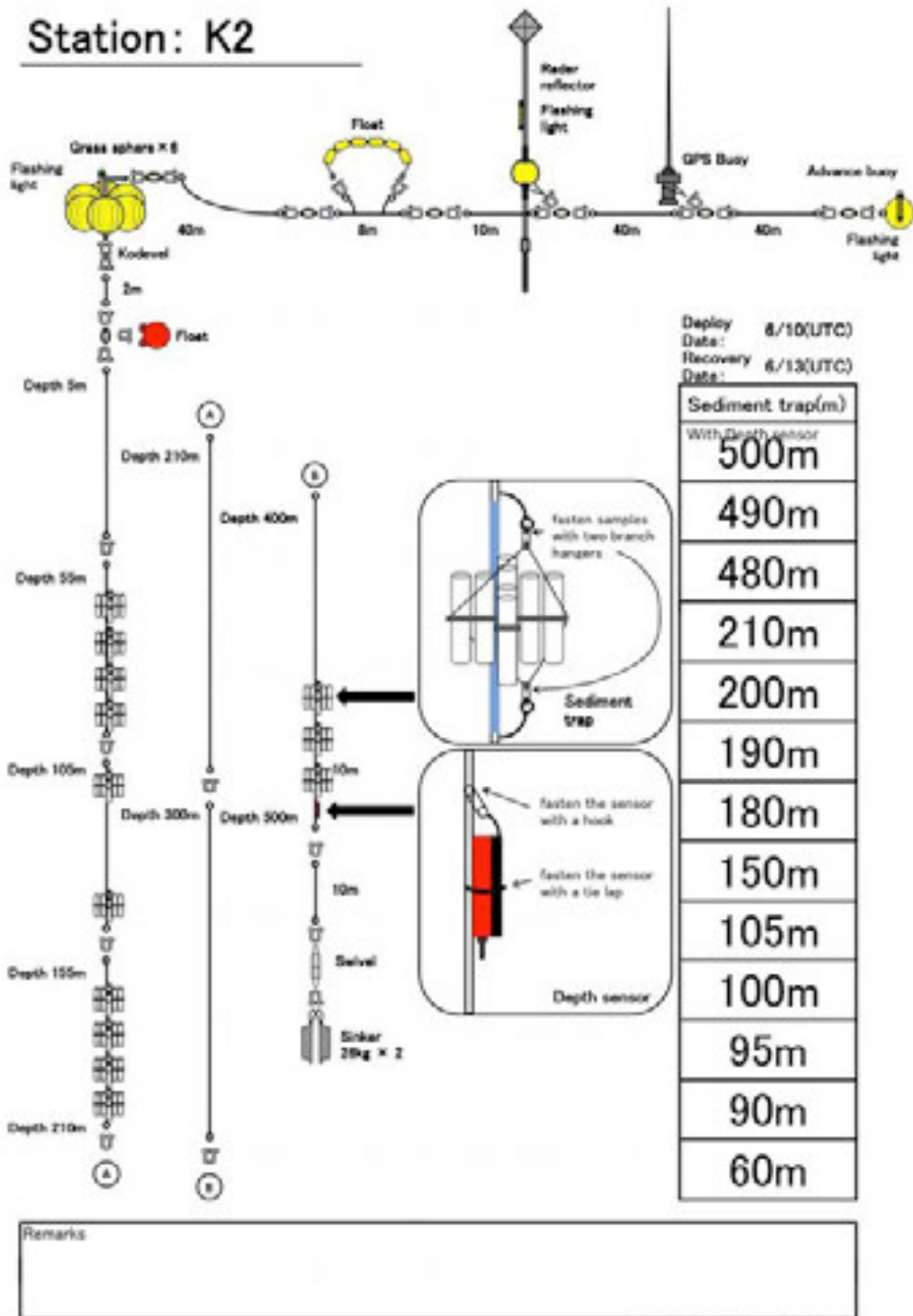
3.6.1 Drifting mooring system

Hajime KAWAKAMI (JAMSTEC MIO)
Makio C. HONDA (JAMSTEC RIGC)
Yoshihisa MINO (Nagoya University/JAMSTEC RIGC)
Katsunori KIMOTO (JAMSTEC RIGC)
Koji HAMASAKI (University of Tokyo)
Ryo KANEKO (University of Tokyo)
Mario UCHIMIYA (National Institute of Polar Research)
Katsuyuki INOUE (University of Tokyo)
Miyo IKEDA (MWJ)
Kanako YOSHIDA (MWJ)
Masahir OORUI (MWJ)

In order to conduct drifting sediment trap experiment at stations K2 and S1, drifting mooring system (drifter) was deployed. This drifter consists of radar reflector, GPS radio buoy (Taiyo TGB-100), flush light, surface buoy, ropes and sinker. On this system, “Knauer” type sediment trap at 13 layers were installed together (Traps of JAMSTEC: 60, 100, 150, 200, and 500 m; traps of Nagoya University: 90, 95, 180, 190, 480, and 490 m; traps of University of Tokyo: 105 and 210 m). Thanks to the effort by MWJ technicians, drifting mooring system was upgraded on board. The configuration is shown in Fig. 3.6.1-1.

The drifter was deployed at 20:10 on 10 June (UTC) at station K2 and at 21:40 on 27 June (UTC) at station S1. The drifter was recovered at 19:10 on 13 June at stations K2 and at 21:00 on 30 June at station S1. The drifter’s position was monitored by using GPS radio. Fig. 3.6.1-2 shows tracks of the drifter. In general, the drifter tended to drift northeastward and southeastward at stations K2 and S1, respectively. At recovery at station S1, the ropes and buoys at the sea surface were tangled.

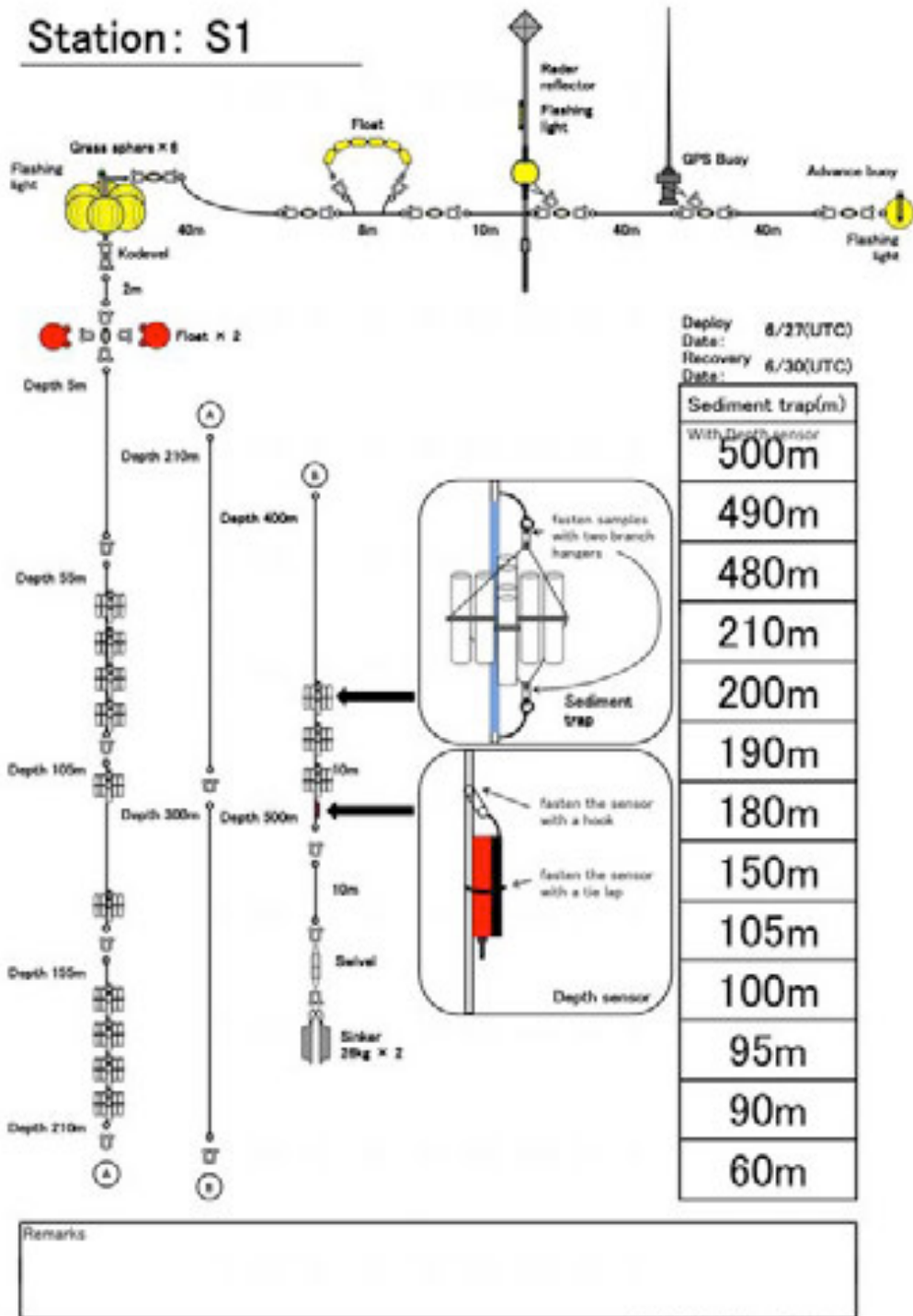
Station: K2



MR12-02 Drifting sediment trap
 Ver. 2012/6/10

Fig. 3.6.1-1 Drifting mooring system at stations K2 and S1.

Station: S1



MR12-02 Drilling sediment trap
Ver. 2012/6/27

Fig. 3.6.1-1 Continued.

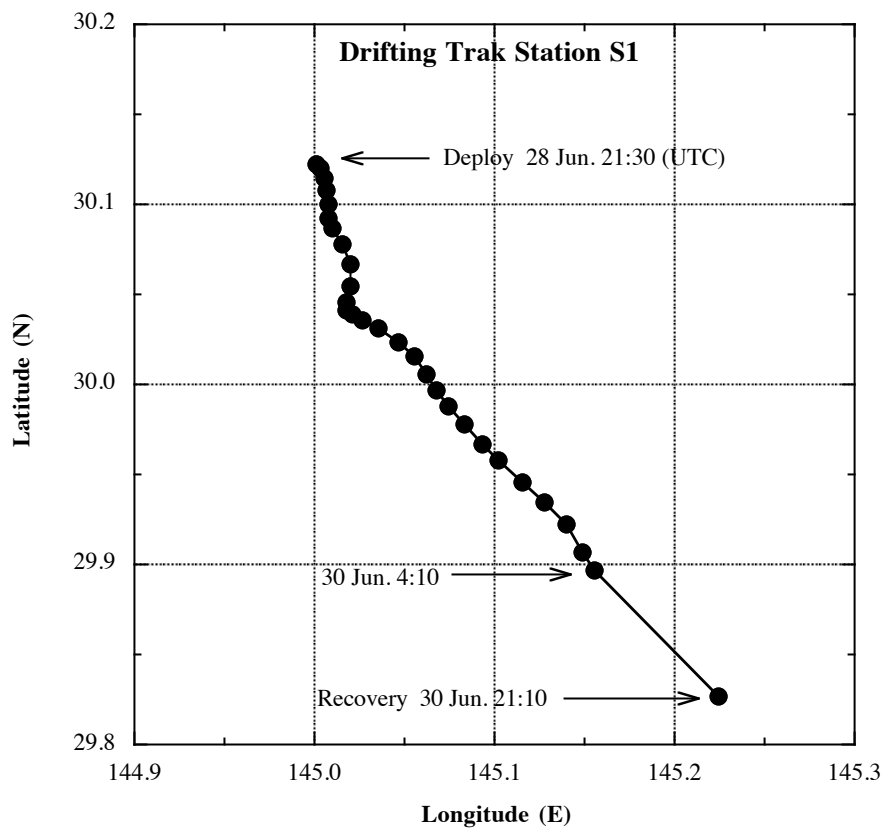
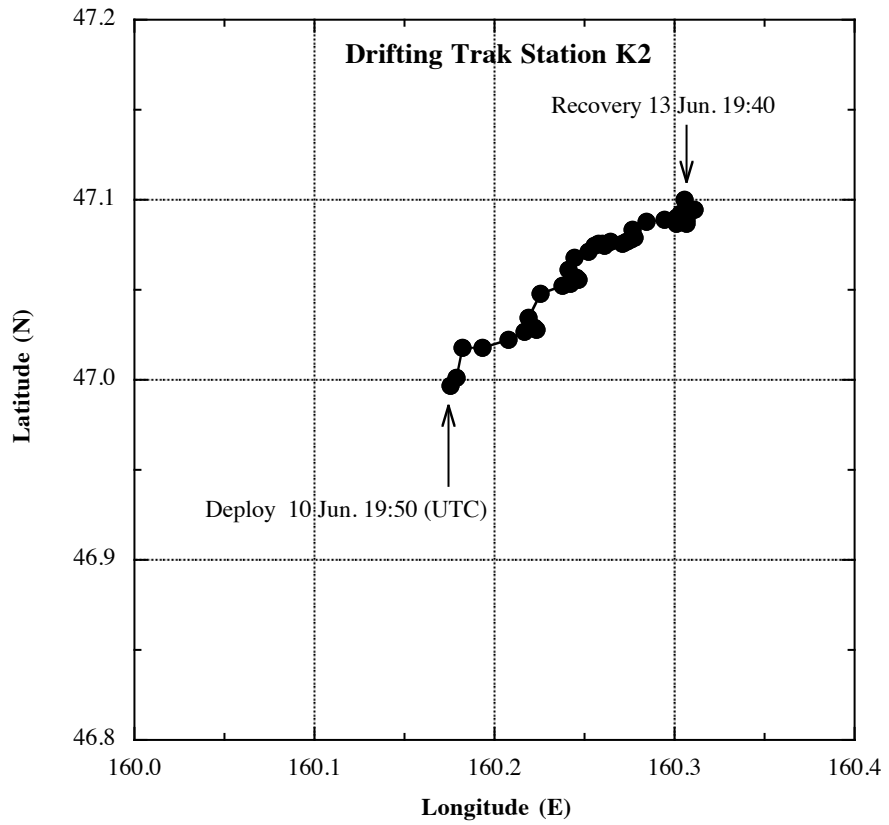


Fig. 3.6.1-2 Track of drifter (GPS buoy) at stations K2 and S1.

3.6.2 Drifting sediment trap of JAMSTEC

Hajime KAWAKAMI (JAMSTEC MIO)

Makio C. HONDA (JAMSTEC RIGC)

Katsunori KIMOTO (JAMSTEC RIGC)

In order to collect sinking particles and measure carbon flux, and zooplankton, “Knauer type” cylindrical sediment trap (Photo 3.6.2-1) was deployed at stations K2 and S1 where measurement of primary productivity was conducted. This trap consists of 8 individual transparent polycarbonate cylinders with baffle (collection area: ca. 0.0038 m², aspect ratio: 620 mm length / 75 mm width = 8.27), which was modified from Knauer (1979). Before deployment, each trap was filled with filtrated surface seawater, which salinity is adjusted to ~ 39 PSU by addition of NaCl (addition of 100 g NaCl to 20 L seawater) were placed in tubes. These were located at approximately 60, 100, 150, 200, and 500 m. After recovery, sediment traps were left for half hour to make collected particles settle down to the bottle. After seawater in acrylic tube was dumped using siphonic tube, collecting cups were took off. Two cups of samples at each layer were used for the study of the foraminifer. Four cups of samples at each layer were filtered thorough Nuclepore filter with a nominal pore size of 0.4μm and GF/F filter by two cups, for respective purposes (total mass flux, trace elements, total particulate carbon, and particulate organic carbon). The other samples were added buffered formalin for archive. The filter and archive samples were kept in freezer and refrigerator by the day when these were analyzed, respectively.



Photo 3.6.2-1 Drifting Sediment Trap.

3.7 Po-210 and export flux

Hajime KAWAKAMI (JAMSTEC MIO)

Makio C. HONDA (JAMSTEC RIGC)

(1) Purpose of the study

The fluxes of POC were estimated from Particle-reactive radionuclide (^{210}Po) and their relationship with POC in the western North Pacific Ocean.

(2) Sampling

Seawater and suspended particulate sampling for ^{210}Po , ^{210}Pb , and POC: 2 stations (stations K2 and S1) and 16 depths (10, 20, 30, 50, 75, 100, 150, 200, 300, 500, 700, 1000, 1500, 2000, 3000, and 4000 m) at each station.

Seawater samples (10 L for ^{210}Po and ^{210}Pb) were taken from Hydrocast at each depth. The seawater samples for ^{210}Po were filtered through polypropylene cartridge filters with a nominal pore size of 0.8 μm on board immediately after water sampling.

In situ filtering (suspended particulate) samples were taken from large volume pump sampler (Large Volume Water Transfer System WTS-6-1-142LV04, McLane Inc.). Approximately 200 and 1000 L seawater was filtered through glass-fiber filter with a nominal pore size of 0.7 μm at each station at 10–200m depths and 300–4000m depths, respectively. The filter samples were divided for ^{210}Po and POC.

(3) Chemical analyses

Dissolved and particulate ^{210}Po was absorbed on 25 mm silver disks electrically, and were measured by α -ray counter (Octéte, Seiko EG&G Co. Ltd.). For total (dissolved + particulate) ^{210}Pb measurement, the same procedure was applied to the seawater samples 18 months later, when ^{210}Po come to radioactive equilibrium with ^{210}Pb .

POC was measured with an elemental analyzer (Perkin-Elmer model 2400II) in land-based laboratory.

(4) Preliminary result

The distributions of ^{210}Po and POC will be determined as soon as possible after this cruise. This work will help further understanding of particle dynamics at the euphotic and deep layers.

3.8 Settling velocity of particles in the twilight zone

Yoshihisa MINO (NAGOYA UNIV. HyARC)

Chiho SUKIGARA (NAGOYA UNIV. HyARC)

(1) Objective

Sinking particles have been considered as the most important vehicle, by which the biological pump sequesters carbon in the ocean interior (Buesseler et al., 2007). As the particles sink they undergo the remineralization processes (fragmented into non-sinking ones and consumed by bacteria etc.) in the twilight zone, which leads to POC flux attenuation with depth. A large number of sediment trap studies have revealed that POC flux attenuation varied seasonally and regionally (Berelson, 2001), so it is required to understand this variability in order to better quantify the magnitude of biological pump. Recent studies pointed out the significance of particle settling velocity, varying three orders of magnitude, as a parameter affecting the flux attenuation (Armstrong et al., 2002, 2009; Trull et al., 2008).

This study aim to determine the settling velocity (SV) of particles collected by sediment trap at around 100 and 200, 500 m depth for the subarctic (station K2) and subtropical (S1) North Pacific Ocean, for further understanding the carbon transfer in the twilight zone.

(2) Materials and methods

Particulate samples were collected in the drifting sediment trap experiments conducted during this cruise (see the chapter 3.6 for details on the sediment trap experiments). The depth of sample collection is 90-95, 180-190, 480-490 m at both stations (K2 and S1). All samples were preserved in the 5% buffered formalin seawater for the SV analysis on shore.

Here we apply the elutriation method (Peterson et al. 2005) to fractionate particles into SV classes using countercurrents of varying speeds. A portion of the sediment trap samples is introduced into the custom-built polycarbonate elutriator and separated into 5 fractions with SVs of >500, 150-500, 50-150, 15-50, <15 m d⁻¹. After the swimmers are removed using the tweezers under microscope, each SV-fraction sample is filtrated onto pre-combusted GF/F filter. The organic carbon content in samples will be determined, which derive the settling velocity spectra of the trapped particles. The carbon and nitrogen isotope abundances are also determined for each SV-fraction.

(3) Data archive

The experimental data sets from this study will be submitted to JAMSTEC Data Integration and Analyses Group (DIAG).

(4) References

- Armstrong et al. (2002), *Deep-Sea Res. II*, 49, 219-236.
- Armstrong et al. (2009), *Deep-Sea Res. II*, 56, 1470-1478.
- Berelson, (2001), *Oceanography*, 14, 59-67.
- Buesseler et al. (2007), *Science*, 316, 567-570.
- Peterson et al. (2005), *Limnol. Oceanogr.: Methods*, 3, 520-532.
- Trull et al. (2008), *Deep-Sea Res. II*, 55, 1684-1695.

3.9 Zooplankton

3.9.1 Community structure and ecological roles

Minoru KITAMURA (JAMSTEC)

(1) Objective

Subarctic western North Pacific is known to be a region with high biological draw down of atmospheric CO₂. And time-series biogeochemical observations conducted at the station K2 have revealed high annual material transportation efficiency to the deep compared to the other time-series sites set in the subtropical regions. Importance of not only sinking particle but also ‘active transport’ by zooplankton on vertical material transport is recently suggested in several area such as Oyashio region, the station BATS or Antarctic Ocean. However, biogeochemical role of zooplankton is not fully estimated in western subarctic gyre, North Pacific. With these backgrounds, goal of the research is to investigate roles of mesozooplankton and micronekton in vertical material transport in the station K2, western subarctic North Pacific. We deployed two types of plankton nets to investigate species and size composition of zooplankton from the surface to the greater deep.

Material transport through microbial food web is one of the pathways which is little understood. To estimate ecological roles of the microzooplankton we will also analyze abundance, vertical distribution and grazing pressure of them.

For comparison to K2 ecosystem, we also conducted same samplings at a new time-series station, S1

(2) Materials and methods

Mesozooplankton and micronekton samplings (IONESS Sampling)

For collection of stratified sample sets, multiple opening/closing plankton net system, IONESS, was used. This is a rectangular frame trawl with nine nets. Area of the net mouth is 1.5 m² when the net frame is towed at 45° in angle, and mesh pore size is 0.33-mm. Volume of filtering water of each net is estimated using area of net mouth, towing distance, and filtering efficiency. The area of net mouth is calibrated from frame angle during tow, the towing distance is calculated from revolutions of flow-meter, and the filtering efficiency is 96% which was directory measured. The net system is towed obliquely. Ship speed during net tow was about 2 knot, speeds of wire out and reeling were 0.1-0.7 m/s and 0.1-0.3 m/s, respectively.

Total eight tows (except three tows for collection of RI samples) of IONESS were done. The stratified sampling layers at stations K2 and S1 were summarized in the Table 3.9.1-1. To understand diel vertical migration of mesozooplankton and micronekton, the samplings were conducted during both day and night. Towing data such as date, time, position, sampling layers are summarized in Table 3.5.1-1.

NORPAC net sampling

A twin-type NORPAC net with fine mesh (100 mm) and flow meters was used. The net was vertically towed 0-50 m and 0-150 m at the Stations K2 and S1. Zooplankton samples were preserved in the 5% buffered formalin seawater for the later analysis.

Nano- and microzooplankton sampling

Seawater samples were collected at eight depths within the euphotic layer in both the stations K2 and S1. The former eight depths corresponded to nominal specific optical depths approximately 100, 50, 35, 17, 12, 7, 3 and 1% light intensity relative to the surface irradiance as determined from the optical profiles obtained by Free-fall system.

Seawater samples were immediately treated with the final concentration of 1% glutaraldehyde and were kept at 4°C until filtering. Each seawater sample were filtered through 1µm pore size Nuclepore filter, pre-stained by irgalan black, at the low vacuum of 15 cmHg, and were double-stained using DAPI (4'6-diamidino-2-phenylindole dihydrochloride) and proflavine (3-6-diamidino-acridine hemisulfate). Just before the finish of filtering, DAPI was added to sample in filtering funnel for the staining DNA. After the DAPI staining, proflavine was also added for the staining of flagella. Both the staining time is five minute. The working solution of DAPI (10 µg/ml) and proflavine (0.033%) were pre-filtered through 0.45 µm pore size of non-pyrogenic Durapore membrane filter (Millipore, Millex-GX). After the filtering, sample filters put on a slide-glass with one drop of immersion oil, and covered with micro cover glass. All preparations were stored in the deep freezer (-80°C) until the observation.

Sampling data such as depths or filtering volume are summarized in Table 3.9.1-2.

Table 3.9.1-1. Summary of IONESS samplings.

MR12-02 IONESS Samplings
 including filtering efficiency, 90% in calculations of filtering volume
 LST: +1100 at K2, -0900 at S1 and F1

Sta.	Low ID	Date & Time			Position		Sampling layer (upper, m) and filtering volume (bottom, m ³)								Remarks		
		LST	m	UTC	in	out	Net No.	0	1	2	3	4	5	6		7	8
K2	02001A	2012.6.11	11:03	2012.6.12	0:03	46°59.82'N, 159°59.31'E	0-1048-1000	1000-750	750-500	500-300	300-200	200-150	150-100	100-50	50-0		
		13:52	2:52	47°03.07'N, 160°00.40'E	3283.6	3151.1	2196.3	951.8	484.0	646.7	483.4	642.3					
	02001B	2012.6.12	22:00	2012.6.12	11:00	46°58.60'N, 159°59.32'E	0-1038-1000	1000-750	750-500	500-300	300-200	200-150	150-100	100-50	50-0		
		0:50	13:50	47°03.96'N, 160°00.45'E	2199.5	3562.8	2364.7	1109.6	580.5	523.2	530.3	404.8					
02001A	2012.6.13	11:13	2012.6.13	0:13	46°56.57'N, 159°59.87'E	0-1060-1000	1000-750	750-500	500-300	300-200	200-150	150-100	100-50	50-0			
		13:52	2:52	47°00.00'N, 160°00.27'E	2499.4	3853.3	3713.0	752.2	479.1	424.9	356.8	408.0					
	02001A	2012.6.14	22:00	2012.6.14	11:00	46°58.87'N, 160°00.71'E	0-1054-1000	1000-750	750-500	500-300	300-200	200-150	150-100	100-50	50-0		
		0:52	13:52	47°04.64'N, 160°00.34'E	3043.2	3791.9	2440.9	711.0	315.3	316.8	431.9	366.7					
02001A	2012.6.15	21:08	2012.6.15	10:08	46°58.13'N, 159°58.73'E	0-250-200	200-40	40-0	0-220-200	200-40	40-0	-	-	-	-	NO IONESS	
		23:59	12:59	46°59.68'N, 159°59.22'E	3616.5	573.7	-	2630.9	626.3	-	-	-	-	-	-	NO IONESS	
S1	02002A	2012.6.28	21:09	2012.6.28	12:09	29°53.03'N, 145°00.17'E	0-225-200	200-25	25-0	0-220-200	200-25	25-0	0-220-200	200-25	25-0	-	NO IONESS
		23:56	14:56	29°53.86'N, 144°57.56'E	3403.0	1008.1	-	3659.0	3499.5	-	2413.1	258.2					
02002A	2012.6.29	10:24	2012.6.29	1:28	30°01.28'N, 145°00.81'E	0-1047-1000	1000-750	750-500	500-300	300-200	200-	200-100	100-50	50-0		4th net was not closed	
		13:21	4:21	29°55.09'N, 144°59.97'E	3112.3	3118.7	2530.8	3283.2	-	1274.5	880.6	881.2			5th net had to be closed		
02003A	2012.6.30	10:35	2012.6.30	1:35	30°00.77'N, 145°00.45'E	0-1033-1000	1000-750	750-500	500-300	300-200	200-150	150-100	100-50	50-0			
		13:29	4:35	30°11.75'N, 144°59.34'E	3275.7	2769.1	2764.7	1410.1	697.3	432.6	471.8	399.2					
02001A	2012.7.1	21:00	2012.7.1	12:00	30°04.02'N, 144°57.73'E	0-1046-1000	1000-750	750-500	500-300	300-200	200-150	150-100	100-50	50-0			
		23:50	14:50	30°08.87'N, 144°59.84'E	3741.0	3162.8	3057.8	1104.4	505.8	834.0	523.1	562.6					
02002A	2012.7.2	21:00	2012.7.2	12:00	30°06.47'N, 144°56.00'E	0-1065-1000	1000-750	750-500	500-300	300-200	200-150	150-100	100-50	50-0			
		23:52	14:52	30°04.68'N, 144°56.21'E	3346.7	3669.2	2318.4	1199.9	622.0	618.5	460.0	517.1					
F1	02003A	2012.7.7	21:00	12:00	30°28.00'N, 141°29.85'E	0-216-200	200-23	23-0	0-200-200	200-23	23-0	-	-	-	-	NO IONESS	
		23:01	14:01	30°34.99'N, 141°33.58'E	3693.7	469.6	-	1306.6	376.5	-	-	-	-	-	-	Two sample due to cool and trouble	

Table 3.9.1-2. Summary of NORPAC net hauls

MR12-02
NORPAC net hauls
 Rewind speed: 1.0 m / sec

Sta.	Date	Time (LST)	Position		Sampling (m)	Mesh	Wire out (m)	Wire angle (°)	Flow-meter readings		Filtering vol. (m ³)	
			Lat.	Long.					#1 net ID:2370	#2 net ID:3120	#1 net	#2 net
K2	2012.6.10	20:35	46°59.30'N	159°59.80'E	50-0	XX13	50	0	572	610	7.4	7.9
		20:46	46°59.27'N	159°59.85'E	150-0	XX13	151	5	1508	1579	19.6	20.5
S1	2012.6.26	21:18	29°58.99'N	145°00.90'E	50-0	XX13	50	0	562	523	7.3	6.8
		21:28	29°58.87'N	145°01.01'E	150-0	XX13	151	5	1580	1577	20.5	20.5
S1	2012.6.27	20:47	29°59.77'N	145°00.59'E	50-0	XX13	50	5	539	568	7.0	7.4
		20:57	29°59.68'N	145°00.67'E	150-0	XX13	151	5	1525	1505	19.8	19.6

Table 3.9.1-3. Summary of water samplings for nano- and microzooplankton.

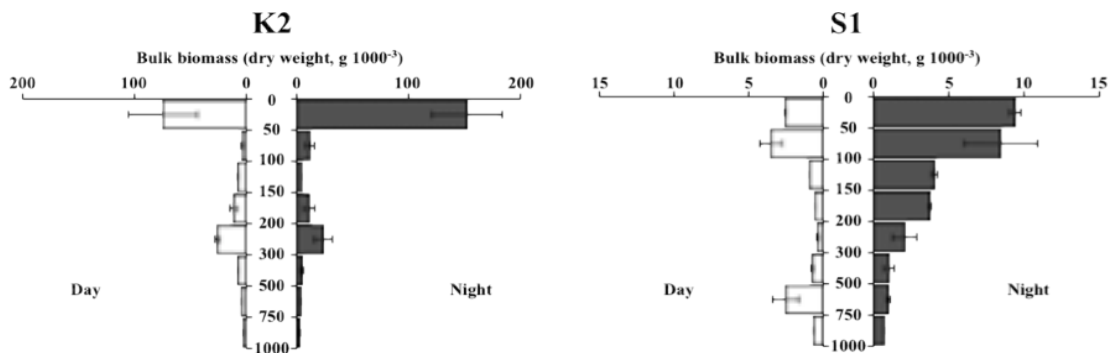
MR12-02

Water samplings for analysis of nano- and microzooplankton abundance

* Local ship time										
Sta.	Date*	Time*	CTD cast ID	Depth (m)	Irradiance (%)	Sample ID	Filtering vol. (ml)	Funnel No.	Preservation	Time filtration
K2	2012.6.11	2:30	K2_2 Shallow (PP 1st)	75	0.1	K2-27	250	1	6:10	2012.6.11 14:00
				40	1	K2-29	250	2		
				27	4.5	K2-31	215	3		
				22	7	K2-32	250	4		
				16	13	K2-33	175	1		
				13	17	K2-34	188	2		
				3	60	K2-36	215	3		
				0	100	K2-S	185	4		
				0	100	K2-S-2	135	1		
				2012.6.14	2:30	K2_2 Shallow (PP 2nd)	0	100		
KNOT	2012.6.17	19:40	KNOT_1 Deep Routine	0	100	KNOT-S	250	2	19:47	2012.6.18 19:30
JKEO	2012.6.19	21:30	JKEO_1 Deep Routine	0	100	JKEO-S	210	1	21:30	2012.6.20 21:20
NKEO	2012.6.21	10:40	NKEO_1 Deep Routine	0	100	NKEO-S-1	185	1	10:50	2012.6.21 19:30
				0	100	NKEO-S-2	250	2		
				0	100	NKEO-S-2	250	2		
S1	2012.6.28	5:30	S1_2 Shallow (PP 1st)	76	0.7	S1-27	500	1	5:30	2012.6.30 2:00
				57	3.5	S1-29	385	2		
				48	6	S1-31	325	3		
				33	13	S1-33	420	4		
				27	18	S1-34	380	1		
				12	40	S1-35	415	2		
				4	65	S1-36	400	3		
				0	100	S1-S	500	4		
				0	100	S1-S	500	4		

(3) Preliminary results

Vertical distributions of mesozooplankton biomass (dry weight) in the stations K2 and S1 are shown below.



(4) Future plans and sample/data archives

All samples are stored at JAMSTEC. Environmental (T, S) and net status (net number, towing distance, etc.) data, which were recorded during each IONESS tow, are stored under Kitamura. Using the samples, I will conduct about

- (a) comparison of zooplankton communities in the two sites,
- (b) identification of dominant species and vertical migrants (diel and ontogenetic),
- (c) estimation of vertically active carbon flux by mesozooplankton.

3.9.2 Grazing pressure of microzooplankton

Minoru KITAMURA (JAMSTEC BIOGEOSS)

Kazuhiko MATSUMOTO (JAMSTEC RIGC)

(1) Objective

To understand material export from surface to deep ocean, not only estimations of primary productivity or vertical flux but also evaluation of grazing impacts at surface is needed. Grazing by larger organisms might bring about efficient vertical carbon transport through repacking phytoplankton into fecal pellets or active carbon transport by diel and ontogenetic migrator. On the other hand, grazing by smaller organisms might have small or negative impact to vertical export. Identification of influential grazers and quantitative estimation of their grazing rates are essential to discuss the carbon cycle in the ocean. Recently, large grazing pressure of not only the crustacean plankton but also microzooplankton has been recognized in the several area. Based on this background, we estimated grazing rate of them.

(2) Materials and methods

Eight dilution incubation experiments were done through the cruise (Table 3.9.2-1). For each experiment 40 l of water were collected from Niskin bottle or bucket. Water was pre-screened through 200 μm mesh to exclude larger zooplankton. Dilution series were prepared with 25, 50, 75, and 100% of natural seawater. Filtered water was obtained by direct gravity flow through a compact cartridge filter (ADVANTEC, MCS-020-D10SR). Incubation of the dilute water was done in transparent polycarbonate bottle. Duplicate or triplicate bottle were prepared. Incubation lasted for 24 h in. All the water samplings, filtering, and incubate items were soaked in 10% HCl and rinsed Milli-Q water between each use on board. Nutrient was added in the incubation bottles. To measure initial and final chl. *a* concentration, experiment water were filtered onto GF/F filter and extracted 6 ml DMF at -20°C until measurement. Chl. *a* was measured fluorometrically (Welshmeyer method) with a Turner Design fluorometer. Phytoplankton cell numbers were also counted using flowcytometry.

Apparent phytoplankton growth rate (d^{-1}) were calculated using following equation:

$$\text{Apparent growth rate} = (1/t)\ln(P_t/P_0)$$

where t is incubation time (day), P_t and P_0 are final and initial Chl. *a* concentration or cell number, respectively. When the apparent phytoplankton growth rate is plotted as a function of dilution factor, the y-intercept and negative slope of the approximate line means true phytoplankton growth (k ; d^{-1}) and grazing coefficient of microzooplankton (g ; d^{-1}), respectively. According to Verity et al. (1993) and Zhang et al. (2006), microzooplankton grazing pressure on primary production (P_p ; %) is calculated as the following equation:

$$P_p = (e^{kt} - e^{(k-g)t}) / (e^{kt} - 1) * 100$$

Through the eight incubation experiments, we tried to estimate true growth rate of phytoplankton, grazing rate of microzooplankton and grazing pressure of microzooplankton on primary production. Incubation states are summarized in Table 3.9.2-2.

Table 3.9.2-1. Dilution experiments, list of samplings.

Station	Date*	Exp. ID.	Time*	Position	Depth m	Irradiance %	Water sampling			Sampler
							Temp. °C	Chl.a µg/l	CTD cast No.	
K2	2012.6.11	K2-1	2:30	46°59.71'N, 160°00.20'E	0	100	4.9	1.12	K2_2 Shallow (PP 1st)	Bucket
	2012.6.11	K2-2	9:00	46°59.99'N, 160°00.00'E	30'	3	4.8	1.39	K2_3 Co/Paloo	Clean Niskin
	2012.6.14	K2-3	2:30	47°03.54'N, 160°17.77'E	0	100	5.2	0.55	K2_8 Shallow (PP 2nd)	Bucket
	2012.6.14	K2-4	8:30	47°00.99'N, 160°03.04'E	31'	5	4.7	0.66	K2_9 Shallow (PE)	Clean Niskin
S1	2012.6.28	S1-1	2:30	30°00.09'N, 144°39.84'E	0	100	23	0.13	S1_2 Shallow (PP 1st)	Bucket
	2012.6.28	S1-2	10:00	30°01.74'N, 144°59.35'E	66'	1.7	18.2	0.49	S1_4 Shallow (Co/Paloo)	Clean Niskin
	2012.7.1	S1-3	2:30	29°53.12'N, 145°05.48'E	0	100	23.5	0.14	S1_6 Shallow (PP 2nd)	Bucket
	2012.7.1	S1-4	8:30	29°49.51'N, 145°12.50'E	62'	2	18.7	0.58	S1_7 Shallow (PE)	Clean Niskin

*Local ship time

Chl.a max. depth

Table 3.9.2-2. Dilution experiments, summary of incubation states.

Exp. ID.	Incubation						Remarks	
	start	Time*	end	Incubation bottle	Temp. °C	Irradiance %		Nutrients addition
K2-1	11 June	4:30	12 June 4:30	1L	4.8-5.2	100	+	Matsumoto FCM
K2-2	11 June	11:40	12 June 9:00	1L	4.8-5.2	2.5	+	Matsumoto FCM
K2-3	14 June	4:20	15 June 5:30	1L	5.1	100	+	Matsumoto FCM
K2-4	14 June	10:30	15 June 10:45	1L	5.1-5.5	100	+	Matsumoto FCM
S1-1	28 June	4:20	29 June 5:00	2L	22.6-23.7	100	+	Matsumoto FCM
S1-2	28 June	12:30	29 June 9:00	1L	18.9	2.5	+	Matsumoto FCM
S1-3	1 July	4:20	2 July 4:30	2L	23.2-23.5	100	+	Matsumoto FCM
S1-4	1 July	11:30	2 July 11:30	1L	18.9	2.5	+	Matsumoto FCM

(3) Preliminary results

All measurements of Chl.a and phytoplankton cell numbers were finished on board. In the Fig. 3.9.2-1, the apparent phytoplankton growth is plotted as a function of dilution factor. The negative slope of the regression equation is the grazing coefficient.

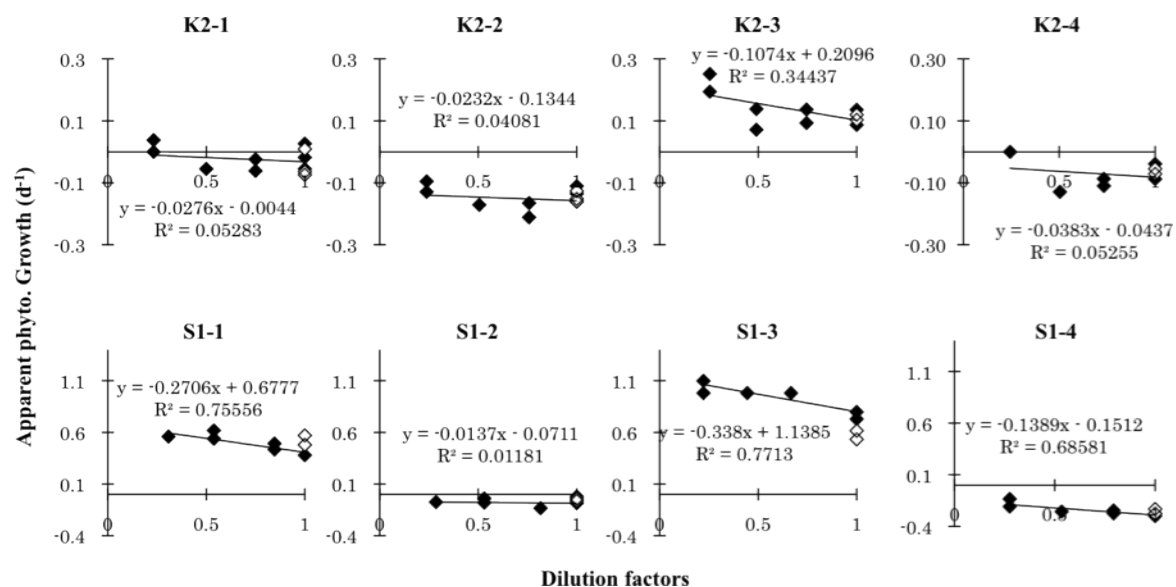


Figure 3.9.2-1. Dilution plots from the eight experiments. Apparent growths of phytoplankton were calculated based on the changes of bulk chlorophyll.

3.10 Biological study for phytoplankton and zooplankton

Katsunori KIMOTO (RIGC, JAMSTEC)

Miyako SATO (RIGC, JAMSTEC)

Yuriko NAKAMURA (RIGC, JAMSTEC)

3.10.1 Planktic Foraminifers and radiolarians

(1) Objective

Planktic foraminifers and radiolarians produce calcium carbonate and siliceous tests respectively and contribute to the material cycles. Planktic foraminifers show wide distributions in the surface water. Recent molecular biological studies revealed the high genetic variations within many planktic foraminifera species. These intra-specific genetic variations considered be the indications of the cryptic speciation and their ecologies could be different among these cryptic species. Moreover, morphological variations which correspond to the genetic populations is confirmed on several species. The water mass structure is considered as one of the factors which affect the distribution of the genetic populations. However, the genetic variability of the planktic foraminifers is not fully understood. In this study, we collected living planktic foraminifer in order to reveal the genetic populations of the planktic foraminifera in the North Pacific Subpolar gyre and the Subtropical gyre.

(2) Methods

Living planktic foraminifera samples were collected by filtration of surface seawater and vertical towing of a NORPAC net (Fig. 3-10-1). Surface seawater taken from onboard seawater tap was filtered using filtration apparatus (63 μm opening). The NORPAC net towing was conducted at station K2 and S1. A closing NORPAC net (63 μm opening) was used in order to obtain depth-stratified samples. The sampling depths and dates of the NORPAC net towing are summarized in Table 3-10-1. A part of selected samples obtained NORPAC net samples were used for phylogenetic analysis.

Samples were removed seawater and completely replaced by 99.5 % ethanol in the onboard laboratory. Then, samples were stored at 4 °C. Some living planktic foraminifer and radiolarian individuals for phylogenetic analysis were picked under a stereomicroscope and cleaned in filtered seawater with fine brushes. Specimens were air dried on the faunal slides and stored at -80 °C.

In this cruise, we tried to collect planktic foraminiferal shells using in-situ pumping (Large Volume Pump, LVP) and drifting traps. Sampling depths are also listed in Table 3-10-1.



Fig.3-10-1 Schematic illustration of closing NORPAC net. Plankton net is open during towing (left), and closed at the top of the sampling depth range by deploying a messenger (right).

(3) Preliminary result on shipboard

Species identifications under stereomicroscope show that planktic foraminifer species at K2 consist of subpolar species while species at S1 is consist of subtropical species. Samples collected Stn. K2 contained *Globigerina bulloides*, *Neogloboquadrina pachyderma*, *Turborotalita quinqueloba*, and *Globigerinita uvula*. Planktic foraminifera species observed in the samples collected in the Stn. S1 include *Globigerinoides ruber*, *G. sacculifer*, small Globigerinids and *Streptochilus globulosus*. The number of individuals collected at S1 was very few compared to the samples collected at K2.

(4) Data archive

The planktic foraminifer samples are stored at JAMSTEC. Molecular phylogenetic and morphological analysis will be conducted. Measurement of shell density by using micro-focus X-ray Computing Tomography will be also performed.

Table 3-10-1. Summary of plankton tow sampling.

Station	Latitude	Longitude	Depth (m)	Equipment	Date	Time	Station	Latitude	Longitude	Depth (m)	Equipment	Date	Time
K2	47° 0' N	140° 0' E	0-20	NORPAC	2012	6 10 0400 UTC	S1	30° 0' N	145° 0' E	0-20	NORPAC	2012	6 26 1034 UTC
K2	47° 0' N	140° 0' E	20-50	NORPAC	2012	6 10 010 UTC	S1	30° 0' N	145° 0' E	20-50	NORPAC	2012	6 26 1041 UTC
K2	47° 0' N	140° 0' E	50-100	NORPAC	2012	6 10 020 UTC	S1	30° 0' N	145° 0' E	50-100	NORPAC	2012	6 26 1107 UTC
K2	47° 0' N	140° 0' E	100-150	NORPAC	2012	6 10 030 UTC	S1	30° 0' N	145° 0' E	100-150	NORPAC	2012	6 26 1118 UTC
K2	47° 0' N	140° 0' E	150-200	NORPAC	2012	6 10 040 UTC	S1	30° 0' N	145° 0' E	150-200	NORPAC	2012	6 26 1130 UTC
K2	47° 0' N	140° 0' E	300-300	NORPAC	2012	6 10 055 UTC	S1	30° 0' N	145° 0' E	300-300	NORPAC	2012	6 26 1200 UTC
K2	47° 0' N	140° 0' E	300-500	NORPAC	2012	6 12 734 UTC	S1	30° 0' N	145° 0' E	300-500	NORPAC	2012	6 26 025 UTC
K2	47° 0' N	140° 0' E	500-700	NORPAC	2012	6 12 005 UTC	S1	30° 0' N	145° 0' E	500-700	NORPAC	2012	6 26 2348 UTC
K2	47° 0' N	140° 0' E	700-1000	NORPAC	2012	6 12 050 UTC	S1	30° 0' N	145° 0' E	700-1000	NORPAC	2012	6 26 2300 UTC
K2	47° 0' N	140° 0' E	0-20	NORPAC	2012	6 13 2228 UTC	S1	30° 0' N	145° 0' E	0-20	NORPAC	2012	6 30 828 UTC
K2	47° 0' N	140° 0' E	20-50	NORPAC	2012	6 13 2238 UTC	S1	30° 0' N	145° 0' E	50-100	NORPAC	2012	6 30 838 UTC
K2	47° 0' N	140° 0' E	50-100	NORPAC	2012	6 13 2341 UTC	S1	30° 0' N	145° 0' E	100-200	NORPAC	2012	6 30 848 UTC
K2	47° 0' N	140° 0' E	100-150	NORPAC	2012	6 13 2352 UTC	S1	30° 0' N	145° 0' E	0-200	NORPAC	2012	6 30 906 UTC
K2	47° 0' N	140° 0' E	150-200	NORPAC	2012	6 13 2358 UTC	S1	30° 0' N	145° 0' E	0-200	NORPAC	2012	6 30 935 UTC
K2	47° 0' N	140° 0' E	200-300	NORPAC	2012	6 13 2358 UTC	S1	30° 0' N	145° 0' E	0-200	NORPAC	2012	6 30 935 UTC
K2	47° 0' N	140° 0' E	30	In-situ Pump	2012	6 14 1500 UTC	S1	30° 0' N	145° 0' E	0-200	NORPAC	2012	6 30 951 UTC
K2	47° 0' N	140° 0' E	50	In-situ Pump	2012	6 14 1800 UTC	S1	30° 0' N	145° 0' E	20	In-situ Pump	2012	6 14 400 UTC
K2	47° 0' N	140° 0' E	100	In-situ Pump	2012	6 14 1900 UTC	S1	30° 0' N	145° 0' E	30	In-situ Pump	2012	6 14 400 UTC
K2	47° 0' N	140° 0' E	125	In-situ Pump	2012	6 14 1900 UTC	S1	30° 0' N	145° 0' E	80	In-situ Pump	2012	6 14 400 UTC
K2	47° 0' N	140° 0' E	150	In-situ Pump	2012	6 14 1900 UTC	S1	30° 0' N	145° 0' E	120	In-situ Pump	2012	6 14 400 UTC
K2	47° 0' N	140° 0' E	175	In-situ Pump	2012	6 14 1900 UTC	S1	30° 0' N	145° 0' E	350	In-situ Pump	2012	6 14 400 UTC
K2	47° 0' N	140° 0' E	200	In-situ Pump	2012	6 14 1900 UTC	S1	30° 0' N	145° 0' E	500	In-situ Pump	2012	6 14 400 UTC
K2	47° 0' N	140° 0' E	300	In-situ Pump	2012	6 14 1900 UTC	S1	30° 0' N	145° 0' E	700	In-situ Pump	2012	6 14 400 UTC
K2	47° 0' N	140° 0' E	40	Drifting Trap	2012	6 13 1900 UTC	S1	30° 0' N	145° 0' E	1000	In-situ Pump	2012	6 14 400 UTC
K2	47° 0' N	140° 0' E	100	Drifting Trap	2012	6 13 1900 UTC	S1	30° 0' N	145° 0' E	60	Drifting Trap	2012	6 13 1900 UTC
K2	47° 0' N	140° 0' E	150	Drifting Trap	2012	6 13 1900 UTC	S1	30° 0' N	145° 0' E	100	Drifting Trap	2012	6 13 1900 UTC
K2	47° 0' N	140° 0' E	200	Drifting Trap	2012	6 13 1900 UTC	S1	30° 0' N	145° 0' E	150	Drifting Trap	2012	6 13 1900 UTC
K2	47° 0' N	140° 0' E	300	Drifting Trap	2012	6 13 1900 UTC	S1	30° 0' N	145° 0' E	200	Drifting Trap	2012	6 13 1900 UTC
K2	47° 0' N	140° 0' E	500	Drifting Trap	2012	6 13 1900 UTC	S1	30° 0' N	145° 0' E	500	Drifting Trap	2012	6 13 1900 UTC

3.10.2 Shell-bearing phytoplankton studies in the western North Pacific

(1) Objectives

Shell-bearing phytoplanktons (Diatoms, Silicoflagellates, and Coccolithophorids) are main primary producer of the ocean, therefore it is important to know their seasonal distribution, interactions, and transgressions of assemblages. Furthermore, hard skeletons of phytoplankton remains in the deep sea sediments and it provide useful information for paleoceanographic changes of sea surface water conditions. In this study, we collected water samples from Stn. K2 and S1 to investigate vertical distributions and their ecology.

(2) Methods

Seawater samples were obtained from upper 200 m water depths at all hydrocast stations by CTD/Niskin systems of 12 L bottle capacity. The locations that were collected seawater were listed in Table 3-10-2.

For coccolithophorid separations, maximally 10 liter seawaters were filtered using 0.45 μm membrane filter (ADVANTEC MFS, Inc., JAPAN) immediately after collection. For diatoms and silicoflagellates separations, maximally 5 liter seawaters were also filtered using 0.45 μm membrane filter.

(3) Future works

Collected samples were analyzed assemblages, diversities and spatial distributions for each taxon at onshore laboratory. These data will be compared with the sediment trap datasets that are moored at St. S1 and K2, same locations with water sampling points in this time. That should be provided the important information of seasonal and spatial variability of phytoplankton related with oceanographic changes in the western north Pacific.

Table3-10-2. Summary of seawater filtration sampling.

Station	Latitude		Longitude		Depth (m)	Volume of water (L)	Date			Time
K2	47	0 N	160	0 E	200	20	2012	6	10	22:00 UTC
K2	47	0 N	160	0 E	150	20	2012	6	10	22:00 UTC
K2	47	0 N	160	0 E	125	20	2012	6	10	22:00 UTC
K2	47	0 N	160	0 E	100	20	2012	6	10	22:00 UTC
K2	47	0 N	160	0 E	75	20	2012	6	10	22:00 UTC
K2	47	0 N	160	0 E	50	20	2012	6	10	22:00 UTC
K2	47	0 N	160	0 E	30	20	2012	6	10	22:00 UTC
K2	47	0 N	160	0 E	10	20	2012	6	10	22:00 UTC
K2	47	0 N	160	0 E	0	20	2012	6	10	22:00 UTC
S1	30	0 N	145	0 E	200	20	2012	6	28	21:30 UTC
S1	30	0 N	145	0 E	150	20	2012	6	28	21:30 UTC
S1	30	0 N	145	0 E	125	20	2012	6	28	21:30 UTC
S1	30	0 N	145	0 E	100	20	2012	6	28	21:30 UTC
S1	30	0 N	145	0 E	75	20	2012	6	28	21:30 UTC
S1	30	0 N	145	0 E	50	20	2012	6	28	21:30 UTC
S1	30	0 N	145	0 E	30	20	2012	6	28	21:30 UTC
S1	30	0 N	145	0 E	10	20	2012	6	28	21:30 UTC
S1	30	0 N	145	0 E	0	20	2012	6	28	21:30 UTC

3.11 Community structures and metabolic activities of microbes

(Studies on the microbial-geochemical processes that regulate the operation of the biological pump in the subarctic and subtropical regions of the western North Pacific – IV)

**Ryo KANEKO (Atmosphere and Ocean Research Institute : AORI,
The University of Tokyo: UT)**

Mario UCHIMIYA (AORI, UT)

Hideki FUKUDA (AORI, UT)

Hiroshi OGAWA (AORI, UT)

Toshi NAGATA (AORI, UT)

Kazuhiro KOGURE (AORI, UT)

Koji HAMASAKI (AORI, UT)

(1) Objective

A significant fraction of dissolved and particulate organic matter produced in the euphotic layer of oceanic environments is delivered to meso- and bathypelagic layers, where substantial transformation and decomposition of organic matter proceeds due to the actions of diverse microbes thriving in these layers. Spatio-temporal variations in organic matter transformation and decomposition in the ocean's interior largely affect patterns in carbon cycling in the global ocean. Thus elucidating diversity, activities and distribution patterns of microbes in deep oceanic waters is fundamentally important in order to better understand major controls of oceanic material cycling in the ocean.

The objective of this study is to determine seasonal variability of microbial diversity and activities during the time-series observation of vertical fluxes at the two distinctive oceanic stations located in the subarctic and subtropical western North Pacific. We investigated i) full-depth profiles of prokaryotic abundance and related biogeochemical parameters including dissolved organic carbon and nitrogen concentrations (potential resources of prokaryotes), and the abundances of viruses (potential predators of prokaryotes), ii) community structures of Bacteria and Archaea and their metabolic activities, iii) sinking velocity and physic-chemical properties of suspended particles in the mixing layer.

(2) Method

Seawater samples were collected from predetermined depths of two CTD casts, i.e. the Atmosphere and Ocean Research Institute (AORI) cast and the Routine cast, conducted at Stations K2 and S1 (see the meta-data sheet for details). Sinking particles were collected by drifting traps to determine fluxes of sinking POC/PON and their weight (see the meta-data sheet for details).

i) Full-depth profiles of prokaryotic activity and abundance and related biogeochemical parameters

- a) Prokaryotic abundance: Flowcytometry
- b) Prokaryotic production: ^3H -leucine incorporation
- c) Virus abundance: Flowcytometry
- d) DOC/DON: Concentrations of dissolved organic carbon and total dissolved nitrogen were determined by the high temperature catalytic oxidation (HTCO) method. The concentration

of dissolved organic nitrogen was calculated by subtracting the concentration of dissolved inorganic nitrogen (determined by Auto-analyzer) from that of total dissolved nitrogen.

ii) Relationship between community structures of Bacteria and Archaea and their metabolic activities

- a) Bacterial community structures: PCR-DGGE method after extracting DNA from particles collected on 0.22 μm -pore-size filters (Sterivex).
- b) Activities of bacteria: Bromodeoxyuridine-incorporating methods

iii) Sinking velocity and physico-chemical properties of suspended particles

- a) Concentrations of particulate organic carbon and nitrogen: Determined using an elemental analyzer for samples collected on GF/F filters.
- b) Weight of suspended solid: Determined by weighing samples collected on pre-weighted GF/F filter.

(3) All results will be submitted to Data Management Office, JAMSTEC after analysis and validation and be opened to public via the web site.

3.12. Dissolved Organic Carbon

Masahide WAKITA (JAMSTEC MIO)

(1) Purpose of the study

Fluctuations in the concentration of dissolved organic carbon (DOC) in seawater have a potentially great impact on the carbon cycle in the marine system, because DOC is a major global carbon reservoir. A change by < 10% in the size of the oceanic DOC pool, estimated to be ~ 700 GtC, would be comparable to the annual primary productivity in the whole ocean. In fact, it was generally concluded that the bulk DOC in oceanic water, especially in the deep ocean, is quite inert based upon ¹⁴C-age measurements. Nevertheless, it is widely observed that in the ocean DOC accumulates in surface waters at levels above the more constant concentration in deep water, suggesting the presence of DOC associated with biological production in the surface ocean. This study presents the distribution of DOC during spring in the northwestern North Pacific Ocean.

(2) Sampling

Seawater samples were collected at stations E03, K2 (Cast 1, 2 and 8), S1 (Cast 1, 2, and 6) and F1, and brought the total to ~130. Seawater from each Niskin bottle was transferred into 60 ml High Density Polyethylene bottle (HDPE) rinsed with same water three times. Water taken from the surface to 250 m is filtered using precombusted (450°C) GF/F inline filters as they are being collected from the Niskin bottle. At depths > 250 m, the samples are collected without filtration. After collection, samples are frozen upright and preserved at ~ -20 °C cold until analysis in our land laboratory. Before use, all glassware was muffled at 550 °C for 5 hrs.

(3) Analysis

Prior to analysis, samples are returned to room temperature and acidified to pH < 2 with concentrated hydrochloric acid. DOC analysis was basically made with a high-temperature catalytic oxidation (HTCO) system improved a commercial unit, the Shimadzu TOC-V (Shimadzu Co.). In this system, the non-dispersive infrared was used for carbon dioxide produced from DOC during the HTCO process (temperature: 680 °C, catalyst: 0.5% Pt-Al₂O₃).

(4) Preliminary result

The distributions of DOC will be determined as soon as possible after this cruise.

(5) Data Archive

All data will be submitted to JAMSTEC Data Management Office (DMO) within 2 years.

3.13 Chlorofluorocarbons

Masahide WAKITA (JAMSTEC MIO)

Ken'ichi SASAKI (JAMSTEC MIO)

(1) Objective

Chlorofluorocarbons (CFCs) are chemically and biologically stable gases that have been synthesized at 1930's. The atmospheric CFCs can slightly dissolve in sea surface water by air-sea gas exchange and then are spread into the ocean interior. The chemical species of CFCs (CFC-11 (CCl₃F), CFC-12 (CCl₂F₂), and CFC-113 (C₂Cl₃F₃)) can be used as transient chemical tracers for the ocean circulation on timescale of several decades. We measured concentrations of CFCs in seawater.

(2) Apparatus

Dissolved CFCs are measured by an electron capture detector (ECD) – gas chromatograph attached with a purging & trapping system.

Table 3-14-1 Instruments

Gas Chromatograph:	GC-14B (Shimadzu Ltd.)
Detector:	ECD-14 (Shimadzu Ltd)
Analytical Column:	
Pre-column:	Silica Plot capillary column [i.d.: 0.53mm, length: 8 m, film thickness: 0.25μm]
Main column:	Connected two capillary columns (Pola Bond-Q [i.d.: 0.53mm, length: 9 m, film thickness: 6.0μm] followed by Silica Plot [i. d.: 0.53mm, length: 14 m, film thickness: 0.25μm])
Purging & trapping:	Developed in JAMSTEC. Cold trap columns are 1/16" SUS tubing packed with Porapak T.

(3) Procedures

3-1 Sampling

Seawater sub-samples for CFC measurements were collected from 12 liter Niskin bottles to 300 ml glass bottles at stations K2 (Cast 1) and S1 (Cast 1) and brought the total to ~80. The bottles were filled by nitrogen gas before sampling. Three times of the bottle volumes of seawater sample were overflowed. The bottles filled by seawater sample were kept in water bathes controlled at 5°C until analysis in our land-based laboratory. The CFCs concentrations were determined as soon as possible after this cruise.

In order to confirm CFC concentrations of standard gases and their stabilities, CFC mixing ratios in air were also analyzed. Air samples were collected into a 200ml glass cylinder at outside of our laboratory.

3-2 Analysis

The analytical system is modified from the original design of Bullister and Weiss (1988). Constant volume of sample water (50ml) is taken into a sample loop. The sample is send into stripping chamber and dissolved CFCs are de-gassed by N₂ gas purging for 8 minutes. The gas sample is dried by magnesium perchlorate desiccant and concentrated on a trap column cooled

down to -50 °C. Stripping efficiencies of CFCs are confirmed by re-stripping of surface layer samples and more than 99.5 % of dissolved CFCs are extracted on the first purge. Following purging & trapping, the trap column is isolated and electrically heated to 140 °C. CFCs are desorbing by electrically heating the trap column, and lead into the pre-column. CFCs are roughly separated from other compounds in the pre-column and are sent to main analytical column. And then the pre-column is switched to another line and flushed by counter flow of pure nitrogen gas. CFCs sent into main column are separated further and detected by an electron capture detector (ECD). Nitrogen gases used in this system was filtered by gas purifier tube packed Molecular Sieve 13X (MS-13X).

Table 3-14-2 Analytical conditions of dissolved CFCs in seawater.

Temperature

Analytical Column:	95 °C
Detector (ECD):	240°C
Trap column:	-50 °C (at adsorbing) & 140 °C (at desorbing)

Mass flow rate of nitrogen gas (99.99995%)

Carrier gas:	15 ml/min
Detector make-up gas:	22 ml/min
Back flush gas:	20 ml/min
Sample purge gas:	130 ml/min

Standard gas (Japan Fine Products co. ltd.)

Base gas:	Nitrogen
CFC-11:	300 ppt (v/v)
CFC-12:	160 ppt (v/v)
CFC-113:	30 ppt (v/v)

(4) Preliminary result

The distributions of CFCs will be determined as soon as possible after this cruise. The standard gases used in this analysis will be calibrated with respect to SIO scale standard gases and then the data will be corrected.

(5) Data archive

All data will be submitted to JAMSTEC Data Management office (DMO) and under its control.

(6) Reference

Bullister, J.L and Weiss R.F. 1988. Determination of CCl₃F and CCl₂F₂ in seawater and air. Deep Sea Research, 35, 839-853.

3.14 Argo float

Toshio SUGA (JAMSTEC RIGC C, not on board): Principal Investigator

Shigeki HOSODA (JAMSTEC RIGC) Operation Leader

Kanako SATO (JAMSTEC RIGC: not on board)

Mizue HIRANO (JAMSTEC RIGC: not on board)

Ryuichiro INOUE (JAMSTEC RIGC: not on board)

Vincent Faure (JAMSTEC RIGC: not on board)

Shinya KOUKETSU (JAMSTEC RIGC: not on board)

Toru IDAI (MWJ)

Naoko MIYAMOTO (MWJ)

Tatsuya TANAKA (MWJ)

Hirokatsu UNO (MWJ)

(1) Objective

The recent studies have shown that the oceanic meso-scale eddies with spatial scales of tens to hundreds kilometers have the potential to affect the transport of material such as nutrient salts and to influence the biological activity of phytoplankton. To clarify relationship between meso-scale eddy and biological activity, we started the observational project from FY2010, named INBOX (Western North Pacific Integrated Physical-Biogeochemical Ocean Observation Experiment). On MR11-05 cruise in FY2011, we observed physical and biogeochemical process associated with meso-scale eddies around the mooring point S1 (30N, 145E) which locates at the south of Kuroshio Extension, to deploy 22 floats with dissolved oxygen sensors (DO-float) in the 150-km square area. On MR12-02 cruise, we decide to observe a warm core eddy itself in the mixed water region off Japan (41N, 147E) as the target because we focus on the meso-scale eddy activity, mixing process of water mass and its growth/decay processes. We also carry out observations of XCTD, shipboard CTD with water sampling, DO-floats and surface drifting buoys. The purpose of XCTD observation is to capture a vertical section of temperature and salinity structure in the warm core eddy to understand complex mixture of variable water mass. Launches of DO floats are done in the warm core eddy and around S1 to continuously measure detailed physical and biogeochemical processes to clarify the correlation with meso-scale phenomena. Also, shipboard CTD observation and water sampling data are done as the purpose of post-calibrations for CTD and DO sensors. Further, to capture the current velocity structure of the eddy, surface drifter buoys are launched at the center of warm core eddy. From these observations, we are able to depict detailed hydrographical and biogeochemical structure of the eddy. Then, these observations totally make it possible to evaluate the relationship between meso-scale eddies and the biological activity together with the data of mooring buoys and research vessels.

(2) Method

We launched 9 APEX floats manufactured by Teledyne Webb Research and one NEMO float by Optimare. Each float equips two sensors: one is a SBE41CP (APEX) or SBE41 (NEMO) CTD sensor manufactured by Sea-Bird Electronics Inc (SBE) to measure temperature, salinity, and pressure and the other is an optode4330 (8 APEX) or 3830 (one APEX and one

NEMO) DO sensor manufactured by Aanderaa Data Instruments (AADI) to measure dissolved oxygen. All CTD sensors and optode4330 had been calibrated in the laboratory before shipping. The specification of the floats is shown in Table 3.14-1 and 3.14-2. Shipboard CTD observation and water sampling are conducted at all points where floats are launched (point E01-E05; see Table 3.14-3). Thirty one XCTDs were launched to cross the warm core eddy (see Table 3.14-5). Three surface drifting buoys were launched at the center of warm core eddy (point E03; see Table 3.14-4). Using XCTD and shipboard CTD data, launch position of DO floats and surface drifting buoys are decided.

The float usually stays at a depth of 1000 dbar, but it dives to a depth of 2000 dbar once per five observations. During the ascent to the sea surface with increasing its buoyancy, the float measures sea water temperature, salinity, pressure and dissolved oxygen. To send the measured data to the Argo data center via the Iridium transmitting system in real time, the float stays at the sea surface in appropriate time, approximately 1 hour (the time out period). Finally the float returns to the parking depth with decreasing buoyancy. The cycle of each float is 1 day. The floats with the iridium telecommunication system can change their operation by commands which are sent by land operators.

Table 3.14-1: Specification of launched float (APEX with Iridium transmission system)

Float Type	APEX float manufactured by Teledyne Webb Research.
CTD sensor	SBE41cp manufactured by Sea-Bird Electronics Inc.
Dissolved oxygen	Optode 4330 or 3830 manufactured by Aanderaa Data Instruments
Cycle	1days
Iridium transmit timeout	90 minutes (The timeout period at the sea surface)
Target Parking Pressure	1000 dbar
Sampling levels	Pressure, temperature, and salinity: Each 2dbar from 2000dbar to surface (High resolution mode) Dissolved oxygen:75 layers
	(2000,1900,1800,1700,1600,1500,1450,1400,1350,1300,1250,1200,1150,1100,1050,1000,950,900,850,800,750,700,650,625,600,575,550,525,500,475,450,425,400,375,350,340,330,320,310,300,290,280,270,260,250,240,230,220,210,200,190,180,170,160,150,140,130,120,110,100,90,80,70,60,50,45,40,35,30,25,20,15, 10,6,and surface,dbar)

Table 3.14-2: Specification of launched float (NEMO with Iridium transmission system)

Float Type	NEMO float manufactured by Optimare.
CTD sensor	SBE41 manufactured by Sea-Bird Electronics Inc.
Dissolved oxygen	Optode 3830 manufactured by Aanderaa Data Instruments
Cycle	1days
Iridium transmit timeout	90 minutes (The timeout period at the sea surface)

Target Parking Pressure	1000 dbar
Sampling layers	Pressure, temperature, salinity, and dissolved oxygen:75 layers
	(2000,1900,1800,1700,1600,1500,1450,1400,1350,1300,1250,1200,1150,1100,1050,1000,950,900,850,800,750,700,650,625,600,575,550,525,500,475,450,425,400,375,350,340,330,320,310,300,290,280,270,260,250,240,230,220,210,200,190,180,170,160,150,140,130,120,110,100,90,80,70,60,50,45,40,35,30,25,20,15, 10,6,and surface,dbar)

Table 3.14-3: Float Launching area and date/time

Float S/N	ARGOS/IMEI ID	Date and Time of Reset (UTC)	Date and Time of launch (UTC)	Location of launch	Observation cycle	Remarks
6193	8816 9249 5973	2012/6/5 09 : 04	2012/6/5 11:41	40-56.48 [N] 147-28.24[E]	1 days	APEX (Optode4330)
202	3000 340 130 25610	2012/6/5 09 : 13	2012/6/5 11:42	40-56.45 [N] 147-28.23[E]	1 days	NEMO (Optode3830)
6188	8816 9249 5967	2012/6/6 05 : 18	2012/6/6 07:07	41-06.32 [N] 147-08.88[E]	1 days	APEX (Optode4330)
6187	8816 9249 5966	2012/6/6 05 : 19	2012/6/6 07:08	41-06.30 [N] 147-08.89[E]	1 days	APEX (Optode4330)
5588	8816 9377 0437	2012/6/6 02 : 09	2012/6/6 04:01	41-09.12 [N] 146-58.75[E]	1 days	APEX (Optode3830)
6192	8816 9249 5983	2012/6/6 02 : 09	2012/6/6 04 : 02	41-09.11 [N] 146-58.78[E]	1 days	APEX (Optode4330)
6189	8816 9249 5979	2012/6/5 22 : 28	2012/6/6 00 : 22	41-14.74 [N] 146-33.42[E]	1 days	APEX (Optode4330)
6190	8816 9249 5980	2012/6/5 22 : 27	2012/6/6 00 : 23	41-14.76[N] 146-33.46[E]	1 days	APEX (Optode4330)
6191	8816 9249 5981	2012/6/5 19 : 09	2012/6/5 05 : 50	41-18.30[N] 146-11.21[E]	1 days	APEX (Optode4330)
6194	88169249 5974	2012/7/2 13:40	2012/7/2 15:04	30-04.41[N] 144-50.19[E]	1 days	APEX (Optode4330)

Table 3.14-4: Surface drifting buoy Launching area and date/time

Buoy S/N	Date and Time of launch (UTC)	Location of launch
117372	2012/6/6 04:03	41-09.11 [N] 146-58.79 [E]
117373	2012/6/6 04:04	41-09.11 [N] 146-58.82 [E]
117374	2012/6/6 04:05	41-09.11 [N] 146-58.83 [E]

Table 3.14-5: XCTD launching area and date/time

St.	Date(UTC)	Time	Latitude	Longitude	Depth [m]	SST [deg-C]	SSS [PSU]	Probe S/N
X01	2012/06/04	15:37	41-29.9617N	145-30.0292E	7058	8.368	32.726	08101739
X02	2012/06/04	16:03	41-25.9579N	145-34.1109E	6976	10.725	33.076	08101736
X03	2012/06/04	16:29	41-21.9462N	145-38.1400E	6693	12.103	33.510	08101759
X04	2012/06/04	16:54	41-17.9591N	145-42.1653E	6453	12.145	33.797	08101737
X05	2012/06/04	17:20	41-13.9853N	145-46.1344E	6019	12.187	33.790	08101738
X06	2012/06/04	17:46	41-09.9859N	145-50.2538E	5738	12.255	33.925	08101740
X07	2012/06/04	18:16	41-05.9581N	145-54.3562E	5495	11.925	33.802	08101735
X08	2012/06/04	18:42	41-01.9802N	145-58.3203E	5487	12.106	33.821	09012693
X09	2012/06/04	19:10	40-57.9953N	146-02.2882E	5341	11.942	33.775	08101703
X10	2012/06/04	19:38	40-54.0225N	146-06.3230E	5302	12.896	33.933	08101760
X11	2012/06/04	20:07	40-50.0081N	146-10.3965E	5251	12.747	33.907	09012692
X12	2012/06/04	20:37	40-46.0113N	146-14.4487E	5208	11.794	33.648	08101762
X13	2012/06/04	21:05	40-42.0140N	146-18.3776E	5173	12.451	33.781	08101765
X14	2012/06/04	22:15	40-42.9750N	146-27.0396E	5202	12.400	33.805	08101763
X15	2012/06/04	22:44	40-41.9816N	146-33.6926E	5212	12.350	33.813	08101764
X16	2012/06/04	23:11	40-41.9866N	146-40.2919E	4965	12.355	33.752	08101766
X17	2012/06/04	23:42	40-41.8504N	146-47.2065E	4187	12.544	33.885	08101761
X18	2012/06/05	00:12	40-40.7841N	146-53.4984E	3516	12.806	33.864	08101770
X19	2012/06/05	00:43	40-42.2114N	147-00.1058E	5219	12.497	33.792	08101769
X20	2012/06/05	01:12	40-42.1796N	147-06.6958E	5312	12.059	33.634	09012694
X21	2012/06/05	01:42	40-41.9437N	147-13.2982E	5302	12.178	33.634	09012652
X22	2012/06/05	02:11	40-41.9882N	147-19.9154E	5294	12.166	33.649	08101768
X23	2012/06/05	02:39	40-41.9980N	147-26.4961E	5290	12.400	33.647	09012645
X24	2012/06/05	03:09	40-41.9452N	147-33.0838E	5287	12.743	33.722	09012645
X25	2012/06/05	03:37	40-41.9204N	147-39.6836E	5302	13.084	33.817	09012644
X26	2012/06/05	04:05	40-41.8579N	147-46.3045E	5330	12.979	33.767	09012647
X27	2012/06/05	04:34	40-41.8020N	147-52.8980E	5356	12.406	33.083	09012650
X28	2012/06/05	05:02	40-41.7836N	147-59.4922E	5397	11.813	33.473	09012651
X29	2012/06/05	05:30	40-41.7504N	148-06.1134E	5405	11.578	33.468	09012649
X30	2012/06/05	06:00	40-41.9004N	148-13.4504E	5469	10.413	33.005	09012646
X31	2012/06/05	06:25	40-41.9744N	148-19.2850E	5419	9.998	33.027	09012648

(3) Preliminary result

The Float S/N, ARGOS ID or IMEI Number, launched date/ time, launched position observation cycle of the float is summarized in Table. 3.14-3. The data will be measured automatically each observation cycle. Nine floats deployed at the center of an anti-cyclonic eddy and moved with surface current (Fig. 3.14-1).

Vertical section of temperature is shown in Fig. 3.14-2. Although the XCTD observation line turns at X13, whole warm core eddy is captured. In the surface layer warm water is seen around the center of eddy and cold water is outside of the eddy.

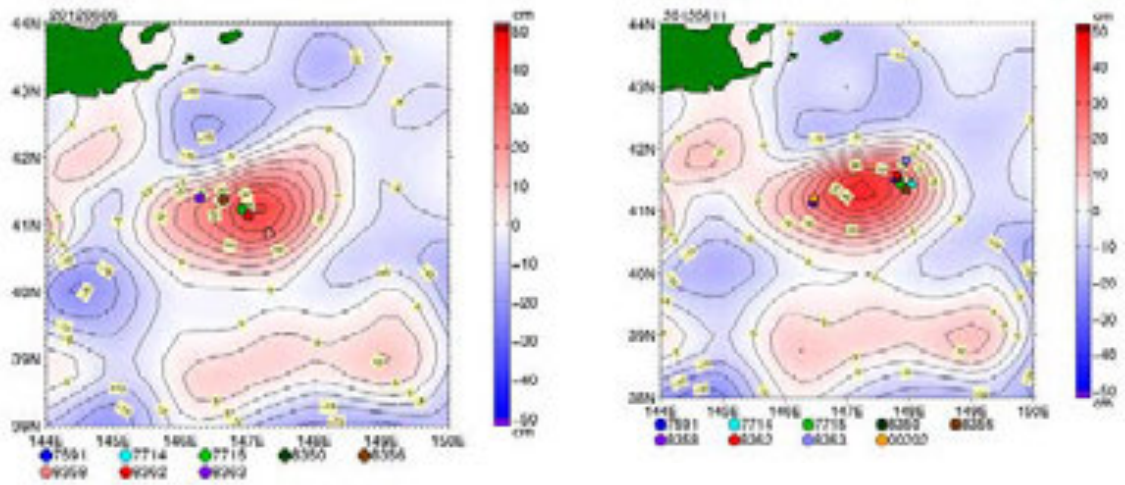


Figure 3.14-1. Float position on June 6, 2012 (left) and June 11, 2012 (right). Background color and contour is sea surface height anomaly map obtained from AVISO. Nine floats were deployed in the warm core eddy, drifting anti-cyclonically with current of meso-scale eddy. One NEMO float (S/N 202) is not seen in the left panel because of float's mission.

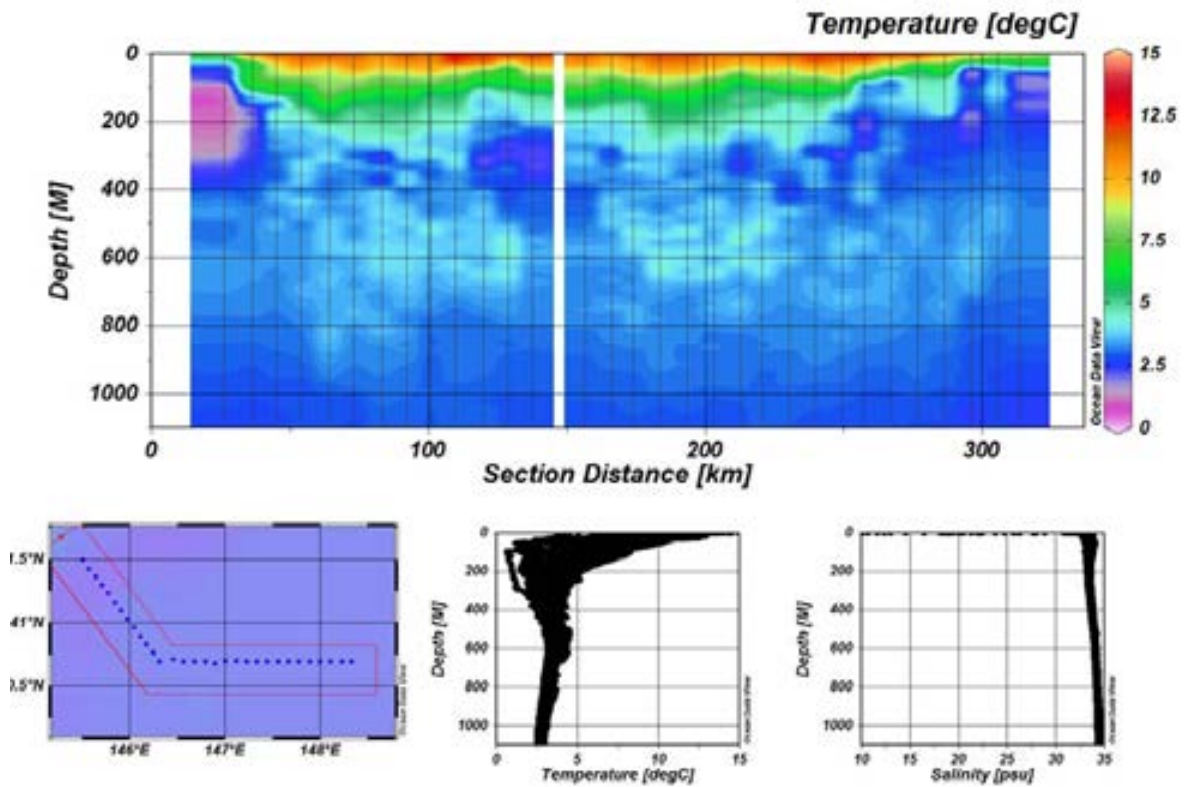


Figure 3.14-2. Vertical section of temperature from XCTD observation (upper panel). XCTD points (lower left), temperature profiles (lower middle) and salinity profiles (lower right) are also shown.

(4) Data archive

The data observed by floats will be released via Global Data Assembly Center (GDAC: <http://www.usgodae.org/argo/argo.html>, or <http://www.coriolis.eu.org/>) and Global Telecommunication System (GTS) by July, 2014.

3.15 Observational research on air-sea interaction in the Kuroshio-Oyashio Extension region : JKEO, NKEO, and KEO buoys

Yoshimi KAWAI	(JAMSTEC RIGC, PI/not on board)
Akira NAGANO	(JAMSTEC RIGC)
Kyoko TANIGUCHI	(JAMSTEC RIGC)
Meghan CRONIN	(NOAA PMEL, not on board)
Keith RONNHOLM	(University of Washington)
David ZIMMERMAN	(University of Washington)
Hirokatsu UNO	(MWJ)
Toru IDAI	(MWJ)
Tomoyuki TAMAMORI	(MWJ)
Masaki TAGUCHI	(MWJ)

(1) Objective

The objective of the moored-buoy observations is to investigate the air-sea interaction around the Kuroshio Extension, where a large amount of heat is released from the ocean. Surface water pCO₂ is also measured at these two buoys to examine the air-sea CO₂ flux. In addition, wave gauges are attached on the K-TRITON buoys. We specially deployed an additional K-TRITON buoy at the NKEO site for one-year intensive observation.

(2) Description of instruments deployed

Each of the K-TRITON and KEO buoys has an anemometer, a thermometer for atmospheric temperature, a hygrometer, a long-wave radiometer, a shortwave radiometer, pCO₂ sensors, a rain gauge, a barometer, current meters, CTs (water temperature and salinity) and CTDs (water temperature, salinity, and pressure). A weather transmitter (Vaisala WXT520), which can measure wind speed, wind direction, air temperature, humidity, rain rate, and air pressure, is installed on each buoy as spare. The K-TRITON buoys also have wave gauges. Photos of the K-TRITON buoy and the KEO buoy are in Fig. 3.15-1.

(3) Operations and preliminary result

I. Deployment and recovery of the K-TRITON buoys at the JKEO site

We deployed buoy at 37° 54.0663'N, 146° 36.5399'E (5380 m) on 19 June 2012 (JKEO6), and recovered a buoy (JKEO5) at 38° 05.059'N 146 26.8701'E (5398 m) which was deployed on 23 February 2011 in the MR11-02 cruise. The processes of the operations are summarized in Table 3.15-1. The mooring diagrams are illustrated in Figs. 3.15-2 and 3.15-3.

II. Deployment of the K-TRITON buoy at the NKEO site

We newly deployed a buoy at 33° 50.6977'N 144° 54.1396'E (5746 m) on 22 June 2012. The process of the operations is summarized in Table 3.15-2. The mooring diagram is illustrated in Fig. 3.15-4.

III. Recovery and deployment of the KEO buoys

We deployed a buoy (KEO10) on 4 July 2012 at 32° 24.939'N, 144° 29.848'E (5774 m), and recovered a buoy (KEO9) on 5 July 2012 at 32° 19.00'N, 144° 32.50'E (5710 m).

On the recovery, the enable command was transmitted to the acoustic releaser, but no respond was received. Attempts to communicate with the release were continued with different

deck units and ship positions. After attempts on an operational boat to reduce possible vessel noise did not improve the status, the recovery was targeted the top 700m only. The line tension was monitored during the recovery operation. The processes of the operations are summarized in Table 3.15-3. The mooring diagrams are illustrated in Figs. 3.15-5 and 3.15-6.

(4) Data archive

The meteorological and oceanic data obtained at the JKEO site, except for pCO₂ and wave data, are open to public (<http://www.jamstec.go.jp/iorgc/ocorp/ktsfg/data/jkeo/index.html>). The data of the KEO buoy are also open to public (<http://www.pmel.noaa.gov/keo/>).

Table 3.15-1. Process of the operations at the JKEO site

Date and time (LST)	
Deployment operation (JKEO6)	
12:44, 19 June	Started deployment operation
13:08	Placed the buoy on the sea surface
14:32	Started deploying the nylon line
15:58	Started deploying the polyolefin line
17:07	Cast anchor
17:40	Finished deployment operation
Recovery operation (JKEO5)	
08:00, 23 June	Started recovery operation
08:30	Attached the tag line to the buoy
09:30	Released the acoustic releaser
11:00	Secured the buoy on deck, and started recovering the wire
12:15	Started recovering the nylon line
13:32	Started recovering the polyolefin line
14:16	Recovered glass balls and acoustic releasers
14:30	Finished recovery operation

Table 3.15-2. Process of the operations at the NKEO site

Date and time (LST)	
Deployment operation (NKEO1)	
08:10, 22 June	Started deployment operation
08:25	Placed the buoy on the sea surface
09:32	Started deploying the nylon line
11:00	Started deploying the polyolefin line
12:30	Cast anchor
13:20	Finished deployment operation

Table 3.15-3. Process of the operation at the KEO site

Date and time (LST)	
Deployment operation (KEO10)	
08:00, 4 July	Started deployment operation
08:31	Placed the buoy on the sea surface
10:06	Started deploying the nylon line
12:54	Cast anchor
13:06	Started CTD observation
14:07	Finished CTD observation
14:21	Calibrated the sinker position
15:30	Confirmed buoy visually
16:22	Confirmed data reception and finished deployment operation
Recovery Operation (KEO9)	
05:55, 5 July	Started recovery operation preparation
06:23	Attached the tag line to the buoy
07:00	Transmitted the commands to the releaser (unsuccessful)
09:00	Transmitted the commands to the releaser from an operational boat (unsuccessful)
12:00	Decided to the partial recovery
13:00	Started operation on the deck
13:56	Started recovering the tag line
14:40	The buoy on deck
15:00	Started recovering the wire
16:40	Disconnected the wire and the nylon line
16:45	Operation ended

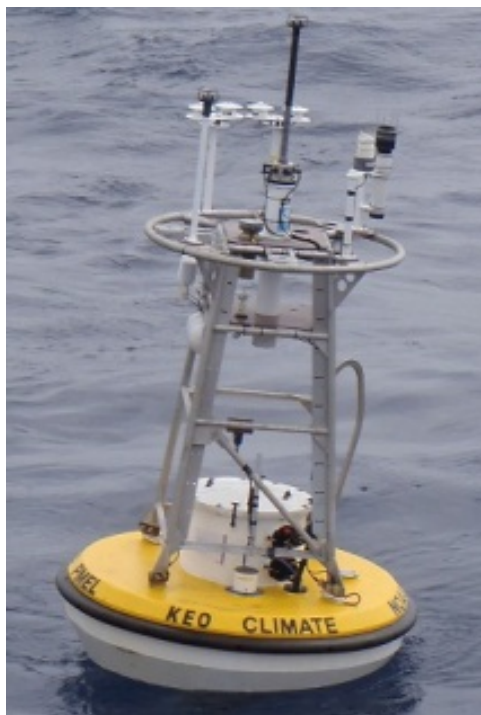


Figure 3.15-1: Deployed (upper left) and recovered (upper right) K-TRITON buoys and KEO buoy (bottom).

JAMSTEC K-TRITON

Mooring ID: JKEO6

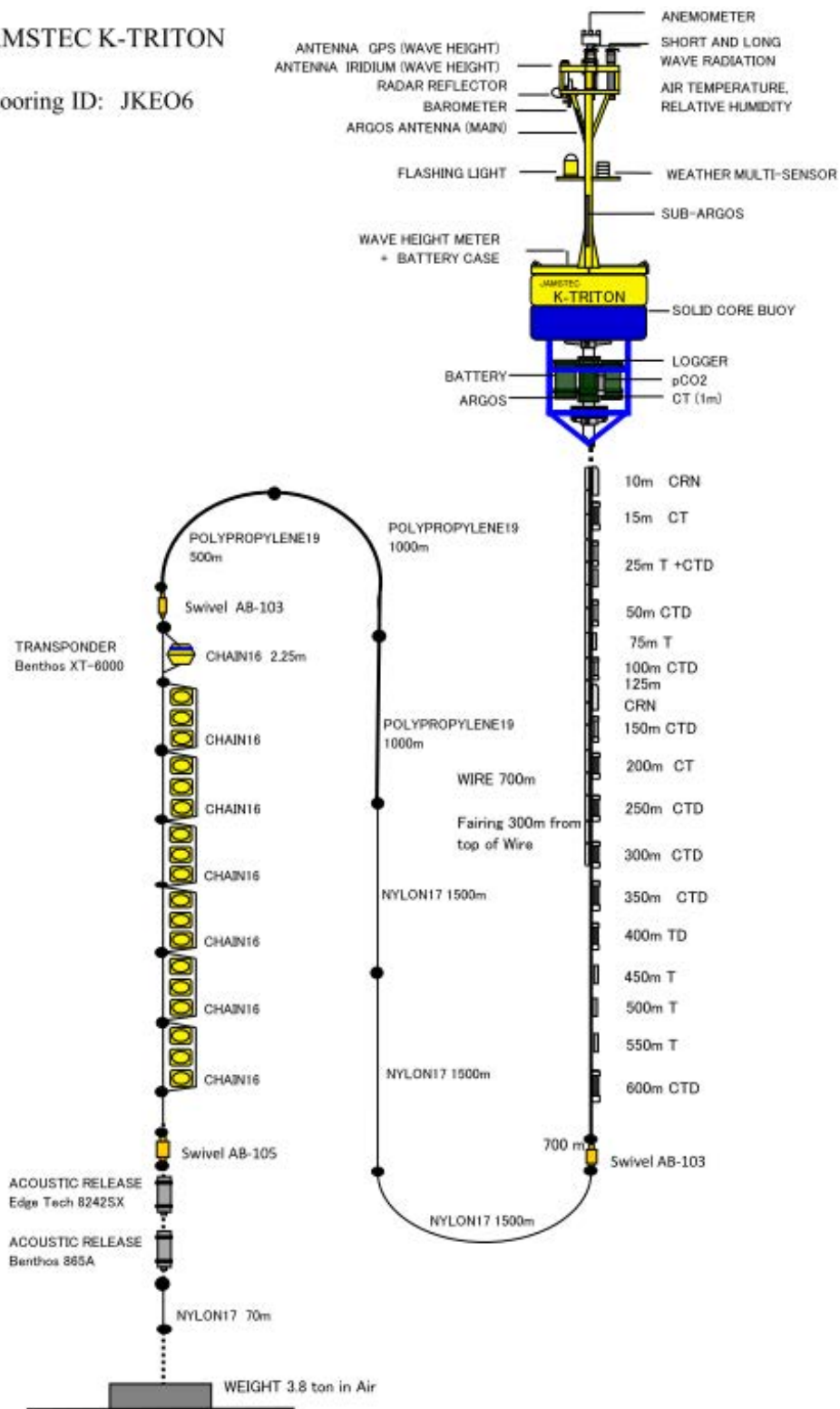


Figure 3.15-2: Mooring diagram of JKEO6 which was deployed in this cruise.

JAMSTEC K-TRITON

Mooring ID: NKEO1

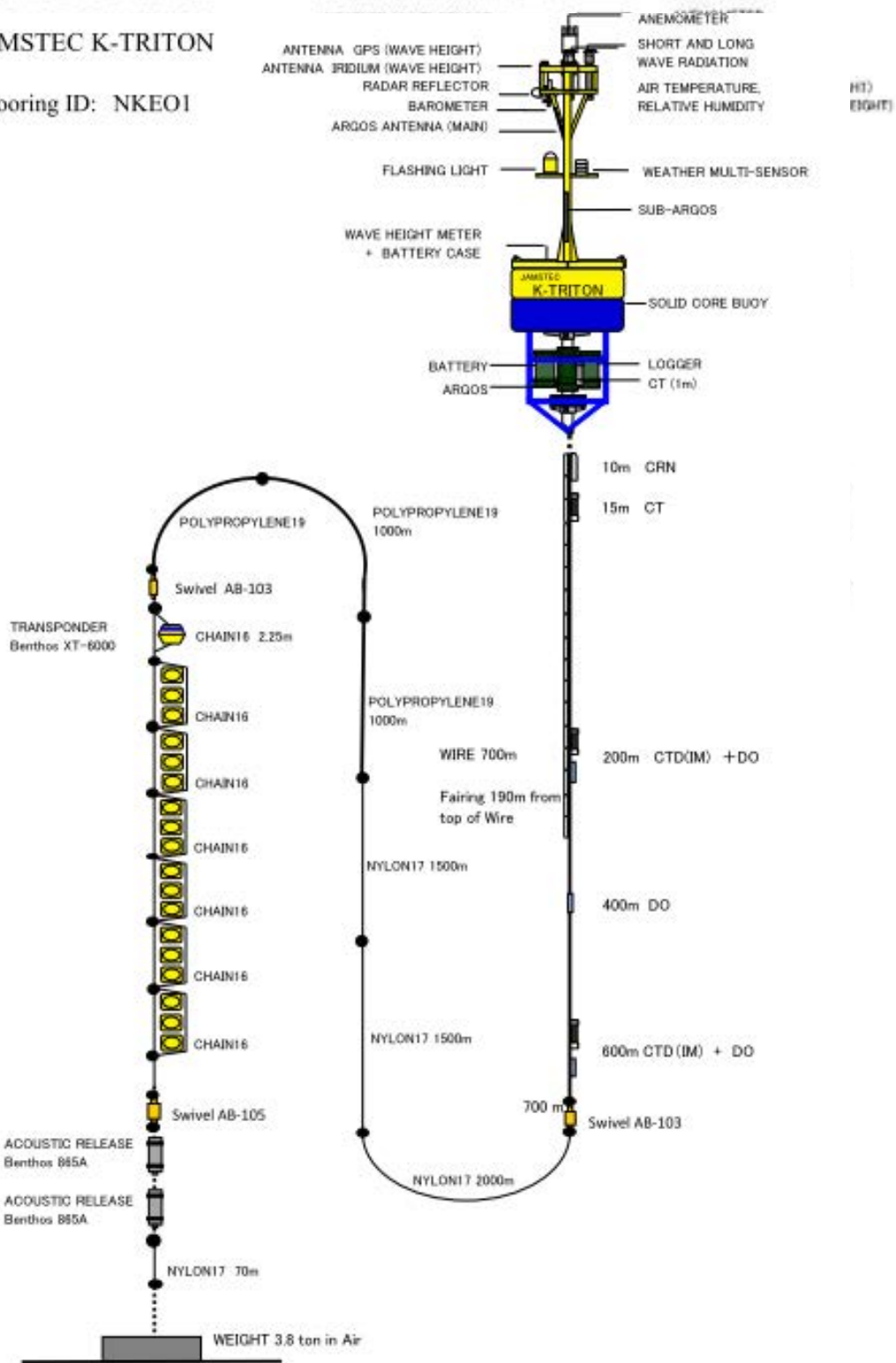


Figure 3.15-3: Mooring diagram of JKEO5 which was deployed in MR11-02 cruise and was recovered in this cruise.

Figure 3.15-4: Mooring diagram of NKEO1 which was deployed in this cruise.

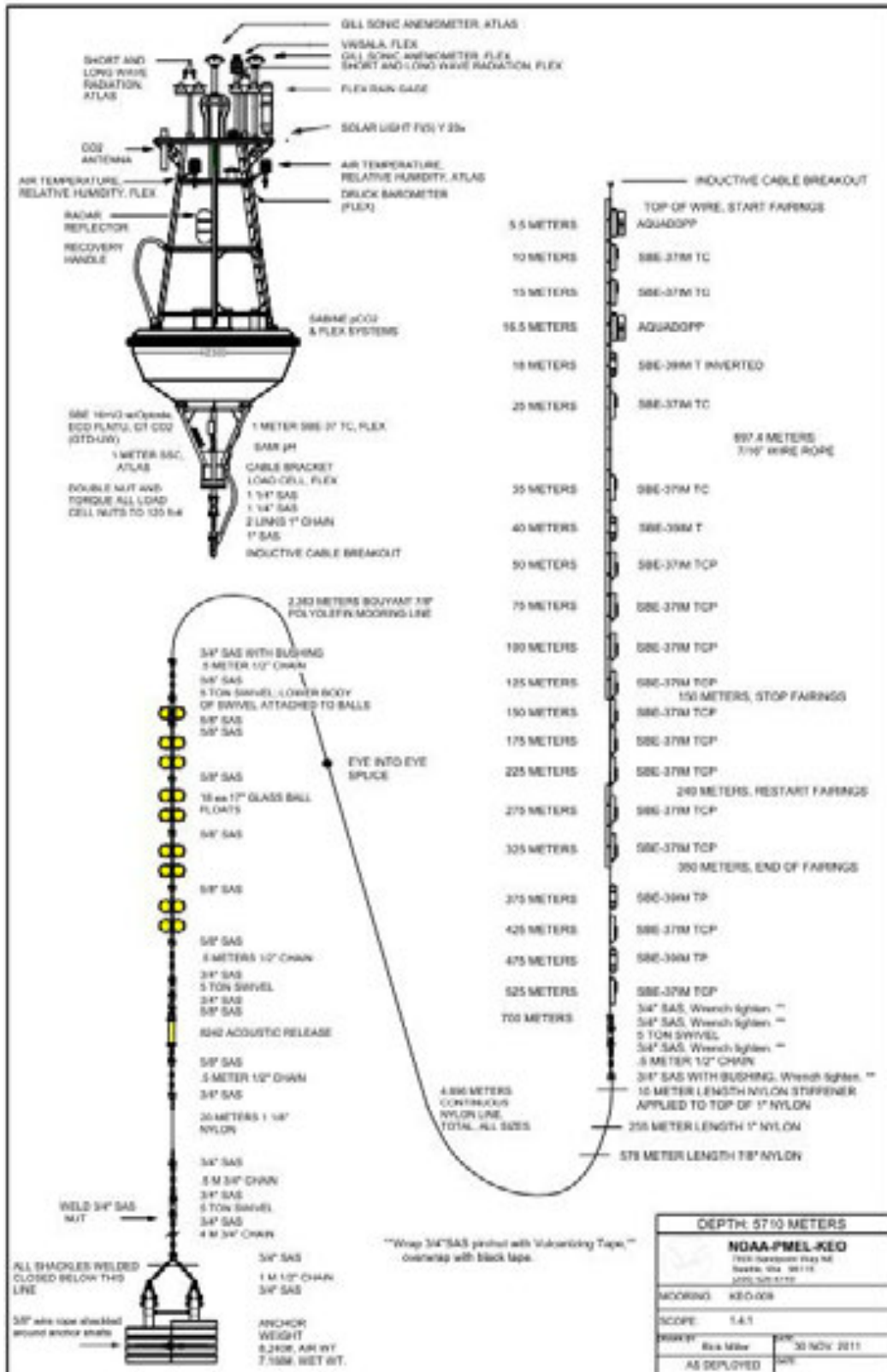


Figure 3.15-5: Mooring diagram of KEO10 which was deployed in this cruise.
 Figure 3.15-6: Mooring diagram of KEO9 which was recovered in this cruise.

3.16 Temporal changes in water properties of abyssal water in the western North Pacific

Hiroshi UCHIDA (JAMSTEC RIGC) (Principal Investigator)

Masahide WAKITA (JAMSTEC MIO)

Akihiko MURATA (JAMSTEC RIGC) (not on board)

(1) Objective

The objective of this study is to clarify temporal changes in water properties of abyssal water in the western North Pacific by means of moored CTD/O₂ observations. The time series data will be used to evaluate sampling error caused by short-term temperature fluctuation for the estimation of bottom water warming in recent decades derived from land-to-land repeat hydrographic data, and to monitor long-term fluctuation of water properties of the abyssal water.

(2) Materials and methods

CTDs used in the mooring observations were SBE-37 SM (Sea-Bird Electronics, Inc., Bellevue, Washington, USA). The SBE-37s had no pump, but included an optional pressure sensor with a range of 7000 m, developed by Paine Electronics, LLC, East Wenatchee, Washington, USA. Oxygen sensors used in the mooring observations were Oxygen Optode model 3830 (Aanderaa Data Instruments AS, Bergen, Norway) from October 2008 to June 2012, and Rinko I (JFE Advantech Co., Ltd., Kobe, Japan) from June 2012. The optode sensor was attached to a datalogger with an internal battery and memory in a titanium housing designed for mooring observation (Compact OPTODE; Alec Electronics Co., Ltd., Kobe, Japan) (Uchida et al., 2008b).

These CTD and oxygen sensors were attached to the acoustic releaser of the BGC mooring system (Table 3.17.1). Depth of the acoustic releasers was 34 m above the sea floor. The SBE-37 and Oxygen Optode data were obtained at a sampling interval of 30 minutes for the first mooring period (from October 2008 to January 2010) and of 1 hour for the other mooring periods.

For in situ calibration before mooring deployment or after mooring recovery, these sensors were attached to the CTD/water-sampling frame and the data sampled at 10 or 12 second intervals will be compared with the simultaneously obtained shipboard CTDO₂ data. For the oxygen sensors, laboratory calibration was also performed at JAMSTEC.

(3) Preliminary result

Time series of potential temperature and oxygen saturation obtained by the mooring observations were shown in Fig. 3.17.1. The CTD data for the first mooring period is not available due to leakage of the CTD sensor. Quality control is not yet performed for the data and will be performed by using a method similar to that of Uchida et al. (2008a, 2009). The data were low-pass-filtered by the running mean with a window of 25 hours. The oxygen data were drifted in time during the mooring period, probably due to a slow time-dependent, pressure-induced effect. Similar drifts were observed in the Wake Island passage Flux Experiment (Uchida et al., 2009).

(4) Data archive

The quality-controlled moored CTD/O₂ data will be submitted to JAMSTEC Data

Integration and Analyses Group (DIAG).

(5) References

- Uchida, H., T. Kawano and M. Fukasawa (2008a): In situ calibration of moored CTDs used for monitoring abyssal water. *J. Atmos. Oceanic Technol.*, 25, 1695-1702.
- Uchida, H., T. Kawano, I. Kaneko and M. Fukasawa (2008b): In situ calibration of optode-based oxygen sensors. *J. Atmos. Oceanic Technol.*, 25, 2271-2281.
- Uchida, H., H. Yamamoto, K. Ichikawa, M. Kawabe and M. Fukasawa (2009): Wake Island Passage Flux Experiment Data Book, JAMSTEC, Yokosuka, Japan, 93 pp.

Table 3.17.1. Summary of mooring observations of abyssal water.

Cruise	Mooring	K2	S1
MR08-05	Deployment	2008/10/28 01:13 (K-2 BGC) 47-00.36 N, 159-58.16 E, 5206 m SBE37 S/N 2757 (5172 m) OPTODE S/N 5 (5172 m)	None
MR10-01	Recovery	2010/01/24 11:20 The SBE 37 was leaked and no data is available for the SBE 37.	None
	In situ calibration	Station S01 cast 2 (SBE37 and OPTODE)	Station S01 cast 2 (SBE37 and OPTODE)
	Deployment	2010/02/15 05:05 (K2 BGC) 47-00.34 N, 159-58.24 E, 5206 m SBE37 S/N 2731 (5172 m) OPTODE S/N 5 (5172 m)	2010/02/03 03:06 (S1 BGC) 30-03.88 N, 144-57.96 E, 5926 m SBE37 S/N 2730 (5892 m) OPTODE S/N 3 (5892 m)
MR10-06	Recovery	2010/10/25 01:41	2010/11/06 01:44
	Deployment	2010/10/31 05:35 (K2 BGC) 47-00.37 N, 159-58.24 E, 5218 m SBE37 S/N 2731 (5184 m) OPTODE S/N 5 (5184 m)	2010/11/10 01:52 (S1 BGC) 30-03.92 N, 144-57.98 E, 5927 m SBE37 S/N 2730 (5893 m) OPTODE S/N 3 (5893 m)
MR11-05	Recovery	2011/06/30 02:04	2011/07/24 21:19
	Deployment	2011/07/04 00:24 (K2 BGC) 47-00.34 N, 159-58.42 E, 5218 m SBE37 S/N 2731 (5184 m) OPTODE S/N 5 (5184 m)	2011/07/28 23:04 (S1 (BGC) 30-03.93 N, 144-58.03 E, 5924 m SBE37 S/N 2730 (5890 m) OPTODE S/N 3 (5890 m)
MR12-02	Recovery	2012/06/09 19:38	2012/06/25 21:50
	In situ calibration	Station K02 cast 6 (SBE37, OPTODE and Rinko [S/N 51 and 52])	Station S01 cast 5 (SBE37 and OPTODE)
	Deployment	2012/06/14 23:57 (K2 BGC) 47-00.40 N, 159-58.22 E, 5222	2012/07/02 02:30 (S1 BGC) 30-03.93 N, 144-58.21 E, 5930

		m SBE37 S/N 2731 (5188 m) Rinko I S/N 51 (5188 m)	m SBE37 S/N 2730 (5896 m) Rinko I S/N 52 (5896 m)
--	--	---	---

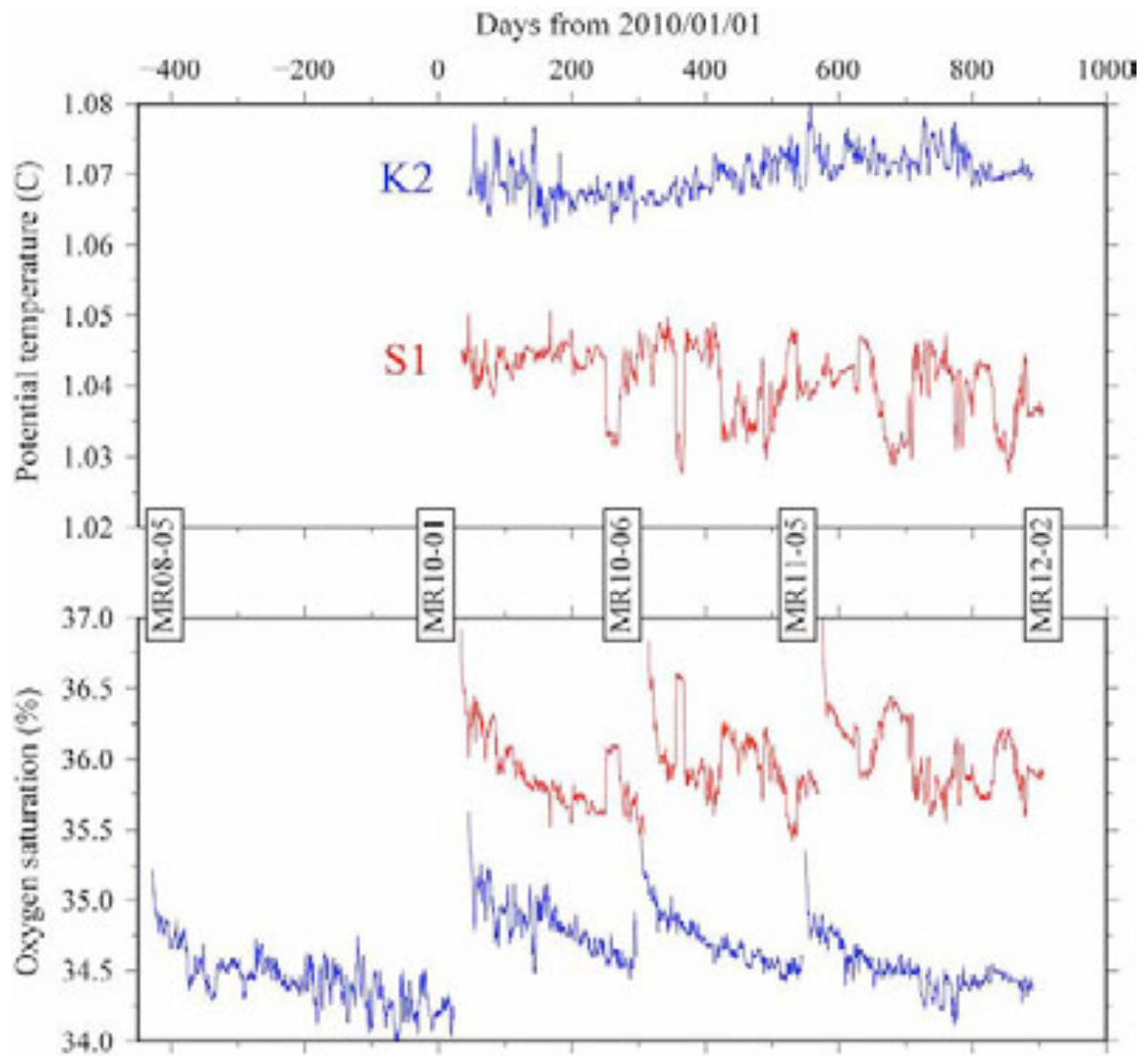


Fig. 3.17.1. Time series of potential temperature and oxygen saturation at 34 m above the sea floor for K2 (blue lines) and S1 (red lines) stations.

3.17. Development of a high-quality dissolved oxygen measurement by an optode-based oxygen sensor

Hiroshi UCHIDA (JAMSTEC RIGC) (Principal Investigator)

Yasuhiro NAGASAWA (JFE Advantech Co., Ltd.)

Masahide WAKITA (JAMSTEC MIO)

Akihiko MURATA (JAMSTEC RIGC) (not on board)

Yuichiro KUMAMOTO (JAMSTEC RIGC) (not on board)

(1) Objective

The objective of this study is to examine characteristics and performances of products and prototypes of optode-based oxygen sensors to develop a high-quality dissolved oxygen measurement by the optode-based oxygen sensors.

(2) Materials and methods

In this cruise, we examined 1) time-dependent, pressure-induced effect for 9 optode-based oxygen sensors (four Rinko I, one prototype of Rinko I [AROD-USB], and four Rinko III, JFE Advantech Co., Ltd., Kobe, Japan) at the CTD station K02 cast 6 by stopping the CTD package at 5000 dbar for 4 hours, 2) performance of prototype of portable optode-based oxygen sensors (five ARO-PR, JFE Advantech Co., Ltd.) by comparing with the dissolved oxygen data by the Winkler's method. Data from the CTD station E01-05, K02, KNT, JKO, and NKO, and the Continuous Sea Surface Water Monitoring System were used for the comparisons. A part of these oxygen sensors was calibrated before the cruise by using the oxygen standard gases based on the calibration equation by Uchida et al. (2010).

(3) Preliminary result

Changes of the oxygen sensor outputs at 5000 dbar were shown in Fig. 3.18.1. The time-dependent, pressure-induced effect on the sensing foil is large for the Rinko, as observed for a Clark electrode oxygen sensor (SBE 43; Sea-Bird Electronics, Inc., Bellevue, Washington). For the SBE 43, the correction method was developed (Edwards et al., 2010). Since characteristics of the effect are similar between the Rinko optode and the SBE 43 electrode, the Rinko can be corrected by means of the same method as that developed for the SBE 43 (Uchida et al., 2010). However, magnitude of this effect seems to be different from each sensor, and it is probably correlated with the degree of aging of the sensing foil. In other words, the correction coefficients for the time-dependent, pressure-induced effect for the Rinko might need to be changed in time according to the degree of aging.

For the Oxygen Optode 3830 (Aanderaa Data Instruments AS, Bergen, Norway), no time-dependent, pressure-induced effect (hysteresis) on the sensors was observed by repeated pressure cycling between 30 and 4050 dbar (Tengberg et al., 2006). However, the sensor output from the Optode 3830 was gradually changed in time as shown in Fig. 3.18.1. Results from the moored observation in the deep ocean suggest that the response of the sensing foil against pressure change is extremely slow for the Oxygen Optode 3830 (see Section 3.17.1 and Uchida et al., 2009).

(4) References

Edwards, B., D. Murphy, C. Janzen and N. Larson (2010): Calibration, response, and hysteresis in deep sea dissolved oxygen measurements. *J. Atmos. Oceanic Technol.*, 27, 920-931,

doi:10.1175/2009JTECHO693.1.

Tengberg, A., J. Hovdens, H.J. Andersson, O. Brocandel, R. Diaz, D. Hebert, T. Americh, C. Huber, A. Körtzinger, A. Khripounoff, F. Rey, C. Rönning, J. Schimanski, S. Sommer and A. Stangelmayer (2006): Evaluation of a lifetime-based optode to measure oxygen in aquatic systems. *Limnol. Oceanogr. Methods*, 4, 7-17.

Uchida, H., G.C. Johnson and K.E. McTaggart (2010): CTD oxygen sensor calibration procedures. The GO-SHIP Repeat Hydrography Manual: A Collection of Expert Reports and Guidelines, IOCCP Report no. 14, ICPO Publication series no. 134, Version 1.

Uchida, H., H. Yamamoto, K. Ichikawa, M. Kawabe and M. Fukasawa (2009): Wake Island Passage Flux Experiment Data Book, JAMSTEC, Yokosuka, Japan, 93 pp.

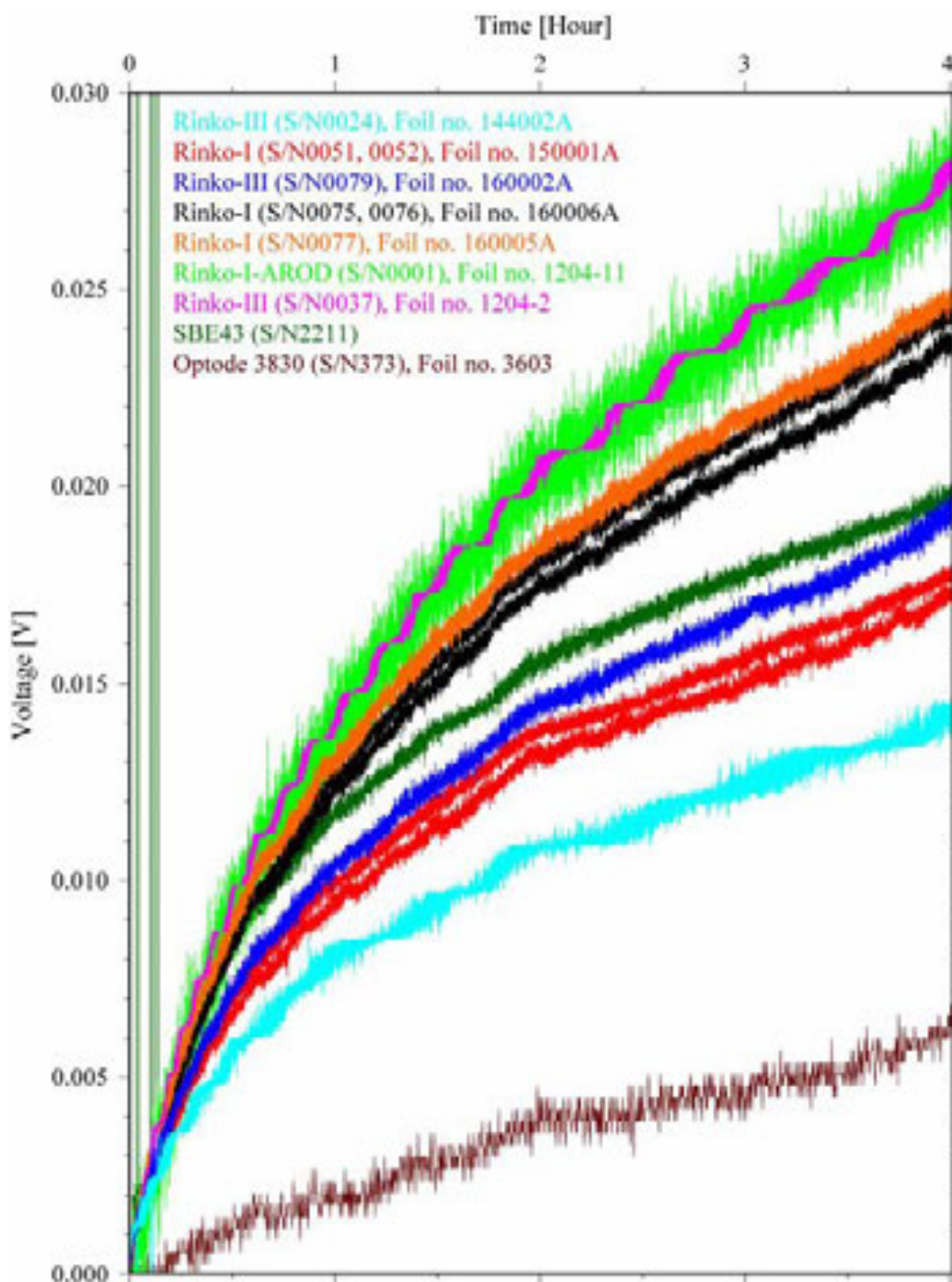


Fig. 3.18.1. Changes of raw sensor output from 11 oxygen sensors at 5000 dbar (maximum depth of the CTD station K02 cast 6). For the Rinko-I, scale of the sensor output (N-value) was changed by multiplying 0.000058 to match the signal from Rinko-III S/N0037 with that from Rinko-I AROD S/N0001. Data from the SBE 43 and Oxygen Optode 3830 are also shown.

3.18 Radiosonde observation for the validation of GOSAT and ship-borne sky radiometer products

Shuji KAWAKAMI	(JAXA EORC, PI/not on board)
Kazuma AOKI	(Toyama University, PI/not on board)
Hirofumi OHYAMA	(JAXA EORC)
Yoshiyuki NAKANO	(JAMSTEC MARITEC)
Tadahiro HAYASAKA	(Tohoku University, not on board)
Yoshimi KAWAI	(JAMSTEC RIGC, not on board)
Kyoko TANIGUCHI	(JAMSTEC RIGC)
Akira NAGANO	(JAMSTEC RIGC)
Katsuhisa MAENO	(GODI)
Harumi OHTA	(GODI)
Toshimitsu GOTO	(GODI)

(1) Objective

We performed the radiosonde observations to obtain vertical profiles of temperature and water vapor for the validation of GOSAT and ship-borne sky radiometer products, and to investigate atmospheric and cloud structure responding to the ocean temperature front of the Kuroshio Extension and Oyashio.

(2) Parameters

According to the manufacturer, the range and accuracy of parameters measured by the radiosonde sensor (RS92-SGPD) are as follows;

Parameter	Range	Accuracy
Pressure	3~1080 hPa	+/- 1 hPa (1080-100 hPa), +/- 0.6 hPa (100-3 hPa)
Temperature	-90~60 °C	+/- 0.5 °C
Humidity	0~100 %	5 %

(3) Method

Atmospheric soundings by radiosondes were carried out in the northwestern Pacific Ocean. In total, 38 soundings were carried out, but one sounding (RS035) failed due to a trouble of the receiver, and one sounding (RS011) stopped at only 3713 m height due to too strong wind (Table 3.19.1, Figure 3.19.1). The main system consisted of processor (Vaisala, DigiCORA Ver.3.64.1), GPS antenna (GA20), UHF antenna (RB21), ground check kit (GC25), balloon launcher (ASAP), and GPS radiosonde sensor (RS92-SGPD).

(4) Preliminary results

Precipitable water calculated from the sounding data is in Figures 3.19.2. It was not calculated for RS011 and RS035.

(5) Data archive

Raw data were recorded in ASCII format every 2 seconds during ascent. These raw data were submitted to the Data Management Group of JAMSTEC just after the cruise.

Table 3.19.1. Radiosonde launch log.

Sounding	Station	Launching	Maximum	Duration
----------	---------	-----------	---------	----------

No.	No.	Date (UT)	Time	Lon	Lat	Altitude	hPa	(sec)
RS001	-	2012/06/06	03:20:52	146.980	41.147	18612	70.3	3168
RS002	K2	2012/06/13	02:29:52	160.004	47.002	22731	37.2	6160
RS003	K2	2012/06/13	09:30:34	160.000	47.000	22549	38.4	5834
RS004	K2	2012/06/13	13:30:24	160.158	47.037	20768	50.4	4786
RS005	-	2012/06/16	02:30:06	159.721	44.485	22417	38.7	5620
RS006	-	2012/06/16	13:30:09	158.988	44.602	22460	38.5	5768
RS007	JKEO	2012/06/19	13:33:42	146.588	37.946	14237	148.6	3658
RS008	-	2012/06/19	15:00:03	146.509	37.742	17723	83.2	3680
RS009	-	2012/06/19	16:30:05	146.379	37.473	15620	118.1	3708
RS010	-	2012/06/19	18:00:19	146.256	37.196	11397	232.8	3690
RS011	-	2012/06/19	19:30:09	146.126	36.915	3713	647.0	3714
RS012	NKEO	2012/06/21	14:30:12	144.898	33.836	18435	74.2	4630
RS013	JKEO	2012/06/23	03:00:16	146.341	38.089	22939	35.9	5938
RS014	-	2012/06/24	14:30:29	141.623	35.785	22795	36.6	5636
RS015	S1	2012/06/26	03:00:03	144.981	30.060	23522	32.5	5594
RS016	S1	2012/06/27	14:29:59	145.018	29.996	23286	33.7	6144
RS017	S1	2012/06/29	03:00:12	144.999	29.986	24402	28.4	7004
RS018	S1	2012/06/30	14:30:41	144.998	29.958	22822	36.6	5420
RS019	S1	2012/07/02	03:00:13	144.962	30.064	25007	25.9	5992
RS020	KEO	2012/07/03	05:59:53	144.463	32.318	25678	23.4	7404
RS021	KEO	2012/07/03	14:30:22	144.721	32.444	23004	35.5	5780
RS022	KEO	2012/07/04	08:00:10	144.516	32.424	17198	91.1	4894
RS023	KEO	2012/07/04	10:00:47	144.588	32.415	18906	68.6	4900
RS024	KEO	2012/07/04	12:00:53	144.627	32.399	17793	82.6	4904
RS025	KEO	2012/07/04	14:00:28	144.605	32.384	19351	63.8	4902
RS026	KEO	2012/07/04	16:00:18	144.620	32.386	18216	76.8	4910
RS027	KEO	2012/07/04	18:00:36	144.612	32.404	19538	61.6	4906
RS028	KEO	2012/07/04	20:00:21	144.572	32.382	17616	84.8	4916
RS029	KEO	2012/07/05	03:00:19	144.533	32.317	24309	29.0	5534
RS030	-	2012/07/05	10:00:21	144.301	32.651	18524	72.9	4900
RS031	-	2012/07/05	12:00:08	144.046	32.998	19278	64.5	4896
RS032	-	2012/07/05	14:00:04	143.824	33.314	20119	56.2	4894
RS033	-	2012/07/05	16:00:06	143.602	33.623	20892	49.5	4888
RS034	-	2012/07/05	18:00:09	143.353	33.944	18220	76.2	4916
RS035	-	2012/07/05	20:00:00	-	-	-	-	-
RS036	F1	2012/07/07	08:00:16	141.475	36.485	24627	27.8	6572
RS037	-	2012/07/09	03:30:42	141.980	36.934	22979	36.1	5450
RS038	-	2012/07/09	14:30:10	142.335	38.451	23398	34.0	5458

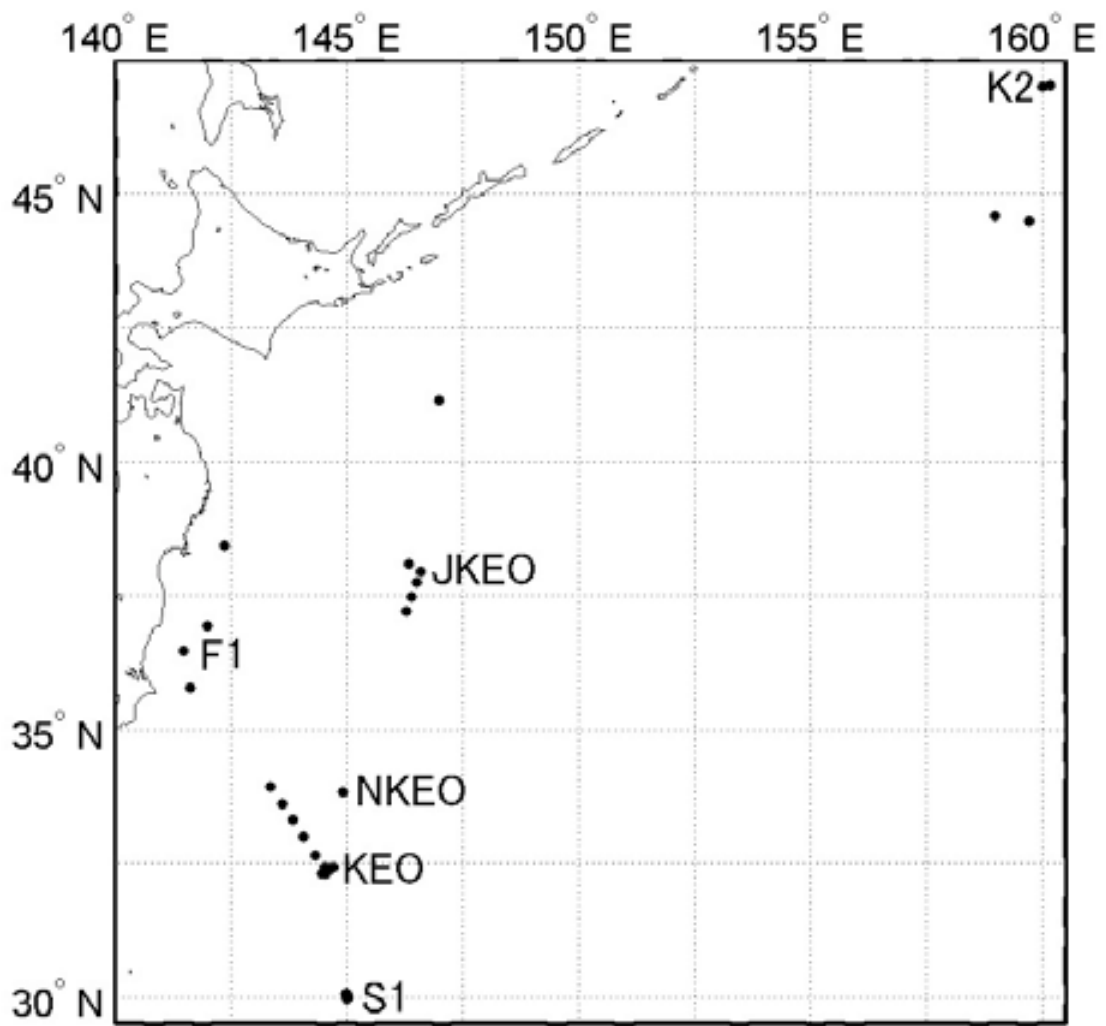


Figure 3.19.1. Positions of the GPS radiosonde (dots).

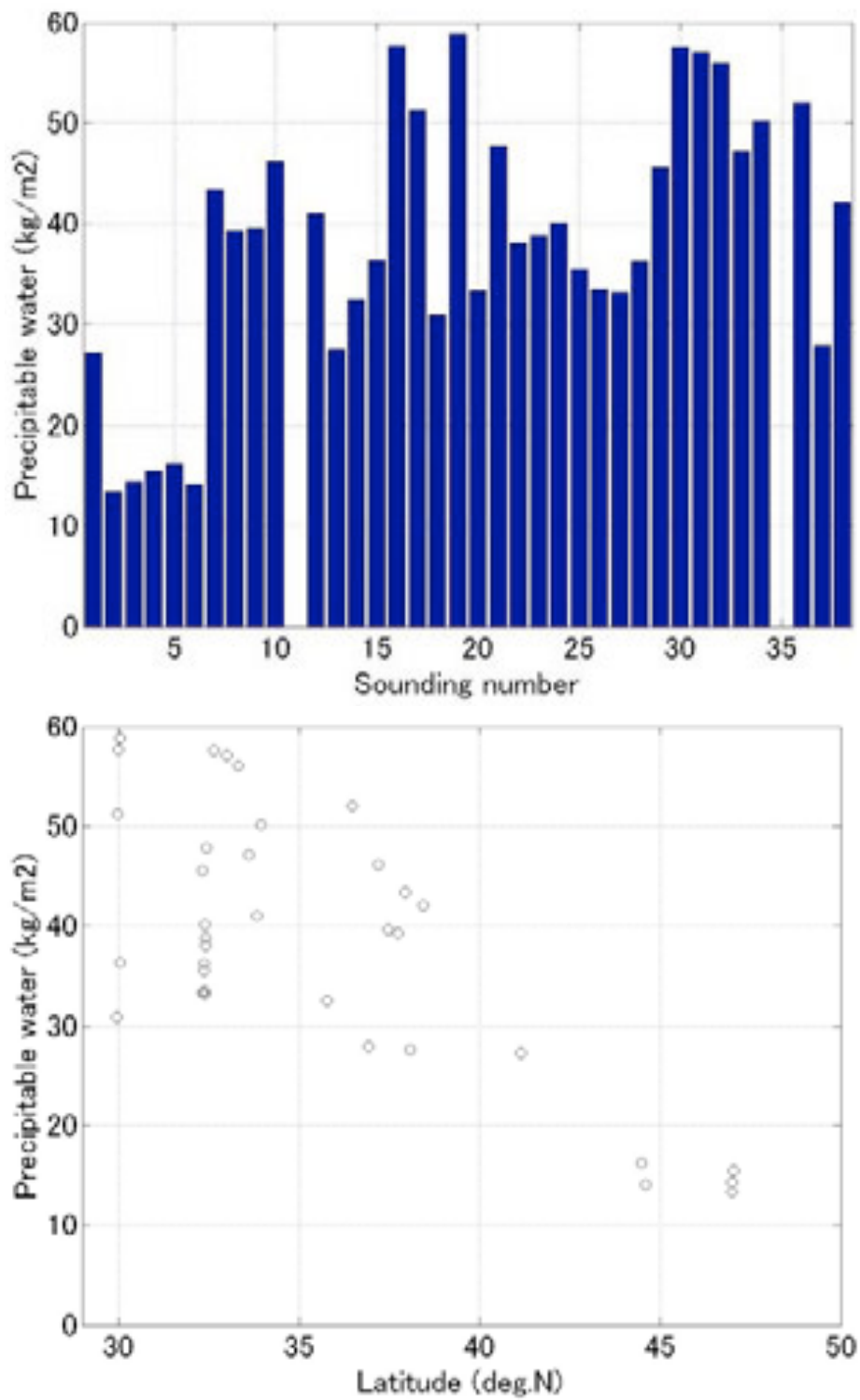


Figure 3.19.2. Precipitable water for (upper) each sounding number and (lower) latitude.

3.19 Sampling for artificial radionuclide from Fukushima

Makio C. HONDA (JAMSTEC)
Hajime KAWAKAMI (JAMSTEC)
Minoru KITAMURA (JAMSTE)

(1) Suspended particles

Suspended particles at two layers were collected at stations K2, S1, and F1. In situ pumping / filtration system (McLane WTS-6-1-142V) was used.

	K2	S1	F1
Sampling date and time (UTC)	14 June 2012 2:30 – 4:30	30 June 2012 6:00 – 8:00	6 July 2012 9:30 – 11:30
Sampling depth (m)	10, 100	10, 100	10, 100
Filter	Versapor (0.8 µm)	Versapor (0.8 µm)	Versapor (0.8 µm)
Sampling volume (m ³) (filtration volume)	10 m: 0.089 100 m: 0.235	10 m: 0.327 100 m: 0.729	10 m: 0.218 100 m: 0.428

Sample on filters were frozen immediately onboard.

(2) Zooplankton samples

At stations K2, S1 and F1, zooplankton for measurement of radionuclides such as Cs were collected by using IONESS system. Details (sampling date and time, sampling layers) are described on Table 3.9.1-1 in section 3.9.1 as “RI-IONESS”.

(3) Seawater

Along cruise track, surface seawater of 20 L were collected (Table 3.19.1). These samples were sent to Woods Hole Oceanographic Institution for measurements of radionuclides.

Table 3.19.1 Surface seawater sampling

SN	On board ID	Sample Category	Sampling Method	Preservation	Date Collected					Latitude			Longitude			Depth [m]	Area	Locality
					YYYY	MM	DD	hh:mm:ss	UTC/IST	Deg.	Min.	N/S	Deg.	Min.	E/W			
1	MR12-02(1) 0 W 1	Seawater	underway pump	room temp.	2012	06	15	20:03	UTC	45	28.3	N	159	52.77	E	0	Western North Pacific	
2	MR12-02(1) KNOT W 2	Seawater	underway pump	room temp.	2012	06	17	7:00	UTC	44	00	N	155	00	E	0	Western North Pacific	KNOT
3	MR12-02(1) JKEO W 3	Seawater	underway pump	room temp.	2012	06	19	9:46	UTC	37	55	N	146	25	E	0	Western North Pacific	JKEO
4	MR12-02(1) 0 W 4	Seawater	underway pump	room temp.	2012	06	19	23:00	UTC	36	21.9	N	145	52.1	E	0	Western North Pacific	
5	MR12-02(1) 0 W 5	Seawater	underway pump	room temp.	2012	06	20	8:50	UTC	35	09	N	145	17	E	0	Western North Pacific	
6	MR12-02(1) NKEO W 6	Seawater	underway pump	room temp.	2012	06	20	23:00	UTC	33	50	N	144	54	E	0	Western North Pacific	NKEO
7	MR12-02(1) 0 W 7	Seawater	underway pump	room temp.	2012	06	23	13:00	UTC	37	38.1	N	144	28.2	E	0	Western North Pacific	
8	MR12-02(1) 0 W 8	Seawater	underway pump	room temp.	2012	06	23	21:10	UTC	37	13.5	N	142	35.8	E	0	Western North Pacific	
9	MR12-02(1) ONA W 9	Seawater	underway pump	room temp.	2012	06	24	6:30	UTC	36	53.88	N	140	53.28	E	0	Western North Pacific	ONAHAMA
10	MR12-02(2) S1 W 1	Seawater	underway pump	room temp.	2012	06	28	1:05	UTC	30	00	N	145	00	E	0	Western North Pacific	S1
11	MR12-02(2) KE0 W 2	Seawater	underway pump	room temp.	2012	07	03	6:05	UTC	32	18.2	N	144	26.5	E	0	Western North Pacific	KEO
12	MR12-02(2) 0 W 3	Seawater	underway pump	room temp.	2012	07	05	23:10	UTC	34	53.9	N	142	40.4	E	0	Western North Pacific	
13	MR12-02(2) 0 W 4	Seawater	underway pump	room temp.	2012	07	06	5:00	UTC	35	59.9	N	141	52.1	E	0	Western North Pacific	
14	MR12-02(2) F1 W 5	Seawater	underway pump	room temp.	2012	07	07	4:47	UTC	36	29.553	N	141	20.710	E	0	Western North Pacific	F1

4. The concentrations of radionuclides in the western North Pacific

Tatsuo AONO (National Institute of Radiological Science: NIRS)

Makoto ONODA (NIRS)

Jian ZHENG (NIRS)

Tetsuya NAKAMURA (Nichiyu Giken Kogyo),

Hajime KAWAKAMI (JAMSTEC)

Makio HONDA (JAMSTEC)

Artificial radionuclides (^{134}Cs , ^{137}Cs and Pu isotopes etc.) in the ocean were mainly delivered by global fallout before the earthquake on March 11th, 2011. The Fukushima Daiichi nuclear power plant (FD1NPP) accident caused emission of radionuclides to atmosphere and ocean after the Great East Japan Earthquake, and the large volume of radioactively contaminated water containing high concentrations of radionuclides were flowed to ocean from the FD1NPP. In order to clarify the distributions and behavior of radioactive cesium in the western North Pacific, as the activity of cesium in seawater have not decreased by pre-accident level of 1.5 ~ 2 mBq/L, seawater samples were collected during this cruise. The collected seawater samples were listed up in Table 1. The seawater samples will be analyzed for Cs with AMP method and a gamma spectrometry using extended range coaxial Ge detector, and for Pu with an alpha spectrometry and ICP-MS in the laboratory. As it is known that some radionuclides, such as Cs, Pb and Pu etc. are transported with particles, the surface sediments were collected with a multiple core sampler in K2, S1 and F1. These samples were partitioned into each 0.5 – 2 cm scale and stored in refrigerator (Sampling detail is described in section 7. Multiple core). The activities of radionuclides (^{137}Cs , ^{134}Cs and Pu isotopes) will be measured with gamma spectrometry and ICP-MS.

Table 1 The list and information of seawater samples collected in the cruise of MR12-02.

Sample number	Date	Time	Location		Note
			Latitude	Longitude	
MR12-02-1	21012.6.4	10:13-10:20	41° 30.559' N	144° 03.510' E	
MR12-02-2	2012.6.4	23:18-23:25	40° 42.000' N	146° 42.945' E	
MR12-02-3	2012.6.5	11:15-11:22	40° 56.293' N	147° 28.438' E	
MR12-02-4	2012.6.5	23:17-23:24	41° 14.237' N	146° 32.935' E	
MR12-02-5	2012.6.6	11:08-11:15	40° 41.199' N	148° 01.236' E	
MR12-02-6	2012.6.7	08:45-08:51	41° 08.596' N	150° 20.882' E	
MR12-02-7	2012.6.7	08:33-08:40	42° 42.363' N	153° 33.921' E	
MR12-02-8	2012.6.9	23:47-23:55	44° 24.124' N	156° 15.509' E	
MR12-02-9	2012.6.9	08:29-08:33	45° 38.148' N	158° 00.795' E	
MR12-02-10	2012.6.10	22:00-23:00	46° 59.661' N	159° 59.862' E	K2 (800m) in a Niskin sampler
MR12-02-11	2012.6.10	22:00-23:00	46° 59.661' N	159° 59.862' E	K2 (600m) in a Niskin sampler
MR12-02-12	2012.6.10	22:00-23:00	46° 59.661' N	159° 59.862' E	K2 (400m) in a Niskin sampler
MR12-02-13	2012.6.10	22:00-23:00	46° 59.661' N	159° 59.862' E	K2 (200m) in a Niskin sampler
MR12-02-14	2012.6.10	22:00-23:00	46° 59.661' N	159° 59.862' E	K2 (150m) in a Niskin sampler
MR12-02-15	2012.6.10	22:00-23:00	46° 59.661' N	159° 59.862' E	K2 (100m) in a Niskin sampler
MR12-02-16	2012.6.10	22:00-23:00	46° 59.661' N	159° 59.862' E	K2 (50m) in a Niskin sampler
MR12-02-17	2012.6.10	22:00-23:00	46° 59.661' N	159° 59.862' E	K2 (25m) in a Niskin sampler
MR12-02-18	2012.6.10	22:00-23:00	46° 59.661' N	159° 59.862' E	K2 (0m) in the surface water
MR12-02-19	2012.6.11	22:00-23:00	47° 00.036' N	160° 00.272' E	K2
MR12-02-20	2012.6.11	22:00-23:00	47° 00.036' N	160° 00.272' E	K2
MR12-02-21	2012.6.11	22:00-23:00	47° 00.036' N	160° 00.272' E	K2
MR12-02-22	2012.6.11	22:00-23:00	47° 00.036' N	160° 00.272' E	K2
MR12-02-23	2012.6.11	22:00-23:00	47° 00.036' N	160° 00.272' E	K2 (Non Acid)
MR12-02-24	2012.6.15	23:23-23:29	44° 59.671' N	159° 51.031' E	
MR12-02-25	2012.6.16	20:00-21:00	44° 18.491' N	157° 09.941' E	
MR12-02-26	2012.6.17	09:30-10:30	43° 59.950' N	154° 59.761' E	KNOT (100m)
MR12-02-27	2012.6.17	09:30-10:30	43° 59.950' N	154° 59.761' E	KNOT (0m) in the surface water
MR12-02-28	2012.6.18	09:35-09:41	40° 17.430' N	149° 45.760' E	
MR12-02-29	2012.6.19	12:30-13:30	37° 56.272' N	146° 35.994' E	JKEO (100m)
MR12-02-30	2012.6.19	12:30-13:30	37° 56.272' N	146° 35.994' E	JKEO (0m) in the surface water
MR12-02-31	2012.6.20	06:09-06:15	35° 32.405' N	145° 29.463' E	
MR12-02-32	2012.6.21	02:00-03:00	33° 50.436' N	144° 54.122' E	NKEO (100m)
MR12-02-33	2012.6.21	02:00-03:00	33° 50.436' N	144° 54.122' E	NKEO (0m) in the surface water
MR12-02-34	2012.6.22	05:59-06:05	34° 15.854' N	144° 53.181' E	
MR12-02-35	2012.6.23	11:05-11:10	37° 44.371' N	144° 54.460' E	
MR12-02-36	2012.6.24	22:05-22:11	37° 10.626' N	142° 22.479' E	
MR12-02-37	2012.6.24	9:04	36° 45.68' N	141° 02.28' E	Onahama
MR12-02-38	2012.6.24	23:03	34° 08.00' N	142° 37.31' E	Onahama--S1
MR12-02-39	2012.6.25	8:58	32° 14.205' N	143° 43.519' E	Onahama--S1
MR12-02-40	2012.6.28	01:10-01:52	30° 01.142' N	144° 58.942' E	S1 (800m) Bottle: 21-22
MR12-02-41	2012.6.28	01:10-01:52	30° 01.142' N	144° 58.942' E	S1 (600m) Bottle: 23-24
MR12-02-42	2012.6.28	01:10-01:52	30° 01.142' N	144° 58.942' E	S1 (400m) Bottle: 25-26
MR12-02-43	2012.6.28	01:10-01:52	30° 01.142' N	144° 58.942' E	S1 (200m) Bottle: 27-28
MR12-02-44	2012.6.28	01:10-01:52	30° 01.142' N	144° 58.942' E	S1 (150m) Bottle: 29-30
MR12-02-45	2012.6.28	01:10-01:52	30° 01.142' N	144° 58.942' E	S1 (100m) Bottle: 31-32
MR12-02-46	2012.6.28	01:10-01:52	30° 01.142' N	144° 58.942' E	S1 (50m) Bottle: 33-34
MR12-02-47	2012.6.28	01:10-01:52	30° 01.142' N	144° 58.942' E	S1 (25m) Bottle: 35-36
MR12-02-48	2012.6.28	01:10-01:52	30° 01.142' N	144° 58.942' E	S1 (0m) Bucket
MR12-02-49	2012.7.2	20:50	31° 10.157' N	144° 41.264' E	S1--KEO
MR12-02-50	2012.7.3	4:07-08:00	32° 19.233' N	144° 28.023' E	KEO (100m) Bottle: 1-2
MR12-02-51	2012.7.3	4:07	32° 19.233' N	144° 28.023' E	KEO (0m) in Lab
MR12-02-52	2012.7.5	15:01	33° 32.028' N	143° 39.919' E	KEO--F1
MR12-02-53	2012.7.5	20:45	34° 27.939' N	142° 59.455' E	KEO--F1
MR12-02-54	2012.7.6	2:37	35° 32.150' N	142° 12.120' E	KEO--F1
MR12-02-55	2012.7.7	01:41-3:58	36° 29.553' N	141° 30.710' E	F1 (800m) Bottle: 1-2 poly-x2
MR12-02-56	2012.7.7	01:41-3:58	36° 29.553' N	141° 30.710' E	F1 (600m) Bottle: 3-4 poly-x2
MR12-02-57	2012.7.7	01:41-3:58	36° 29.553' N	141° 30.710' E	F1 (400m) Bottle: 5-6 poly-x2
MR12-02-58	2012.7.7	01:41-3:58	36° 29.553' N	141° 30.710' E	F1 (200m) Bottle: 7-8 poly-x2
MR12-02-59	2012.7.7	01:41-3:58	36° 29.553' N	141° 30.710' E	F1 (150m) Bottle: 9-10 poly-x2
MR12-02-60	2012.7.7	01:41-3:58	36° 29.553' N	141° 30.710' E	F1 (100m) Bottle: 11-12 poly-x2
MR12-02-61	2012.7.7	01:41-3:58	36° 29.553' N	141° 30.710' E	F1 (50m) Bottle: 13-14 poly-x2
MR12-02-62	2012.7.7	01:41-3:58	36° 29.553' N	141° 30.710' E	F1 (25m) Bottle: 15-16 poly-x2
MR12-02-63	2012.7.7	01:41-3:58	36° 29.553' N	141° 30.710' E	F1 (0m) in Lab
MR12-02-64	2012.7.7	01:41-3:58	36° 29.553' N	141° 30.710' E	F1 (0m) in Lab
MR12-02-65	2012.7.7	01:41-3:58	36° 29.553' N	141° 30.710' E	F1 (0m) in Lab
MR12-02-66	2012.7.7	01:41-3:58	36° 29.553' N	141° 30.710' E	F1 (0m) in Lab
MR12-02-67	2012.7.9	6:07	37° 18.024' N	142° 07.403' E	F1--HaChinohe
MR12-02-68	2012.7.9	12:32	38° 13.087' N	142° 19.538' E	F1--HaChinohe
MR12-02-69	2012.7.9	21:18	39° 23.733' N	142° 17.665' E	F1--HaChinohe

5. A study of the cycles of global warming related materials using their isotopomers in the western North Pacific

Chisato YOSHIKAWA (Tokyo Institute of Technology)

Osamu YOSHIDA (Rakuno Gakuen University)

Sebastian O. DANIELACHE (Tokyo Institute of Technology)

Yuki OKAZAKI (Rakuno Gakuen University)

Naohiro YOSHIDA (Tokyo Institute of Technology)

5.1 Aims of this study

This study aims to reduce the uncertainties of sinks and sources of global warming related materials by using “isotopomers”, a useful tracer of material cycles. In this study, to understand the cycles of global warming related materials in the western North Pacific, we conducted air and water sampling for isotopomer analysis of methane (CH₄), nitrous oxide (N₂O) and related substances (NO₃⁻, NH₄⁺ and Chlorophyll-a) and carbonyl sulfide (OCS). Moreover, to quantitatively understand the cycles and estimate the budgets, we develop a marine isotopomer model for global warming related materials and evaluate the model by using the results of isotopomer analysis.

5.2 Sampling elements

All sampling elements of Tokyo Institute of Technology and Rakuno Gakuen University group at hydrographic and air sampling stations are listed below.

Table 1. Parameters and hydrographic station numbers for samples collection.

Parameters	Hydrographic stations
1. Concentrations of dissolved CH ₄	K2-Deep, K2-Shallow2, KNOT, JKEO, NKEO, S1-Deep, S1-Shallow2, KEO
2. Concentrations of dissolved N ₂ O	K2-Deep, KNOT, JKEO, NKEO, S1-Deep, KEO
3. δ ¹⁵ N and δ ¹⁸ O values of NO ₃ ⁻	K2-Deep, K2-Shallow1, KNOT, JKEO, NKEO, S1-Deep, S1-Shallow1, KEO, F1
4. δ ¹⁵ N, SP and δ ¹⁸ O values of dissolved N ₂ O	K2-Deep, S1-Deep
5. δ ¹³ C values of dissolved CH ₄	K2-Shallow2, S1-Shallow2
6. δD values of dissolved CH ₄	K2-Shallow2, S1-Shallow2
7. δ ¹⁵ N of NH ₄	K2-Shallow1, S1-Shallow1
8. δ ¹⁵ N of Chlorophyll <i>a</i>	K2-Shallow1, S1-Shallow1
A. Air samples for concentration and isotopomer values of CH ₄ and N ₂ O	K2, S1
B. Air samples for concentration and δ ³⁴ S values of OCS	K2, S1

5.3 Methane

(1) Introduction

Atmospheric methane (CH₄) is a trace gas playing an important role in the global carbon cycle as a greenhouse gas. Its concentration has increased by about 1050 ppbv from 700 ppbv since the pre-industrial era (IPCC, 2007). In order to understand the current global methane cycle, it is necessary to quantify its sources and sinks. At present, there remain large uncertainties in the estimated methane fluxes from sources to sinks. The ocean's source strength for atmospheric methane should be examined in more detail, even though it might be a relatively minor source, previously reported to be 0.005 to 3% of the total input to the atmosphere (Cicerone and Oremland, 1988; Bange et al., 1994; Lelieveld et al., 1998).

To estimate an accurate amount of the methane exchange from the ocean to the atmosphere, it is necessary to explore widely and vertically. Distribution of dissolved methane in surface waters from diverse locations in the world ocean is often reported as a characteristic subsurface maximum representing a supersaturation of several folds (Yoshida et al., 2004). Although the origin of the subsurface methane maximum is not clear, some suggestions include advection and/or diffusion from local anoxic environment nearby sources in shelf sediments, and in situ production by methanogenic bacteria, presumably in association with suspended particulate materials (Karl and Tilbrook, 1994; Katz et al., 1999). These bacteria are thought to probable live in the anaerobic microenvironments supplied by organic particles or guts of zooplankton (Alldredge and Cohen, 1987).

So, this study investigates in detail profile of methane concentration and stable isotopic distribution in the water column in the western North Pacific to clarify methane dynamics and estimate the flux of methane to the atmosphere.

(2) Materials and methods

Seawater samples are taken by CTD-CAROUSEL system attached Niskin samplers of 12 L at 5-22 layers and surface layer taken by plastic bucket at 2-8 hydrographic stations as shown in Table 1. Each sample was carefully subsampled into 30, 125, 600 ml glass vials to avoid air contamination for analysis of methane concentration, carbon isotope ratio, and hydrogen isotope ratio respectively. The seawater samples were poisoned by 20 µl (30 and 125 ml vials) or 100 µl (600 ml vial) of mercuric chloride solution (Tilbrook and Karl, 1995; Watanabe et al., 1995), and were closed with rubber and aluminum caps. These were stored in a dark and cool place until we got to land, where we conducted gas chromatographic analysis of methane concentration and mass spectrometric analysis of carbon and hydrogen isotopic composition at the laboratory.

The analytical method briefly described here: The system consists of a purge and trap unit, a desiccant unit, rotary valves, a gas chromatograph equipped with a flame ionization detector for concentration of methane, GC/C/IRMS for carbon isotope ratio of methane, GC/TC/IRMS for hydrogen isotope ratio of methane, and data acquisition units. The entire volume of seawater in each glass vial was processed all at once to avoid contamination and loss of methane. Precisions obtained from replicate determinations of methane concentration, and carbon and hydrogen isotope ratios were estimated to be better than 5%, and 0.3‰ and 3‰, respectively, for the usual concentration of methane in seawater.

(3) Expected results

Subsurface maximum concentrations of methane ($>3 \text{ nmol kg}^{-1}$) were expected to be observed in the western North Pacific. A commonly-encountered distribution in the upper ocean with a methane peak within the pycnocline (e.g., Ward et al., 1987; Owens et al., 1991; Watanabe et al., 1995). Karl and Tilbrook (1994) suggested the suboxic conditions would further aid the development of microenvironments within particles in which methane could be produced. The organic particles are accumulated in the pycnocline, and methane is produced in the micro reducing environment by methanogenic bacteria. Moreover, in situ microbial methane production in the guts of zooplankton can be expected (e.g., Owens et al., 1991; de Angelis and Lee, 1994; Oudot et al., 2002; Sasakawa et al., 2008). Watanabe et al. (1995) pointed out that the diffusive flux of methane from subsurface maxima to air-sea interface is sufficient to account for its emission flux to the atmosphere. In the mixed layer above its boundary, the methane is formed and discharged to the atmosphere in part, in the below its boundary, methane diffused to the bottom vertically. By using concentration and isotopic composition of methane and hydrographic parameters for vertical water samples, it is possible to clarify its dynamics such as production and/or consumption in the water column.

(4) References

- Aldredge, A. A., Y. Cohen: Can microscale chemical patches persist in the sea? Microelectrode study of marine snow, fecal pellets, *Science*, 235, 689-691, 1987.
- Bange, H. W., U. H. Bartell, S. Rapsomanikis, and M. O. Andreae: Methane in the Baltic and the North seas and a reassessment of the marine emissions of methane, *Global Biogeochem. Cycles*, 8, 465-480, 1994.
- Cicerone, R. J., and R. S. Oremland: Biogeochemical aspects of atmospheric methane, *Global Biogeochem. Cycles*, 2, 299-327, 1988.
- de Angelis, M. A., and C. Lee: Methane production during zooplankton grazing on marine phytoplankton, *Limnol. Oceanogr.*, 39, 1298-1308, 1994.
- Karl, D. M., and B. D. Tilbrook: Production and transport of methane in oceanic particulate organic matter, *Nature*, 368, 732-734, 1994.
- Katz, M. E., D. K. Pak, G. R. Dickkens, and K. G. Miller (1999), The source and fate of massive carbon input during the latest Paleocene thermal maximum, *Science*, 286, 1531-1533.
- Lelieveld, J., P. J. Crutzen, and F. J. Dentener (1998), Changing concentration, lifetime and climate forcing of atmospheric methane, *Tellus Ser. B*, 50, 128-150.
- Oudot, C., P. Jean-Baptiste, E. Fourre, C. Mormiche, M. Guevel, J-F. TERNON, and P. L. Corre: Transatlantic equatorial distribution of nitrous oxide and methane, *Deep-Sea Res., Part I*, 49, 1175-1193, 2002.
- Owens, N. J. P., C. S. Law, R. F. C. Mantoura, P. H. Burkill, and C. A. Llewellyn: Methane flux to the atmosphere from the Arabian Sea, *Nature*, 354, 293-296, 1991.
- Sasakawa, M., U. Tsunogai, S. Kameyama, F. Nakagawa, Y. Nojiri, and A. Tsuda (2008), Carbon isotopic characterization for the origin of excess methane in subsurface seawater, *J. Geophys. Res.*, 113, C03012, doi: 10.1029/2007JC004217.
- Tilbrook, B. D., and D. M. Karl: Methane sources, distributions and sinks from California coastal waters to the oligotrophic North Pacific gyre, *Mar. Chem.*, 49, 51-64, 1995.

- Ward, B. B., K. A. Kilpatrick, P. C. Novelli, and M. I. Scranton: Methane oxidation and methane fluxes in the ocean surface layer and deep anoxic waters, *Nature*, 327, 226–229, 1987.
- Watanabe, S., N. Higashitani, N. Tsurushima, and S. Tsunogai: Methane in the western North Pacific, *J. Oceanogr.*, 51, 39–60, 1995.
- Yoshida, O., H. Y. Inoue, S. Watanabe, S. Noriki, M. Wakatsuchi: Methane in the western part of the Sea of Okhotsk in 1998-2000, *J. Geophys. Res.*, 109, C09S12, doi:10.1029/2003JC001910, 2004.

5.4 Nitrous oxide and related substances

(1) Introduction

Nitrous oxide is a very effective heat-trapping gas in the atmosphere because it absorbs outgoing radiant heat in infrared wavelengths that are not captured by the other major greenhouse gases, such as water vapor and CO₂. The annual input of N₂O into the atmosphere is estimated to be about 16 Tg N₂O-N yr⁻¹, and the oceans are believed to contribute more than 20% of the total annual input (IPCC, 2007).

N₂O is produced by the biological processes of nitrification and denitrification (Dore et al., 1998; Knowles et al., 1981; Rysgaard et al., 1993; Svensson, 1998; Ueda et al., 1993). Depending on the redox conditions, N₂O is produced from inorganic nitrogenous compounds (NH₄ or NO₃⁻), with subsequently different isotopic fractionation factors. The isotopic signatures of N₂O confer constraints on the relative source strength, and the reaction dynamics of N₂O biological production pathways are currently under investigation. Furthermore, isotopomers of N₂O contain more easily interpretable biogeochemical information as to their sources than obtained from conventional bulk ¹⁵N and ¹⁸O measurements (Yoshida and Toyoda, 2000).

The Pacific Ocean is the largest of the world's five oceans (followed by the Atlantic Ocean, Indian Ocean, Southern Ocean, and Arctic Ocean) (CIA, www) and expected to be important for the biogeochemical and biological cycles. Thus, the study of N₂O production and nutrients dynamics are very important to examine the origins of N₂O in seawater and to estimate the inventory of N₂O from this region with respect to the troposphere.

(2) Materials and methods

Seawater samples are taken by CTD-CAROUSEL system attached Niskin samplers of 12 L at 5-22 layers and surface layer taken by plastic bucket at 2-8 hydrographic stations as shown in Table 1. Air samples were also collected into pre-evacuated stainless-steel canisters (total 2 stations, Tables 1).

Seawater samples for N₂O concentration and isotope analyses were subsampled into two glass vials: one 30 ml vial for concentration analysis and two 125 ml glass vials for isotopomer ratio analysis. The subsamples were then sterilized with saturated HgCl₂ solution (about 20 μL per 100 ml seawater). The vials were sealed with butyl-rubber septa and aluminum caps, taking care to avoid bubble formation, and then brought back to the laboratory and stored at 4°C until analysis. Dissolved and air N₂O concentrations and its isotopic compositions will be measured by GC/ECD and/or GC/IRMS.

Water sample for isotope analysis of NO₃⁻ were collected into a 50-ml syringe equipped

with a DISMIC® filter (pore size: 0.45 µm). The sample was then filtrated into a polypropylene tube. The tube was stored at -20°C until analysis. Isotope ratios of NO₃⁻ will be measured by denitrifer method (Sigman et al., 2001) in which N₂O converted from nitrate is measured by using GC/IRMS.

Water sample for isotope analysis of isotope analysis of NH₄⁺ were collected into a 1L polypropylene bottle. The sample was then filtrated and divided into ten polypropylene bottles. The bottles were stored at -20°C until analysis. Isotope ratios of NH₄⁺ will be measured by diffusion method (Sigman et al., 1997) in which N₂O converted from nitrate is measured by using GC/IRMS.

Water sample for isotope analysis of isotope analysis of Chlorophyll pigments were collected into six-ten 1L light-blocking polypropylene bottles. The samples were filtered under reduced pressure and collected on two-three Whatman GF/F filfers. The filters were wrapped in aluminum foil and stored at -20°C until analysis. Chlorophyll pigments were extracted and split into each pigments by HPLS. Isotope ratios of Chlorophyll pigments were measured by using EA-IRMS.

(3) Expected results

In the surface layer, N₂O concentration of water affects the sea-air flux directly (Dore et al., 1998). However the pathway of N₂O production in surface layer is still unresolved. In the surface layer, N₂O is predominantly produced by nitrification, but also by nitrifer-denitrification and denitrification if oxygen concentration is low in the water mass or particles (Maribeb and Laura, 2004). Concentrations and isotopomer ratios of N₂O together with those values of substrates for N₂O (NO₃⁻, NH₄⁺ and Chlorophyll) will reveal the pathway of N₂O production in the surface layer (especially euphotic zone).

In deeper layer, N₂O could be produced through *in situ* biological processes of settling particles or fecal pellets derived from phytoplankton or zooplankton, and N₂O maximum was indeed observed at 600-800 m depth in the North Pacific (Popp et al., 2002; Toyoda et al., 2002). However, following problems have not been resolved: (i) what the major pathway for the N₂O maximum is and (ii) whether the N₂O is produced *in situ* or transported from other area.

Although there are reports on distribution of concentration and isotopomer ratio of N₂O in the North Pacific (Toyoda et al., 2002), this study will be the first one which reveals the distribution and production pathway of N₂O by using N₂O isotopomer ratios together with those ratios of substrates for N₂O.

(8) References

- Dore, J.E., Popp, B.N., Karl, D.M. and Sansone, F.J.: A large source of atmospheric nitrous oxide from subtropical North Pacific surface water, *Nature*, 396, 63-66, 1998.
- IPCC, Climate Change 2007: The Physical Science Basis. Contribution of Working Group I to the Fourth Assessment Report of the Intergovernmental Panel on Climate Change, edited by S. Solomon et al., pp. 996, Cambridge University Press, Cambridge, United Kingdom and New York, NY, USA, 2007.
- Knowles, R., Lean, D.R.S. and Chan, Y.K.: Nitrous oxide concentrations in lakes: variations with depth and time, *Limnology and Oceanography*, 26, 855-866, 1981.
- Maribeb, C.-G. and Laura, F.: N₂O cycling at the core of the oxygen minimum zone off

- northern Chile, *Marine Ecology Progress Series*, 280, 1-11, 2004.
- Popp, B. N., et al.: Nitrogen and oxygen isotopomeric constraints on the origins and sea-to-air flux of N₂O in the oligotrophic subtropical North Pacific gyre, *Global Biogeochem. Cycles*, 16(4), 1064, 2002. doi: 10.1029/2001GB001806.
- Rysgaard, S., Risgaard-Petersen, N., Nielsen, L.P. and Revsbech, N.P.: Nitrification and denitrification in lake and estuarine sediments measured by the ¹⁵N dilution technique and isotope pairing, *Applied and Environmental Microbiology*, 59, 2093-2098, 1993.
- Sigman, D.M., Altabet, M.A., Michener, R.H., McCorkle, D.C., Fry, B., Holmes, R.M., 1997. Natural abundance level measurement of the nitrogen isotopic composition of oceanic nitrate: an adaptation of the ammonia diffusion method. *Marine Chemistry* 57, 227–242.
- Sigman, D. M., K. L. Casciotti, M. Andreani, C. Barford, M. Galanter, and J. K. Boehlke: A bacterial method for the nitrogen isotopic analysis of nitrate in seawater and freshwater, *Anal. Chem.*, 73, 4145-4153, 2001.
- Svensson, J.M.: Emission of N₂O, nitrification and denitrification in a eutrophic lake sediment bioturbated by *Chironomus plumosus*, *Aquatic Microbial Ecology*, 14, 289-299, 1998.
- Toyoda, S., H. Iwai, K. Koba, and N. Yoshida: Isotopomeric analysis of N₂O dissolved in a river in the Tokyo metropolitan area, *Rapid Commun. Mass Spectrom.*, 23 (6), 809-821, 2009. doi: 10.1002/rcm.3945.
- Toyoda, S., N. Yoshida, T. Miwa, Y. Matsui, H. Yamagishi, U. Tsunogai, Y. Nojiri, and N. Tsurushima: Production mechanism and global budget of N₂O inferred from its isotopomers in the western North Pacific, *Geophys. Res. Lett.*, 29 (3), 7-1-7-4, 2002.
- Ueda, S., Ogura, N. and Yoshinari, T.: Accumulation of nitrous oxide in aerobic ground water, *Water Research*, 27, 1787-1792, 1993
www.cia.gov/cia/publications/factbook/geos/zn.html
- Yoshida, N. and Toyoda, S.: Constraining the atmospheric N₂O budget from intramolecular site preference in N₂O isotopomers, *Nature*, 405, 330-334, 2000.

5.5 Carbonyl sulfide

(1) Introduction

Carbonyl sulfide (COS) is the most abundant (about 500 pptv) and most stable (life time is about 16 years) gaseous sulfur species in the background (remote) atmosphere. It is oxidized in the stratosphere to form sulfate aerosols which may influence the radiation budget at the Earth's surface and the stratospheric ozone cycle (Crutzen, 1976). It is emitted from natural sources such as microbial metabolism of sulfur in the ocean and terrestrial environment and anthropogenic sources such as sulfur industry and combustion of fossil fuel and biomass (Chin and Davis, 1993; Watts, 2000; Kettle et al., 2002). Its major sinks are considered to be soil and plant uptake, reaction with OH and O radicals, and photolysis in the stratosphere. However, estimated fluxes of the sources have large uncertainty because they are based on limited observations of COS concentration, and COS budget has not been closed yet. Therefore, isotopic study of COS may provide constraints for relative source strength as well as information on reaction pathways in its formation and destruction processes. Sulfur isotope ratio of COS in the atmosphere or source gasses has not been reported so far, although there is a study on sulfur isotope fractionation in the stratospheric COS which suffers from low analytical precision by balloon-born infrared spectroscopy (Leung et al., 2002).

In this study, we are developing a high-sensitive, high-precision, and rapid analytical system for concentration and sulfur isotope ratios of COS that is applicable to trace COS in environment. Our purpose of this cruise is to collect maritime air samples which contain background COS or COS emitted from nearby oceanic sources for the isotopic analysis.

(2) Materials and methods

Air samples were collected at 2 stations listed in Tables 1. At each station, ambient air near the bridge (about 10 m above sea level) was pressurized into two stainless-steel canisters (6L) at 5 atm (absolute pressure) using a sampling device which consists of a diaphragm pump, a back-pressure regulating valve, a desiccant tube packed with $\text{Mg}(\text{ClO}_4)_2$, and stainless tubes and connectors. Inner surface of the SS canisters are deactivated to prevent COS adsorption or decomposition during sample storage.

(3) Expected results

First, concentration analysis will be performed to determine the sample size and detail procedure for isotopic measurement. Then, stability of COS in the glass bottle and canister will be checked by periodic analysis of concentration using an aliquot of the same sample. Finally, sulfur isotope ratio will be measured by the newly developed analytical system. If succeeded, sulfur isotope ratio of atmospheric COS will be revealed for the first time.

(4) References

- Crutzen, P. J.: The possible importance of OCS for the sulfate layer of the stratosphere, *Geophys. Res. Lett.*, 3, 73-76, 1976.
- Chin, M., and D. D. Davis: Global sources and sinks of OCS and CS₂ and their distributions, *Global Biogeochem. Cycles*, 7 (2), 321-337, 1993.
- Kettle, A. J., U. Kuhn, M. von Hobe, J. Kesselmeier, and M. O. Andreae: Global budget of atmospheric carbonyl sulfide: Temporal and spatial variations of the dominant sources and sinks, *J. Geophys. Res.*, 107 (D22), 4658, 2002.
- Leung, F.-Y., A. J. Colussi, and M. R. Hoffmann: Isotopic fractionation of carbonyl sulfide in the atmosphere: Implications for the sources of background stratospheric sulfate aerosol, *Geophys. Res. Lett.*, 29 (10), 1474, 2002.
- Watts, S. F.: The mass budgets of carbonyl sulfide, dimethyl sulfide, carbon disulfide and hydrogen sulfide, *Atmos. Environ.*, 34, 761-779, 2000.

6. Validation of GOSAT products over sea using a ship-borne compact system for measuring atmospheric trace gas column densities

Shuji KAWAKAMI (JAXA EORC)
Hirofumi OHYAMA (JAXA SAPC)
Yoshiyuki NAKANO (JAMSTEC)

(1) Objective

Greenhouse gases Observing SATellite (GOSAT) was launched on 23 January 2009 in order to monitor the global distributions of atmospheric greenhouse gas concentrations: column-averaged dry-air mole fractions of carbon dioxide (CO₂) and methane (CH₄). A network of ground-based high-resolution Fourier transform spectrometers provides essential validation data for GOSAT. Vertical CO₂ profiles obtained during ascents and descents of commercial airliners equipped with the in-situ CO₂ measuring instrument are also used for the GOSAT validation. Because such validation data are obtained mainly over land, there are very few data available for the validation of the over-sea GOSAT products. The objectives of our research are to acquire the validation data over sea using an automated compact instrument and to compare the acquired data with the over-sea GOSAT products.

(2) Description of instruments deployed

The column-averaged dry-air mole fractions of CO₂ and CH₄ can be estimated from absorption by atmospheric CO₂ and CH₄ that is observed in a solar spectrum. An optical spectrum analyzer (OSA, Yokogawa M&I co., AQ6370) was used for measuring the solar absorption spectra in the near-infrared spectral region. A solar tracker (PREDE co., ltd.) and a small telescope (Figure 1) collected the sunlight into the optical fiber that was connected to the OSA. The solar tracker searches the sun every one minute until the sunlight with a defined intensity is detected. The measurements of the solar spectra were performed during solar zenith angles of <80°. In addition, radiosonde observations, which were collocated with the GOSAT overpass time (both daytime and nighttime), were made to obtain vertical profiles of atmospheric temperature and humidity.

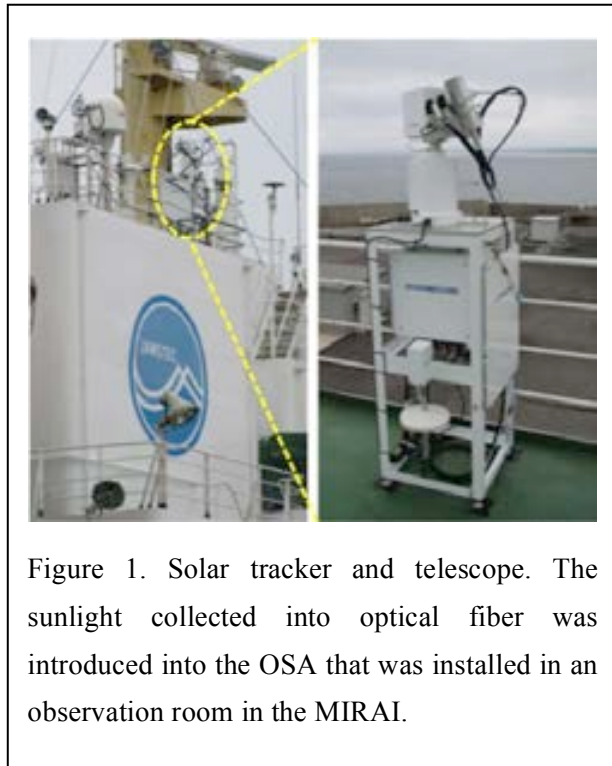


Figure 1. Solar tracker and telescope. The sunlight collected into optical fiber was introduced into the OSA that was installed in an observation room in the MIRAI.

(3) Analysis method

The CO₂ absorption spectrum at the 1.6 μm band measured with the OSA is shown in Figure 2. The absorption spectrum can be simulated based on radiative transfer theory using assumed atmospheric profiles of pressure, temperature, and trace gas concentrations. The

column abundance of CO₂ (CH₄) was retrieved by adjusting the assumed CO₂ (CH₄) profile to minimize the differences between the measured and simulated spectra. Figure 3 shows an example of spectral fit performed for the spectral region with the CO₂ absorption lines. The column-averaged dry-air mole fraction of CO₂ (CH₄) was obtained by taking the ratio of the CO₂ (CH₄) column to the dry-air column.

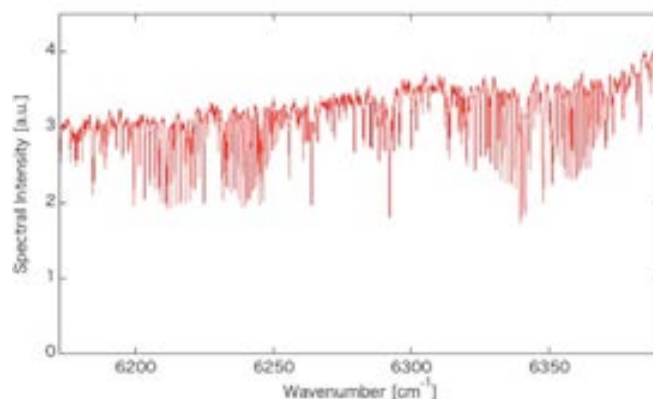


Figure 2. 1.6 μm CO₂ absorption spectrum measured with the OSA.

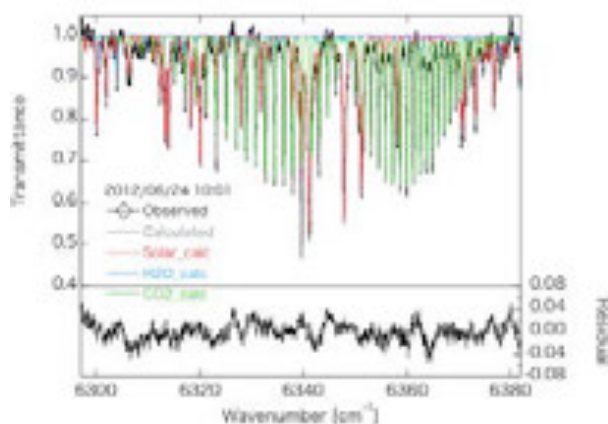


Figure 3. Spectral fit performed for the 6297–6382 cm⁻¹ region using an OSA spectrum. Open diamonds denote the measured spectrum, and the solid line denotes the spectrum calculated from the retrieval result. The residual between the measured and calculated spectra is also shown.

(4) Data archive

The column-averaged dry-air mole fractions of CO₂ and CH₄ retrieved from the OSA spectra will be submitted to JAMSTEC Data Integration and Analyses Group (DIAG).

7. Multiple Core (MC)

Makio HONDA (JAMSTEC RIGC)

Hajime KAWAKAMI (JAMSTEC MIO)

Tatsuo AONO (NIRS)

Makoto ONODA (NIRS)

Steven MANGANINI (WHOI)

Katsunori KIMOTO (JAMSTEC RIGC): Sampling leader

Miyako SATO (JAMSTEC RIGC)

Yuriko NAKAMURA (JAMSTEC RIGC)

Sayaka KAWAMURA (Marine Works Japan Co. Ltd): Leg.1 Operation Leader

Yasushi HASHIMOTO (Marine Works Japan Co. Ltd) : Leg.2 Operation Leader

(1) Objective

After the hit of East Japan Huge Earthquake occurred in 11, March, 2011, the artificial radioactive leakage from the Fukushima Daiichi Nuclear plants occurred. Huge amount of artificial radioactive nuclides that is emitting from the atomic reactors flew into the Pacific Ocean, and polluted ambient environments. Thus observation of diffusion of radionuclides is quite important to evaluate affection to natural environments, especially marine biosphere. In this cruise, we collected bottom sediments from our time-series stations: K2, S1 and F1 to observe the concentrations of radionuclides on the seafloor and evaluate the pollution of the bottom water environments about a year and half after that tragedy.

(2) Instruments and methods

A Multiple Corer (MC) was used in this cruise, consists of main body (620kg weight) and 4 pipes, which are 3 acryl pipes and 1 polycarbonate pipe. Core barrel is 60cm length and 74mm inside diameter.

When we started lowering the MC, a speed of wire out is set to be 0.5m/s, and then gradually increased to be 1.0m/s. The MC was stopped at a depth about 30~50m above the sea floor for 3~5minutes to stabilize of the sampler. After the sampler was stabilized, the wire was wound off at 0.3m/s, and we watched carefully a tension meter. When the MC touches the bottom, wire tension leniently decreases by the loss of the sampler weight. After confirmation that the MC touch seafloor, the wire out was stopped then another 4~7m rewinding. After waited 20~40 seconds, the wire was wound in at 0.3m/s until the tension gauge indicates that the corer left the bottom. After left the bottom, which wire was wound in at the maximum speed. The MC came back ship deck, the core barrel was detached main body.

Onboard, core was sliced each 5 mm thickness for the first 20 mm, 10 mm

(3) Results

Results of MC recoveries were summarized in Table 7.1. At stations K2 and S1, surface seafloor sediment with length of longer than 30 cm were successfully collected. At station F1, surface seafloor sediment with about 10 cm was also collected. Operation logs at respective stations are shown in Table 7.2 (a) (b) (c).

(4) Future works

Recovered core materials were distributed to some institutes. Radionuclides such as ^{134}Cs , ^{137}Cs , ^{238}U , ^{239}Pu and ^{240}Pu will be analyzed with γ ray spectrometry and/or radiochemical techniques by Kanazawa University, National Institute of Radiological Sciences (NIRS) and Woods Hole Oceanographic Institution (WHOI).

Table 7.1 MC coring summary

Date (maddy)	Core ID	Sampling Site	Location	Lat.	Lon.	Depth(m)	HAND No.	Core length(cm)*	Tension max.(t)	Remarks
2012.6.12	MC01	K2	The North Western North Pacific	47°00.7113' N	139°49.3035' E	5.156	HAND2	31	5.32	acryl pipe
							HAND3	32		acryl pipe
							HAND6	32		acryl pipe
							HAND7	30		polycarbonate pipe
6/29/2012	MC02	S1	Western North Pacific	30°11.9789' N	143°05.9095' E	5.938	HAND2	36.8	6.02	
							HAND3	37.5		
							HAND6	29.1		polycarbonate pipe
							HAND7	36.7		
7/7/2012	MC03	F1	Western North Pacific	36°29.0903' N	141°20.0104' E	1.322	HAND2	17.2	2.20	
							HAND3	15.2		
							HAND6	15.6		polycarbonate pipe
							HAND7	14.2		
							HAND8	9.0		flap valve catcher

*Core length was measured the cores vertically

**Latitude and Longitude was used the ship's position.

Table 7.2 (a) Operation log at station K2

Area: The North Western North Pacific
 Sampling Site: St.K2

Weather: Cloudy
 Wind direction: 15deg. Wind speed: 9.8m/s
 Current direction: 334.9deg. Current speed: 0.6knot

Time* (UTC)	Depth (m)	Wire length (m)	Latitude	Longitude	Tension (ton)	Wire speed (m/s)	Wire in/out (↑ / ↓)	Remarks
19:02	5160	-			-	-	-	Start the operation.
19:04	5157	0	47°00.6994' N	159°49.3087' E	0.4	0.0	-	MC on surface**, Reset the wire length. Wire out (-0.8m/s).
19:15	5159	500			0.9	0.0	-	Wire stop. Start the swell compensator. Wire out (-1.0m/s).
19:24	5157	1000			1.3	1.0	↓	
19:32	5159	1500			1.6	1.0	↓	
19:41	5157	2000			2.0	1.0	↓	
19:49	5157	2500			2.4	1.0	↓	
19:57	5157	3000			2.8	1.0	↓	
20:07	5157	3500			3.3	1.0	↓	
20:14	5157	4000			3.8	1.0	↓	
20:23	5156	4500			4.2	1.0	↓	
20:31	5157	5000			4.5	1.0	↓	
20:34	5157	5110			4.8	0.0	-	Wire stop.
20:39	5153	5110			5.0	-0.3	↓	Wire out.
20:42:03	5156	5150	47°00.7113' N	159°49.3035' E	Min. 4.0	0.3	↓	MC hit the bottom**, Wire out 5m.
20:42	5155	5155			4.4	0.0	-	Wire stop.
20:42	5156	5155			4.5	-0.3	↓	Wire out 2m.
20:42	5157	5157			4.2	0.0	-	Wire stop.Wait 30 seconds.
20:43	5161	5157			4.5	-0.3	↑	Wire in.
20:44:30	5188	5144	47°00.7133' N	159°49.3044' E	Max. 5.2	0.3	↑	MC left the bottom** Wire in (-1.2m/s).
20:46	5157	5000			5.1	1.2	↑	
20:53	5161	4500			4.6	1.2	↑	
21:00	5158	4000			4.3	1.2	↑	
21:07	5158	3500			3.8	1.2	↑	
21:14	5160	3000			3.4	1.2	↑	
21:21	5162	2500			2.9	1.2	↑	
21:28	5164	2000			2.4	1.2	↑	
21:35	5165	1500			2.0	1.2	↑	
21:42	5164	1000			1.5	1.2	↑	
21:51	5162	500			0.9	0.0	-	Stop the swell compensator. Wire in (-0.9m/s).
21:58	5165	0	47°00.9404' N	159°49.5043' E	0.7	-0.6	↑	MC on surface.
22:00	5163	-			-	-	-	MC on deck.

*LST: UTC +11h

**Latitude and Longitude was used the ship's position.

Table 7.2 (b) Operation log at station S1

Cruise Name: MR12-02_Leq2 Operator: Yasushi Hashimoto(MWJ)
 Date (UTC): 2012/6/29
 Core Number: MC02
 Area: Western North Pacific
 Sampling Site: St.S1

Weather: Fine and Cloudy
 Wind direction: 268 deg. Wind speed: 9.8 m/s
 Current direction: 136 deg. Current speed: 0.4 knot

Time* (UTC)	Depth (m)	Wire (m)	Latitude	Longitude	Tension (ton)	Wire (m/s)	Wire (↑/↓)	Remarks
20:58	5942	-			0.6	-	-	Start the operation.
20:59	5941	0	30°12.0077' N	145°05.9405' E	0.5	0.0	-	MC on surface**, Reset the wire length. Wire out (-1.0m/s).
21:10	5937	500			1.0	0.0	*	Wire stop. Start the swell compensator. Wire out (-1.0m/s).
21:19	5936	1000			1.3	1.0	↓	
21:27	5935	1500			1.6	1.0	↓	
21:34	5933	2000			2.2	1.0	↓	
21:43	5935	2500			2.4	1.0	↓	
21:51	5938	3000			3.0	1.0	↓	
21:59	5936	3500			3.4	1.0	↓	
22:07	5939	4000			3.7	1.0	↓	
22:15	5939	4500			4.2	1.0	↓	
22:23	5934	5000			4.6	1.0	↓	
22:32	5937	5500			4.9	1.0	↓	
22:39	5935	5900			5.6	0.0	*	Wire stop (to stabilize the MC for 3 minutes)
22:42	5941	5900			5.5	-0.3	↓	Wire out.
22:44:35	5938	5924	30°11.9786' N	145°05.9090' E	Min. 4.73	0.3	↓	MC hit the bottom**, Wire out 6m.
22:44	5935	5931			5.2	0.0	-	Wire stop. Wait 20 seconds.
22:45	5932	5931			5.2	-0.3	↑	Wire in.
22:46:51	5936	5914	30°11.9779' N	145°05.9098' E	Max. 6.82	0.3	↑	MC left the bottom** Wire in (-1.2m/s).
22:52	5935	5500			5.3	1.2	↑	
22:59	5934	5000			5.3	1.2	↑	
23:06	5935	4500			4.7	1.2	↑	
23:13	5932	4000			4.4	1.2	↑	
23:20	5943	3500			3.8	1.2	↑	
23:27	5937	3000			3.3	1.2	↑	
23:34	5935	2500			2.8	1.2	↑	
23:41	5939	2000			2.4	1.2	↑	
23:48	5938	1500			2.1	1.2	↑	
23:55	5938	1000			1.6	1.2	↑	
0:03	5929	500			0.9	0.0	-	Stop the swell compensator. Wire in (-1.0m/s).
0:16	5927	0	30°11.4979' N	145°05.8807' E	0.8	0.5	↑	MC on surface.**
0:18	5931	-			-	-	-	MC on deck.

*LST: UTC +9h.

**Latitude and Longitude was used the ship's position.

Table 7.2 (c) Operation log at station F1

Cruise Name: MR12-02_Leg2 Operator: Yasushi Hashimoto(MWJ)
 Date: (UTC) 2012/7/7
 Core Number: MC03
 Area: Western North Pacific
 Sampling Site: St.F1
 Weather: Cloudy
 Wind direction: 17 deg. Wind speed: 11.0 m/s
 Current direction: 31.1 deg. Current speed: 1.6 knot

Time* (UTC)	Depth (m)	Wire (m)	Latitude	Longitude	Tension (ton)	Wire (m/s)	Wire (↑ / ↓)	Remarks
23:14	1343	-			0.6	-	-	Start the operation.
23:16	1337	0	36°28.9667' N	141°30.1130' E	0.5	0.0	-	MC on surface**, Reset the wire length. Wire out (~1.0m/s).
23:27	1326	500			1.0	0.0	-	Wire stop. Start the swell compensator. Wire out (~1.0m/s).
23:36	1326	1000			1.3	1.0	↓	
23:42	1322	1300			1.7	0.0	-	Wire stop (to stabilize the MC for 3 minutes)
23:45	1323	1300			1.6	-0.3	↓	Wire out.
23:47:23	1322	1326	36°29.0933' N	141°30.0104' E	Min. 1.05	0.3	↓	MC hit the bottom**, Wire out 4m.
23:47	1322	1330			1.1	0.0	-	Wire stop.Wait 20 seconds.
23:48	1322	1330			1.1	-0.3	↑	Wire in.
23:48:58	1323	1323	36°29.0933' N	141°30.0168' E	Max. 2.20	0.3	↑	MC left the bottom** Wire in (~1.0m/s).
23:54	1323	1000			1.6	1.0	↑	
0:04	1314	500			1.0	0.0	-	Stop the swell compensator. Wire in (~1.0m/s).
0:14	1308	0	36°29.2702' N	141°30.1000' E	0.7	0.5	↑	MC on surface.**
0:16	1304	-			-	-	-	MC on deck.

*LST: UTC +9h

**Latitude and Longitude was used the ship's position.

8. Geophysical observation

8.1 Swath Bathymetry

Takeshi MATSUMOTO (University of the Ryukyus): Principal Investigator (not on-board)

Masao NAKANISHI (Chiba University): Principal Investigator (not on-board)

Katsuhisa MAENO (Global Ocean Development Inc.: GODI) - leg2 -

Harumi OTA (GODI) - leg1 -

Toshimitsu GOTO (GODI) - leg1, 2 -

Ryo KIMURA (Mirai Crew) - leg1, 2 -

(1) Introduction

R/V MIRAI is equipped with a Multi narrow Beam Echo Sounding system (MBES), SEABEAM 3012 Upgrade Model (L3 Communications ELAC Nautik) and Sub-bottom Profiler (SBP), Bathy2010 (SyQwest). The objective of MBES and SBP is collecting continuous bathymetric and sub-bottom data along ship's track to make a contribution to geological and geophysical investigations and global datasets.

(2) Data Acquisition

The "SEABEAM 3012 Upgrade Model" on R/V MIRAI was used for bathymetry mapping during the MR12-02 cruise from 4 June to 10 July 2012.

To get accurate sound velocity of water column for ray-path correction of acoustic multibeam, we used Surface Sound Velocimeter (SSV) data to get the sea surface (6.2m) sound velocity, and the deeper depth sound velocity profiles were calculated by temperature and salinity profiles from CTD, XCTD data by the equation in Del Grosso (1974) during the cruise.

Table 8.1-1 shows system configuration and performance of SEABEAM 3012 Upgrade Model.

Table 8.1-1 System configuration and performance

SEABEAM 3012 Upgrade Model (12 kHz system)

Frequency:	12 kHz
Transmit beam width:	1.6 degree
Transmit power:	20 kW
Transmit pulse length:	2 to 20 msec.
Receive beam width:	1.8 degree
Depth range:	100 to 11,000 m
Beam spacing:	0.5 degree athwart ship
Swath width:	150 degree (max)
	120 degree to 4,500 m
	100 degree to 6,000 m
	90 degree to 11,000 m
Depth accuracy:	Within < 0.5% of depth or +/-1m, whichever is greater, over the entire swath. (Nadir beam has greater accuracy; typically within < 0.2% of depth or +/-1m, whichever is

greater)

Sub-bottom Profiler (3.5kHz system)

Frequency:	3.5 kHz
Transmit beam width:	23 degree
Transmit pulse length:	0.5 to 50 msec
Strata resolution:	Up to 8 cm with 300+ Meters of bottom penetration; bottom type dependant
Depth resolution:	0.1 Feet, 0.1 Meters
Depth accuracy:	±10 cm to 100 m, ± .3% to 6,000 m

(3) Preliminary Results

The results will be published after primary processing.

(4) Data Archives

Bathymetric data obtained during this cruise will be submitted to the Data Management Group (DMG) in JAMSTEC, and will be archived there.

8.2 Sea surface gravity

Takeshi MATSUMOTO (University of the Ryukyus): Principal Investigator (not on-board)

Masao NAKANISHI (Chiba University): Principal Investigator (not on-board)

Katsuhisa MAENO (Global Ocean Development Inc.: GODI) - leg2 -

Harumi OTA (GODI) - leg1 -

Toshimitsu GOTO (GODI) - leg1, 2 -

Ryo KIMURA (Mirai Crew) - leg1, 2 -

(1) Introduction

The local gravity is an important parameter in geophysics and geodesy. We collected gravity data at the sea surface.

(2) Parameters

Relative Gravity [CU: Counter Unit]

$$[\text{mGal}] = (\text{coef1: } 0.9946) * [\text{CU}]$$

(3) Data Acquisition

We measured relative gravity using LaCoste and Romberg air-sea gravity meter S-116 (Micro-g LaCoste, LLC) during the MR12-02 cruise from 4 June 2012 to 11 July 2012.

To convert the relative gravity to absolute one, we measured gravity using portable gravity meter (Scintrex gravity meter CG-5), at Sekinehama as the reference points.

(4) Preliminary Results

Absolute gravity table is shown in Tabel 8.2-1.

Table 8.2-1

No.	Date	U.T.C.	Port	Absolute Gravity (mGal)	Sea Level (cm)	Draft (cm)	Gravity at Sensor* ¹ (mGal)	L&R Gravity* ² (mGal)
#01	30-May-12	03:53	Sekinehama	980371.92	278	633	980373.06	12614.27
#02	13-Jul-12	03:32	Sekinehama	980371.95	247	641	980373.00	12614.42

*¹: Gravity at Sensor = Absolute Gravity + Sea Level*0.3086/100 + (Draft-530)/100*0.2654

*²: LaCoste and Romberg air-sea gravity meter S-116

(5) Data Archives

Surface gravity data obtained during this cruise will be submitted to the Data Management Group (DMG) in JAMSTEC, and will be archived there.

8.3 Sea Surface magnetic field

Takeshi MATSUMOTO(University of the Ryukyus): Principal Investigator (not on-board)

Masao NAKANISHI (Chiba University): Principal Investigator (not on-board)

Katsuhisa MAENO (Global Ocean Development Inc.: GODI) - leg2 -

Harumi OTA (GODI) - leg1 -

Toshimitsu GOTO (GODI) - leg1, 2 -

Ryo KIMURA (Mirai Crew) - leg1, 2 -

1) Three-component magnetometer

(1) Introduction

Measurements of magnetic force on the sea are required for the geophysical investigations of marine magnetic anomaly caused by magnetization in upper crustal structure. We measured geomagnetic field using a three-component magnetometer during the MR12-02 cruise from 4 June 2012 to 11 July 2012.

(2) Principle of ship-board geomagnetic vector measurement

The relation between a magnetic-field vector observed on-board, \mathbf{H}_{ob} , (in the ship's fixed coordinate system) and the geomagnetic field vector, \mathbf{F} , (in the Earth's fixed coordinate system) is expressed as:

$$\mathbf{H}_{ob} = \mathbf{A} \mathbf{R} \mathbf{P} \mathbf{Y} \mathbf{F} + \mathbf{H}_p \quad (a)$$

where \mathbf{R} , \mathbf{P} and \mathbf{Y} are the matrices of rotation due to roll, pitch and heading of a ship, respectively. \mathbf{A} is a 3 x 3 matrix which represents magnetic susceptibility of the ship, and \mathbf{H}_p is a magnetic field vector produced by a permanent magnetic moment of the ship's body. Rearrangement of Eq. (a) makes

$$\mathbf{B} \mathbf{H}_{ob} + \mathbf{H}_{bp} = \mathbf{R} \mathbf{P} \mathbf{Y} \mathbf{F} \quad (b)$$

where $\mathbf{B} = \mathbf{A}^{-1}$, and $\mathbf{H}_{bp} = -\mathbf{B} \mathbf{H}_p$. The magnetic field, \mathbf{F} , can be obtained by measuring \mathbf{R} , \mathbf{P} , \mathbf{Y} and \mathbf{H}_{ob} , if \mathbf{B} and \mathbf{H}_{bp} are known. Twelve constants in \mathbf{B} and \mathbf{H}_{bp} can be determined by measuring variation of \mathbf{H}_{ob} with \mathbf{R} , \mathbf{P} and \mathbf{Y} at a place where the geomagnetic field, \mathbf{F} , is known.

(3) Instruments on R/V MIRAI

A shipboard three-component magnetometer system (Tierra Technica SFG1214) is equipped on-board R/V MIRAI. Three-axes flux-gate sensors with ring-cored coils are fixed on the fore mast. Outputs of the sensors are digitized by a 20-bit A/D converter (1 nT/LSB), and sampled at 8 times per second. Ship's heading, pitch, and roll are measured utilizing a Inertial Navigation System (Fiber Optical Gyro) installed for controlling attitude of a Doppler radar. Ship's position (GPS) and speed data are taken from LAN every second.

(4) Data Archives

These data obtained during this cruise will be submitted to the Data Management Group (DMG) in JAMSTEC, and will be archived there.

(5) Remarks

1. For calibration of the ship's magnetic effect, we made a "Figure eight" turn (a pair of clockwise and anti-clockwise rotation). The periods were follows;
 - i) 05:38 - 06:05 UTC, 14 Jun. around at 47-00N,159-59E
 - ii) 10:20 - 10:51 UTC, 30 Jun. around at 30-03N,144-59E
 - iii) 07:00 - 07:24 UTC, 08 Jul. around at 36-30N,141-31E

2) Cesium magnetometer

(1) Introduction

Measurement of total magnetic force on the sea is required for the geophysical investigations of marine magnetic anomaly caused by magnetization in upper crustal structure.

(2) Data Period

13:52 UTC 15 Jun. - 05:00 UTC 17 Jun.

(3) Specification

We measured total geomagnetic field using a cesium marine magnetometer (Geometrics Inc., G-882) and recorded by G-882 data logger (Clovertech Co., Ver.1.0.0). The G-882 magnetometer uses an optically pumped Cesium-vapor atomic resonance system. The sensor fish towed 500 m behind the vessel to minimize the effects of the ship's magnetic field. Table 8.3-1 shows system configuration of MIRAI cesium magnetometer system.

Table 8.3-1 System configuration of MIRAI cesium magnetometer system.

Dynamic operating range:	20,000 to 100,000 nT
Absolute accuracy:	$< \pm 2$ nT throughout range
Setting: Cycle rate;	0.1 sec
Sensitivity;	0.001265 nT at a 0.1 second cycle rate
Sampling rate;	1 sec

(4) Data Archive

Total magnetic force data obtained during this cruise was submitted to the Data Management Group (DMG) of JAMSTEC, and archived there.

8.4 Tectonic history of the mid-Cretaceous Pacific Plate

Masao NAKANISHI (Graduate School of Science, Chiba University)

The Pacific Plate is the largest oceanic lithospheric plate on the Earth. The Pacific Plate was born around 190 Ma, Middle Jurassic (Nakanishi et al., 1992). The tectonic history of the Pacific Plate has been exposed by many studies based on magnetic anomaly lineations. However, the tectonic history in some periods is still obscure because of lack of geophysical data. To reveal the entire tectonic history of the Pacific Plate from Middle Jurassic to the present, increase in geophysical data is indispensable.

In the seafloor around the stations K2 and KNOT there are several topographic features that bear on tectonic evolution of the mid-Cretaceous Pacific Plate. The seafloor in the survey area was formed at the Pacific-Izanagi Ridge (e.g., Mammerickx, and Sharman, 1988). They proposed a significant reorganization of the plate boundaries of the Pacific Plate in the period.

The detailed bathymetric survey exposed the topographic expression of the en echelon troughs south of the station K2 (Figure 1). The width of the troughs is about 15 km. The depth of the troughs has a southeastward deepening from 5800 m to 6200 m. The northern edge is steeper than the southern edge. The relative height of the northern edge is more than 500 m, but that of the southern edge is 300-500 m. The troughs trend roughly parallel to the fracture zones, suggesting an origin related to seafloor spreading of the Pacific-Izanagi Ridge.

The geomagnetic measurement was also conducted by the cesium-vapor magnetometer. The magnetic anomalies are calculated by International Geomagnetic Reference Field (International Association of Geomagnetism and Aeronomy, Working Group V-MOD, 2010). The figure 2 shows magnetic anomaly profiles along the ship track. The amplitude of magnetic anomalies in the detailed bathymetric survey area is less than 200 nT. That of the transit from the survey area to the station KNOT is more than 300 nT.

References

- International Association of Geomagnetism and Aeronomy, Working Group V-MOD, International Geomagnetic Reference Field, 2010: the eleventh generation. *Geophys. J. Int.*, 83, 3, 1216-1230, December 2010. DOI: 10.1111/j.1365-246X.2010.04804.x.
- Mammerickx, J., and G. F. Sharman, 1988: Tectonic Evolution of the North Pacific During the Cretaceous Quiet Period, *J. Geophys. Res.*, 93, B4, 3009-3024, doi:10.1029/JB093iB04p03009.

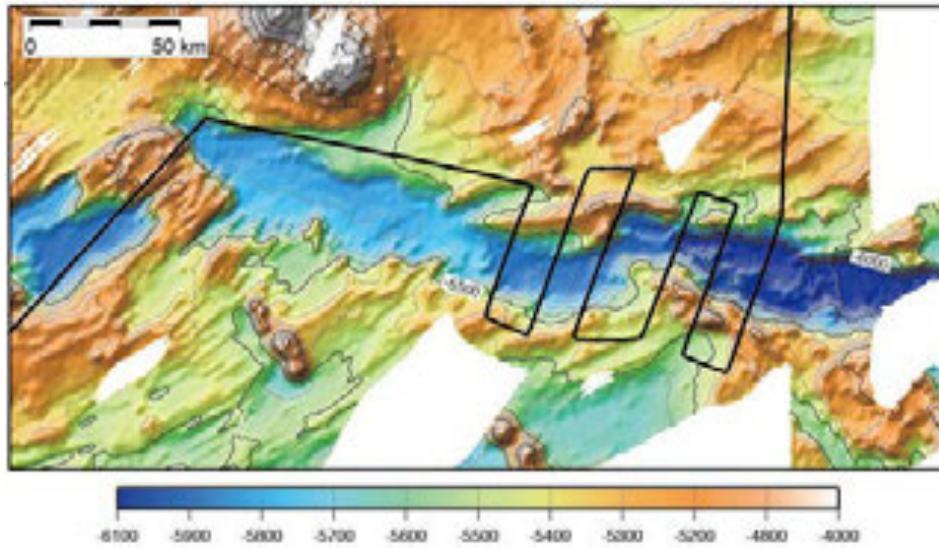


Figure 1. Bathymetric map of the detailed bathymetric survey area made by bathymetric data collected in this cruise and previous cruises by R/V MIRAI and other research vessels. Contour interval is 100 m. Bathymetry is illuminated from the northwest. The black line represents the ship track.

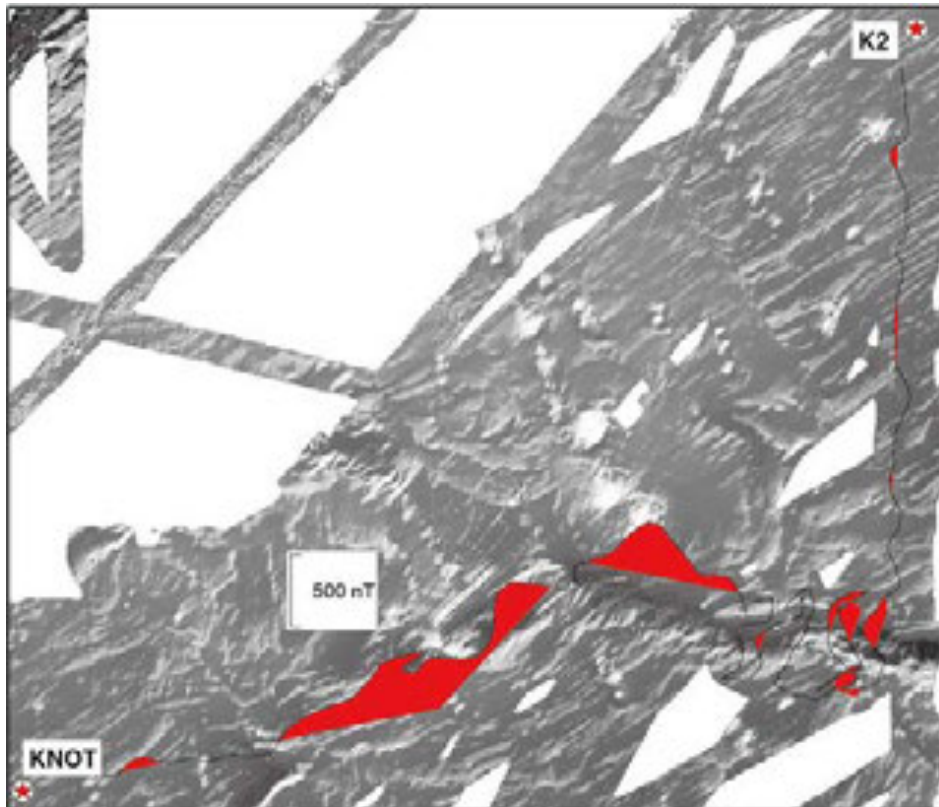


Figure 2. Magnetic anomaly profiles plotted along the ship track and overlaid on bathymetric map. Positive anomalies are filled in red.

9. Satellite Image Acquisition (MCSST from NOAA/HRPT)

Makio HONDA	(JAMSTEC)	
Katsuhisa MAENO	(Global Ocean Development Inc.: GODI)	- leg2 -
Harumi OTA	(GODI)	- leg1 -
Toshimitsu GOTO	(GODI)	- leg1, 2 -
Ryo KIMURA	(Mirai Crew)	- leg1, 2 -

(1) Objectives

It is our objectives to collect data of sea surface temperature in a high spatial resolution mode from the Advance Very High Resolution Radiometer (AVHRR) on the NOAA polar orbiting satellites and to build a time and depth resolved primary productivity model.

(2) Method

We receive the down link High Resolution Picture Transmission (HRPT) signal from NOAA satellites. We processed the HRPT signal with the in-flight calibration and computed the sea surface temperature by the Multi-Channel Sea Surface Temperature (MCSST) method. A daily composite map of MCSST data is processed for each day on the R/V MIRAI for the area, where the R/V MIRAI located.

We received and processed NOAA data throughout MR12-02 cruise from 4 June 2012 to 12 July 2012.

The sea surface temperature data will be applied for the time and depth resolved primary productivity model to determine a temperature field for the model.

(3) Data archives

The raw data obtained during this this cruise will be submitted to the Data Management Group (DMG) in JAMSTEC, and will be archived there.